Profiling chemokine signalling bias of CCR4, CCR7 and CCR10

Christopher James Kelly

A thesis submitted to the College of Medicine, Veterinary and Life Sciences, University of Glasgow in fulfillment of the requirements for the degree of Doctor of Philosophy

October 2018

Institute of Infection, Immunity and Inflammation
University of Glasgow
120 University Place
G12 8TA

Author’s declaration

I declare that, except where explicit reference is made to the contribution of others, that this thesis is the result of my own work and has not been submitted for any other degree at the University of Glasgow or any other institution.

Signature .....

Printed name: Christopher James Kelly

List of abbreviations

7 transmembrane domains (7TM)

Adult t-cell leukaemia/lymphomas (ATLL)

Angiotensin 2 type 1 receptor (AT1R)

Atypical chemokine receptors (ACKRs)

Bioluminescence resonance energy transferred (BRET)

Bone marrow derived dendritic cell (BMDC)

Calcitonin gene-related peptide (CGRP)

Cells from 4 days into the BMDC differentiation protocol (D4)

Cells from 7 days into the BMDC differentiation protocol (D7)

Central memory T-cells (Tcm)

Central nervous system (CNS)

Cutaneous lymphocyte antigen positive (CLA+)

CXCL12-abundant reticular (CAR) cells

Dendritic cells (DCs)

Dopamine D2 receptor (D2R)

Double negative thymocytes (DNTs)

Double positive thymocytes (DPT)

Doxycycline (DOX)

Dulbecco's minimal essential medium (DMEM)

Dulbecco's phosphate buffered saline, calcium and magnesium free (DPBS)

Effector memory T-cells (Tem)

Endoneuraminidase-N (endo-N)

Foetal calf serum (FCS),

G-protein coupled receptor kinases (GRKs)

G-protein coupled receptors (GPCRs)

Gene/genes of interest (GOI)

Granulocyte-macrophage colony stimulating factor (GM-CSF)

Guanidine diphosphate (GDP)

Guanidine nucleotide exchange factor (GEF)

Guanidine triphosphate (GTP)

Hanks balanced salt solution (HBSS, Gibco)

Hematopoietic stem cells (HSC)

High endothelial venules (HEVs)

High fidelity (HF)

Human immune deficiency virus (HIV)

Human T-lymphotropic virus 1 (HTLV-1)

Imiquimod treated (Imq)

Immunoprecipitation (IP)

Interferon alpha (INFa)

Interleukin 4 IL-4

Knockout mouse strain (KO)

Lipopolysaccharide (LPS)

-Logarithm of 50% maximal response (pEC_{50})

-Logarithm of dissociation constant (pK_i)

Lymph nodes (LNs)

Mean fluorescence intensity (MFI)

Medullary thymic epithelial cells (mTECs)

Mesenchymal stem cells (MSCs)

Mitogen-activated protein kinase (MAPK)

Molecular weight (MW)

Nanoluciferase (nLuc)

Natural killer (NK)

Neural cell adhesion molecule (NCAM)

Neuropilin 2 (NRP2)

No-chemokine control (NC)

Percentage staining/band density compared to WT (%WT)

Pertussis toxin (PTX)

Polyethylenimine (PEI)

Polymerase chain reaction (PCR)

Polysialic acid (pSia)

Post-translational modifications (PTMs)

Rat corticotropin releasing factor receptor (CRF1R)

Regulatory T-cell (Treg)

Relative efficacy (RA)

Renilla luciferase (rLuc)

Reverse transcription quantitative PCR (qPCR)

Rheumatoid arthritis (RA)

Secondary lymphoid organs (SLOs),

Single positive (i.e. CD4+ or CD8+) thymocytes (SPTs)

Sphingosine-1-phosphate 1 receptor (S1P1R)

Standard deviation (SD)

Streptavidin-BV421 (SABV421)

Streptavidin-PE (SAPE)

Systematic protein affinity strength modulation (SPASM)

T-helper 2 (Th2)

TATA binding protein (TBP)

Tertiary lymphoid organs (TLOs)

Tissue culture (TC)

Toll like receptor (TLR)

Toll-like receptor 7 (TLR7)

Tris-acetate-EDTA (TAE)

Tumour associated macrophages (TAMs)

Tumour necrosis factor alpha (TNFa, Miltenyi)

Unnatural amino acids (UAA)

Unstimulated bone marrow (D0)

Vascular endothelial growth factor D (VEGF-D)

Vehicle treated (Veh)

Wildtype (WT)

Yellow fluorescent protein (YFP)

Acknowledgements

I would like to thank my supervisors Gerard Graham and Graeme Milligan for their support and advice over the years, and for giving me the freedom to follow my own path. I would also like to thank the GLAZgo discovery centre for funding and supporting me throughout my time at the university.

Thanks to everyone on level 3 (and beyond), past and present. It's been a fantastic experience getting to know everyone and I really couldn't have asked for a better or friendlier environment to spend the last 4 years in. I think it's fair to say I've made a number of lifelong friends here. I would especially like to thank Sam and Robin, who did take on the slightly onerous task of living with me. I'm not easy to live with at the best of times, and don't imagine I improved during the final few stages. I definitely wouldn't have made over the finish line without you guys, and I owe you a lot for that.

Lastly, I'd like to thank my entire family, but in particular my parents, without whom I both literally and figuratively wouldn't be here. It's not always been easy, but you helped turn impossible in to not-easy on more than one occasion, and I don't think I can thank you enough for that. I promise, this time I will actually stop being a student once I've finished here.

Table of Contents

List of figures/tables

Abstract

Inflammatory chemokine signalling is implicated in a broad range of pathologies and has been intensely researched. However, chemokine receptors remain poorly druggable. This may be due to the complexity of chemokine signalling; multiple chemokines can bind a single receptor, and an individual chemokine can bind multiple receptors. Additionally, many receptors demonstrate signalling bias, where different ligands elicit diverse responses. Bias signalling is an area of emerging interest with relevance in drug development, and there is a call to better characterise chemokine signalling bias. CCR4, CCR7 and CCR10 share a similar molecular evolution; each interacts with a ligand pair resultant from gene duplication, with one ligand in each pair being "dominant" in receptor activation, i.e. able to fully activate the receptor triggering recruitment of G-proteins and β-arrestin. It may be possible, with a greater understanding of the underlying biology of biased signalling, to generate future antagonists of these receptors that selectively inhibit individual signalling pathways, as has been demonstrated previously with other GPCRs.

Biased signalling is believed to result from slight variation in ligand/receptor binding that lock the receptor in specific conformations for coupling to signalling apparatus. In an effort to visualise these subtle differences, a novel unnatural amino acid (UAA) capture based methodology was attempted. An expression vector for a UAA compatible tRNA/Synthetase pair, as well as mutants of 16 residues of CCR7, were generated. UAA integration was observed with all 16 mutants, however protein level and ligand binding varied significantly between sites of integration. UV crosslinking of ligand and receptor was attempted, but no combination of chemokine and substitution site demonstrated successful chemokine capture.

In an effort to fully profile the bias of CCRs 4, 7 and 10, BRET based methods were employed to assess β-arrestin and G-protein recruitment by the receptors in response to their cognate ligands. These data confirmed the reported bias, that CCL22, 19 and 21 trigger β-arrestin recruitment to CCR4, 7 and 10 respectively, but CCL17 and CCL28 failed to trigger recruitment, and CCL21 did so at poorer efficiency than CCL19. Interestingly, this pattern remained at the level of G-protein recruitment also, in contrast to the previously reported signalling properties of these chemokines.

Recently, CCR7 was identified as a target of ST8sia4 mediated polysialylation, with significant effects on the biological activity of CCL21. As such, the role of ST8sia4 in chemokine biology was further examined. These data revealed that HEK293T cells, as well

as other adherent cell lines, demonstrate little to no expression of ST8sia4. Reintroduction of polysialic acid modification of CCR7 restored the capacity of CCL21 to compete with labelled CCL19 on HEK293T cells, resulting in a partial phenocopy of primary cells in the same assay, and resulted in a shift in potency of CCL21 for β–arrestin recruitment. This was mirrored at the level of G-protein recruitment, indicating that the previously noted lack of G-protein in response to CCL21 was most likely due to the lack of polysialylation of CCR7. Conversely, inclusion of ST8sia4 expression in the assessment of CCR4 signalling demonstrated no change from previous experiments. CCR10 however was revealed to be a previously undescribed target of ST8sia4 mediated polysialylation, with implications for the signalling potential of both of its cognate ligands.

1 Introduction

1.1 Overview

Since their initial identification in the 1980s, chemokines have emerged as perhaps the key instigators of directed cellular migration, in a process referred to as chemotaxis (Rot and von Andrian, 2004). In this capacity they are best described for their role in the immune system, giving rise to their title of chemotactic cytokines, abbreviated to chemokines. Although diverse in physiological function all chemokines share a number of traits. They all adopt a conformation maintained by a tetracysteine motif (with the exception of the XCL chemokines), are all quite small at an average molecular weight of around 10 kDa, and signal through coupling with a group of class A G-protein coupled receptors (GPCRs) known as the chemokine receptors . Beyond their role in the immune system a number of chemokines have demonstrated additional functional roles. The CXCR4/CXCL12 signalling axis is often regarded as the primordial chemokine/receptor pairing in the system, and its genetic ablation results in a 100% mortality rate of offspring and a number of defects in the cardiovascular system, in the urinary tract and in the central nervous system (Ara *et al.*, 2005; Takabatake *et al.*, 2009; Zhu and Murakami, 2012). This would indicate extensive developmental functions of CXCL12/CXCR4. Chemokines are also important in the processes of angiogenesis and wound healing, mediating their effects either through the recruitment of cells capable of tissue remodelling, or through direct non-chemotactic signalling events downstream of chemokine receptors (Behm *et al.*, 2012).

It is in their function in the immune system, however, that chemokines are most studied. As demonstrated by the utilisation of CXCR4 blockade to free hematopoietic stem cells (HSC) into circulation for collection and transplant, the CXCL12/CXCR4 axis is important in directing and maintaining HSC residence in the bone marrow under basal conditions, a form of homeostatic signalling (Devine *et al.*, 2008). In the context of insult or injury chemokine signalling spatially and temporally coordinates the reaction of the immune system. An example could be the breaking of the skin barrier introducing pathogen, resulting in the release of an initial wave of Toll like receptor (TLR) dependent danger signals. These include CXCL1 secreted by keratinocytes, signalling through CXCR2 and contributing to neutrophil recruitment, in an initial attempt to contain infection (Sanz and Kubes, 2012). This would be an example of inflammatory chemokine signalling. If the pathogen is not cleared by the innate response, an adaptive immune response may be required. Dermal or epidermal dendritic cells (DCs) uptake antigen, upregulating CCR7 expression and leading to their recruitment to lymph nodes (LNs) (Ohl *et al.*, 2004). Here

they can interact with naïve T-cells basally recruited by CCR7 ligands, initiating an adaptive immune response (Förster, Davalos-Misslitz and Rot, 2008). In this context CCR7 signalling could be considered both inflammatory for DCs, as they do not express CCR7 basally, and homeostatic for naïve T-cells, which routinely travel in and out of secondary lymphoid organs (SLOs), surveying for DCs presenting their specific antigen.

Chemokines can also be considered pathogenic under a number of contexts. CCR5 is used as a co-receptor for human immune deficiency virus (HIV) cellular entry, with maraviroc (a CCR5 antagonist) being effectively used in disease management (Tan *et al.*, 2013). Other viruses have become highly adept at manipulating the chemokine system for their own gain. Kaposi's sarcoma-associated herpesvirus encodes a viral chemokine, vMIP-II, capable of antagonising CXCR4 and promiscuously binding CC and CXC receptors (Qin *et al.*, 2015). Others like human cytomegalovirus encode viral chemokine receptors like US28, a constitutively active receptor capable of binding CC, CXC and CX_3C chemokines and sculpting the immune system as a result (Burg *et al.*, 2015). In cancer, aberrant chemokine signalling can aid in the development of disease in a number of ways. Recruitment of tumour associated macrophages (TAMs) and other inflammatory mediators aids tumorigenesis through upregulation of angiogenesis and tissue remodelling (Allavena *et al.*, 2008). This process is necessary for the expansion of tumour size beyond certain metabolic limitations and is considered a hallmark of cancer development (Hanahan and Weinberg, 2011). The deposition of metastatic lesions is also linked with chemokine signalling, for example metastasis of breast cancer to the bone marrow, lungs and LNs is often linked to CXCR4:CXCL12 signalling (Gangadhar, Nandi and Salgia, 2010). Inflammatory signalling is also very important in various autoimmune diseases. In rheumatoid arthritis (RA) an influx of leukocytes is recruited and retained in the joint synovium, a process heavily associated with aberrant chemokine signalling, inducing inflammation and damaging the surrounding tissue (Szekanecz *et al.*, 2006).

Despite extensive study, in the 3 decades since their discovery, there is still a great deal we do not fully understand about the chemokine system.

1.2 The chemokines

As stated previously, chemokines share a few common features, such as their size (~8-14 kDa) and general 3D structure. They can however be sub-divided for characterisation based on a number of further criteria. The distinctive structure of chemokines is maintained through disulfide bonding between highly conserved cysteine residues. Generally, there are

4 conserved cysteine residues found in chemokines, giving the tetracysteine motif typical of the family, with 2 found near the N-terminus, 1 near the C-terminus and a fourth in-between, forming 2 disulfide bonds (figure 1.2.1). The absence or addition of amino acid residues between the 2 N-terminal cysteines allows for the classification of chemokines as either CC, CXC or CX_3C. Additionally, there are the XC chemokines, which lack 2 of the 4 cysteines but maintain a similar structure (figure 1.2.1) (Zlotnik and Yoshie, 2000). At present 28 CC, 17 CXC, 1 CX_3C and 2 XC chemokines have been identified (summarised in table 1.2.1) (Hughes and Nibbs, 2018). CXC chemokines can also be referred to as α-chemokines, and CC as β-chemokines.

Due to their shared structure and sequence homology, the extensive repertoire of chemokines identified today are thought to have derived from duplication events of a single ancestral chemokine (Zlotnik, Yoshie and Nomiyama, 2006). This principle of chemokine evolution is supported by the observation that the genes for chemokines are frequently clustered in common genomic loci, with a cluster of CXC chemokine genes found on chromosome 4 in humans and a cluster of CC chemokine genes on chromosome 17. These clusters represent the largest groupings of genes for their respective families, though smaller mini-clusters for others are also observed as are non-clustered chemokine genes (summarised in figure 1.2.2).

CXC chemokines can also be further subdivided as either ELR+ or ELR- (Belperio *et al.*, 2000). This classification refers to a 3 amino acid motif consisting of glutamic acid, lysine and arginine, which is present at the N-terminus of these chemokines next to the CXC motif. These include CXCL1, 2, 3, 5, 6, 7 and 8, and which bind CXCRs 1 and 2. These ELR+ positive chemokines are considered pro-angiogenic, contributing to the re-vascularisation of injured or ischemic tissue, as well as neo-vascularisation of lesional tissues (Bizzarri *et al.*, 2006). ELR- CXC chemokines, conversely, are broadly considered angiostatic, i.e. they have either no or even inhibitory effects on angiogenesis (Airoldi and Ribatti, 2011). Interestingly, mutagenesis of CXCL8 to remove this ELR motif results in a functional switch from angiogenic to angiostatic (Strieter *et al.*, 1995). The primary cellular mediators of these angiogenic effects are vascular endothelial cells, which express CXCR2, migrate in response to ELR+ chemokines in vitro and promote the vascularisation of corneal pockets in vivo.

Although divisible by sub-family as either CC, CXC, CX_3C and XC, chemokines are also frequently grouped by function as either homeostatic or inflammatory.

1.2.1 Homeostatic chemokines

As mentioned previously, the CXCL12/CXCR4 signalling axis is considered homeostatic, that is CXCL12 expression occurs basally and is generally unaffected by inflammatory insult, and subsequent signalling through CXCR4 is constant. Indeed, this signalling axis could be considered the archetypal homeostatic signalling axis, as demonstrated by its extensive roles both in organogenesis and in the mature immune system (Anders, Romagnani and Mantovani, 2014). Disruption of any aspect of this signalling axis is perinatally lethal in mice (Ma *et al.*, 1998; Ara *et al.*, 2005; Yu *et al.*, 2011), a rarity amongst knockout mouse strains (KO) targeting the chemokine system. It is through this signalling axis that HSCs are recruited and retained in the bone marrow, with CXCL12 expression from CXCL12-abundant reticular (CAR) cells in the bone marrow stroma aiding in retention of CXCR4+ HSCs (Rankin, 2012). CXCL12/CXCR4 signalling is also used to maintain stem cell-like properties and tissue localisation of other progenitor cell populations as well, such as neural and mesenchymal stem cells (Zhu *et al.*, 2012; Hu *et al.*, 2013). During embryogenesis CXCL12/CXCR4 guidance cues are vitally important in the development of the cardiovascular and renal systems, ensuring the correct direction of cellular movement of cardio, endothelial and epithelial pre-cursors to form these tissues (Raman, Sobolik-Delmaire and Richmond, 2011). The dual roles of CXCL12/CXCR4 signalling in vascular development and the maintenance of stem cell populations in tissues also makes this chemokine/receptor interaction vital in wound healing and re-vascularisation (Bermudez *et al.*, 2011).

As well as extensive functions during development, stem-cell renewal and wound healing, CXCL12/CXCR4 signalling also has additional immune functions. In concert with CCL25/CCR9, CCL17/CCL22/CCR4 and CCL19/CCL21/CCR7, CXCL12/CXCR4 signalling regulates the step-wise transition of immature lymphocytes through the thymus during their development (Takahama, 2006). Somewhat similarly, the sequential presentation of the chemokines of CCR7 in SLOs is vital in instigating mature DC; naïve/memory T-cell interactions, a critical step in initiating an adaptive immune response (Comerford *et al.*, 2013). As well, the CXCL13/CXCR5 signalling axis is a requirement of B-cell homing into SLOs, again a critical event in the development of antigen specific humoral immune responses (Ansel *et al.*, 2000). Additionally, signalling by CCL17 and CCL22 through CCR4, and CCL27 through CCR10, recruits a number of T-cell subsets into the skin, and CCL28/CCR10 signalling in mucosal epithelial tissues helps with IgA producing plasmablast retention, important for the maintenance of barrier immunity. The

functions of CCR4, CCR7 and CCR10 will be discussed in further detail later in this Chapter.

Homeostatic signalling can also be pathogenic in a number of circumstances. CXCL12/CXCR4 signalling is arguably the best characterised in this respect, as might be expected. In chronic inflammatory conditions for example, CXCL12 can drive the formation of tertiary lymphoid organs (TLOs) (Corsiero *et al.*, 2012), which can be counter-productive to the resolution of inflammation. CXCL12/CXCR4 signalling is also often utilised in the invasion and metastatic dissemination of a number of cancers (Sun *et al.*, 2010). CCR7 signalling is also often exploited by cancers to aid in the deposition of LN metastasis, and CCR4 driven migration to the skin is a hallmark of adult t-cell leukaemia/lymphomas (ATLL). Again, these aspects of CCR4 and CCR7 biology will be discussed further in later sections.

1.2.2 Inflammatory chemokines

In contrast to the homeostatic chemokines, inflammatory chemokines are rapidly upregulated, usually in response to inflammatory insult . These inflammatory chemokines are expressed by a plethora of cell-types in response to damage or attack (Rollins, 1997). Amongst the CXC chemokines these include CXCL1, 2, 3, 5, 6, 7 and 8 . These chemokines signal through the receptors CXCR1 and 2 and in doing so recruit neutrophils to the site of damage or infection (Zlotnik and Yoshie, 2012). Amongst the inflammatory CC chemokines there are CCL2, 3, 4, 6, 7, 8, 9, and 15 which signal through CCR1, 2, 3 and 5 (Charo and Ransohoff, 2006). This alludes to an interesting division between the inflammatory and homeostatic chemokines. Namely that, for the most part, the homeostatic chemokines interact with specific receptors whereas the inflammatory chemokines are able to interact with multiple receptors (Culley *et al.*, 2006). The inverse is also true, as the inflammatory (but not most homeostatic) receptors themselves similarly bind multiple chemokines (Berchiche *et al.*, 2011) (summarised in figure 1.2.3). This considerable multiplicity of ligand/receptor combinations and cross-talk is often referred to as “redundancy” in the system. The idea being that, in order to ensure a robust immune infiltrate to sites of infection, a multitude of chemokines/receptors serving the same function has evolved and duplicated to ensure this broad activity (Mantovani, 1999). However, it is perhaps hasty to write off this explosion in inflammatory chemokines as simple redundancy. As can be seen (figure 1.2.3), chemokines vary in the repertoire of receptors they can bind. In addition, they display differing affinities for different receptors (Corbisier *et al.*, 2015). When considering this, and the fact that redundancy to this degree

is rare in biological systems, it is possible that these chemokines serve non-redundant functions that have yet to be fully elucidated.

Once again, inflammatory chemokine signalling can also be pathogenic in a number of contexts. As might be expected, chronic inflammatory conditions are perpetuated by the recruitment of cellular mediators of inflammation, which is frequently chemokine driven process. In the case of RA, recruitment of inflammatory cells of the myeloid compartment to the joint synovium is critical to pathogenesis (Szekanecz *et al.*, 2006). As such, pharmacological blockers of CCR1, 2 and 5 have been considered in the treatment of RA, however to date no such treatment has been successful in clinical trials (Lebre *et al.*, 2011). Developing tumours also benefit from the exploitation of inflammatory chemokines. For example, CCL2 and CCL5 can be expressed either by cancer cells or the surrounding stroma and recruit TAMs to the tumour site, a critical step in the establishment of the tumour microenvironment (Farajzadeh Valilou *et al.*, 2018). In addition, inflammatory chemokine signalling may be utilised in metastasis (Borsig *et al.*, 2014)

1.3 The chemokine receptors

Chemokines mediate their actions through the chemokine receptors, a group of class A GPCRs (GPCRs). These are grouped as either CCR, CXCR, CX3CR or XCR in accordance with the chemokines that signal through them. For the most part a chemokine receptor is restricted in the family of chemokines it can bind, i.e. a CCR will bind CC chemokines only, and a CXC chemokine can only bind to a CXCR. At present 10 CCRs, 6 CXCRs, 1 CX_3CR and XCR1 have been identified in humans (Zlotnik and Yoshie, 2012). These receptors, and the chemokines they bind, are summarised in table 1.1. Chemokine receptors belong to the Class A GPCR, or rhodopsin-like, family of GPCRS and share a number of structural features consistent with members of this family (Allen, Crown and Handel, 2007). These being that they consist of an unstructured N-terminus, with 7 helical transmembrane domains (7TM) embedded in cellular membranes, connected by extracellular and intracellular loops and finally a C-terminal tail, with extracellular loops thought to be involved in ligand interaction, and intracellular loops and the C-terminus involved in interaction with signalling pathways.

1.3.1 Chemokine receptor signalling

As stated, the chemokine receptors are GPCRs, and therefore belong to the most extensive family of signal transduction receptors encoded for by the human genome. Consequently, they share a number of common features with other GPCRs in terms of how they translate

external stimuli (i.e. interaction with ligands) to internal effects (i.e. cytoskeletal rearrangement, modulation of gene expression etc). In general, GPCRs follow a distinct series of events in order to mediate intracellular signalling that begins with association of the ligand with the receptor (Hanlon and Andrew, 2015). This results in conformational changes in receptor structure that facilitate recruitment of heterotrimeric G-protein complexes by the receptor and allows it to act as a guanidine nucleotide exchange factor (GEF). These heterotrimeric complexes consist of Gα, Gβ and Gγ subunits. GPCRs activate signalling pathways by acting as a GEF, stripping the low energy and stable guanidine diphosphate (GDP) molecule from the Ga subunit and allowing guanidine triphosphate (GTP) to bind with it. This dissociates the Gα subunit from the heterotrimeric complex, while the Gβ and Gγ subunits remain in complex with each other. While both the (now GTP bearing) Gα subunit and the remaining Gβγ complex can signal through the activation of secondary messenger pathways, it is the Gα subunit that confers selectivity of receptor signalling through the activation of different secondary messengers. The repertoire of Gα proteins available to GPCRs is extensive (Cotton and Claing, 2009), however with the chemokine system it is generally accepted that signalling of chemokine receptors is predominantly through coupling to Gi or Go α sub-units. This is due to the observation that chemotaxis is pertussis toxin (PTX) sensitive, a hallmark of Gi/o signalling (Katada, 2012). Although there is increasing evidence of other G-protein/chemokine receptor couplings, and therefore variable signalling outcomes as a result, only Gi/o signalling will be considered in this introduction. The free Gi/o subunit inhibits adenylate cyclase and reduces cellular cAMP levels as a result, initiating the downstream signalling cascade that results from GPCR/ligand interaction.

The remaining Gβγ complex has been shown to recruit GPCR kinases (GRKs) to the receptor (Luttrell *et al.*, 1999), however it has also been suggested that disassociation of the heterotrimeric G-protein complex from the receptor following Gα activation is sufficient for GRK/GPCR interaction (Palczewski *et al.*, 1991). In either case, GRKs phosphorylate key residues on the C-terminus of receptors. This leads to recruitment of β-arrestin 1 and/or 2 to the receptor (Peterson and Luttrell, 2017). This will either trigger receptor internalisation, leading to degredation of bound ligand followed by cycling back to the membrane, or receptor desensitisation; where β-arrestin remains bound to the receptor and inhibits subsequent signalling events. (summarised in figure 1.3.1). The mobilised Gβγ complex is also considered to be critical to instigating chemotaxis. Over-expression of Gβγ sequestering proteins was sufficient to abrogate chemotaxis to CXCL8 by HEK293 cells expressing it's receptor (Ourne, 1997). Additionally, singular rescue of

Gβ expression in the model organism *Dictyostelium discoideum,* restored the chemotactic phenotype of these cells, whereas similar rescue experiments with Gα subunits failed to do so (Janetopoulos, Jin and Devreotes, 2016).

1.3.2 Atypical chemokine receptors

In addition to the classic chemokine receptors, there are other chemokine binding receptors that are not involved in G-protein signalling. These are the atypical chemokine receptors (ACKRs), of which 4 have been identified thus far. Like the GPCRs, these atypical receptors have a 7TM structure but lack what is known as the DRYLAIV motif (Ulvmar, Hub and Rot, 2011). This is a conserved peptide sequence on the second intracellular loop of GPCRs that facilitates G-protein binding. As such they do not interact with G-proteins and are sometimes referred to as "silent" receptors. This may be something of a misnomer however, as ACKRs have been shown to associate with the β-arrestins, which can activate signalling cascades independently of G-protein activity such as the mitogen-activated protein kinase (MAPK) pathway (Peterson and Luttrell, 2017). However, ACKRs are instead thought to facilitate their immunomodulatory activates by scavenging of the chemokines they bind, thereby removing them from the local environment and sculpting the immune system as a result (Nibbs and Graham, 2013). Some ACKRs, like ACKR2, scavenge an extensive number of chemokines and can therefore have a broad impact on immune activity. The known ACKRs, and the chemokines they bind, are listed in table 1.2.1.

1.3.3 Chemokine/receptor interaction

As mentioned before, chemokine receptor (and indeed all GPCR) signalling results from structural changes in the receptor following binding to ligand. Chemokines are said to follow what is known as a 2-site binding model, dependent on the shared structural features of chemokines (Rajagopalan and Rajarathnam, 2006). In this model, the N-loop (the unstructured chain of amino acids that runs from the N-terminus to the first β-sheet) interacts with the N-terminus of the receptor. This interaction is believed to anchor the chemokine/receptor binding and denote receptor selectivity, as mutagenesis studies of CXCL10 (a cognate ligand of CXCR3) indicated that swapping the N-loop region of this chemokine with that of CXCL8 allowed it to interact with CXCRs 1&2 (Clark-Lewis *et al.*, 1994). The N-terminus of the chemokine then interacts with transmembrane domains of the receptor. It is believed that this interaction initiates signalling functions of the

receptor, as alteration of the N-terminus has previously been shown to mitigate function while having little effect on receptor binding of CCL5 (Proudfoot *et al.*, 1996).

While undoubtedly useful in assessing the relationship between chemokines and their receptors, the 2-site model may be something of an over-simplification. Recent work characterising the interactions of CXCL12/CXCR4 indicated that, while both monomeric and dimeric versions of CXCL12 could bind the receptor, monomeric CXCL12 bound a wider area of the receptor beyond what would be described in the traditional 2-site model (Ziarek *et al.*, 2017). The functional consequence of this was that monomeric CXCL12 was capable of triggering G-protein and β-arrestin recruitment by the receptor. However, dimeric CXCL12, which more closely followed a 2-site binding model, triggered recruitment of G-proteins alone by CXCR4. As well as providing insight into the structural requirements of full receptor activation, this study could also indicate that biased agonism may be dependent on structural differences in receptor/ligand binding. Signalling bias will be discussed in greater detail in subsequent sections.

Chemokine receptors, like many other proteins, also undergo additional post-translational modifications (PTMs). Some are critical to simply maintaining structure, for example the formation of disulfide bonds between cysteine residues of the extracellular portions of chemokine receptors is critical to receptor stability (Rummel *et al.*, 2013). Others however can affect chemokine/receptor interactions. For example, sulfation of tyrosine residues in the N-terminus of CCR5 has been shown to improve affinity of CCL3 and CCL4 for the receptor (Farzan *et al.*, 1999). In addition, chemokine receptors can carry large carbohydrate modifications. This is referred to as glycosylation and is known to occur on asparagine (N-linked) or serine/threonine residues (O-linked) of the receptor N-terminus (Szpakowska *et al.*, 2012). However, the exact impact of this PTM is not entirely clear, as many chemokine receptors show little impact on ligand binding or functional outcomes from deglycosylation, such is the case with CXCL12 binding to mutants of CXCR4 lacking N-terminal asparagine residues (Huskens *et al.*, 2007). However, glycans can be additionally decorated with other sugar groups, such as sialic acid, and the presence of sialic acid on O-linked glycans of CCR5 also improved CCL3 and CCL4 affinity (Bannert *et al.*, 2001). It is clear that the interaction between chemokine and receptor is highly complicated and can be influenced by a wide array of factors, and that a holistic understanding of chemokine binding as it relates to the biology of these molecules is still lacking. Like many GPCRs, chemokine receptor are frequently phosphorylated on their C-terminus, with selective deletion of serine and threonine residues, or complete ablation of the C-terminus, significantly attenuating receptor internalisation and desensitisation (Stone

et al., 2017). The chemokine receptor CXCR4 is also ubiquitinated (Marchese and Benovic, 2001), a PTM that serves to promote receptor degredation in lysosomes but has little effect on receptor internalisation. Finally, CCR5 is also modified by palmitoylation (Percherancier *et al.*, 2001), dependent on a cluster of three cysteine residues in the receptors C-terminus. Mutation of all three residues blocks receptor palmitoylation and impairs cell surface trafficking of the receptor.

1.3.4 Pharmacological targeting of the chemokine system

With extensive involvement in embryogenesis, the function of the immune system, in the development of cancer and spread of metastasis, and in the pathophysiology of various inflammatory conditions, the chemokine system is a demonstrably attractive target for therapeutic intervention. Indeed, targeting of GPCRs for therapeutic effect is a highly successful strategy. Case in point; at present around 34% of drugs approved for use by the US Food and Drug administration target GPCRs (Hauser *et al.*, 2017). As mentioned before, various viruses have evolved to exploit chemokine biology to their own advantage. The Kaposi's sarcoma associated virus encodes a highly promiscuous viral chemokine (vMIPII), while the human cytomegalovirus encodes a constitutively active chemokine receptor (US28), and in doing so each successfully sculpt the immune response to their advantage. So, manipulation of the chemokine system is clearly feasible and advantageous in a number of contexts, however at present there are very few widely available drugs that target chemokine receptors.

Interest in targeting the chemokine system arguably ramped up with the discovery that HIV utilised chemokine receptors to elicit cellular entry, namely CCR5 and CXCR4 (Berger, Murphy and Farber, 1999). Indeed, the observation that peoples of northern European descent that carried a natural mutation that effectively ablated CCR5 expression (known as Δ32 CCR5) were highly protected from HIV transmission confirmed the validity of targeting chemokine receptors in the treatment of the disease (Chatterjee *et al.*, 2012). Intensive research efforts lead to the development of maraviroc, a small molecule CCR5 antagonist that effectively blocked cellular entry of HIV, that is still used in HIV treatment (Tan *et al.*, 2013). HIV is known to switch receptor tropism from CCR5 to CXCR4 during the development of the disease. As such, efforts were made to develop antagonists of CXCR4 that would similarly inhibit viral entry (Hendrix *et al.*, 2004). While ultimately not useable in the treatment of HIV, the CXCR4 antagonist plerixafor did prove useful in the mobilisation of HSCs from the bone marrow into the circulation, where they could be collected for transplantation into immune-compatible recipients (Devine *et al.*,

2008). Additionally, there is mogamulizumab, a humanised monoclonal antibody against CCR4 (Yoshie and Matsushima, 2015). mogamulizumab was licensed for the treatment of relapsed ATLL in Japan in 2012 and is thought to initiate immune destruction of cells expressing CCR4 by relying on the same mechanisms as the humoral arm of the immune system. Side-effects have been noted with mogamulizumab treatment, presumably associated with non-specific destruction of CCR4 expressing cells. However as of August of 2018, it was approved for use by the U.S. food and drug administration, potentially indicating more widespread use of anti-CCR4 treatment in the near future.

These success stories however are very much the minority, and many more compounds targeting the chemokine system have been developed but never made it through clinical trials. This is particularly true of targeting inflammatory chemokine receptor signalling, as at present no compounds that target inflammatory chemokine receptors are licensed for use in inflammatory disease. Various antagonists of CCR1, 2 and 5 have been trailed in the treatment of RA for example, but ultimately failed to deliver improved patient outcomes (Horuk, 2009; Lebre *et al.*, 2011). This discrepancy between the great potential in targeting of the chemokine system, and the reality that to date no drugs targeting inflammatory chemokine signalling are available, could be attributable to a number of factors.

Chemokine signalling is highly sensitive, needing only a minor amount of ligand/receptor interaction to elicit physiological responses. As such a compound targeting chemokine receptors may require over 90% receptor coverage before achieving any effect in some cases (Dairaghi *et al.*, 2011). Small molecule inhibitors are well known to suffer from non-specific binding to protein and lipid in sera, and as such achieving this high dosing may prove difficult. As well, the previously noted complexity of shared receptors amongst the inflammatory chemokines, and the highly complex inflammatory environment established in diseases such as RA (Szekanecz *et al.*, 2006), can limit the effectiveness of targeting specific chemokine receptors. Further complicating the chemokine system is the observation of signalling bias by some chemokine receptors.

1.3.5 Biased agonism in chemokine biology

Biased agonism is an area of increasing focus in GPCR research, and stems from the understanding that, rather than simply adopting an “on” or “off” structural conformation, GPCRs can occupy multiple active states due to their dynamic nature in the membrane (Kenakin and Christopoulos, 2013). These different active states then recruit different repertoires of signalling partners (i.e. G-proteins and the β-arrestins) as a result. Active

states generally need to be stabilised by binding of ligand to receptor, and it is proposed that subtle structural differences in the ligand/receptor interface help to shape these different active conformations (Anderson, Solari and Pease, 2016). This is referred to as ligand bias and can be described as 2 or more ligands interacting with the same receptor, generating unique signalling profiles as a result that cannot be attributed to different ligand affinites. Further forms of bias have been described, such as receptor bias (where the same ligand generates a different signalling profile when binding different receptors), or tissue bias (where the signalling profile of the same ligand/receptor combination changes depending on the cellular context examined) (Jørgensen, Rosenkilde and Hjortø, 2018), however ligand bias will be the focus going forward.

Functional selectivity of ligands for certain GPCRs may be integral to their biology. The serotonin 5HT2A receptor activates Akt signalling pathways in response to serotonin but not N-methyltryptamines, a metabolite of serotonin (Schmid and Bohn, 2010). Treatment with either ligand causes head twitching behaviour in mice, however in β-arrestin 2 KO animals this behaviour is selectively lost with serotonin treatment, indicating the requirement of this signalling partner for the receptor's activity in response to serotonin. As well, the μ-opioid receptor has been demonstrated to selectively recruit β–arrestin 2 upon interaction with morphine but recruits both β-arrestin 1 and 2 in response to enkephalin (Groer *et al.*, 2011). Such examples could indicate that biased agonism functions as a means of fine-tuning signalling responses of certain GPCRs in complex environments.

Targeted activation or inhibition of one signalling pathway over another is an exciting prospect as it may provide more targeted therapies than are currently available with fewer side-effects. For example, the κ opioid receptor presents a promising target for treatment for pain management with selective agonists. The variable outcomes of signalling through this receptor are considered to be dependent on the recruitment of different signalling partners, with activation of the G-protein pathway resulting in the desired analgesic properties of receptor agonism, and activation of β-arrestin resulting in the undesirable side-effect of dysphoria (Zhou *et al.*, 2013). As such, a number of small molecule agonists that selectively activate G-proteins to the receptor have been developed (Zhou *et al.*, 2013; Lovell *et al.*, 2015). The angiotensin 2 type 1 receptor (AT1R) represents another potential target for pathway selective treatment. Signalling by angiotensin 2 through the receptor is both harmful and protective, with G-protein signalling considered to mediate the deleterious vasoconstrictive effects of angiotensin 2, and β-arrestin signalling mediating the beneficial inotropic effects of the ligand (Violin, Soergel and Lark, 2012).

Consequently, compounds that selectively inhibit G-protein signalling, but leave β-arrestin signalling pathways available, have already been evaluated in a model of heart failure (Violin *et al.*, 2010). Here they demonstrated improved physiological outcomes when compared with a pan-AT1R antagonist.

Biased agonism has been described with a number of chemokine receptors, namely CCRs 1, 2, 4, 5, 7 and 10, CXCR3 and ACKRs 2 and 3 (Anderson, Solari and Pease, 2016). Signalling bias can manifest itself with these receptors in a number of ways. For example, CCL5 appears more potent than either CCL3 or 4 in activating Ca^{2+} flux in cells expressing CCR5 (Oppermann *et al.*, 1999). This would indicate that CCL5 is dominant in receptor activation despite having similar receptor affinity to the other 2 chemokines. However, Ca^{2+} flux could be completely abrogated by PTX treatment for CCL5 and CCL4, but not CCL3 (Leach, Charlton and Strange, 2007). This could indicate that CCL3 can signal through CCR5 through Gi/o independent G-protein/receptor couplings. In addition, the chemokines binding CCR2 all display broad recruitment profiles of β-arrestin 1 and 2, with the exception of CCL13 which showed little capacity to initiate β-arrestin 1 recruitment by CCR2 (Berchiche *et al.*, 2011). CCL21 is capable of signalling through interactions with CCR7 via a pathway that is both G-protein and β-arrestin independent, whereas CCL19 does not. Here, oligomers of CCR7 allowed for receptor phosphorylation by Src kinase. This phosphorylation of CCR7 allowed CCL21 to signal through the SHP2 pathway and enhanced chemotaxis to the chemokine (Hauser *et al.*, 2016).

However, many GPCRs demonstrate a form of bias that is perhaps clearer-cut than these examples. The interaction of monomeric and dimeric CXCL12 with CXCR4 (as discussed previously in this chapter) demonstrated a form of signalling bias that resulted from effectively the same ligand. This was namely that one “ligand” was able to activate both G-protein and β-arrestin signalling by CXCR4 and was therefore balanced (monomeric CXCL12), whereas the other was biased toward G-protein signalling only (dimeric CXCL12). While it is interesting that oligomerisation state had this effect on CXCL12 activity, it does follow what in some respects is an archetypal form of bias. This being a receptor interacting with both balanced ligands, and with those biased towards G-protein signalling (summarised in figure 1.3.2). This has been demonstrated with a number of chemokine/receptor combinations, however is arguably most interesting when discussing CCRs 4, 7 and 10. Unlike the inflammatory chemokine receptors, which bind multiple chemokines and demonstrate significant cross-talk, or other homeostatic receptors, which often interact with a single chemokine, all 3 of these receptors interact with only a pair of ligands. These are CCL17 and 22 with CCR4, CCL19 and 21 with CCR7 and CCL27 and

28 with CCR10 (Mariani *et al.*, 2004; Rajagopal *et al.*, 2013; Corbisier *et al.*, 2015). Within each pairing it has been reported previously that one ligand is balanced (CCL22, CCL19 and CCL27), and the other is G-protein biased (CCL17, CCL21 and CCL28). The fact that such a model of biased agonism in ligand pairs has emerged on at least 3 separate occasions, and with receptors that demonstrate such distinct expression and functional profiles, could indicate an evolutionary advantage in forming a ligand pair with diverse signalling properties. As such further study of the signalling bias of these receptors is warranted.

1.4 CCR4 in health and disease

CCR4 emerged relatively recently in the evolution of the chemokine system, being found in reptiles along with the likes of CCR5 and CX_3CR1 (Nomiyama, Osada and Yoshie, 2011). In terms of its expression on mature cells of the immune system, CCR4 is considered the dominant chemokine receptor expressed by T-cells of the T-helper 2 (Th2) and regulatory T-cell (Treg) lineages (Bonecchi *et al.*, 1998; Hirahara *et al.*, 2006), and it is through these cells that most of the physiological effects of CCL17 and CCL22 are exerted. CCR4 expression has also been reported in cutaneous lymphocyte antigen positive (CLA+) T-cells, Th17 cells, Th22 cells, some subsets of natural killer (NK) cells and airway eosinophils as well (Yoshie and Matsushima, 2015). However, for simplicity's sake, the immune-developmental functions of CCR4 signalling and its roles in Th2 and Treg activity and associated pathology will be discussed here.

Both CCL17 and CCL22 are expressed in the thymus (Imai *et al.*, 1996; Godiska *et al.*, 1997), and their signalling through CCR4 is thought to be important in T-cell development. In essence, immature thymocytes undergo sequential expression of chemokine receptors during various stages of selection and development (Takahama, 2006). The cognate ligands of these receptors are expressed differentially by the thymic stroma, depending on the tissue microenvironment, and therefore guide developing thymocytes through the thymus. Immature thymocytes enter the cortex of the thymus, where they interact with stromal cells and travel through the thymic cortex in a CXCR4/CCR7 dependent manner . At this stage they express neither CD4 nor CD8 and are therefore referred to as double negative thymocytes (DNTs). Expression of CXCR4/CCR7 is down-regulated as CCR9 is upregulated, leading to migration of DNTs from the cortex to the subcapsular zone. Here they will undergo selection and either start to express CD4 and CD8, becoming double positive thymocytes (DPT), or will undergo apoptosis. DPTs that survive then undergo further differentiation and highly self-reactive DPTs undergo deletion at this time,

eventually becoming single positive (i.e. CD4+ or CD8+) thymocytes (SPTs). SPTs upregulate expression of CCR4 and CCR7 during differentiation (Cowan *et al.*, 2014), and expression of the ligands of these receptors by stromal cells of the thymic medulla draws these cells into this region to continue selection. In the medulla, SPTs are again exposed to self-antigens by medullary thymic epithelial cells (mTECs), and those SPTs that are auto-reactive are either destroyed or pushed into a regulatory phenotype. The ligands of CCR4, however, are predominantly produced by medullary thymic DCs in the thymus (Hu *et al.*, 2015). These cells help to discern auto-reactive SPTs by presenting self-antigens from all tissues of the body, serving to identify those auto-reactive SPTs that strongly bind self-antigen (which are destroyed), those which demonstrate no binding (which continue the differentiation programme) and those that demonstrate lower affinity binding (which can develop into Tregs). As such, CCR4 signalling appears critical in the process of immune education and the establishment of central tolerance. Those SPTs that do not react to self-antigen however can continue to develop and leave the thymic medulla and enter the circulation as naïve T-cells. This final egress from the thymus however is not thought to be mediated by upregulation of a chemokine receptor, but instead the Sphingosine-1-phosphate 1 receptor (S1P1R) (Matloubian *et al.*, 2004).

In this context, CCR4 signalling is homeostatic, but could be argued to serve a redundant function with CCR7 in recruitment of SPTs into the medulla. However, expression of CCR4 and CCR7 are temporally distinct, with CCR4 expression seen earlier in SPT development. Deletion of CCR7 does not completely block medullary entry of SPTs either, whereas PTX treatment does (Ehrlich *et al.*, 2009), indicating the involvement of other chemokine receptors in this process. In addition, genetic ablation of CCR4 results in the accumulation of self-reactive T-cells in secondary lymphoid organs (Hu *et al.*, 2015), such as the LNs, however it has no effect on the levels of Treg subtypes (Cowan *et al.*, 2014). This could indicate that CCR4 and CCR7 serve non-redundant functions in the development and maturation of T-cells and in the maintenance of central tolerance.

CCR4 expression is detectable during the earliest stages of in vitro differentiation of Th2 cells (Morimoto, 2005). In addition, generation of DCs from monocytes by treatment with granulocyte-macrophage colony stimulating factor (GM-CSF) (a common cytokine of both Th1 and Th2 cells) and Interleukin 4 IL-4 (a Th2 specific cytokine) enhanced the production of CCL17 by these cells (Imai *et al.*, 1999). This would indicate that skewed differentiation conditions can alter the chemokine production of antigen presenting cells (APCs), and therefore the kind of T-cells they can attract with them. Th2 driven immune responses are also generally associated with allergic reactions. Indeed, nasal antigen

challenge resulted in an increased number of CCR4+ T-cells found in biopsies taken from patients suffering from allergic rhinitis compared to healthy controls, and allergen challenge in the lungs of asthma sufferers was shown to increase the levels of CCR4 ligands (Banfield *et al.*, 2010). Additionally, blockade of CCR4 activity using small molecule antagonists has demonstrated some protective effects in mouse models of allergic asthma (Y. Zhang *et al.*, 2017). As such, it appears that pharmacological intervention with CCR4 antagonists could be effective in the treatment of some allergic pathologies and would presumably exert their effects through attenuating Th2 recruitment.

However, such a treatment strategy would need to account for the noted expression of CCR4 on Treg cells. Loss of CCR4 expression by Tregs reduces their prevalence in the skin and lungs of mice, and can exaggerate the immune response to antigen challenge, resulting in an increase in lymphocytic infiltration in these tissues (Sather *et al.*, 2007). In addition, recruitment of tolerising Tregs into cardiac allografts in mice has been demonstrated to be CCR4 dependent (Lee *et al.*, 2005). However, the activity of Tregs can be pathogenic in a number of contexts. Tregs are frequently recruited into the tumour microenvironment, where their immunomodulatory activities are exploited to sculpt the immune response to the developing tumour (Ondondo *et al.*, 2013). They are recruited, in part, by the expression of CCL17 and/or CCL22 by tumour cells themselves or infiltrating innate immune cells (Mizukami, 2008; Maolake *et al.*, 2016). Tregs can be selectively recruited and activated in primary breast cancers for example in a CCL22 dependent manner (Gobert *et al.*, 2009), and the presence of CCR4+ Tregs often correlates with a poorer prognosis for patients in the diagnosis of multiple different cancers (Curiel *et al.*, 2004; Watanabe *et al.*, 2010; Svensson *et al.*, 2012).

As stated previously, CCR4 is one of the few chemokine receptors that is successfully targeted for therapeutic effect, and the humanised anti-CCR4 antibody mogamulizumab has been licensed for the treatment of relapsed and chemotherapy resistant ATLL in Japan for many years now (Makita and Tobinai, 2017). CCR4 expression is frequently high in ATLL cells, leading to the notion that these cancers are derived from cells of either the Th2 or Treg lineage (Yoshie *et al.*, 2002). This is in keeping with the frequency with which ATLL lesions form in the skin, as the expression of the ligands of CCR4 is frequently associated with the skin, hence the strong correlation of CCR4 expression in skin-tropic T-cells (Soler *et al.*, 2003; Yoshie and Matsushima, 2015). FOXP3 is a transcription factor critical to Tregs, and its expression is also frequently elevated in ATLL (Karube *et al.*, 2004), which could indicate that Tregs are the most likely source. However, infection of T-cells with Human T-lymphotropic virus 1 (HTLV-1) is a frequent event in ATLL

pathogenesis (Malpica *et al.*, 2018), and has been shown to elevate expression of FOXP3 (Miyazato and Matsuoka, 2014). It might therefore be hasty to attribute ATLL solely to Treg cells. As well as being used in the treatment of ATLL, mogamulizumab has also been considered as an adjuvant to targeted vaccination with tumour antigens, with enhanced induction of antigen specific responses in vitro from peripheral blood mononuclear cells (PBMCs) of melanoma patients following Treg depletion (Sugiyama *et al.*, 2013). In addition, a small molecule antagonist of CCR4 was also successfully evaluated as an adjuvant to immunotherapy in mouse models of cancer, with an increased production of antigen specific CD8+ T-cells resulting from anti-CCR4 treatment (Pere *et al.*, 2011).

Although targeting of CCR4 has been successful, particularly in treatment of ATLL, there have been complications associated with depletion of Treg cells, including at least one fatality (Ishida *et al.*, 2013). Given the observation of bias of CCR4 ligands (Mariani *et al.*, 2004), as well as a noted distinct conformation of the receptor that can only bind CCL22 (Viney *et al.*, 2014a), it may be possible to more selectively target CCR4 in the future. As such, further characterisation of CCR4, its ligands and their biased agonism, is of interest.

1.5 CCR7 in health and disease

CCR7 is more evolutionarily ancient than CCR4, first emerging in jawed, bony vertebrates (Nomiyama, Osada and Yoshie, 2011). As stated previously, CCR7 demonstrates a number of roles in the maturation of lymphoid cells in the thymus, helping to aid navigation through the thymus at various stages of development (as discussed previously). It is also potentially involved in the initial migration into the thymus of T-cell precursors in a CCL21 dependent manner. CCR7 and its ligands also act in the development of SLOs as well, as the genetic deletion of CCR7, or loss of CCR7 ligands in the plt/plt mouse line, results in significantly reduced LN size, and a loss in demarcation between microanatomical regions (Förster *et al.*, 1999; Gunn *et al.*, 1999). CCR7 does appear to share this function with another homeostatic chemokine axis, that of CXCR5/CXCL13, as a double KO of these receptors results in greater disruption to healthy LN development than either single KO (Ohl *et al.*, 2003).

While the developmental functions of CCR7 and its ligands are obviously important, with its genetic ablation resulting in significant loss of naïve T-cell development in the thymus (Cowan *et al.*, 2014), the functions of CCR7 are arguably best described in their role in adaptive immunity. Following maturation, naïve T-cells express CCR7 and use the receptor to survey SLOs throughout the body, and genetic ablation of CCR7 results in near

complete loss of naive T-cell in LNs and generally altered tissue distribution (Förster *et al.*, 1999). B-cells also use CCR7 signalling to navigate to, and within, LNs (Park *et al.*, 2012), however they do not display as severely altered tissue distribution as naïve T-cells in KO animals. DCs express CCR7 upon encountering antigen and undergoing maturation (Sallusto *et al.*, 1998). In the skin mature DCs migrate in response to functional gradients of CCL21 into afferent lymphatics vessels to reach the LN (Weber *et al.*, 2013), where they can interact with naïve T-cells that possess a compatible T-cell receptor to the antigen the DCs are presenting. In addition, CCR7 is expressed on central memory T-cells (Tcm) but not effector memory T-cells (Tem), as the former survey SLOs in case of encounter with their corresponding antigen again whereas the latter do not enter SLOs (Sallusto *et al.*, 2014). Interestingly, in addition to CCR4 expression, CCR7 expression has also been demonstrated on Tregs, and is a requirement for their regulatory effects in the LNs (Schneider *et al.*, 2007). It is clear therefore that CCR7 signalling is critical in the functions of nearly all aspects of the adaptive immune system at some stage and a fundamental link between the innate and adaptive immune systems.

Within LNs, CCR7 intricately co-ordinates the movement of cells to facilitate antigen presentation. Naive T-cells and Tcms enter the LN via the high endothelial venules (HEVs), and are drawn to the T-cell zone via expression of CCL19 and CCL21 by the fibroblastic reticular cells which also produce IL-7, a critical cytokine in naïve T-cell survival (Link *et al.*, 2007). B-cells, conversely, migrate to the B-cell follicles in response to CXCL13/CXCR5 signalling. Within the T-cell zone, naïve T-cells remain very motile so as to increase the probability of encountering their cognate antigen. This has been shown to be CCR7 dependent, as T-cells from CCR7 KO mice demonstrate decreased motility in wildtype (WT) LNs, and WT T-cells demonstrate decreased motility in the LNs of plt/plt mice (Worbs *et al.*, 2007). Residence of naïve T-cells in the T-cell zone is determined by a balance between CCR7 and S1P1R (Comerford *et al.*, 2013), as constant signalling through CCR7 is thought to not only desensitise the receptor, but also promote expression of S1P1R by the cells and subsequent egress from the LN (Shannon *et al.*, 2012). DCs enter the LN via a slightly different route: they migrate into afferent lymphatics in a CCL21 dependent manner and then drain into the subcapsular sinus of the LN. From here they follow gradients of CCR7 ligands, maintained by the atypical chemokine receptor ACKR4, to the paracortical area of the LN (Ulvmar *et al.*, 2014). Here they can present antigen to naïve and central memory T-cells. DCs themselves can also express CCL19 in order to attract naïve T-cells in the LN (Katou *et al.*, 2003).

Due to its extensive functions in the immune system, aberrant CCR7 activity can cause considerable harmful effects. TLOs form in areas of persistent inflammatory insult, and CCR7 KO animals spontaneously form TLOs in mucosal tissues (Davalos-Misslitz *et al.*, 2007). However, CCR7 KO animals are also protected from further TLO formation in the joint synovia during models RA (Wengner *et al.*, 2007). Over-expression of CCL21 has been shown to enhance the formation of TLOs in various tissues, including the liver (Grant *et al.*, 2002). This disparity between a damaging phenotype at rest and protective phenotype during inflammation is most likely attributable to developmental defects in the T-cell compartment that promote an autoimmune environment in peripheral tissues at rest. As stated earlier, CCR7 expression by tumours is frequently associated with metastasis of various cancers to the LNs, and consequently poorer prognosis for patients (Dai *et al.*, 2017; Xiong *et al.*, 2017). As well as directing cancerous cells to the LNs, CCR7 signalling has also been shown to directly enhance epithelial to mesenchymal transition (EMT) of tumour cells (Li *et al.*, 2016; Xu *et al.*, 2017; Zhong *et al.*, 2017), a critical step in establishing an invasive and migratory phenotype. CCR7 has demonstrated other additional effects in cancer, as its inhibition has been shown to encourage apoptosis and supress growth in cancer cells (Chi *et al.*, 2015; L. Zhang *et al.*, 2017). CCR7 may also be involved in tumour remodelling, as CCR7 over-expression induced vascular endothelial growth factor D (VEGF-D) in non-small cell lung cancer cells in vitro, and CCR7 expression correlates with VEGF-D in vivo (Sun *et al.*, 2015). Consequently, there is a constant drive to better understand the biological and pathophysiological functions of CCR7.

1.6 CCR10 in health and disease

Like CCR7, CCR10 first emerged in in jawed, bony vertebrates (Nomiyama, Osada and Yoshie, 2011), and interacts with 2 ligands; CCL27 and CCL28 (Morales *et al.*, 1999; Wang *et al.*, 2000). Unlike the ligands of CCRs 4 and 7, CCL27 and CCL28 display significant differences in their tissue localisation at rest, with CCL27 expressed almost exclusively by epidermal keratinocytes in the skin (Homey *et al.*, 2000), and CCL28 expressed by the epithelium of various mucosal tissues (Pan *et al.*, 2000), where it additionally acts directly as an anti-microbial agent (Hieshima *et al.*, 2003). CCR10 expression has been reported on a wide variety of cell types (Xiong *et al.*, 2012), however broadly speaking CCR10 expressing cells can grouped as; skin-tropic subtypes of various T-cell lineages including Th22 cells, δγ T-cells, Tem and Treg cells (Eyerich *et al.*, 2009; Jin *et al.*, 2010; Xia *et al.*, 2014), IgA producing B-cells of the mucosal epithelia (Morteau *et al.*, 2008) and skin-homing mesenchymal stem cells (MSCs) (Alexeev *et al.*, 2013). In

this respect, it is clear that CCR10 and its ligands are critical in the maintenance of immune homeostasis of barrier tissues.

In the skin the functions of CCR10 appear to be both distinct from, and overlapping with, those of CCR4, depending on the study. For example, in one instance expression of CCL27 could be induced by the application inflammatory cytokines, and direct injection of CCL27 recruited lymphocytes to the skin whereas antibody neutralisation of the chemokine attenuated recruitment following inflammatory insult (Homey *et al.*, 2002). Conversely, other studies have demonstrated through adoptive transfer experiments that CCL27 neutralisation had little effect on WT CD4+ T-cell infiltration into inflamed skin, with effects of CCL27 neutralisation only noted when CCR4 KO T-cells were analysed (Reiss *et al.*, 2001). In another study, neutralisation of both CCR4 and CCR10 ligands demonstrated a cumulative protective effect in multiple models of inflammation compared with targeting either receptor individually (Mirshahpanah *et al.*, 2008). This discrepancy between studies is concerning, however, CCR4/CCR10 co-expression has been demonstrated on the T-cell infiltrate of atopic dermatitis lesions, but not in psoriatic lesions, where CCR10 expression alone is observed (Vestergaard *et al.*, 2003). This could indicate that the requirements of CCR4 and CCR10 are disease, and context, specific.

The role of CCL28/CCR10 in the biology of IgA plasmablasts is arguably more consistent. Immunisation via mucosal tissues increased the prevalence of antigen-specific IgA producing B-cells compared to the more traditional route, and that migration of these cells into mucosal tissues could be blocked by the administration of CCL28 neutralising antibodies (Cha *et al.*, 2011). Additionally, the inclusion of CCL27 expression elements in the delivery of a plasmid-based vaccine against HIV increased the prevalence of antigen specific IgA plasmablasts in multiple tissues of mice, and increased IgA antibody titre in bronchiolar lavage from macaques (Kraynyak *et al.*, 2010). Similarly, co-delivery of a CCL28 expression vector and HIV virus like particles (VLP) demonstrated an increase in antigen specific humoral responses compared with no chemokine or CCL19/HIV-VLP controls (Rainone *et al.*, 2011). Collectively, such studies indicate a critical role for CCR10 in IgA plasmablast function, and are in agreement with the assessment of CCR10 KO animals which demonstrate an absence of such cells in some mucosal tissues (Morteau *et al.*, 2008).

As might be expected, CCR10 expression is frequently upregulated in a number of skin associated T-cell lymphomas in a similar manner to CCR4 (Yoshie *et al.*, 2002; Notohamiprodjo *et al.*, 2005; Fujita *et al.*, 2006). CCR10 overexpression was also

observed in human cutaneous melanoma and glioblastoma samples, and correlated with a poorer prognosis for patients (Kühnelt-Leddihn *et al.*, 2012; Chen *et al.*, 2014). Additionally, like CCR7, CCR10 signalling can directly promote a more aggressive phenotype in breast cancer cells (Lin *et al.*, 2017). Given its extensive roles in barrier immunity, and frequent association with cancer, CCR10 biology represents an area of increasing research interest.

1.7 Aims of the project

The work described herein was intended to assess the bias presented by CCRs 4, 7 and 10 in unprecedented detail. To this end, 3 main strategies were followed with the following goals;

1: Unnatural amino acids (UAA), integrated in place of individual residues of CCR7, were used in an attempt to covalently capture either CCL19 and CCL21. This was done as this technology had been used previously to determine the binding pocket of a peptide ligand with its cognate GPCR (Coin et al., 2013), so may have been of use in determining the binding interface of CCL19 and CCL21. It was hoped that such a map would indicate subtle differences in receptor/ligand interaction between the 2 chemokines, and consequently reveal a structural basis for their observed selective functions.

2: Recruitment of signalling apparatus (Gi proteins and the β-arrestins) by CCRs 4, 7 and 10 in response to their respective ligands was assessed utilising bioluminescence resonance energy transferred (BRET) based methods. It was hoped that, using such methods, it would be possible to build a signalling profile of these receptors in previously undescribed detail (for CCR4 and CCR10).

3: Finally, recent publications indicated that polysialylation of CCR7 was critical to CCL21 instigated migration, and that in its absence CCR7 expressing cells were almost completely refractory to CCL21 (Kiermaier *et al.*, 2016). Observations made during the course of these studies indicated that CCR7 expressed in HEK293T cells may be similarly refractory to CCL21. As such, assessment was made of ST8sia4 expression (a polysialyltransferase required for CCR7 polysialylation) in HEK293T, and the role this restricted PTM may have in signalling behaviour of CCR7 ligands was evaluated. Potential polysialylation of CCR4 and CCR10 was also assessed.

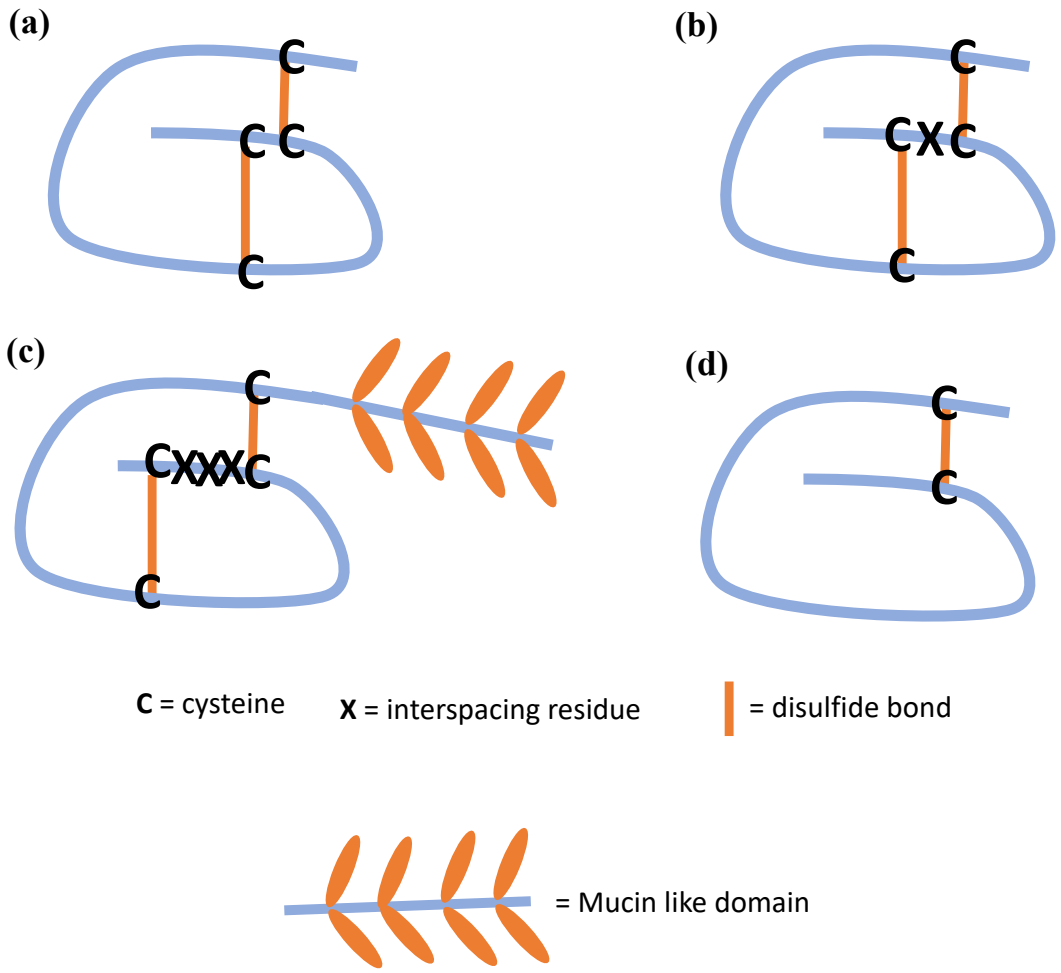

Figure 1.2.1 Schematic representation of chemokines

Representations of chemokines of the (a) CC, (b) CXC, (c) CX3C and (d) XC subfamilies are shown

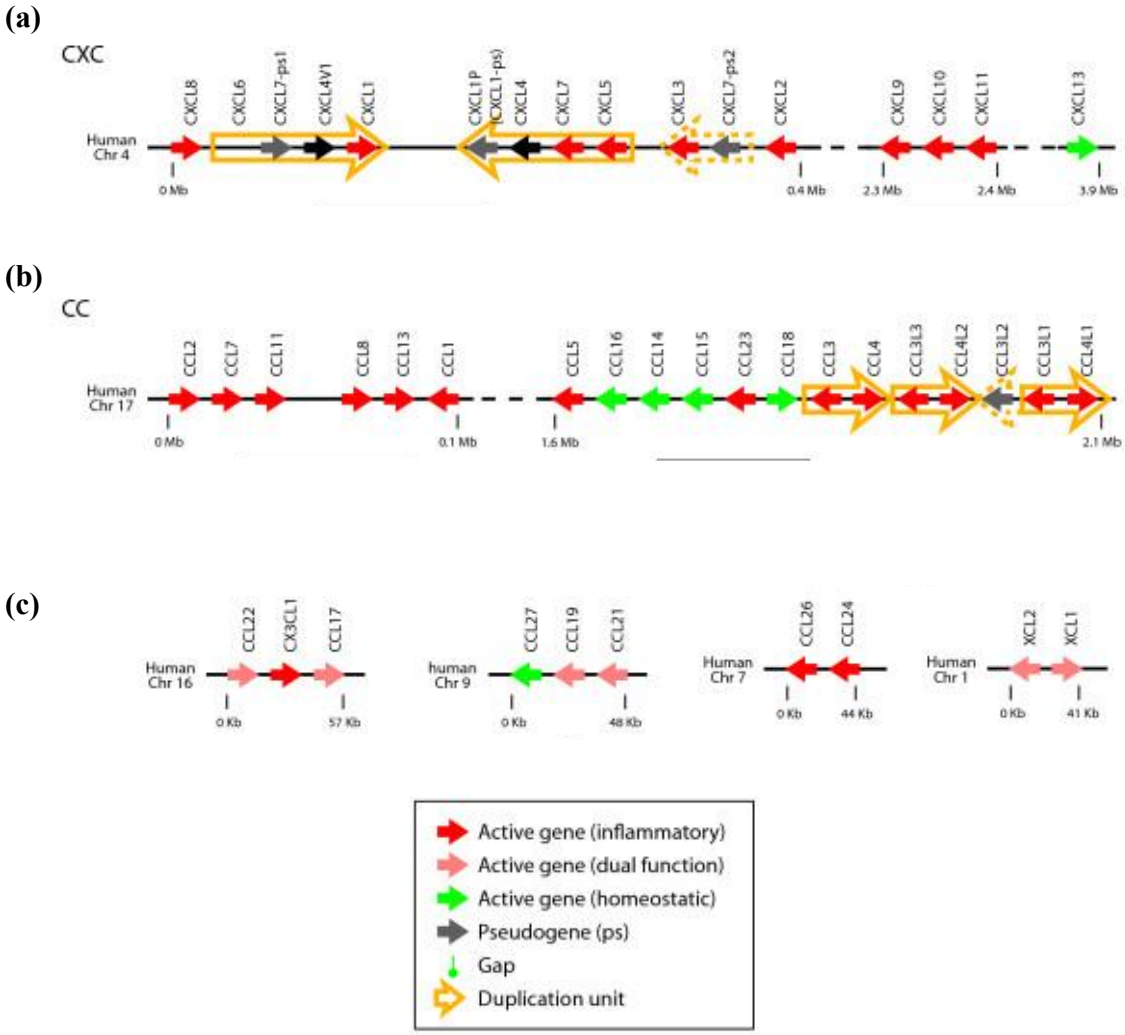

Figure 1.2.2 Genomic loci of chemokine gene clusters

The genomic loci of the major (a) CXC, (b) CC, and (c) minor gene clusters for human chemokines are shown. Adapted from Zlotnik, Yoshie and Nomiyama, 2006.

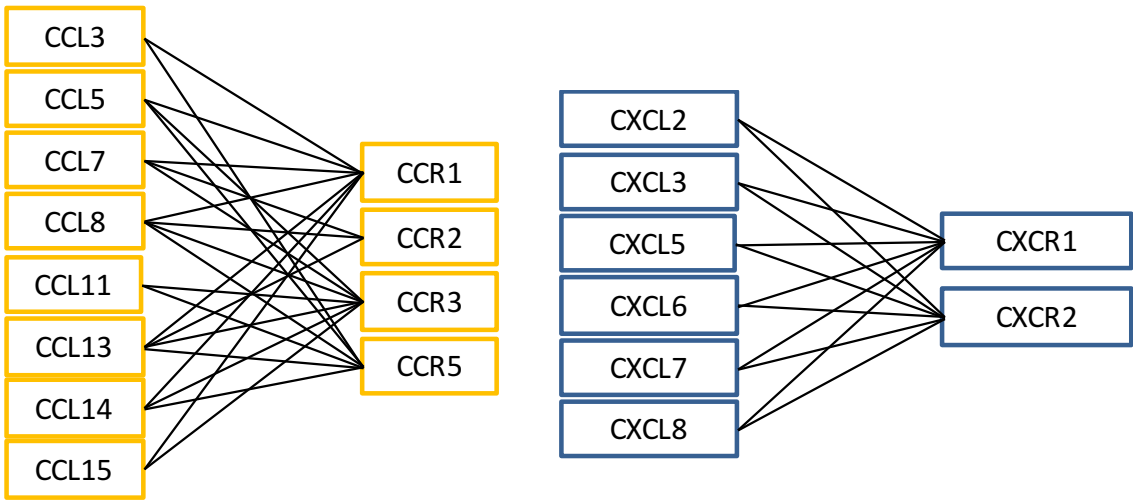

Figure 1.2.3 Inflammatory chemokine/receptor cross-talk

Inflammatory chemokines and their receptors demonstrate considerable promiscuity.

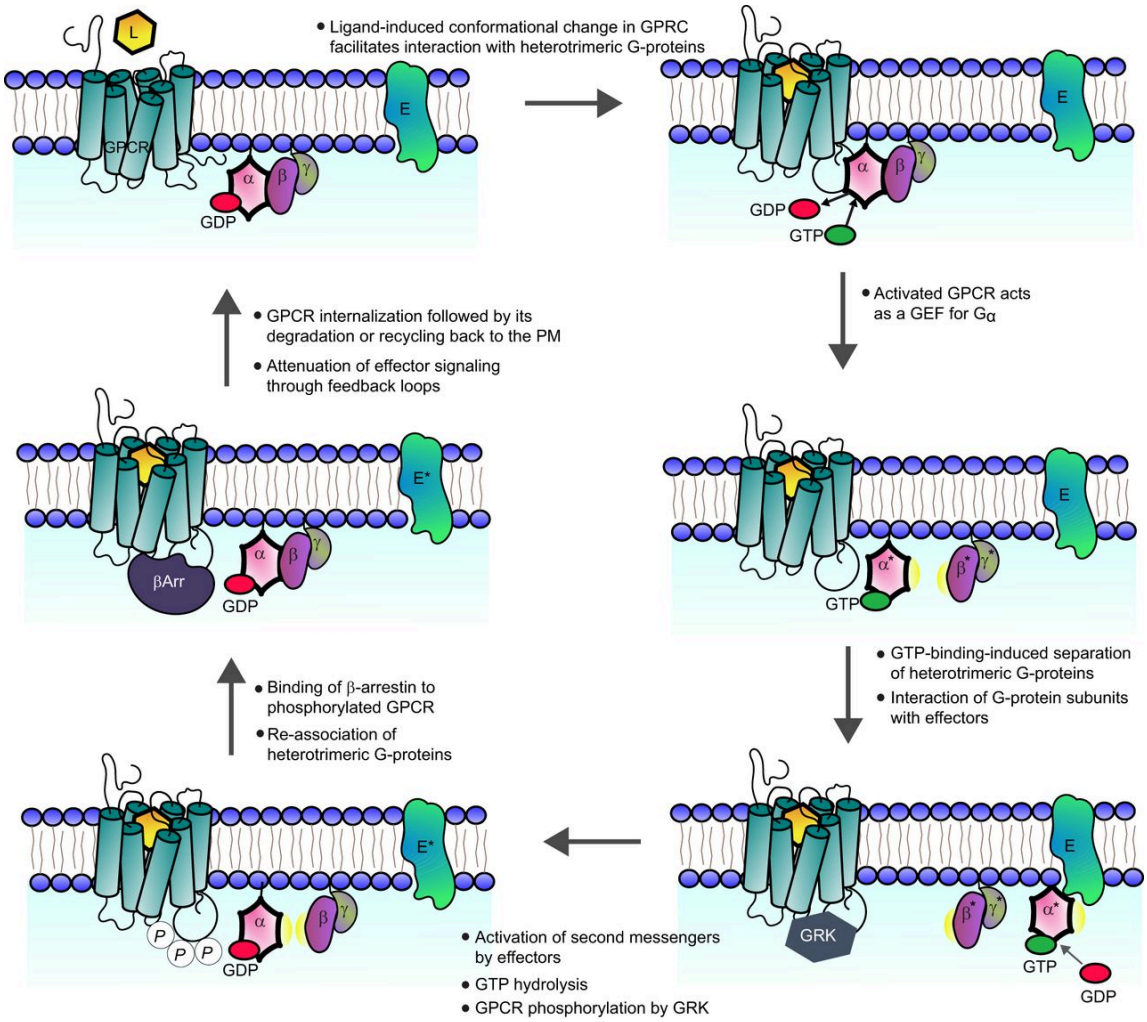

Figure 1.3.1 Signalling events during GPCR activation

Schematic representation of the sequential recruitment of signalling machinery following ligand/GPCR interaction. In brief, association of ligand and receptor initiates GDP/GTP transfer on Gα subunits, causing it to disassociate from the heterotrimeric G-protein complex. This frees Gα to initiate secondary messenger signalling events and allows for receptor phosphorylation by GRKs. The phosphorylated receptor then recruits β-arrestin, triggering receptor internalisation, ligand degradation and/or receptor desensitisation. The now inactive receptor traffics back to the cell surface, available to interact with ligand again. Adapted from Hanlon and Andrew, 2015.

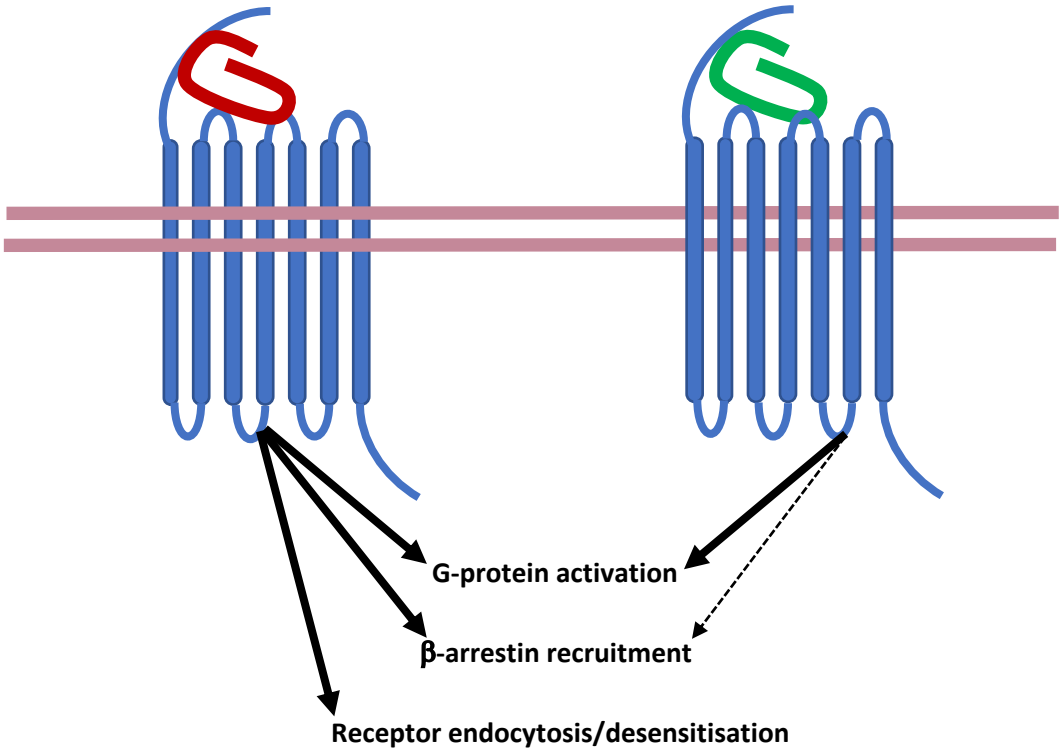

Figure 1.3.2 Basic representation of biased agonism of chemokine receptors

Biased agonism, refers to the ability of distinct ligands to activate different signalling pathways from the same receptor. Frequently, this manifests as one or more ligands being balanced, i.e. able to recruit G-proteins and β-arrestin and able to trigger receptor internalisation and desensitisation, and another which signals predominantly or entirely through G-protein coupling and does not desensitise or internalise the receptor.

Receptor:	*Chemokines*
CXCR Subfamily	
CXCR1	CXCL6, CXCL7, CXCL8, acPGP
CXCR2	CXCL1, CXCL2, CXCL3, CXCL5, CXCL6, CXCL7, CXCL8, acPGP, MIF
CXCR3	CXCL4 (CXCR3-B), CXCL9, CXCL10, CXCL11, CXCL13, CCL21 (mouse)
CXCR4	CXCL12, MIF, ubiquitin
CXCR5	CXCL13
CXCR6	CXCL16
CCR Subfamily	
CCR1	CCL3, CCL3L1, CCL5, CCL7, CCL8, CCL13, CCL14, CCL15, CCL16, CCL23
CCR2	CCL2, CCL7, CCL8, CCL13, CCL16, β-defensin 2,3
CCR3	CCL3L1, CCL5, CCL7, CCL11, CCL13, CCL14, CCL15, CCL24, CCL26, CCL28
CCR4	CCL17, CCL22
CCR5	CCL3, CCL3L1, CCL4, CCL4L1, CCL5, CCL8, CCL11, CCL16
CCR6	CCL20, β-defensin-2
CCR7	CCL19, CCL21
CCR8	CCL1, CCL18
CCR9	CCL25
CCR10	CCL27, CCL28
XCR Subfamily	
XCR1	XCL1, XCL2
CX3CR Subfamily	
CX3CR1	CX3CL1, CCL26 (human)
Atypical (Nonchemotactic, Recycling or Scavenger Receptors)	
ACKR1	CXCL1, CXCL2, CXCL3, CXCL7, CXCL8, CCL2, CCL5, CCL11, CCL13, CCL14, CCL17
ACKR2	CCL2, CCL3, CCL3L1, CCL4, CCL4L1, CCL5, CCL7, CCL8, CCL11, CCL12, CCL13, CCL14, CCL17, CCL22, CCL23, CCL24
ACKR3	CXCL11, CXCL12
ACKR4	CCL19, CCL21, CCL25, CXCL13
ACKR5	CCL19, chemerin

Table 1.2.1 Human chemokines receptors and the chemokines they bind

Table listing all chemokines receptors identified in humans to date and their cognate ligands. Generated with data from Zlotnik and Yoshie, 2012.

2 Materials and Methods

2.1 RNA extraction and cDNA conversion

The methods employed in RNA extraction varied depending in the biological source. For all extractions from cellular suspension (from cell lines or PBMCs), up to $1x10^7$ cells were washed x1 in Dulbecco's phosphate buffered saline, calcium and magnesium free (DPBS, Invitrogen), then disrupted in 350 µl buffer RLT (Qiagen RNeasy mini kit) supplemented with 1% v/v β-mercaptoethanol. Disrupted cells were passed through a 25-gauge needle 5 times to shear genomic DNA. From here, the Qiagen RNeasy mini kit was utilised in accordance with manufacturer's instructions, with the inclusion of an additional on-column DNA digestion step (RNase free DNase Set, Qiagen). RNA was eluted in 30 µl nuclease free water (Qiagen). RNA/DNA concentration was quantified using the Nanodrop 1000 spectrophotometer (ThermoFisher Scientific).

For RNA extraction from tissues, tissue was initially fixed in RNAlater (ThermoFisher Scientific) overnight at 4 ºC, then transferred to a 2 ml RNase/DNase free reaction tube with 2x 5 mm stainless steel balls and 1 ml Qiazol lysis reagent (Qiagen). Tissue was homogenised for 15 minutes using the TissueLyser LT (Qiagen), then left to rest at room temperature for 5 minutes before adding 200 µl chloroform. This was spun at 12000 g for 15 minutes at 4 ºC, and cleared supernatant transferred to a RNeasy mini kit column. From here the manufacturer's instructions were followed as before. In either case purified RNA was either kept on ice or stored at -80 ºC.

RNA was converted to cDNA through the use of the High-Capacity RNA-to-cDNA kit, in accordance with manufacturer's instructions (Applied Biosystems). Either 500 ng or 1 µg RNA was converted and diluted either 1/5 or 1/10 respectively for downstream use.

2.2 PCR, DNA digest and purification

2.2.1 PCR

Primers for the amplification of genes of interest (GOI) were designed to include compatible restriction sites for plasmid ligation and/or epitope tags. All primers designed and used for the work described herein were manufactured by Integrated DNA Technologies and are listed in table 2.2.1. Q5 high fidelity polymerase (New England Biosciences/NEB) was utilised in all PCR reactions unless otherwise stated. 25 µl PCR

reactions were prepared as follows; 5X Q5 Reaction Buffer 5 µl, 10 mM dNTPs 0.5 µl, 10 µM Forward Primer 1.25 µl, 10 µM Reverse Primer 1.25 µl, template DNA 1 µl, Q5 High-Fidelity DNA Polymerase 0.25 µl, 5X Q5 High GC Enhancer 5 µl and Nuclease-Free Water 10.75 µl. PCR reaction was performed in 200 µl flat lid PCR tubes (StarLab) using a Veriti 96-well thermocycler (Applied Biosciences) using the following programme;

STEP	TEMP	TIME
Initial Denaturation	98°C	30 seconds
35 Cycles	98°C	10 seconds
	*50–72°C	15 seconds
	72°C	30 seconds/kb
Final Extension	72°C	2 minutes
Hold	4°C	

* the annealing temperature was primer specific and calculated using the NEB Tm calculator, http://tmcalculator.neb.com/#!/main

PCR products were visualised on gels prepared with Ultra-pure agarose (Invitrogen) supplemented with 0.5 µg/ml ethidium bromide. Percentage agarose used was dependent on the fragment size to be visualised, but generally followed the following; <500 base pair (bp) = 2% w/v, 0.5-2.5 kilo bp (kb) = 1-1.5% w/v, >2.5 kb = 0.75% w/v. Product size was determined by the use of a DNA ladder (1 kb or 100 bp ladder depending on target size, Promega). Prior to loading of DNA, samples were mixed with an appropriate volume of loading buffer (6x blue/orange loading dye, supplied with DNA ladders). Agarose was dissolved in 1x Tris-acetate-EDTA (TAE) buffer (Tris-acetate 40 mM, EDTA 0.05 M), and ethidium bromide added once the agarose/TAE mix had sufficiently cooled. This was then poured into pre-made casters and allowed to set. DNA samples were run (in 1x TAE buffer) by gel electrophoresis, at constant 100 volts (V). DNA was visualised by UV transillumination using the Alpha Innotech gel dock. Where required, PCR products were purified using the Qiaquick PCR purification kit in accordance with manufacturer's instructions (Qiagen), and DNA eluted in 30 µl nuclease free water.

2.2.2 DNA digests

Digests were performed using restriction enzymes purchased from NEB. Where available high fidelity (HF) versions of these enzymes were used. The quantity of DNA and the specific enzyme used varied dependent on the requirements of individual experiments (relative figures are annotated with the restriction enzymes used). In general, 25 µl digest reactions were prepared as follows; 2.5 µl 10x cutsmart buffer, 0.5-1 µg DNA, 0.5 µl of

each restriction enzyme and nuclease free water up to 25 µl. These reactions were incubated at 37 ºC unless otherwise stated, and from 1 hour to overnight. Digest products were visualised in the same manner as described for PCR products.

2.3 Cloning and sub-cloning, mutagenesis programme, bacterial transformation and culture, and plasmid purification

2.3.1 Cloning and sub-cloning

Plasmids were prepared from either newly amplified GOI or digested products from pre-existing plasmids. Where a digest included the plasmid backbone, 1 µl of calf intestinal alkaline phosphatase was added (NEB) and sample incubated for a further 30 minutes at 37 ºC to prevent spontaneous ligation. Following digestion, reactions were run on 0.75% agarose gels as described above. Digested bands were excised from the gel, and DNA purified utilising the QIAquick gel extraction kit (Qiagen) in accordance with manufacturer's instructions. Purified DNA was eluted in 30 µl nuclease free water. Ligation of inserts into plasmid backbones was performed utilising T4 DNA ligase (Promega), with a 3:1 molar excess of insert to plasmid being employed in all such reactions. Ligation reactions were prepared as follows; 1 µl 10x ligase buffer, 100 ng plasmid DNA, 3x molar excess insert DNA, 0.5 µl T4 DNA ligase, and nuclease free water up to a total volume of 10 µl. Reactions were incubated overnight at 4 ºC. 5 µl of this reaction was used in subsequent transformations. All new plasmids were prepared in this manner, with the exception of tR4-8.3 and TAG substitution mutants of CCR7.

The specific strategy employed in generating tR4-8.3 is discussed in chapter 3 of this thesis (figure 3.2.8), however in brief pAcBac2.tR4-OMeYRS/GFP* (a gift from Peter Schultz, Addgene plasmid # 50831 (Chatterjee *et al.*, 2013)), was digested with SfiI and NotI-HF. Due to the different temperature requirements of these enzymes digest was carried out initially at 37 ºC for 1 hour then 50 ºC for a further hour. The target fragment featured incompatible overhanging ends for ligation, so the reaction was subsequently treated with DNA Polymerase I, Large (Klenow) Fragment (NEB), with 0.5 µl each of dNTP and Klenow added to the reaction before incubation at 37 ºC for a further 30 minutes. This reaction was run out on a gel and target fragment extracted and purified as before. Ligation reaction was performed as before with the omission of additional insert DNA, and 5 µl used in subsequent transformation experiments.

2.3.2 Generation of CCR7 TAG substitution mutants

All TAG substitution mutant plasmids were generated using the GeneArt Site Directed Mutagenesis System (Invitrogen). The TAG stop codon was introduced in place of the codon corresponding to residues of interest, in accordance with the methodology set out for UAA integration previously (Coin *et al.*, 2013). All mutagenesis primer pairs followed the same design principle; with 100% complementarity to each other and the mutation in the exact middle, flanked by 15-18 nucleotides either side. These are listed in table 2.2.1. PCR reactions were prepared as follows;

10X AccuPrime Pfx Reaction buffer	2.5 µl
10X Enhancer	2.5 µl
Primer mix (10 µM each)	0.75 µl
WT CCR7 plasmid template (20 ng/µl)	0.5 µl
DNA Methylase	0.5 µl
25x SAM*	1 µl
AccuPrime Pfx	0.2 µl
PCR water	17 µl

*25x SAM was prepared as a fresh dilution of 200x SAM, provided in the kit

This kit utilises a single PCR programme that initially methylates the original template plasmid before generating linear fragments of the whole plasmid including the desired mutation. This allows for the template to be selectively degraded following bacterial transformation due to the expression of McrBC endonuclease by the strain used (One Shot MAX Efficiency DH5α-T1R Competent Cells, Invitrogen). PCR was performed according to the following programme:

STEP	**TEMP**	**TIME**
Template methylation	37°C	20 minutes
Methylase heat inactivation/initial denaturation	94°C	2 minutes
18 cycles	94°C	20 seconds
	57°C	30 seconds
	68°C	3.5 minutes
Final Extension	68°C	5 minutes
Hold	4°C	indefinitely

The linear PCR product generated by this reaction then underwent *in vitro* recombination to create a new plasmid. The recombination product was prepared as follows; 2 µl 5x

reaction buffer, 2 µl PCR product, 1 µl 10 x Enzymer mix and 5 µl nuclease free water. This was incubated at room temperature for 10 minutes before recombination reaction was halted by the addition of 0.5 µl EDTA, and 2 µl of the reaction used in subsequent transformations.

2.3.3 Bacterial culture and transformation

One Shot MAX Efficiency DH5α-T1R Competent Cells were used in all transformation experiments, and aseptic technique was employed throughout all preparative and experimental procedures. Both Luria-Bertani (LB) Broth and LB agar were prepared in-house and sterilised by core facility staff. LB agar was melted, allowed to cool before the addition of selection antibiotics, and poured into 90 mm petri dishes (Fisher Scientific). Once set, agar plates were stored inverted at 4 ºC until required. Ampicillin stock was created from Ampicillin sodium salt (Sigma-Aldrich) and reconstituted at 50 mg/ml in 50% ethanol, then stored at -20 ºC. Gentamicin was used from a 10 mg/ml commercially available solution (Sigma-Aldrich). The ingredients of LB broth, agar plate and SOC media (provided with competent cells) are listed below;

Medium	**Component**	**Concentration**
Luria-Bertani (LB) Broth	Tryptone	1% (w/v)
	Yeast extract	0.5% (w/v)
	NaCl	1% (w/v)
	Sterilize by autoclaving	
LB agar plates	Agar	15 g/L
	LB-broth	1x
	Ampicillin	50 µg/ml
	Gentamicin (tR4-8.3 only)	10 µg/ml
SOC media (provided with competent cells)	Tryptone	2% (w/v)
	Yeast extract	0.5% (w/v)
	NaCl	10 mM
	KCl	2.5 mM
	$MgCl_2$	10 mM
	$MgSO_4$	10 mM
	Glucose	20 mM

Transformations were performed as follows; competent cells were defrosted in their vial on ice for no more than 20 minutes before the addition of 2-5 µl ligation/recombination reaction, mixed by gently tapping the vial. Vials were then placed in ice for 12 minutes,

before heat shocking the cells for 30 seconds at 42 ºC in a preheated water bath, then returned to the ice for a further 2 minutes. 250 µl SOC media was then added, and cells incubated at 37 ºC for 1 hour with constant, gentle agitation. A volume sufficient to allow for individual colonies to be picked (15-250 µl depending on the plasmid) was spread on to pre-dried agar plates using disposable plastic inoculation loops (VWR) and allowed to grow for 12-18 hours at 37 ºC. Individual colonies were picked by sterile pipette tip and dispersed in 30 µl sterile water. Plasmid preparations were prepared with either QIAprep spin miniprep (Qiagen) or PureLink HiPure Plasmid Midiprep (Invitrogen), depending on required yield.

For mini-preps 5 µl of the bacterial mix was added to 1 ml LB broth, supplemented with equivalent selection anti-biotics to those used when setting up agar plates, and incubated for 1 hour at 37 ºC under constant agitation. This was then transferred to an additional 4 ml LB broth and incubated overnight at 37 ºC in a shaking incubator before DNA harvest using the QIAprep kit in accordance with manufacturer's instructions. Plasmid was eluted in 50-100 µl nuclease free water. Midi-preps were prepared by adding the entire bacteria/water mix to a total volume of 50-100 ml LB (+selection antibiotics) and incubated overnight at 37 ºC in a shaking incubator. DNA was then harvested in accordance with the manufacturer's instructions, and DNA reconstituted in 0.5-1 ml nuclease free water at 37 ºC until completely dissolved. All new plasmids were evaluated by restriction digest and PCR against inserted GOI where applicable. Newly developed plasmids were sent for sanger sequencing by Eurofins Genomics to evaluate their open reading frames (ORFs) for any point mutations and determine if mutagenesis reactions inserted the desired changes to sequence. Plasmids used in this study are listed in table 2.3.1.

2.4 Mammalian cell culture, transfections and stable cell line generation

Although multiple cell lines have been used in the works described in this thesis, common handling and incubation conditions were used. Sterile technique was employed throughout, with all procedural steps conducted in a laminar flow hood with HEPA filtration, regularly sterilised with 70% ethanol throughout, and using sterile equipment, plastics and reagents. Cells were incubated under temperature, humidity and atmospheric controlled conditions, namely 37 ºC, 5% CO_2 and 95% humidity. As stated, multiple cell lines have been employed here, however these can be broadly grouped in to 2 categories.

2.4.1 Culturing of adherent cells

HEK293T, COS-7 and 3T3 cell lines were obtained from pre-existing stocks held by the group. RAW cells were kindly gifted by Jennifer Mitchell, and all adherent cell lines were maintained in either 75 or 150 cm^2 tissue culture (TC) treated, vented cap flasks (Corning). HEK293T, COS-7 and 3T3 cells were maintained in Dulbecco's minimal essential medium (DMEM) plus 10% heat inactivated foetal calf serum (FCS), 2mM L-glutamine and 1% streptomycin and penicillin (all Invitrogen), subsequently referred to as DMEM+. RAW cells were maintained in RPMI-1640 (Invitrogen), with the same additional components as DMEM+, here referred to as RPMI+. All media and reagents were pre-warmed before use. Typically, cells were grown until 70-80% confluent before passage. Cells were lifted from their flasks by first aspirating and discarding the spent media then washing the cell layer carefully with DPBS. Following aspiration of the DPBS, 2-4ml Trypsin-EDTA (0.25%) was added, depending on flask size, and the flask returned to the incubator for 5-10 minutes until all cells detached and were in a single cell suspension. 8-16ml DMEM+ or RPMI+ was then added to neutralise the trypsin, and 1/10 of the total volume transferred to a new flask with fresh media. Where cells had to be lifted from 10 cm^2 or multi-well tissue culture plates for downstream applications, the same basic conditions were used, with a volume of trypsin sufficient to completely cover the cell layer applied, and 4x this volume of DMEM+ added to neutralise it. Please note that Flp-In T-REx 293 cells, and the stable cell lines generated from them, are maintained in the same manner however require the addition of selection anti-biotics to the media. This will be detailed further in sections relating to the establishment of stable cell lines.

2.4.2 Culturing of cells in suspension

Non-adherent cell lines (HUT78, U937, THP1, Jurkat, and L1.2) were all maintained in 25 or 75 cm^2 vented cap TC flasks, using RPMI+ media, in a total volume of 5-20 ml. When cell number reached a density exceeding $1x10^6$/ml (initially determined by count with a haemocytometer then visually), $1/10^{th}$ of the total volume was transferred to fresh flasks with new media.

2.4.3 Freezing down and recovery of cell lines

In order to maintain cell stocks, cell lines would be regularly frozen down. For adherent cell lines this initially required cells to be lifted into a single cell suspension, and then transferred to a 50 ml centrifuge tube (Greiner). Suspension cells were transferred directly to 50 ml tubes. Cells were pelleted by centrifugation at 300 g for 5 minutes. Supernatant

was discarded, and pellet resuspended in DPBS then spun down again. Supernatant was again discarded, and cells resuspended in freezing media (10% DMSO v/v in FCS) at a density of 1-10x10^6 cells/ml. 1 ml of this cell suspension was transferred to 2 ml cryo-vials (Alpha Laboratories) and placed in a Mr Frosty freezing container freezing vessel (ThermoFisher Scientific), containing isopropanol. The vessel was placed in the -80°C freezer overnight to allow gradual cooling (1°C per minute), and the now frozen vials transferred to liquid nitrogen tanks for long-term storage.

Recovery of frozen cells was performed as follows; frozen vials were rapidly defrosted at 37 ºC, and the entire volume of cell suspension transferred to a labelled 15 ml centrifuge tube (Greiner) containing 10 ml of either DMEM+ or RPMI+. Cells were pelleted as before and supernatant discarded. The cell pellet was then dispersed in 10 ml DMEM+ or RPMI+ before being spun down again. Supernatant was again discarded, with cells resuspended in fresh media then transferred to a fresh TC flask.

2.4.4 Transfection of mammalian cells with plasmid DNA

2.4.4.1 Transfection of HEK293T cells with Lipofectamine 2000

Transfection of cells for flow cytometry, western blotting and UAA integration was conducted with Lipofectamine 2000 transfection reagent (Invitrogen). HEK293T cells were seeded on to 12 or 6 well TC plates or 10 cm^2 TC dishes (Corning) at a density sufficient to give ~90% confluence when transfected 24 hours later. Lipofectamine 2000 was used in a 3:1 excess of plasmid DNA, i.e. for every 1 μg plasmid 3 μg lipofectamine 2000 was used. The quantity of plasmid used varied depending on experiment, but generally was 0.5-1 μg per well of a 12-well plate, 1.25-2.5 μg with 6-well plates and 4-10 μg per 10cm^2 dish, diluted in 125, 250 or 500 μl Opti-mem (Invitrogen) respectively. Lipofectamine 2000 reagent was diluted in an equivalent volume of Opti-mem, then combined with the plasmid dilution. The plasmid/lipofectamine mix was then incubated at room temperature for 5 minutes, during which time the media on cells was refreshed. The plasmid/lipofectamine mix was then added to the media, and cells analysed 48 hours later.

2.4.4.2 Transfection of HEK293T and Flp-In T-REx 293 cells with Polyethylenimine (PEI)

Transfection of cells for β-arrestin recruitment and immunoprecipitation (IP) experiments and for the generation of stable cell lines using the Flp-In system were performed using PEI (25kD linear, Polysciences). In all cases, cells were seeded on to 10 cm^2 TC dishes as

described previously, and transfection conducted 24 hours after seeding. Transfection for the generation of stable cell lines will be discussed in greater detail in a later section. PEI was used at a 6:1 excess of plasmid DNA. For β-arrestin recruitment assays 4 μg receptor-YFP expressing plasmid and 1 μg β-arrestin 1 or 2-rLuc expressing plasmid (±4 μg ST8sia4-HA expressing plasmid) was used and diluted in 500 μl sterile 150 mM NaCl. For IP experiments 4 μg each of receptor expressing plasmid and either empty vector or ST8sia4-HA expressing plasmid was diluted in the same volume. PEI was diluted in 500 μl 150 mM NaCl also and combined with the plasmid dilution. The plasmid/PEI mix was incubated for 10 minutes at room temperature while the media on cells was refreshed, then applied into the refreshed media. Transfected cells were utilised 48 hours later.

2.4.5 Generation of stable cell lines using the Flp-In system

Stable cell lines for the inducible expression of systematic protein affinity strength modulation (SPASM) biosensors of Gi1/2 and Gi3 recruitment to CCRs 4, 7 and 10, were generated using the Flp-In T-REx methodology (Ward, Alvarez-Curto and Milligan, 2011). Flp-In T-REx 293 cells were maintained in DMEM+ supplemented with the selection antibiotics Blasticidin S HCl (Invitrogen, used at 5 μg/ml final concentration) and Zeocin (Invitrogen, used at 50 mg/ml final concentration). 10 cm^2 TC dishes were seeded with Flp-In T-REx 293 cells at sufficient density to be >90% confluent 24 hours later. When >90% confluent cells were transfected with SPASM biosensors for each receptor/G-protein combination in a 1:8 ratio with pOG44 plasmid, using PEI as the transfection reagent as described above. Following 2 days incubation transfected cells are replated at a lower density in 75 cm^2 TC flasks, and successful transfectants were selected for with DMEM+ supplemented with Blasticidin S HCl (Invitrogen) at 5 μg/ml and Hygromycin Gold (Invivogen) at 200 μg/ml for ~2 weeks, exchanging spent media every 5-7 days, which removes non-adherent dead cells. Surviving cells are then pooled and maintained in the same selection media from this point.

2.5 Flow cytometry, generation of biotinylated chemokines and competition assays

2.5.1 Flow cytometry

Expression of chemokine receptors of interest was evaluated by flow cytometry. When assessing adherent cells (HEK293T) these were prepared as a single cell suspension as described (Section 2.4.1), washed x2 in PEB (DPBS, 0.5% w/v BSA, 2 mM EDTA), and

resuspended at $5x10^6$ cells/ml in PEB and kept at 4 ºC. Non-adherent cells (BMDCs) were washed x2 in PEB and resuspended at $5x10^6$ cells/ml in PEB and kept at 4 ºC. All proceeding washes and staining steps are conducted at 4 ºC. Cells were stained utilising a novel chemokine-based detection method (Le Brocq *et al.*, 2014). For analysis of CCR7, site-specific biotinylated CCL19 (Almac Sciences) was prepared at a stock concentration of 1 μM in 0.5% BSA and stored at -20 ºC. Staining with the chemokine was performed at a concentration of 25 nM, meaning that in a staining volume of 100 μl, 2.5 μl of biotinylated CCL19 is used. Prior to staining, the chemokine was conjugated to either streptavidin-PE (SAPE) or streptavidin-BV421 (SABV421) (both from Biolegend) in a ratio of 2.5 μl chemokine to 5 μl SAPE/SABV421 and incubated at 4 ºC for 30 mins. Cells were stained by adding 7.5 μl CCL19-SAPE to a total volume of 100 μl cell suspension and incubated for 30 mins at 4 ºC. For CCR4, CCL22 directly conjugated to the fluorophore AF647 (Almac) was used at a staining concentration of 25 nM as well and was added directly to a total volume of 100 μl cell suspension. After staining cells were washed twice, resuspended in 500 μl PEB buffer, with 1 μl DRAQ7 live/dead discriminant (Biostatus) added immediately before analysis. Samples were analysed with the MACSQuant bench top cytometer. Post-acquisition analysis was carried out using FlowJo. Where quoted, MFI represents Geometric mean of all single, live cells in the relevant channel.

2.5.2 In-house biotinylation of chemokines

Human CCL19, CCL22 and CCL27 (Peprotech) were biotinylated using the One-Step Antibody Biotinylation Kit (Miltenyi), in accordance with manufacturer's instructions. In brief, chemokines were reconstituted in DPBS at a concentration of 100 μg/ml, and 100 μl of mixed with the lyophilised reagent provided. This was then incubated for 24 hours at 18 ºC. Remaining non-biotinylated chemokine was incubated under the same conditions for use as a control in subsequent experiments. Following this, chemokine was diluted with 0.5% BSA to a final concentration of 1 μM and stored at -20 ºC. In-house biotinylated chemokines were either used in the same manner as those purchased from Almac, with pre-conjugation to SAPE/SABV421 before staining, or were used unconjugated to label cells. In this 2-step process cells were incubated with the in-house biotinylated chemokine first for 30 minutes, washed x1 in PEB, stained with an equivalent of 5 μl SAPE/100 μl stain for a further 30 minutes, then prepared and analysed as before.

2.5.3 Competition assays

CCL17, 19, 21 and 22 (Peprotech) were reconstituted in 0.5% BSA at a concentration of 10 μM. Where site-specific biotinylated CCL19 was used this was pre-conjugated to SAPE as described above. CCL22-AF647 was used directly. In-house biotinylated CCL22 was used in a 2-step staining process as described in section 2.5.1. In all instances a mix of unlabelled cold competitor and labelled chemokines was created as follows;

	Starting concentration:	**Volume:**	**Final Concentration (in 100 μl stain):**
Labelled Chemokine	1 μM	2.5-7.5 μl	25 nM
Unlabelled Chemokine	10 μM-0.3 nM	10 μl	1 μM-0.03 nM
PEB	n/a	up to 20 μl	n/a

20 μl of these mixes was used to stain prepared cells in a total volume of 100 μl and prepared and analysed as described in section 2.5.1. IC50 values were calculated from the MFI values obtained using an XY table in Prism 6 software (GraphPad), and the following equation; Y=Bottom + (Top-Bottom)/(1+10^((X-LogIC50))). pK_i values were generated using the Cheng-Prusoff equation, as described previously (Lazareno and Birdsall, 1993).

2.6 Protein analysis; western blotting, UV crosslinking and IPs

The following buffers were produced in house for use in protein analysis. 10x PBS was produced by core facility staff.

Solution	Component	Concentration
10 x PBS	NaCl	1.37 M
	KCl	27 mM
	Na_2HPO_4	100 mM
	KH_2PO_4	17.6 mM
1x PBS	10x PBS	10% (v/v)
PBST (0.05%)	PBS	1x
	Tween 20	0.05% (v/v)
5% Milk PBST	PBST	1x
	Skimmed milk powder (Marvel)*	5% (w/v)
Triton X lysis buffer	Trtiton X-100	1% (v/v)
	Tris (pH 8)	10 mM
	EDTA (pH7.4)	5 mM
	NaCl	150 mM
SDS-Urea lysis buffer	Tris (pH 6.8)	100 mM
	Sodium dodecyl sulfate (SDS)	4% (w/v)
	Urea	8 M
	Glycerol	20% (v/v)
	EDTA (pH 7.4)	20 mM
	bromophenol blue	0.014% (v/v)
RIPA buffer	Tris-HCl (pH 7.4)	50 mM
	NP-40	1% (v/v)
	deoxycholate	0.25% (w/v)
	NaCl	150 mM
	EDTA (pH 7,4)	1 mM
1 M DTT	Dithiothreitol	1 M
Coomassie blue buffer	Methanol	50% (v/v)
	Acetic acid	10% (v/v)
	Coomassie blue R-250	0.25% (w/v)
Coomassie destain buffer	Methanol	5% (v/v)
	Acetic acid	7.5% (v/v)
Glycine elution buffer	Glycine	200 mM (pH adjusted to 2.5)
Tris Base	Tris	1 M (pH adjusted to 10.4)

Unless otherwise stated, all buffers are prepared in dH_2O

2.6.1 Preparation of protein lysates

Please note that extraction of protein from HEK293T cells is conducted at 4 ^oC throughout all stages. Whole cell lysate was obtained with Triton X lysis buffer and RIPA buffer as follows; 1 Pierce protease inhibitor mini tablet (ThermoFisher Scientific) was dissolved in 10 ml of lysis buffer. TC media was aspirated, and cell layers washed once with PBS. Cell

layers were then lifted by mechanical disruption in PBS and transferred to 1.5 ml reaction tubes (Greiner). Cells were pelleted at 300 g for 5 minutes, supernatant removed, and pellets disrupted in lysis buffer (50-200 µl depending on cell number), and constantly agitated for 15 minutes. Lysate was then cleared by centrifugation at 17000 g for 15 minutes, and supernatant transferred to fresh reaction tubes.

Whole cell lysate was obtained with SDS-Urea lysis buffer as follows; 1 Pierce protease inhibitor mini tablet was dissolved in 10 ml of lysis buffer. TC media was aspirated, and cell layers washed once with PBS. Cells were then disrupted directly in the lysis buffer, scraped from the plate with an inverted 1000 µl pipette tip, and transferred to 1.5 ml reaction tubes. Lysate was passed through a 25-gauge needle 5 times to shear genomic DNA.

Protein concentration was determined using the Pierce BCA protein assay kit (ThermoFisher Scientific), in accordance with manufacturer's instructions. An equivalent volume of cleared lysis buffer was added to each BSA standard sample to account for background reactivity with the buffer. Unless used immediately, protein lysates were snap frozen in dry ice and stored at -20 ^{o}C.

2.6.2 Western blotting

Unless otherwise stated here or previously, all reagents used in this section were obtained from ThermoFisher Scientific. Lysate sufficient to give 20 µg total protein was made up to a standard volume of 13 µl with additional lysis buffer. Samples were denatured with 5 µl Bolt LDS sample buffer (Invitrogen), reduced with 2 µl 1 M DTT and incubated at 37 ^{o}C for 30 mins. 7.5 µl Novex sharp pre-stained protein standard and the entire volume of each sample were loaded onto 15 well, 4-12% Bolt Bis-Tris plus gels, and run with1x Bolt MES running buffer (5% v/v 20x Bolt MES running buffer) at 200 V and 500 mA for 30-60 minutes. PVDF membrane was pre-activated by incubation in methanol for 30 seconds. Protein was transferred to PVDF membrane in accordance with manufacturer's instructions in transfer buffer (5% v/v 20x Bolt transfer buffer, 10% v/v methanol, 0.1% v/v Bolt Antioxidant) at 20 V and 500 mA for 60 minutes. Membranes were blocked in 5% Milk PBST for 90 mins then incubated in a dilution of the primary antibody in 5% Milk PBST overnight at 4 ^{o}C under. Membranes were washed briefly in PBS, then for 10 minutes in PBST (x3) and then incubated in the secondary antibody diluted in 5% Milk PBST for 1 hour at room temperature. Membranes were again washed briefly in PBS, then for 10 minutes in PBST (x3), dried and exposed to Pierce ECL western blotting substrate

for 2 mins. Proteins of interest were then visualised by exposure to x-ray film (Carestream) under dark room conditions, with multiple exposures obtained in all instances, and developed using the Konica-Minolta SRX-101A film processor. Where applicable, quantification was carried out using ImageJ software and the gel analyser tool by defining pixel density in a standardised region of interest and subtracting background pixilation. Where required, membranes were stripped using Restore stripping buffer in accordance with manufacturer's instructions. Below is a list of primary and secondary antibodies used throughout this thesis.

Primary/Secondary	Epitope/Isotype	Clone/Host species	Dilution	Manufacturer
Primary	FLAG, IgG1	M2, mouse	1;5000	Sigma Aldrich
Primary	GAPDH (human), IgG	n/a, rabbit	1;5000	Generon
Primary	CCL19 (human), IgG	EPR7044(2), rabbit	1;2000	Abcam
Primary	CCL21 (human), IgG	EPR6218, rabbit	1;2000	Abcam
Primary	HA, IgG	n/a, rabbit	1;5000	SantaCruz
Primary	polysialic acid, IgG2a	735, mouse	1;5000	absolute antibody
Primary	polysialic acid, IgM	2-2B, mouse	1;1000	Merck
Primary	GFP	n/a, sheep	1;10000	generated in-house
Secondary	anti-rabbit IgG-HRP	n/a, goat	1;5000-10000	Jackson ImmunoResearch
Secondary	anti-mouse IgG-HRP	n/a, goat	1;5000	R&D Systems
Secondary	anti-goat IgG-HRP*	n/a, donkey	1;20000	R&D Systems
Secondary	anti-mouse IgM HRP	n/a/goat	1;10000	Abcam

* anti-goat IgG HRP readily detected sheep antibodies and was the secondary utilised with the anti-GFP primary.

2.6.3 Coomassie blue staining

Protein gels were prepared and ran as described in 2.6.2, however instead of transfer to PVDF, gels were stained in Coomassie blue buffer for 4 hours. Following this, background Coomassie staining was removed by incubation in Coomassie de-stain buffer for 4 hours. Representative images were captured by camera.

2.6.4 UAA integration and crosslinking

When integrating UAA into TAG substitution mutants of CCR7 the transfection protocol described in section 2.4.4.1 was followed as described, with the exception that media was changed to DMEM+ supplemented with 1 mM p-azidophenyalanine (Bachem) 4-8 hours prior to transfection, instead of during transfection. This allowed time for UAA cell

loading and for media pH to equilibrate. All steps of this procedure are conducted at 4 ºC. 48 hours following transfections cells were harvested in the same manner as described for flow cytometry analysis in section 2.5.1, then split into 2 aliquots and transferred to 1.5 ml reaction tubes. Cells were resuspended in 200 µl PEB supplemented with either CCL19 or CCL21 (100 nM), incubated for 15 mins then transferred to disposable cuvettes (Fisher Scientific) before being exposed to UV radiation (365 nm) for 40 mins by handheld dual UV lamp (Fisher Scientific), with occasional agitation. Alternatively, cell layers were undisturbed, and instead washed x1 in DPBS, exposed to equivalent conditions as cells analysed in suspension (using CCL19 only), then lifted by mechanical disruption of the cell layer in DPBS. From this point, protein was extracted in RIPA buffer as described in section 2.6.1.

2.6.5 Immunoprecipitation of chemokine receptors and polysialylated proteins

Lysate was obtained in 500 µl RIPA buffer from whole 10 cm^2 TC plates transfected with chemokine receptors of interest ±ST8sia4-HA as described in section 2.6.1. Protein L agarose beads (SantaCruz) were used in all IP experiments, and all steps are conducted 4 ºC and performed in 1.5 µl reaction tubes, and all incubation steps are performed under constant agitation by end over end tumbler. For IP using anti-FLAG (M2) the following protocol was used; 20 µl Protein L bead suspension and 1 µl mouse IgG1 isotype control antibody (Biolegend) were added to lysates. These were incubated for 30 minutes, then beads pelleted by centrifugation at 1000 g for 1 minute. Supernatant was transferred to a fresh reaction tube, and 1 µl anti-FLAG (M2) antibody added. Samples were incubated with constant agitation for 1 hour, then 20 µl bead suspension added, before being left to incubate overnight. Beads were pelleted by centrifugation as before, supernatant discarded, and then resuspended in 500 µl RIPA buffer supplemented with protease inhibitor cocktail (as described in section 2.6.1). This wash step was repeated 3 additional times, before protein was eluted in 25 µl glycine elution buffer by constantly mixing buffer and beads for 30 seconds, before neutralising pH with the addition of 2.5 µl Tris base. From here, eluted protein was prepared for western blotting as described in section 2.6.2, with the exception that protein concentration was not determined, and a standard volume was loaded on to gels instead. For IP using anti-pSia (735) adjustments had to be made due to the target epitope's instability. In effect, the same protocol as employed in anti-FLAG IPs was used with the following adjustments; no pre-clear step was employed, incubation time was shortened from overnight to 4 hours, and protein was eluted by denaturing and

reducing of the bead mix in 25 µl of 2xLDS with 100 mM DTT for 15 minutes at 37 ºC. Beads were again pelleted, and supernatant carefully aspirated and used directly for western blotting as described in section 2.6.2.

2.7 Epifluorescent microscopy

24 hours following transfection of HEK293T cells on a 12-well plate with CCR4, 7 or 10-YFP (as described in section 2.4.4.1) cells were harvested as before, resuspended in 1 ml DMEM+ and 500 µl transferred to a chamber of 4-chamber microscope slide (Lab-TEK). 24 hours after this each chamber was washed once with 250 µl DPBS, incubated for 20 mins in 4% paraformaldehyde at room temperature, washed again with DPBS and allowed to air dry. Slides were mounted with mounting medium +DAPI (Vector Laboratories) and visualised on the Axio IMager.M2 microscope with a 40x objective (40x/0,75 Ph2), and imaged using the AxioCam MRM monochromatic camera.

2.8 Aldara model and qPCR

2.8.1 The Aldara model of psoriasiform inflammation

The Aldara model has been well described previously (van der Fits *et al.*, 2009). In brief, 8-week-old female C57BL/6 mice had their dorsal skin shaved near the base of the tail. A quarter sachet of Aldara cream (Meda AB) (~62.5 mg) or equivalent volume of control cream ((Boots Aqueous Cream/10% Vaseline Lanette Cream) was applied daily, up to a total of 5 days. Mice were weighed daily and culled if their body weight reduced by over 20 % during the course of the procedure, in agreement with Home Office Requirements. Mice were euthanised 4, 12 and 24 hours after the initial Aldara treatment and 24 hours after the 3- and 5-day treatments by rising concentration of CO_2. Dorsal skin samples were removed, and RNA harvested and converted to cDNA as described in section 2.1 and 2.2. The preceding was performed by Louis Nerurkar, who kindly gifted cDNA excess to his own requirements for the analysis performed here.

2.8.2 Determination of relative expression by quantitative reverse transcription-PCR (qPCR)

qPCR primers for GOI were designed from the available main mRNA sequence listed on genbank (NCBI), using the Primer3 web tool (Koressaar and Remm, 2007) in accordance with the following conditions; primer length between 18 and 23 bp (20 bp optimal), primer GC content between 40 and 65% (50% optimal), primer annealing temperature (Tm)

between 59.5 ºC and 61 ºC (60 ºC optimal), max self-complementarity of 2, max 3' self-complementarity of 1, amplicon size 50-150bp, no more than two G or C bases in last 5 at 3' end and no stretches of G or C exceeding 4 nucleotides. Where possible, primers were designed to span exon junctions. All primers were checked for specificity using the NCBI Primer-BLAST web tool (Ye *et al.*, 2012).

cDNA was prepared as described in section 2.1. No template (NTC), nuclease free water (water) and no reverse transcriptase (-RT) controls were used where appropriate. The following reaction mix represents the quantities per individual well and was scaled up as required; 5 µl PerfeCTa 2x master mix (Quantabio), 3.85 µl nuclease free water, 0.75 µl each of forward and reverse primer (from a 100 mM primer stock). 9 µl of reaction mix was dispensed into each required well of a 384 well qPCR plate (StarLab), and 1 ml diluted cDNA, water or -RT control was added to the appropriate well, with triplicate measures analysed for each sample. qPCR was performed using the QuantStudio7 Flex Real-Time PCR system (ThermoFisher Scientific), according to the following programme;

STEP	TEMP	TIME
Initial Denaturation	95°C	20 seconds
40 Cycles amplification	95°C	1 second
	60°C	20 seconds
Melt curve analysis	95°C	15 seconds
	60°C	1 second
	95°C	15 seconds

For analysis of Aldara experiments and BMDC expression, Ct values were obtained, and coefficient of variation between triplicates assessed as follows; triplicates with a coefficient of variation >2.5% (standard deviation (SD) = 0.5) had an outlier excluded if the indicated Ct value was >1.5 from the median value within each triplicate. Expression was expressed relative to a housekeeping gene (TATA binding protein, or TBP), presented as $2^{-\Delta\Delta Ct}$ which was calculated for each individual sample as follows; $\Delta Ct = Ct_{goi}/Ct_{TBP}$, $\Delta\Delta Ct = \Delta Ct_{sample} - \Delta Ct_{average\ of\ control\ group}$, $2^{-\Delta\Delta CT} = 2^{\wedge} \Delta\Delta Ct \times -1$.

This methodology was not applicable to the analysis of ST8sia4 expression in cell lines, as a control group cannot be assigned when comparing between different cell lines from different species. Instead, comparison was made to a defined standard for each gene. "Standards" were generated as follows; primers were designed for the amplification of a 500 bp region of mRNA encompassing the qPCR amplicon, PCR performed, samples run

on a gel and the relevant band excised, purified and DNA concentration quantified as described in sections 2.2.1 and 2.3.1. DNA copy number was determined as follows; concentration/molecular weight x $6.23x10^{23}$. The standard was initially diluted 1/100 to give a 10^{-2} stock, then further diluted by 1/10 serial dilution to give a standard range of 10^{-4} to 10^{-9}. For human ST8sia4 the expression vector for this gene had already been established and was used in a similar copy number to the generated standards. A standard curve was generated by analysing 10^{-4} to 10^{-9} copies of this standard in triplicate to determine the copy numbers of samples. Outliers are excluded as described above, and expression conveyed as a function of $QT_{GOI}/QT_{TBP.}$

qPCR and standard primers are listed in table 2.2.1.

2.9 Bioluminescence resonance energy transfer (BRET) experiments

BRET experiments followed a slightly different methodology depending on the signalling partners being assessed. For β-arrestin recruitment assays cells were transfected as described in section 2.4.4.2, and removed from their 10 cm^2 TC plates by washing once in DPBS, incubating in 2 ml trypsin-EDTA, neutralising the trypsin with 8 ml DMEM+, transferring the cellular suspension to 50 ml centrifuge tubes and diluting this suspension with an additional 10 ml DMEM+. 100 µl of these suspensions were seeded onto white 96-well tissue culture plates (Corning) pre-treated with poly-d-lysine (Sigma-Aldrich), and allowed to adhere overnight. For G-protein recruitment assays, cells were lifted in the same manner but subsequently resuspended in DMEM+ (without selection antibiotics). Cell density was determined and adjusted to $6x10^5$ cells/ml, and expression of the SPASM biosensors induced by the administration of 100 ng/ml doxycycline hyclate (Sigma-Aldrich). 100 µl cell suspension was then seeded as described above and allowed to adhere overnight. On the day of analysis cells were washed once with 100 µl Hanks balanced salt solution (HBSS, Gibco), then equilibrated in HBSS (80 µl) for >30 mins. 10 µl of a 25 µM solution of Coelentrazine h (NanoLight Technology, 301) was added to each well (2.5 µM final concentration) and incubated for 10 mins at 37 °C. 10x dilutions of CCLs 17, 19, 21, 22, 27 or 28 (Peprotech) were prepared such that administration of 10 µl of these dilutions gave a final concentration range between 1 µM and 0.01 nM in the well, depending on experimental conditions. Chemokine was administered, and plates incubated at room temperature for 5-10 minutes. Spectral emission was detected at 475 nm for the donor (rLuc/nLuc) and 535 nm for the acceptor (YFP). Gain for YFP and luciferase emissions was adjusted based in untreated controls such that the ratio of YFP/luciferase was close to

1. Plates were then read on the Pherastar FS plate reader. In β-arrestin recruitment kinetics experiments the same basic methodology was followed, except a single final concentration of 100 nM of chemokine was used, gain for YFP/Luciferase set at a standard setting of 3600/3200 (this broadly results in a ratio of 1 for experiments with an rLuc donor), and readings taken continually over a 30-minute period.

All β-arrestin expressing plasmids were kindly gifted by Dr Brian Hudson. In all experiments BRET ratio is determined as YFP emission/rLuc emission. pEC_{50} were determined using Graphpad 6 software with the following equation; Y=Bottom + (Top-Bottom)/(1+10^((LogEC50-X))). Half-time and maximal response values from kinetics experiments were determined with the following equation; Y=Y0 + (Plateau-Y0)*(1-exp(-K*x)). Relative efficacy and bias factors were determined as described previously (Gundry *et al.*, 2017).

2.10 Bone marrow derived dendritic cell (BMDC) differentiation

BMDCs were differentiated from the bone marrow of female C57BL/6 mice. The following was performed by Paul Burgoyne, who kindly gifted excess cells at various stages of the differentiation protocol for use here. The femurs and tibia were dissected out, and muscle and connective tissue removed by washing in ethanol under sterile conditions. Sterile conditions were maintained from here forward. Cleaned bones were rinsed in DPBS. The bone tips were removed by dissection scissors and bone marrow flushed using RPMI+ and a 26-gauge needle and 5 ml syringe. Collected bone marrow was then forced through a 40 μm filter (Greiner) and subsequently flushed with an additional 5 ml RPMI+ to create a single cell suspension. Cell density was determined, and cells pelleted by centrifugation at 300 g for 5 minutes. Cells were suspended at a density of $1x10^6$/ml in RPMI supplemented with 20 ng/ml granulocyte-macrophage colony stimulating factor (GM-CSF, Miltenyi) and transferred to petri dishes (10ml/petri). Following 2 and 4 days in culture, non-adherent cells were transferred to fresh plates, and 2ml RPMI+ with 20 ng/ml GM-CSF was added. After 7 days in culture non-adherent cells were pelleted and resuspended in RPMI+ supplemented with 100 ng/ml lipopolysaccharide (LPS, Sigma-Aldrich) and 50 ng/ml tumour necrosis factor alpha (TNFα, Miltenyi), plated on fresh petri dishes and incubated overnight. RNA was extracted from unstimulated bone marrow (D0), cells at day 4 of the differentiation protocol (D4) and cells at day 7, prior to stimulation with LPS/TNFα. Day 8 stimulated cells were used for flow cytometry analysis.

2.11 Statistical analysis

All data were analysed using Prism 6 software. The specific statistical tests applied, and replicates analysed are listed in the relevant figure legends or in the appropriate section of this chapter (Materials and Methods). Differences were considered significant when $p=<0.05$.

Name	Description	Sequence
Forward HindIII CCR4	Primer against human CCR4 introducing a 5' HindIII restriction site	ACTTAAGCTTatgaaccccacggatatagc
Forward BamHI CCR4	Primer against human CCR4 introducing a 5' BamHI restriction site	cccGGATCCatgaaccccacggatatagca
Reverse CCR4 FLAG XhoI	Primer against human CCR4 introducing a C-terminal FLAG tag and a 3' XhoI restriction site	GACTCGAGctaCTTGTCGTCATCGTCTTTGTAGTCcagagcatcatggagatcatg
Reverse CCR4 KpnI	Primer against human CCR4 introducing a 3' KpnI restriction site	CACGGTACCcagagcatcatggag
Reverse CCR4 NotI	Primer against human CCR4 introducing a 3' NotI restriction site	CaaGGCGGCCGCAcagagcatcatggagat
Forward CCR7 47TAG Mutagenesis	Mutagenesis primers compatible with Geneart site directed mutagenesis kit, introducing a TAG stop codon substitution at the indicated site	CTTTGTTCGAGTCTTAGTGCTCCAAGAAGGA
Reverse CCR7 47TAG Mutagenesis	Mutagenesis primers compatible with Geneart site directed mutagenesis kit, introducing a TAG stop codon substitution at the indicated site	TCCTTCTTGGAGCACTAAGACTCGAACAAAG
Forward CCR7 48TAG Mutagenesis	Mutagenesis primers compatible with Geneart site directed mutagenesis kit, introducing a TAG stop codon substitution at the indicated site	TTTGTTCGAGTCTTTGTAGTCCAAGAAGGACGTGCG
Reverse CCR7 48TAG Mutagenesis	Mutagenesis primers compatible with Geneart site directed mutagenesis kit, introducing a TAG stop codon substitution at the indicated site	CGCACGTCCTTCTTGGACTACAAAGACTCGAACAAA
Forward CCR7 50TAG Mutagenesis	Mutagenesis primers compatible with Geneart site directed mutagenesis kit, introducing a TAG stop codon substitution at the indicated site	TTCGAGTCTTTGTGCTCCTAGAAGGACGTGCGGAACTTT
Reverse CCR7 50TAG Mutagenesis	Mutagenesis primers compatible with Geneart site directed mutagenesis kit, introducing a TAG stop codon substitution at the indicated site	AAAGTTCCGCACGTCCTTCTAGGAGCACAAAGACTCGAA
Forward CCR7 51TAG Mutagenesis	Mutagenesis primers compatible with Geneart site directed mutagenesis kit, introducing a TAG stop codon substitution at the indicated site	TCTTTGTGCTCCAAGTAGGACGTGCGGAACT
Reverse CCR7 51TAG Mutagenesis	Mutagenesis primers compatible with Geneart site directed mutagenesis kit, introducing a TAG stop codon substitution at the indicated site	AGTTCCGCACGTCCTACTTGGAGCACAAAGA
Forward CCR7 52TAG Mutagenesis	Mutagenesis primers compatible with Geneart site directed mutagenesis kit, introducing a TAG stop codon substitution at the indicated site	TCTTTGTGCTCCAAGAAGTAGGTGCGGAACTTTAAAGCC
Reverse CCR7 52TAG Mutagenesis	Mutagenesis primers compatible with Geneart site directed mutagenesis kit, introducing a TAG stop codon substitution at the indicated site	GGCTTTAAAGTTCCGCACCTACTTCTTGGAGCACAAAGA
Forward CCR7 53TAG Mutagenesis	Mutagenesis primers compatible with Geneart site directed mutagenesis kit, introducing a TAG stop codon substitution at the indicated site	GTGCTCCAAGAAGGACTAGCGGAACTTTAAAGCC
Reverse CCR7 53TAG Mutagenesis	Mutagenesis primers compatible with Geneart site directed mutagenesis kit, introducing a TAG stop codon substitution at the indicated site	GGCTTTAAAGTTCCGCTAGTCCTTCTTGGAGCAC
Forward CCR7 54TAG Mutagenesis	Mutagenesis primers compatible with Geneart site directed mutagenesis kit, introducing a TAG stop codon substitution at the indicated site	GCTCCAAGAAGGACGTGTAGAACTTTAAAGCCTGGT
Reverse CCR7 54TAG Mutagenesis	Mutagenesis primers compatible with Geneart site directed mutagenesis kit, introducing a TAG stop codon substitution at the indicated site	ACCAGGCTTTAAAGTTCTACACGTCCTTCTTGGAGC
Forward CCR7 55TAG Mutagenesis	Mutagenesis primers compatible with Geneart site directed mutagenesis kit, introducing a TAG stop codon substitution at the indicated site	CCAAGAAGGACGTGCGGTAGTTTAAAGCCTGGTTCCT
Reverse CCR7 55TAG Mutagenesis	Mutagenesis primers compatible with Geneart site directed mutagenesis kit, introducing a TAG stop codon substitution at the indicated site	AGGAACCAGGCTTTAAACTACCGCACGTCCTTCTTGG
Forward CCR7 56TAG Mutagenesis	Mutagenesis primers compatible with Geneart site directed mutagenesis kit, introducing a TAG stop codon substitution at the indicated site	GGACGTGCGGAACTAGAAAGCCTGGTTCCT
Reverse CCR7 56TAG Mutagenesis	Mutagenesis primers compatible with Geneart site directed mutagenesis kit, introducing a TAG stop codon substitution at the indicated site	AGGAACCAGGCTTTCTAGTTCCGCACGTCC
Forward CCR7 57TAG Mutagenesis	Mutagenesis primers compatible with Geneart site directed mutagenesis kit, introducing a TAG stop codon substitution at the indicated site	GACGTGCGGAACTTTTAGGCCTGGTTCCTCCCT
Reverse CCR7 57TAG Mutagenesis	Mutagenesis primers compatible with Geneart site directed mutagenesis kit, introducing a TAG stop codon substitution at the indicated site	AGGGAGGAACCAGGCCTAAAAGTTCCGCACGTC
Forward CCR7 58TAG Mutagenesis	Mutagenesis primers compatible with Geneart site directed mutagenesis kit, introducing a TAG stop codon substitution at the indicated site	GACGTGCGGAACTTTAAATAGTGGTTCCTCCCTATCATG
Reverse CCR7 58TAG Mutagenesis	Mutagenesis primers compatible with Geneart site directed mutagenesis kit, introducing a TAG stop codon substitution at the indicated site	CATGATAGGGAGGAACCACTATTTAAAGTTCCGCACGTC
Forward CCR7 59TAG Mutagenesis	Mutagenesis primers compatible with Geneart site directed mutagenesis kit, introducing a TAG stop codon substitution at the indicated site	CGGAACTTTAAAGCCTAGTTCCTCCCTATCATG
Reverse CCR7 59TAG Mutagenesis	Mutagenesis primers compatible with Geneart site directed mutagenesis kit, introducing a TAG stop codon substitution at the indicated site	CATGATAGGGAGGAACTAGGCTTTAAAGTTCCG
Forward CCR7 60TAG Mutagenesis	Mutagenesis primers compatible with Geneart site directed mutagenesis kit, introducing a TAG stop codon substitution at the indicated site	GGAACTTTAAAGCCTGGTAGCTCCCTATCATGTACTCC
Reverse CCR7 60TAG Mutagenesis	Mutagenesis primers compatible with Geneart site directed mutagenesis kit, introducing a TAG stop codon substitution at the indicated site	GGAGTACATGATAGGGAGCTACCAGGCTTTAAAGTTCC
Forward CCR7 61TAG Mutagenesis	Mutagenesis primers compatible with Geneart site directed mutagenesis kit, introducing a TAG stop codon substitution at the indicated site	GGAACTTTAAAGCCTGGTTCTAGCCTATCATGTACTCCATCAT
Reverse CCR7 61TAG Mutagenesis	Mutagenesis primers compatible with Geneart site directed mutagenesis kit, introducing a TAG stop codon substitution at the indicated site	ATGATGGAGTACATGATAGGCTAGAACCAGGCTTTAAAGTTCC
Forward CCR7 62TAG Mutagenesis	Mutagenesis primers compatible with Geneart site directed mutagenesis kit, introducing a TAG stop codon substitution at the indicated site	AAAGCCTGGTTCCTCTAGATCATGTACTCCATC
Reverse CCR7 62TAG Mutagenesis	Mutagenesis primers compatible with Geneart site directed mutagenesis kit, introducing a TAG stop codon substitution at the indicated site	GATGGAGTACATGATCTAGAGGAACCAGGCTTT
Forward CCR7 63TAG Mutagenesis	Mutagenesis primers compatible with Geneart site directed mutagenesis kit, introducing a TAG stop codon substitution at the indicated site	TTTAAAGCCTGGTTCCTCCCTTAGATGTACTCCATCATTTGTTTC
Reverse CCR7 63TAG Mutagenesis	Mutagenesis primers compatible with Geneart site directed mutagenesis kit, introducing a TAG stop codon substitution at the indicated site	GAAACAAATGATGGAGTACATCTAAGGGAGGAACCAGGCTTTAAA

Forward HindIII CCR7	Primer against human CCR7, introducing a 5' HindIII restriction site	CATGAAGCTTATGGACCTGGGGAAACCA
Forward BamHI CCR7	Primer against human CCR7, introducing a 5' BamHI restriction site	cccGGATCCatggacctggggaaaccaatg
Reverse CCR7 FLAG BamhI (1 AA missing from FLAG)	Primer against human CCR7, introducing a c-terminal FLAG tag and 3' BamHI restriction site (nb there is a codon missing from the FLAG tag)	GACTGGATCCTTATTTATCATCGTCGTCA
Reverse CCR7 FLAG XhoI	Primer against human CCR7, introducing a C-terminal FLAG tag and 3' XhoI restriction site	GACTCGAGctaCTTGTCGTCATCGTCTTTGTAGTCtggggagaaggtggtggtggt
Reverse CCR7 KpnI	Primer against human CCR7, introducing 3' KpnI restriction site	CACGGTACCTGGGGAGAAGGTGGT
Reverse CCR7 NotI	Primer against human CCR7, introducing 3' NotI restriction site	aaGGCGGCCGCATGGGGAGAAGGTGGTGGT
Reverse CCR10 NotI	Primer against codon optimised CCR10, introducing a 3' NotI restriction	GGCGGCCGCAATTATCCCAGCTAAGGCT
Forward HindIII CCR10	Primer against human CCR10, introducing a 5' HindIII restriction site	TTAAGCTTGCCACCATGGGAACCGAG
Forward BamHI CCR10	Primer against human CCR10, introducing a 5' BamHI restriction site	cccGGATCCatggggacggaggccacagag
Reverse CCR10 FLAG XhoI	Primer against human CCR10, introducing a C-terminal FLAG tag and 3' XhoI restriction site	GACTCGAGctaCTTGTCGTCATCGTCTTTGTAGTCgttgtcccaggagagactgtg
CCR10 KpnI	Primer against human CCR10, introducing 3' KpnI restriction site	CACGGTACCgttgtcccaggagagact
CCR10 NotI	Primer against human CCR10, introducing 3' NotI restriction site	CaaGGCGGCCGCAgttgtcccaggagagactgtgg
Forward HindIII ST8sai4	Primer against human ST8sia4 introducing a 5' HindIII restriction site	ACTTAAGCTTCCCAAGATGCGCTCCATTA
Reverse ST8sia4 HA XhoI	Primer against human ST8sia4 introducing a C-terminal HA tag and a 3' XhoI restriction site	ttCTCGAGttaAGCGTAATCTGGAACATCGTATGGGTATTGCTTTACACACTTTCCTG
Reverse ST8sia4 HA TaV2A BamHI	Primer for introducing a TaV2A self-cleavage site to ST8sia4-HA, with a 5' AgeI and 3' BamHI restriction sites either side of the sequence	CATGGATCCgggtccGGGATTTTCCTCCACGTCCCCGCATGTTAGAAGACTTCCCCTGCCCTCTCCGGAGCCACCGGTAGCGTAATCTGGAACATCGTA
Sequencing Tet-R	Sequencing primer, originating in Tet-R element	GGCGAGTTTACGGGTTGTTA
Sequencing forward pcDNA5	Sequencing primer, originating upstream of ORF in CMV promotor	CATAGAAGACACCGGGAC
Sequencing forward ST8sia4	Sequencing primer, originating in ST8sia4 ORF	TGTCAGAGGTTACTGGCT
Sequencing forward eYFP	Sequencing primer, originating in eYFP ORF	TGAAGCAGCACGACTTCT
Sequencing forward CCR4	Sequencing primer, originating in CCR4 ORF	ATCACCAGTTTGGCTACA
Sequencing forward CCR7	Sequencing primer, originating in CCR7 ORF	GTGGCCATCGTCCAGGCT
Sequencing forward CCR10	Sequencing primer, originating in CCR10 ORF	GGCCGCGCACACTTGGTC
Sequencing reverse pcDNA5	Sequencing primer, originating downstream of ORF in primer backbone	TAGAAGGCACAGTCGAGG
Forward Standard TBP	Primers for the generation of 500 bp PCR product from the indicated target, containing the amplicon of the corresponding qPCR primers	CAGTACAGCAATCAACATCT
Reverse Standard TBP	Primers for the generation of 500 bp PCR product from the indicated target, containing the amplicon of the corresponding qPCR primers	AGGGAACTTCACATCACAGC
Forward Standard ST8sia4	Primers for the generation of 500 bp PCR product from the indicated target, containing the amplicon of the corresponding qPCR primers	TATCTGTGGTCAAGAGCAGT
Reverse Standard ST8sia4	Primers for the generation of 500 bp PCR product from the indicated target, containing the amplicon of the corresponding qPCR primers	TGCCTATCCATCACTTAGACTTATT
Forward qPCR CCL17	qPCR primer against indicated target	CCAGGGATGCCATCGTGTTT
Reverse qPCR CCL17	qPCR primer against indicated target	CCTCAGCGGGAAGGTCATG
Forward qPCR CCL22	qPCR primer against indicated target	CACCCTCTGCCATCACGTTT
Reverse qPCR CCL22	qPCR primer against indicated target	CGGCACAGATATCTCGGTTCT
Forward qPCR TBP	qPCR primer against indicated target	TCTGGAATTGTACCGCAGCTT
Reverse qPCR TBP	qPCR primer against indicated target	CCGTGGCTCTCTTATTCTCATGA
Forward qPCR ST8sia4	qPCR primer against indicated target	AGGAGATTGACAGCCACAACTT
Reverse qPCR ST8sia4	qPCR primer against indicated target	TCCGAAAGCCTCCAAATGCT
Forward qPCR ST8sia4 (human)	qPCR primer against indicated target	CACCAATGAAGAATCGCAGGTT
Reverse qPCR ST8sia4 (human)	qPCR primer against indicated target	GTGTAATCTAGCTCCTGTGGTGG
Forward qPCR TBP (human)	qPCR primer against indicated target	GCTGGAAAACCCAACTTCTG
Reverse qPCR TBP (human)	qPCR primer against indicated target	AGGATAAGAGAGCCACGAACC
Forward Standard TBP (human)	Primers for the generation of 500 bp PCR product from the indicated target, containing the amplicon of the corresponding qPCR primers	GGGCACCACTCCACTGTATC
Reverse Standard TBP (human)	Primers for the generation of 500 bp PCR product from the indicated target, containing the amplicon of the corresponding qPCR primers	CATCTTCTCACAACACCACCA

Table 2.2.1 List of primers used in this study

List of primers designed for use in this study, including descriptions of their intended function and sequence

Plasmid	Description:	Selection	Column4
pAcBac.tR4.OMeYRS.GFP	Plasmid intended for generation of baculovirus particles in SF9 cells that can be used for viral transduction of mammalian cells. This viral delivery system introduces a tRNA/Synthetase pair capable of charging multiple unnatural amino acids, as well as a single codon TAG mutant GFP, used as a reporter of UAA integration. (Chatterjee A et al, 2013)	Ampicillin, Gentamycin	n/a
tR4-8.3	Modified version of pAcBac.tR4.OMeYRS.GFP with large sections of the original viral genome removed, inlcuding the GFP reporter. This plasmid delivers a tRNA/Synthetase pair capable of charging multiple unnatural amino acids more suitable for transient transfection of mammalian cells.	Ampicillin, Gentamycin	n/a
pEF6 /V5-His TOPO TA Empty Vector	Insertless pEF6 backbone, suitable for cloning/sub-cloning and transient transfection.	Ampicillin	Blasticidin
pcDNA3.1(+) empty vector	Insertless pcDNA3 backbone	Ampicillin	Neomycin
pOG44	Flp-Recombinase expression vector for use in the Flp-In stable cell generation system.	Ampicillin	n/a
ST8sia4-HA (pcDNA5/FRT/TO)	Expression vector for human ST8sia4, including a C-terminal HA tag for ease of detection. Suitable for transient transfection and generation of stable DOX inducble cell lines with the Flp-In Trex system	Ampicillin	Hygromycin
ST8sia4-HA.TaV2A (pcDNA5/FRT/TO)	Expression vector for human ST8sia4, including a C-terminal HA tag for ease of detection. Inframe and downstream of this is a self-cleaving TaV2A sequence, with a 5' AgeI and 3' BamHI restriction site for subsequent ligation and generation of a bi-cistronic expression vector.	Ampicillin	Hygromycin
b-arrestin 2-nanoLuciferase (pcDNA3)	Expression vector for nano-luciferase tagged (N-terminal) b-arrestin 2	Ampicillin	Neomycin
b-arrestin1-renilla Luciferase (pcDNA3)	Expression vector for renilla-luciferase tagged (N-terminal) b-arrestin 1	Ampicillin	Neomycin
b-arrestin2-renilla Luciferase (pcDNA3)	Expression vector for renilla-luciferase tagged (N-terminal) b-arrestin 2	Ampicillin	Neomycin
CCR4-eYFP (pcDNA5/FRT/TO)	Expression vector for human CCR4, including a C-terminal eYFP tag. Suitable for transient transfection and generation of stable DOX inducble cell lines with the Flp-In Trex system	Ampicillin	Hygromycin
ST8sia4-HA.TaV2A.CCR4-eYFP (pcDNA5/FRT/TO)	Bicistronic expression vector for ST8sia4-HA and CCR4-eYFP. Suitable for transient transfection and generation of stable DOX inducble cell lines with the Flp-In Trex system	Ampicillin	Hygromycin
CCR4-Gi1/2 (pcDNA5/FRT/TO)	Expression vector for a human CCR4 SPASM biosensor of Ga subunit recruitment (Gi1/2). Suitable for generation of stable DOX inducble cell lines with the Flp-In Trex system	Ampicillin	Hygromycin
ST8sia4-HA.TaV2A.CCR4-Gi1/2 (pcDNA5/FRT/TO)	Bicistronic expression vector for human ST8sia4-HA and CCR4 SPASM biosensor of Ga subunit recruitment (Gi1/2). Suitable for generation of stable DOX inducble cell lines with the Flp-In Trex system.	Ampicillin	Hygromycin
CCR4-Gi3 (pcDNA5/FRT/TO)	Expression vector for a human CCR4 SPASM biosensor of Ga subunit recruitment (Gi3). Suitable for generation of stable DOX inducble cell lines with the Flp-In Trex system.	Ampicillin	Hygromycin
ST8sia4-HA.TaV2A.CCR4-Gi3 (pcDNA5/FRT/TO)	Bicistronic expression vector for human ST8sia4-HA and CCR4 SPASM biosensor of Ga subunit recruitment (Gi3). Suitable for generation of stable DOX inducble cell lines with the Flp-In Trex system.	Ampicillin	Hygromycin
CCR7-FLAG (pcDNA5/FRT/TO)	Expression vector for human CCR7, including a C-terminal FLAG tag. Suitable for transient transfection and generation of stable DOX inducble cell lines with the Flp-In Trex system	Ampicillin	Hygromycin
CCR7-eYFP (pcDNA5/FRT/TO)	Expression vector for human CCR7, including a C-terminal eYFP tag. Suitable for transient transfection and generation of stable DOX inducble cell lines with the Flp-In Trex system	Ampicillin	Hygromycin
ST8sia4-HA.TaV2A.CCR7-eYFP (pcDNA5/FRT/TO)	Bicistronic expression vector for ST8sia4-HA and CCR7-eYFP. Suitable for transient transfection and generation of stable DOX inducble cell lines with the Flp-In Trex system	Ampicillin	Hygromycin
CCR7-eYFP (pcDNA3)	Expression vector for human CCR7, including a C-terminal eYFP tag. Suitable for transient transfection.	Ampicillin	Neomycin
CCR7-Gi1/2 (pcDNA5/FRT/TO)	Expression vector for a human CCR7 SPASM biosensor of Ga subunit recruitment (Gi1/2). Suitable for generation of stable DOX inducble cell lines with the Flp-In Trex system.	Ampicillin	Hygromycin
ST8sia4-HA.TaV2A.CCR7-Gi1/2 (pcDNA5/FRT/TO)	Bicistronic expression vector for human ST8sia4-HA and CCR7 SPASM biosensor of Ga subunit recruitment (Gi1/2). Suitable for generation of stable DOX inducble cell lines with the Flp-In Trex system.	Ampicillin	Hygromycin
CCR7-Gi3 (pcDNA5/FRT/TO)	Expression vector for a human CCR7 SPASM biosensor of Ga subunit recruitment (Gi3). Suitable for generation of stable DOX inducble cell lines with the Flp-In Trex system.	Ampicillin	Hygromycin
ST8sia4-HA.TaV2A.CCR7-Gi3 (pcDNA5/FRT/TO)	Bicistronic expression vector for human ST8sia4-HA and CCR7 SPASM biosensor of Ga subunit recruitment (Gi3). Suitable for generation of stable DOX inducble cell lines with the Flp-In Trex system.	Ampicillin	Hygromycin
CCR7-FLAG 47 TAG (pcDNA5/FRT/TO)	Expression vector for TAG codon substitution mutant human CCR7 (Leu47Stop), including a C-terminal FLAG tag. Suitable for transient transfection and generation of stable DOX inducble cell lines with the Flp-In Trex system	Ampicillin	Hygromycin
CCR7-FLAG 48 TAG (pcDNA5/FRT/TO)	Expression vector for TAG codon substitution mutant human CCR7 (Cys48Stop), including a C-terminal FLAG tag. Suitable for transient transfection and generation of stable DOX inducble cell lines with the Flp-In Trex system	Ampicillin	Hygromycin
CCR7-FLAG 50 TAG (pcDNA5/FRT/TO)	Expression vector for TAG codon substitution mutant human CCR7 (Lys50Stop), including a C-terminal FLAG tag. Suitable for transient transfection and generation of stable DOX inducble cell lines with the Flp-In Trex system	Ampicillin	Hygromycin
CCR7-FLAG 51 TAG (pcDNA5/FRT/TO)	Expression vector for TAG codon substitution mutant human CCR7 (Lys51Stop), including a C-terminal FLAG tag. Suitable for transient transfection and generation of stable DOX inducble cell lines with the Flp-In Trex system	Ampicillin	Hygromycin
CCR7-FLAG 52 TAG (pcDNA5/FRT/TO)	Expression vector for TAG codon substitution mutant human CCR7 (Asp52Stop), including a C-terminal FLAG tag. Suitable for transient transfection and generation of stable DOX inducble cell lines with the Flp-In Trex system	Ampicillin	Hygromycin
CCR7-FLAG 53 TAG (pcDNA5/FRT/TO)	Expression vector for TAG codon substitution mutant human CCR7 (Val53Stop), including a C-terminal FLAG tag. Suitable for transient transfection and generation of stable DOX inducble cell lines with the Flp-In Trex system	Ampicillin	Hygromycin
CCR7-FLAG 54 TAG (pcDNA5/FRT/TO)	Expression vector for TAG codon substitution mutant human CCR7 (Arg54Stop), including a C-terminal FLAG tag. Suitable for transient transfection and generation of stable DOX inducble cell lines with the Flp-In Trex system	Ampicillin	Hygromycin
CCR7-FLAG 55 TAG (pcDNA5/FRT/TO)	Expression vector for TAG codon substitution mutant human CCR7 (Asp55Stop), including a C-terminal FLAG tag. Suitable for transient transfection and generation of stable DOX inducble cell lines with the Flp-In Trex system	Ampicillin	Hygromycin
CCR7-FLAG 56 TAG (pcDNA5/FRT/TO)	Expression vector for TAG codon substitution mutant human CCR7 (Phe56Stop), including a C-terminal FLAG tag. Suitable for transient transfection and generation of stable DOX inducble cell lines with the Flp-In Trex system	Ampicillin	Hygromycin
CCR7-FLAG 57 TAG (pcDNA5/FRT/TO)	Expression vector for TAG codon substitution mutant human CCR7 (Lys57Stop), including a C-terminal FLAG tag. Suitable for transient transfection and generation of stable DOX inducble cell lines with the Flp-In Trex system	Ampicillin	Hygromycin

CCR7-FLAG 58 TAG (pcDNA5/FRT/TO)	Expression vector for TAG codon substitution mutant human CCR7 (Ala58Stop), including a C-terminal FLAG tag. Suitable for transient transfection and generation of stable DOX inducble cell lines with the Flp-In Trex system	Ampicillin	Hygromycin
CCR7-FLAG 59 TAG (pcDNA5/FRT/TO)	Expression vector for TAG codon substitution mutant human CCR7 (Trp59Stop), including a C-terminal FLAG tag. Suitable for transient transfection and generation of stable DOX inducble cell lines with the Flp-In Trex system	Ampicillin	Hygromycin
CCR7-FLAG 60 TAG (pcDNA5/FRT/TO)	Expression vector for TAG codon substitution mutant human CCR7 (Phe60Stop), including a C-terminal FLAG tag. Suitable for transient transfection and generation of stable DOX inducble cell lines with the Flp-In Trex system	Ampicillin	Hygromycin
CCR7-FLAG 61 TAG (pcDNA5/FRT/TO)	Expression vector for TAG codon substitution mutant human CCR7 (Leu61Stop), including a C-terminal FLAG tag. Suitable for transient transfection and generation of stable DOX inducble cell lines with the Flp-In Trex system	Ampicillin	Hygromycin
CCR7-FLAG 62 TAG (pcDNA5/FRT/TO)	Expression vector for TAG codon substitution mutant human CCR7 (Pro62Stop), including a C-terminal FLAG tag. Suitable for transient transfection and generation of stable DOX inducble cell lines with the Flp-In Trex system	Ampicillin	Hygromycin
CCR7-FLAG 63 TAG (pcDNA5/FRT/TO)	Expression vector for TAG codon substitution mutant human CCR7 (Iso63Stop), including a C-terminal FLAG tag. Suitable for transient transfection and generation of stable DOX inducble cell lines with the Flp-In Trex system	Ampicillin	Hygromycin
CCR7-FLAG 47TAG eYFP (pcDNA3)	Expression vector for TAG codon substitution mutant human CCR7 (Leu47Stop), including a C-terminal eYFP tag. Suitable for transient transfection.	Ampicillin	Neomycin
CCR7-FLAG 62TAG eYFP (pcDNA3)	Expression vector for TAG codon substitution mutant human CCR7 (Pro62Stop), including a C-terminal eYFP tag. Suitable for transient transfection.	Ampicillin	Neomycin
CCR10-FLAG (pcDNA5/FRT/TO)	Expression vector for human CCR10, including a C-terminal FLAG tag. Suitable for transient transfection and generation of stable DOX inducble cell lines with the Flp-In Trex system	Ampicillin	Hygromycin
CCR10-eYFP (pcDNA5/FRT/TO)	Expression vector for human CCR10, including a C-terminal eYFP tag. Suitable for transient transfection and generation of stable DOX inducble cell lines with the Flp-In Trex system	Ampicillin	Hygromycin
ST8sia4-HA.TaV2A.CCR10-eYFP (pcDNA5/FRT/TO)	Bicistronic expression vector for ST8sia4-HA and CCR10-eYFP. Suitable for transient transfection and generation of stable DOX inducble cell lines with the Flp-In Trex system	Ampicillin	Hygromycin
CCR10-Gi1/2 (pcDNA5/FRT/TO)	Expression vector for a human CCR10 SPASM biosensor of Ga subunit recruitment (Gi1/2). Suitable for generation of stable DOX inducble cell lines with the Flp-In Trex system.	Ampicillin	Hygromycin
ST8sia4-HA.TaV2A.CCR10-Gi1/2 (pcDNA5/FRT/TO)	Bicistronic expression vector for human ST8sia4-HA and CCR10 SPASM biosensor of Ga subunit recruitment (Gi1/2). Suitable for generation of stable DOX inducble cell lines with the Flp-In Trex system.	Ampicillin	Hygromycin
CCR10-Gi3 (pcDNA5/FRT/TO)	Expression vector for a human CCR10 SPASM biosensor of Ga subunit recruitment (Gi3). Suitable for generation of stable DOX inducble cell lines with the Flp-In Trex system.	Ampicillin	Hygromycin
ST8sia4-HA.TaV2A.CCR10-Gi3 (pcDNA5/FRT/TO)	Bicistronic expression vector for human ST8sia4-HA and CCR10 SPASM biosensor of Ga subunit recruitment (Gi3). Suitable for generation of stable DOX inducble cell lines with the Flp-In Trex system.	Ampicillin	Hygromycin
CCR10-Gi3 (pcDNA5/FRT/TO)	Expression vector for a human CCR10 SPASM biosensor of Ga subunit recruitment (Gi3). Suitable for generation of stable DOX inducble cell lines with the Flp-In Trex system.	Ampicillin	Hygromycin

Table 2.3.1 List of plasmids used in this thesis

A list of plasmids used in this thesis, including intended function and compatible bacterial and mammalian selection antibiotics

3 Integration and crosslinking with unnatural amino acids

3.1 Introduction

Like many GPCRs, some chemokine receptors demonstrate signalling bias (Corbisier *et al.*, 2015). This is a phenomenon wherein two or more ligands binding the same receptor produce a unique signalling profile. A number of chemokine receptors have demonstrated a form of signalling bias that can be broadly described as a pair of ligands binding a receptor, with both resulting in recruitment of heterotrimeric G-protein complexes to the receptor, but only one also recruiting β-arrestin and resulting in receptor internalisation and desensitisation. In this scenario the chemokine that readily recruits both G-proteins and β-arrestin is considered balanced, whereas the chemokine that selectively recruits G-proteins is considered biased toward G-protein mediated signalling. This skewed signalling profile is observed with several chemokine receptors interacting with only a pair of ligands, such as CCR4 (with CCL17 and CCL22), CCR7 (with CCL19 and CCL21) and CCR10 (with CCL27 and CCL28) (Mariani *et al.*, 2004; Rajagopal *et al.*, 2013; Corbisier *et al.*, 2015).

The ability of different ligands to recruit signalling apparatus in unique ways is considered to be a result of subtle variations in receptor:ligand interaction that lead to the adoption of distinct active conformations by the receptor (Ziarek *et al.*, 2017). This could provide the opportunity to target GPCRs with compounds that preferentially inhibit one ligand or signalling pathway over another, with biased agonism currently being considered in new drug development (Rankovic, Brust and Bohn, 2016). However, this requires highly detailed structural information of the particular residues involved in ligand binding. Such data are typically obtained from crystal structures of the receptor of interest complexed with its cognate ligands. This can prove highly technically challenging when evaluating GPCRs (as well as other transmembrane proteins), with chemical modifications often being required to stabilise the receptor, and frequently obtaining only partial structures or structures of a poorer resolution than needed (Ghosh *et al.*, 2015). As all of these factors can heavily influence the interpretation of these data there is a call for alternative approaches to obtain highly detailed readouts of receptor: ligand interactions that don't rely on crystallography.

One such approach is to make use of the expanded genetic code. This is an umbrella term for the integration of amino acids with unique and useful properties (not found in nature) into proteins of interest (Wang and Schultz, 2002). Different UAAs have highly diverse

properties, however broadly speaking they are incorporated into target proteins in the same manner. The codon of the residue to be replaced is substituted with one that corresponds to no natural amino acid, frequently the amber stop codon TAG (Takimoto *et al.*, 2009). This stop codon is then suppressed by the exogenous expression of a tRNA and synthetase pair capable of charging and integrating UAA into the translated protein product in response to the amber stop codon TAG. The result is a protein that, other than the site of UAA substitution, is near-identical to the WT, with minimal disruption to structure and ligand interaction properties. One such UAA, p-azidophenylalanine, carries the additional sidechain modification of an azide group. At rest this azide group is inert, however following UV irradiation at 365 nm expels an N_2 molecule leaving a highly reactive nitrene group behind (Shao *et al.*, 2015). This volatile nitrene group displaces hydrogen from any CH, OH or NH bond in the nearby vicinity, resulting in the covalent capture of any such molecule within a distance of 8.9 Å of the activated UAA (Coin *et al.*, 2013). The principal being that if the substituted residue is involved in ligand binding it will be within this distance, resulting in covalent capture of the ligand. Otherwise the nitrene group will quench in the aqueous environment surrounding the cell.

Using this methodology, it has been possible to image the binding pocket of a GPCR (rat corticotropin releasing factor receptor, CRF1R) with one of its endogenous protein ligands, urocortin 1 (Coin *et al.*, 2013). Here, p-azidophenyalanine was substituted for all residues considered apical and therefore potentially ligand binding, and crosslinking performed in the presence of Urocortin 1. The resulting receptor:ligand adducts could be visualised by western blotting, with both ligand and receptor size-shifting to the same position on the blot (summarised in figure 3.1). Those substitution sites demonstrating successful crosslinking were then mapped to an available structure of the receptor to visualise the binding pocket of Urocortin 1.

It was hoped that this technique could be utilised to visualise the binding pockets of CCL19 and CCL21 on CCR7, highlighting any structural differences that may account for the skewed signalling profile between these two chemokines. Described herein is the establishment of a CCR7 expression vector introducing the FLAG epitope tag to the C-terminus, as well as sixteen TAG substitution mutants of CCR7 ranging from the 47th (leucine) to the 63rd (isoleucine) amino acids (figure 3.1.2), and the development of tRNA/Synthetase expression plasmid suitable for p-azidophenyalanine charging in transient transfections. Expression levels of these mutants and their capacity to bind a fluorescently labelled CCL19 was evaluated (Le Brocq *et al.*, 2014). However, no

successful crosslinking of CCR7 with either CCL19 or CCL21 was demonstrated at any site of substitution tested.

3.2 Establishment and evaluation of CCR7 and tRNA/Synthetase expression vectors

3.2.1 Cloning of CCR7 and plasmid evaluation

Primers were designed to introduce the FLAG epitope to the C-terminus of CCR7, a new TAA stop codon and HindIII and BamHI restriction sites to the 5' and 3' ends of the transcript respectively. This would allow for ready detection of the receptor by western blotting without relying on receptor specific antibodies, allow for TAG codon suppression and provide broad compatibility with numerous expression vectors. CCR7 was amplified from cDNA generated from human peripheral blood monocytes (PBMCs) from two healthy donors (figure 3.2.1a). Interestingly, a second round of PCR from the previous PCR product showed poor amplification. This raised concerns as to the nature of the original PCR product, however digestion with SacI produced the expected band pattern of 591, 318 and 273 bp from the predicted transcript (figure 3.2.1b).

CCR7 transcript and empty pEF6 expression vector were digested with HindIII and BamHI and purified, and CCR7 ligated into the vector. Each ligation reaction was transformed twice into DH5α max efficiency competent cells. Multiple colonies were picked for each transformant. The presence of the insert was confirmed by PCR against CCR7 (figure 3.2.2a), generating a band of ~1.4 kb, and digestion with PstI, producing the expected band pattern of 4.7, 1.7 and 0.5 kb (figure 3.2.2b). One plasmid from each donor (51.2.30.1 & 52.2.250.1) was sent for sequencing which confirmed no point mutations were present in the ORF. Eukaryotic cell expression was evaluated by two separate means.

Firstly, a fluorescently coupled CCL19 was used to evaluate expression, cell surface localisation and ligand binding capacity of CCR7 expressed in HEK293T cells by FACS (figure 3.2.3) and demonstrated robust staining in CCR7-FLAG transfected cells only. A CCR7 "positive" gate was applied based on the main negative population from empty vector transfected cells, which indicated transfection efficiencies of 63.6 % for 51.2.30.1 and 89.2% for 52.2.250.1. It should be noted that this measure of transfection efficiency only assesses surface expression of CCR7 rather than total, and a certain degree of non-specific background staining with CCL19-SAPE is expected due to glycan binding of the chemokine. A single plasmid from one donor (52.2.250.1) was used from this point forward. Transfection with increasing quantities of plasmid resulted in an increase in cell

surface expression, as determined by CCL19-SABV421 staining at 4 ºC. This plateaued around 600-800 ng per well of a 12-well plate (figure 3.2.4). Again, a CCR7 positive gate was applied based on staining of the empty vector control and indicated increasing transfection efficiencies of 29.4, 60.9, 74.1, 80.2 and 83.1 %, ranging from 200 ng to 1 μg.

Secondly whole cell lysate of cells transfected with either empty vector or CCR7-FLAG was harvested in TritonX 100, SDS-Urea or RIPA lysis buffers, and reduced with either 100 or 400 mM DTT (figure 3.2.5a), in an effort to determine optimal sample preparation conditions for the resolution of clean bands. Bands of a size consistent for CCR7-FLAG (~45 kDa) were observed with TritonX 100 and RIPA lysis buffers. SDS-Urea buffer however failed to produce bands of the correct predicted size, and in fact appear to have distorted the relevant lanes of the gel. This could be due to the high urea concentration in this buffer. Various denaturing temperatures were also evaluated, with 37 ºC for 20 minutes determined to give the best resolution of bands of the predicted size (figure 3.2.5b). Two distinct bands were observed, presumed to be the pro and glycosylated forms of CCR7 (Schaeuble *et al.*, 2011). Collectively these data indicated that the expression vector successfully expressed CCR7, that it trafficked to the cell surface and was capable of binding one of its cognate ligands.

3.2.2 Establishment of a tRNA/Synthetase expressing plasmid

As mentioned previously, exogenous expression of a compatible tRNA/Synthetase pair is required for full length expression of UAA bearing mutant proteins. Recently published work on the expanded genetic code utilised viral transduction to introduce a tRNA/Synthetase pair capable of charging multiple UAAs along with a TAG mutant of GFP to report successful translation (Chatterjee *et al.*, 2013). The genome of this virus is available in plasmid form (pAcBac2.tR4-OMeYRS-GFP*) and with the promoters present on the tRNA, synthetase and GFP cassettes, is useable in transient transfection (figure 3.2.6). When analysed by flow cytometry the construct demonstrated limited “leaky” expression of GFP in the absence of p-azidophenyalanine (figure 3.2.7a), with cells demonstrating GFP fluorescence distinct from empty vector controls, as has been reported previously with TAG-codon suppression systems (Chatterjee *et al.*, 2013). Interestingly, in terms of transfection efficiency (as determined by applying a GFP+ gate based on empty vector transfected cells) there aren’t substantial differences between cells incubated without and with UAA, with an increase from 39.1% to 48% transfected cells with the inclusion of UAA in the culture media (figure 3.2.7 a&b). However, we observe a clear shift in fluorescent intensity when UAA is included in the culture media, with the

emergence of a distinct population of high-GFP expressing cells (figure 3.2.7c&d). While the GFP reporter is useful in determining successful UAA integration, the addition of another TAG bearing mutant transcript could complicate co-transfection with TAG mutants of CCR7. Additionally, the large size of the plasmid restricts transfection efficiency. A strategy was devised to remove the GFP cassette and some sections of the viral genome, utilising SfiI and NotI digestion, Klenow polymerase and blunt end ligation (summarised in figure 3.2.8). This should produce a new 8.3 kb expression vector for the tRNA/Synthetase pair only, dubbed "tR4-8.3", which was confirmed by digestion with AgeI and NheI (figure 3.2.9). This provided a new tRNA/Synthetase expression system that would be more effective in downstream applications.

3.3 Generation and evaluation of 16 TAG substitution mutants of CCR7

3.3.1 Expression of C-terminal protein products in the absence of UAA charging

Primers were designed for use with the Geneart site-directed mutagenesis kit to introduce the TAG stop codon in place of that for a range of 16 amino acids. These encompass a region from the N-terminal domain into the first 2 loops of the first transmembrane domain (figure 3.1.2), selected due to the high likelihood of involvement in chemokine/receptor interaction based on the two-site model of chemokine binding. The resultant plasmids were evaluated by restriction digest and sent for sequencing to confirm that the TAG codon substitution was successful, and that no other mutations were present in the CCR7 ORF. These were transfected into cells (without UAA or tR4-8.3) and evaluated by Western blotting to determine if a similar "leaky" expression to that noted when transfecting cells with the original pAcBac2.tR4-OMeYRS-GFP* alone could be seen with the mutants of CCR7 (figure 3.2.10a). Expression of a protein product of higher than expected molecular weight (>260 kDa), unchanged by varying denaturing conditions, was observed. Coomassie blue staining indicated that this could not be attributed to non-specific binding of the antibody to high quantities of an unknown protein product, potentially revealing in-frame expression of the C-terminal FLAG tag in the absence of either a tRNA/Synthetase pair or UAA (figure 3.2.10b). In order to further evaluate this a C-terminally tagged eYFP fused variant of CCR7, compatible with flow cytometric and epifluorescent microscopy analysis, was developed, as well as two TAG mutants of this construct at an early (leucine 47) and later (proline 62) site of substitution. When assessed by FACS analysis it became apparent that expression of the C-terminal tag by the TAG mutants exceeded that observed with WT CCR7-YFP (figure 3.2.11 a-c), in broad agreement with previous Western blot

data. Additionally, epiflourescent microscopy demonstrated altered cellular localisation of the mutants compared with WT with a concentrated YFP signal observed near the nucleus of the cell, as opposed to the more diffuse distribution of WT CCR7 (figure 3.2.11 d-f). This would confirm that, while expression of TAG mutants of CCR7 is observed in the absence of UAA or tRNA/Synthetase, the resultant product is not analogous to WT CCR7.

3.3.2 Evaluation of UAA bearing mutants of CCR7 and attempted UV crosslinking with CCL19 or CCL21

The ORFs for all 16 mutants as well as wild type CCR7-FLAG were excised from the pEF6 background using the HindIII and XhoI restriction sites and ligated into the pcDNA5/FRT/`TO plasmid backbone. This was done as unpublished observations indicated that this background could provide superior expression of inserts, and could also be used to generate stable cell lines using the Flp-In system if desired. Next TAG mutants of CCR7-FLAG in this new vector were assessed while co-transfecting with tR4-8.3, and when supplemented with p-azidophenyalanine. Full-length receptor expression is confirmed with all 16 CCR7 mutants (figure 3.2.12 a). Unlike with the GFP reporter of pAcBac2.tR4-OMeYRS-GFP*, no full-length CCR7 is observed when either tR4-8.3 or UAA was omitted (figure 3.2.12 b&c). Staining with labelled CCL19 indicated cell surface localisation and ligand binding with most UAA bearing mutants (2 examples shown in figure 3.2.13 c&d). Expression of these mutants was compared with WT by band densitometry (Western blot) and MFI (FACS) (figure 3.2.14). These data indicated significant variation in both level of protein and ligand binding between substitution sites, but also significant differences between level of expression and ligand binding at some substitution sites (summarised in table 3.2.1). These data indicate that stop-codon suppression occurs with the new tRNA/Synthetase plasmid, that expression of CCR7 with UAA substitution is feasible, and that the resultant receptor is capable of trafficking to the cell surface and binding CCL19. It would also appear that expression and chemokine binding do not always correlate, potentially indicating altered ligand binding properties with UAA integration.

Finally, UV crosslinking was attempted at each site of UAA integration with CCL19 or CCL21 either with cells in suspension in cuvettes (figure 3.2.15, figure 3.2.16), or directly on the tissue culture plate with CCL19 only (figure 3.2.17). Staining of chemokine and receptor at the same molecular weight was not observed with any of the mutants tested, indicating that covalent capture of chemokine by UAA bearing CCR7 has not occurred. Staining was only seen with CCL21 at a molecular weight below that predicted for CCR7 and is most likely representative of an oligomer of CCL21. Interestingly a size shift

potentially consistent with the crosslinking of receptors was observed when the assay was performed directly on a tissue culture plate (figure 3.2.17). This could indicate successful activation of the UAA, followed by non-specific binding to other molecules of CCR7. However, no concurrent signal is seen with a-CCL19 staining.

3.4 Discussion

At present there are relatively few complete crystal structures of chemokine receptors, particularly in an unmodified ligand bound state. An arguably disproportionate number of these structures are of CCR5 and CXCR4 (Tan *et al.*, 2013; Qin *et al.*, 2015), presumably due to their critical role in HIV pathogenesis making them higher interest targets. Indeed, of the few available and efficacious small molecule antagonists against chemokine receptors, only maraviroc (CCR5) and plerixafor (CXCR4) are routinely used clinically. This correlation between the availability of detailed structural information and development of effective antagonists can hardly be considered incidental. Given its attractive position as a drug target, and the lack of complete structural information, it was hoped that UAA mutants of CCR7 and UV crosslinking with CCL19 or CCL21 could be utilised to map the interface between CCR7 and these chemokines. As well as providing information on critical residues in ligand binding, it was hoped that this mapping would reveal subtle differences between CCL19 and CCL21 binding that might account for the biased agonism observed with this receptor.

To this end a CCR7 expression vector was established and evaluated. Initial attempts at amplification of the CCR7-FLAG ORF proved challenging (figure 3.2.1 a), potentially due to the long reverse primer (designed to introduce the FLAG tag) having a propensity to form complex secondary structures. However once established in a plasmid, digests, PCR (figure 3.2.2 a&b) and sequencing confirmed successful insertion of CCR7-FLAG. Expression in HEK293T cells was evaluated using fluorescently labelled CCL19 and flow cytometry (figure 3.2.3). This indicated not only that the CCR7 protein could be expressed in eukaryotic cells, but also that it traffics to the cell surface and can bind one of its natural ligands, confirming that our new plasmids expressed WT CCR7. Increasing the amount of plasmid transfected into HEK293T did initially increase cell surface expression (figure 3.2.4), however this experienced a plateau in effect around 600-800 ng plasmid/well. This suggested that our planned co-transfection strategy of 500 ng receptor to 500 ng tRNA/synthetase should allow for detectable cell surface expression of CCR7. A variety of harvesting and denaturing conditions were evaluated (figure 3.2.5), with RIPA lysis buffer, 100 mM DTT and incubation at 37 ºC for 20 minutes being utilised in all subsequent

western blotting experiments due to these conditions providing the best resolution of CCR7-FLAG at the predicted molecular weight of 43 kDa, with the heavier, glycosylated, form of the receptor also observed.

Integration of UAAs into TAG substitution mutants requires the expression of exogenous translational machinery, namely a tRNA to bind the non-canonical amino acid, and a corresponding synthetase to charge it (Takimoto *et al.*, 2009). Unfortunately, the tRNA/synthetase plasmid utilised in mapping CRF1R could not be obtained. Instead another potentially usable construct was obtained. This came from work aiming to develop a viral transduction strategy for the evaluation of UAA integration via simultaneous delivery of tRNA, synthetase and a TAG mutant of GFP (Chatterjee *et al.*, 2013). The viral genome was available in the plasmid repository Addgene (pAcBac2.tR4-OMeYRS-GFP*, figure 3.2.6), which could be utilised in transient transfection as well. Transfection of HEK293T with this construct indicated that expression of GFP can be observed when no UAA is provided (figure 3.2.7 a&b). This is presumably due to limited read through of the amber stop codon (Loughran *et al.*, 2018), resulting in integration of an unknown canonical residue and ultimately translation of a functional GFP. Although this is in transient transfections rather than viral transduction, this is in keeping with observations from the original research article (Chatterjee *et al.*, 2013), and a clear shift in fluorescence intensity is observed with the inclusion of UAA (figure 3.2.7 c&d). While including GFP as a reporter for UAA integration is tempting, stop codon suppression can be inefficient in terms of generating protein, with most systems including multiple copies of the tRNA cassettes in an attempt to overcome this (Schmied *et al.*, 2014). Consequently, including multiple TAG substitution mutants in the transfection could attenuate translational efficiency. A two-step restriction and blunt-end ligation strategy was devised in order to remove the GFP cassette from the plasmid along with other elements included to aid viral transduction that would be less useful here (figure 3.2.8). This has the obvious advantage of ensuring all stop-codon suppressing activity is directed towards mutants of CCR7, as well as allowing a higher copy number with the same mass of plasmid. Success of this strategy was determined by digest (figure 3.2.9), and UAA integration activity (as indicated in later experiments).

16 TAG substitution mutants of CCR7, encompassing the hinge region from the N-terminal domain down into the first transmembrane domain, were generated. These were selected for initial screening in part because of the importance of this region in the classical “two-site” model of chemokine binding (Rajagopalan and Rajarathnam, 2006), and the observation of successful crosslinking quite deep into the helices of CRF1R with

Urocortin1 (Coin *et al.*, 2013). Given previous observations of mutant GFP expression in the absence of UAA, a selection of 10 CCR7-FLAG mutants were assessed for translation without UAA (figure 3.2.10). These data indicated that a robust FLAG signal could be observed by western blotting for all mutants tested, that this was of higher indicated molecular weight than WT CCR7 and could not be resolved to a similar size with any denaturing condition tested. Staining of an identical gel with Coomassie blue revealed total protein distribution and did not show the presence of any large amount of protein product in this region that might have led to non-specific binding of the anti-FLAG antibody. YFP-fused versions of WT CCR7 and 2 TAG mutants were generated and evaluated by flow cytometry and epifluorescent microscopy (figure 3.2.11). These data demonstrated a similar pattern of increased expression from that seen in WT, as well as altered sub-cellular localisation compared to WT.

This observation of in-frame expression of C-terminal epitope tags and fluorescent proteins, downstream of the substituted TAG codon and without UAA, raises a number of questions. Primarily, does this represent a read-through past the TAG stop codon, or does translation cease at the stop codon but begin again from a subsequent methionine residue within the ORF? This is difficult to answer for a number of reasons. The molecular weight would indicate the mutants are, if anything, a larger protein than the WT which fits with neither scenario. However, it seems unlikely that these proteins result from read-through of the TAG codon, as this would be expected to result in very little protein and would represent a single site of substitution with a canonical amino acid. As such it would be expected, if anything, to generate a full-length version of CCR7 with very similar properties to WT, which doesn't fit with our observations of high expression, altered cellular localisation, and increased weight on a Western blot. There is some evidence for truncated, intracellular CCR7 in colorectal cancer cell lines and tissues (Na *et al.*, 2008). These findings were determined to be the result of truncated mRNA transcripts that lacked the coding region for the signal peptide of CCR7, presumed to result from alternative splicing or post-transcriptional changes to the mRNA. The loss of this signal peptide would account for the intracellular localisation and may be in line with our own findings.

However, while alternative splicing and posttranslational modifications might be possible from endogenous expression, a plasmid-based expression vector obviously does not contain a genomic like exon/intron structure and should read as a single ORF after being transcribed. It may be possible that in an over-expression system such as this the premature stop codon allows for priming from an otherwise internal methionine, resulting in a truncated version of CCR7 that lacks the signal peptide and thus accumulates

intracellularly (in keeping with our microscopy data), and a smaller, more readily translatable transcript that might account for the increased expression observed by flow cytometry. However, this doesn't account for the increase in indicated molecular weight, and it is impossible to definitively account for this for the time being.

Expression of full-length CCR7 was observed for all 16 TAG mutants when both UAA and tR4-8.3 are included (figure 3.2.16), with visible differences in expression apparent between different sites of substitution. Based on the mapping of CRF1R there is an expectation that different sites would be more amenable to UAA integration than others, resulting in different levels of expression. As crosslinking is only possible at the cell surface, CCL19 staining was once again used to determine if the UAA bearing mutants could traffic to the cell surface and bind chemokine (figure 3.2.13). These data indicated greater variability in ligand binding inconsistent with total protein expression, as determined by western blotting. Expression of each mutant was normalised to the WT receptor in each assay and compared between western blotting and flow cytometry (figure 3.2.14). This revealed several substitution sites where protein level did not correlate with ligand binding, with UAA substitution significantly attenuating (leucine 47, cysteine 48), or perhaps more surprisingly improving (lysine 50, tryptophan 59, phenylalanine 60, isoleucine 63) binding to CCL19. This could not be attributed to any consistent change in size, charge or polarity (table 3.2.2) and could be due to slight structural changes affecting the interaction with CCL19. This is somewhat concerning, as the rationale for using UAAs in this fashion is that they cause minimal disturbance to receptor structure (and consequently ligand binding), compared with other methods. However, these data would appear to indicate that even relatively minor disturbances to overall receptor structure (and/or residue properties) can significantly alter binding profile, making this an important caveat to consider when using this methodology to infer structural relationships.

Finally, crosslinking to CCL19 or CCL21 was attempted with UAA bearing mutants of CCR7 (figure 3.2.15, 16 & 17). However successful crosslinking could not be observed at any site of substitution. Considerable efforts at optimisation were attempted, including altering chemokine concentration, UV irradiation time, performing the assay with cells in suspension or directly on the cell layer, however crosslinking could still not be observed. When performed on cell layers a size shift of CCR7 that could represent adducts of CCR7 itself was observed. The region in which these substitution mutants have been generated does sit within a predicted CCR7 oligomerisation interface (Hauser *et al.*, 2016). However, it isn't possible to conclusively demonstrate this from these data. More importantly, it still does not result in chemokine crosslinking.

It is generally reported that crosslinking can only occur when receptor and ligand are within a distance of 8.9 Å, otherwise the activated UAA quenches in the aqueous environment surrounding the cell. It is possible that none of the 16 sites tested sit in close enough proximity to the chemokine, and that a wider screen of substitution sites may result in successful crosslinking. Given that the selected region tested is considered important to chemokine binding it is perhaps more likely that issues still exist in the methodology that prevent successful crosslinking. However, given the surprising effect UAA integration can have on ligand binding, and how this could impact on interpretation of crosslinking data, important considerations would need to be made before pursuing this methodology further.

In summary, successful translation of UAA bearing mutants of CCR7 capable of ligand binding has been shown. These mutants can demonstrate altered binding properties from WT CCR7, although for the most part total expression and chemokine binding capacity are not significantly different. However most importantly, crosslinking has not been observed at any site of UAA integration.

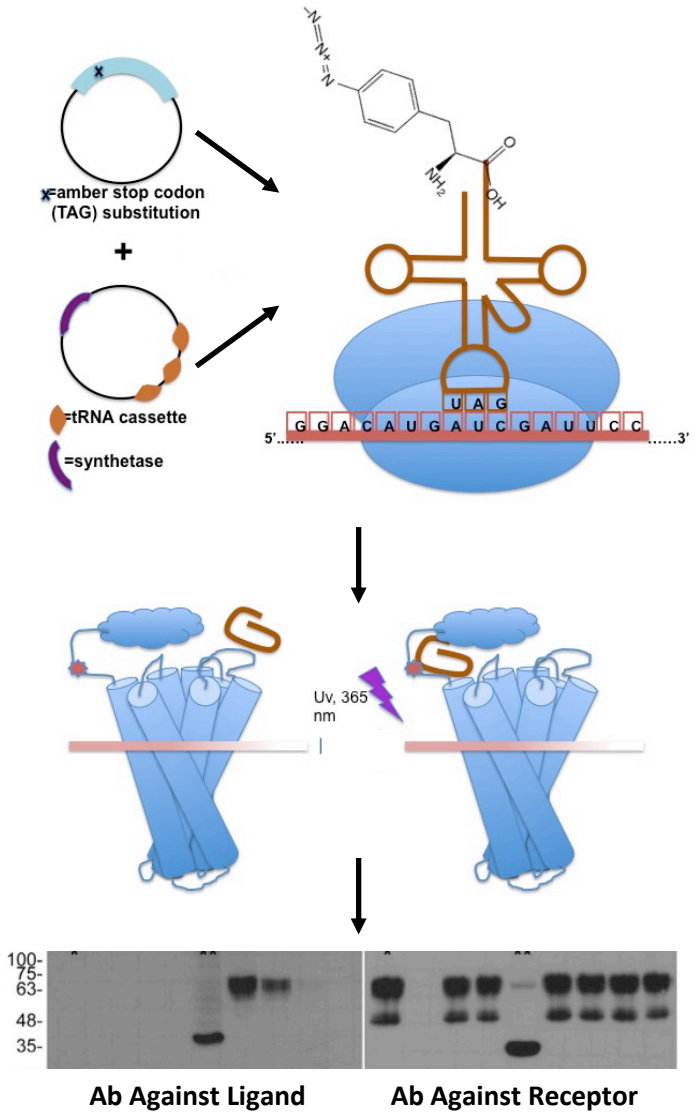

Figure 3.1.1 Graphical representation of UAA charging and incorporation into a GPCR and photo-crosslinking with ligand.

Plasmids expressing a TAG substitution mutant of a GPCR of interest and a tRNA/synthetase pair capable of charging and incorporating UAA in response to the TAG stop codon are co-transfected into eukaryotic cells in the presence of a UAA such as p-azidophenylalanine. This results in suppression of the amber stop codon and translation of full length receptor including the UAA at the desired site. When ligand is incubated with cells expressing this mutant receptor it binds the receptor and the UAA can be activated. In the case of p-azidophenylalanine this results in expulsion of a molecule of N_2 from the azide group, leaving a highly reactive nitrene that can covalently capture proteins within a distance of 8.9 Å. The resultant receptor/ligand adduct is visualised by western blotting, and if crosslinking has occurred successfully then ligand and receptor are separately detectable at the same size. Final panel adapted from Coin et al 2013

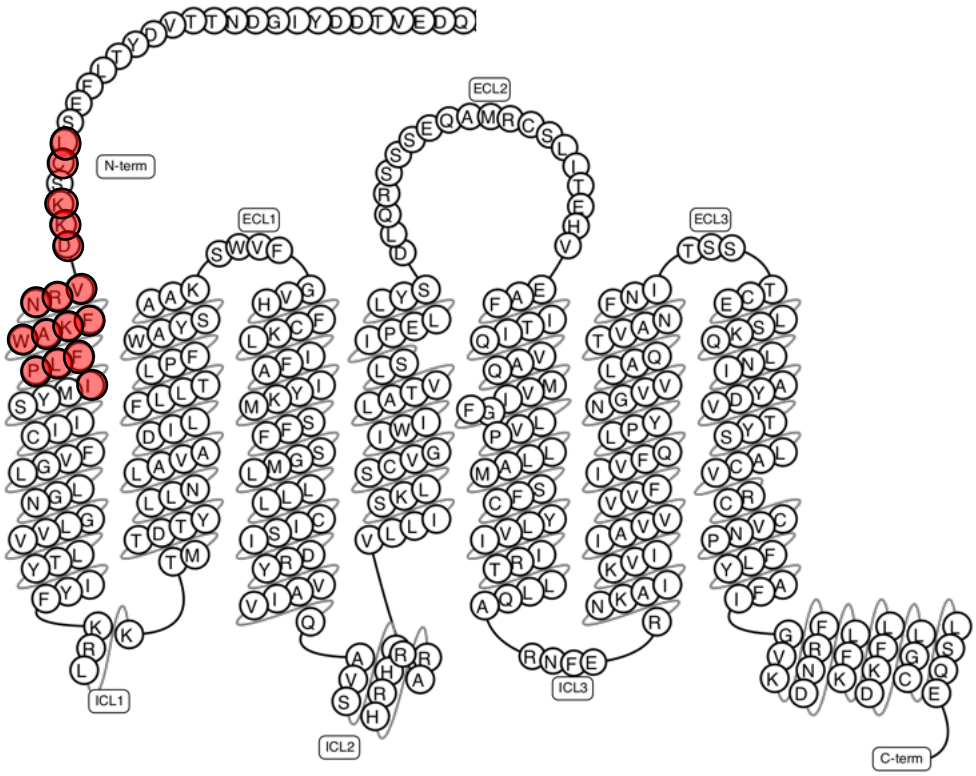

Figure 3.1.2 Schematic representation of CCR7 with TAG substitution mutants highlighted.

The selected sites for UAA integration are highlighted in red. Snake plot representation of CCR7 was adapted from http://gpcrdb.org/family/001_003_002_007/

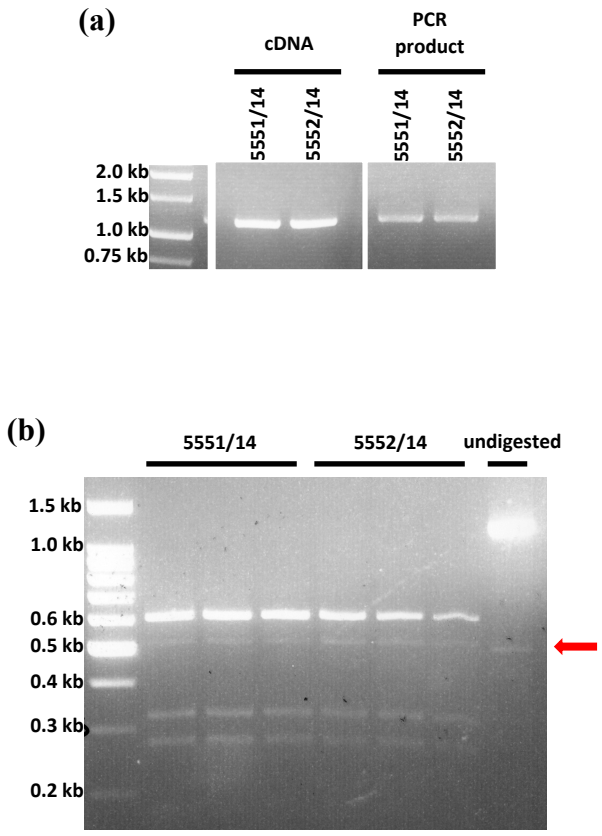

Figure 3.2.1 Amplification and digestion of CCR7-FLAG insert from human PBMC cDNA

(a) A band of estimated size 1.2 kb is produced when using CCR7 targeting primers against cDNA generated from human PBMC RNA. A second round of PCR from this fragment using the same primers does not result in significant amplification. (b) Digestion of the predicted CCR7 sequence with SacI produced fragments of size in keeping with the predicted bands of 591 bp, 318 bp and 273 bp. Although an additional band of around 500 bp was also seen in each digestion it is also present in the undigested controls (red arrow). This most likely represents a non-specific product from the initial PCR.

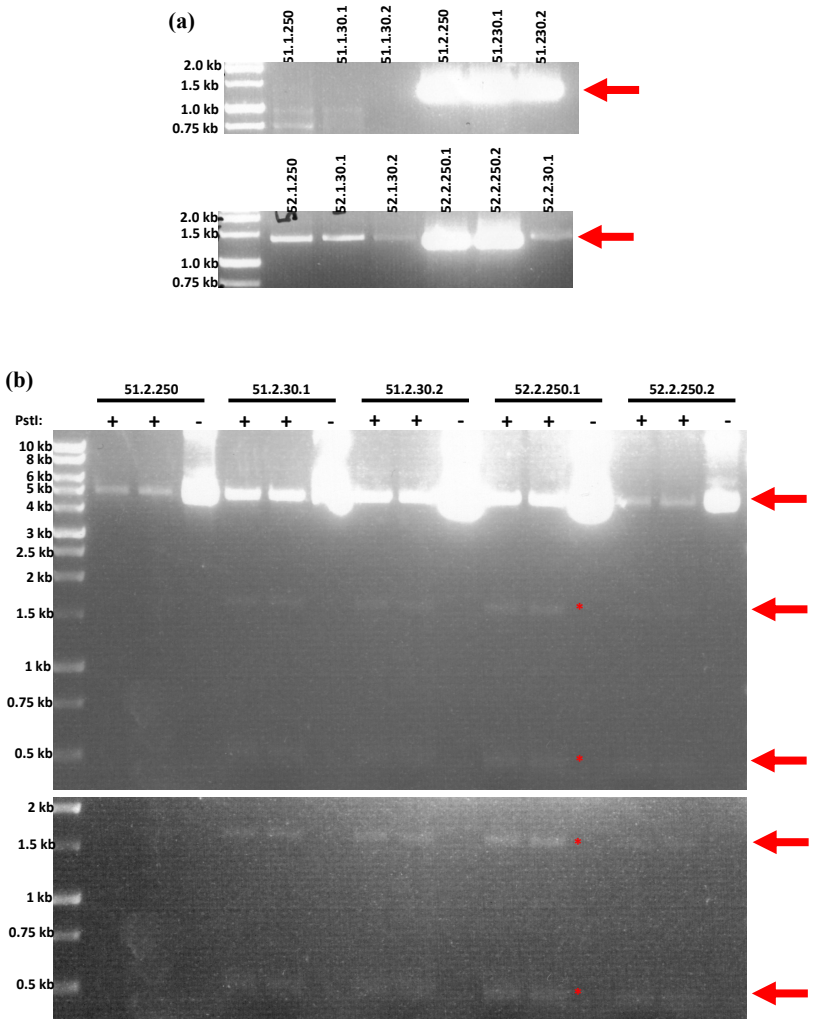

Figure 3.2.2 Evaluation of CCR7-FLAG (pEF6) plasmids by PCR and PstI digestion.

(a) PCR from 12 picked and denatured colony products, using a forward CCR7 primer and the reverse sequencing primer from the pEF6/V5-His-TOPO kit, generated a 1.4 kb PCR fragment, confirming successful insertion of CCR7-FLAG in the correct orientation for 5 out of 12 clones. (b) Digestion of the resultant plasmids with PstI produced fragments consistent with the predicted digestion products of 4.7, 1.7 and 0.5 kb. Images represent a baseline and contrast/brightness adjusted version of the same gel capture respectively. Red arrows highlight bands of interest.

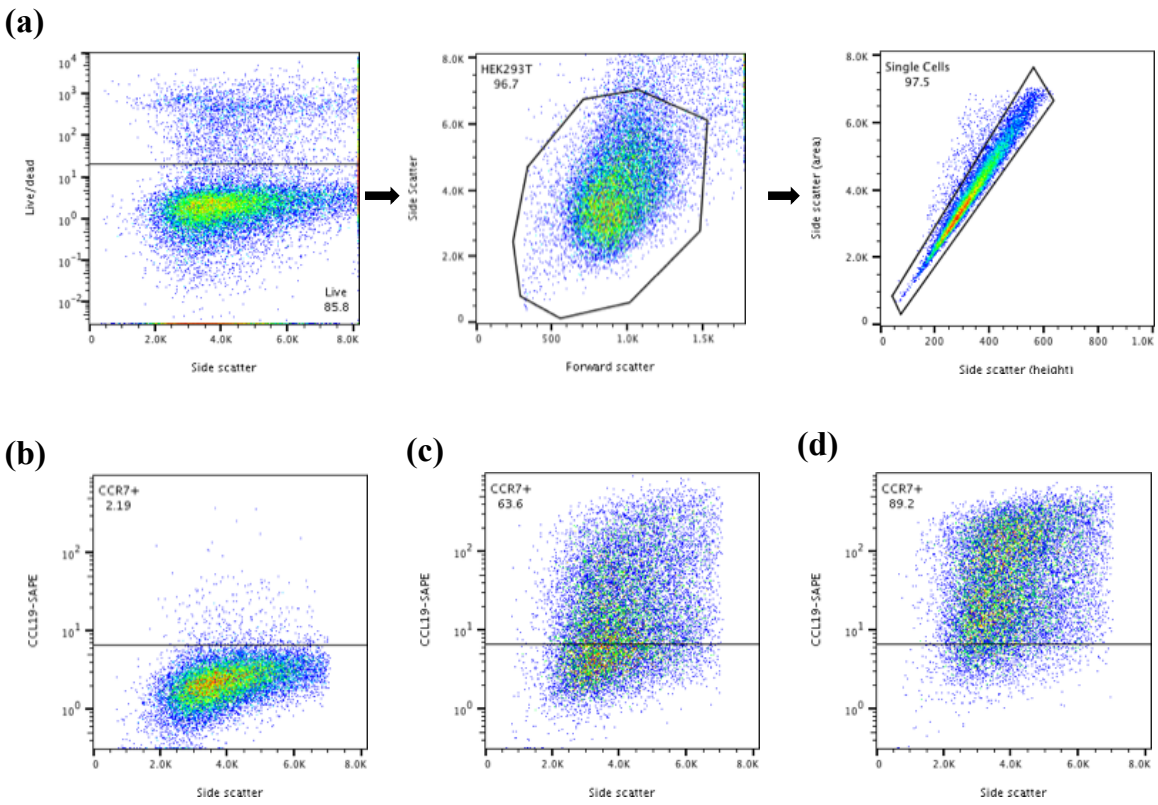

Figure 3.2.3 FACS analysis of CCR7 expressing HEK293T cells indicates cell surface expression of the receptor.

(a) HEK293T cells were analysed by flow cytometry. The gating strategy above was used to determine single, live HEK293T cells for analysis of expression of CCR7 (as indicated by staining with pre-conjugated biotinylated CCL19: streptavidin PE). From left to right, live cells were determined by DRAQ7 exclusion, with a gate applied on non-fluorescent cells. The main population of HEK293T cells was determined by comparing size (forward scatter) with granularity (side scatter), and single cells evaluated by comparing the height and area measures obtained for side scatter. With slight modifications this gating strategy was used on all subsequent FACS analysis using fluorescently bound chemokines. Staining with CCL19 is shown for HEK293T cells transiently transfected with empty vector (b), CCR7 clone 51.2.30.1 (c) and 52.2.250.1 (d). A CCR7 “positive” gate is applied based on the empty vector control in order to account for non-specific binding of CCL19 to cell surface glycans.

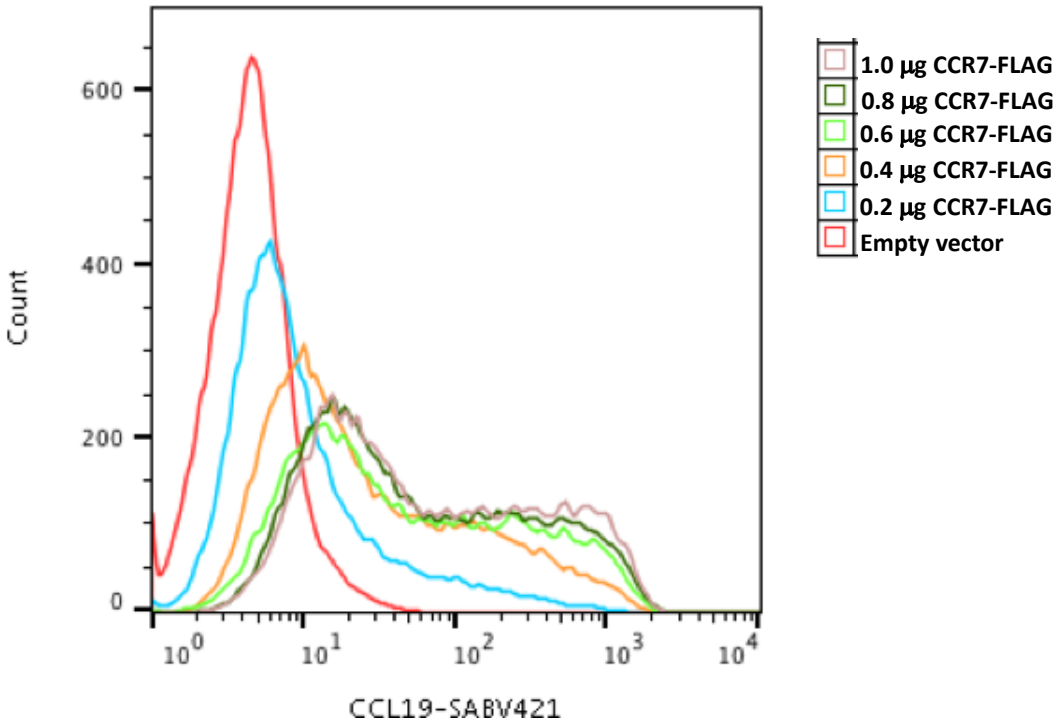

Figure 3.2.4 Surface expression of CCR7 plateaus with increasing plasmid concentration.

Increasing quantities of plasmid were transiently transfected into HEK293T cells seeded on a 12-well tissue culture plate. Transfected cells were again subjected to FACS analysis 48 hours post-transfection and stained with fluorescently labelled CCL19 (streptavidin-BV421) at a concentration of 25 nM. Cell count (Count, y-axis) and the fluorescence intensity of chemokine staining (CCL19-SABV421, x-axis) were plotted against each other.

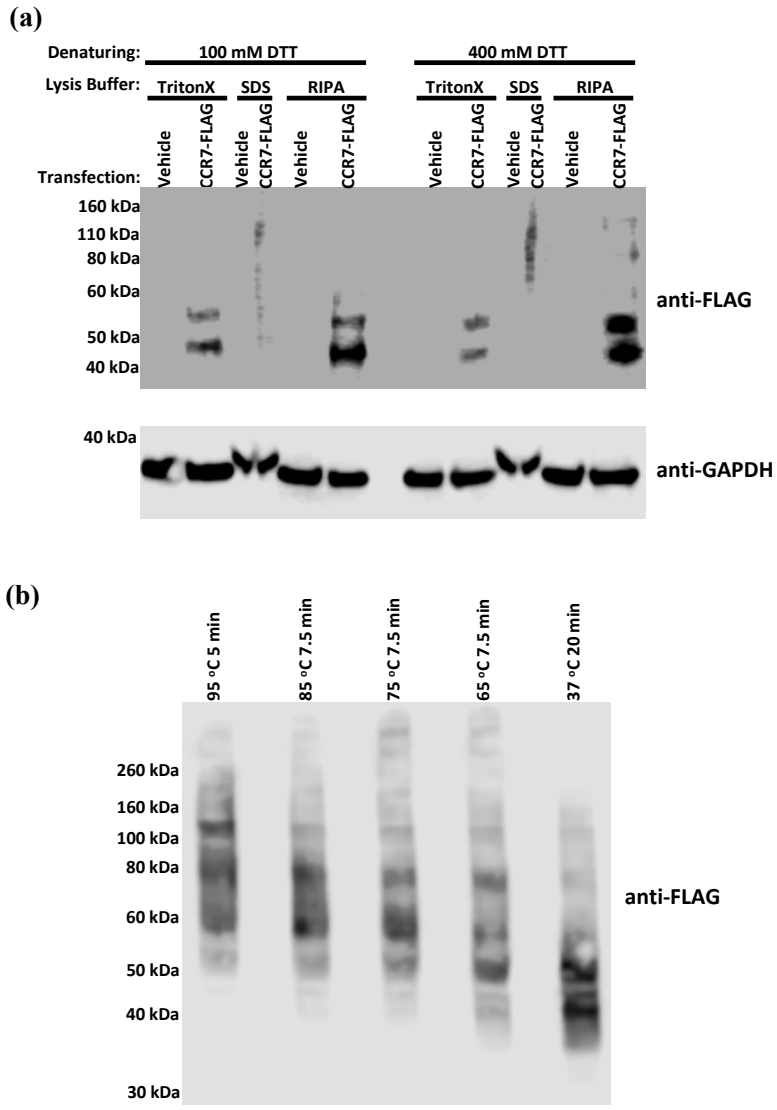

Figure 3.2.5 Western blotting for CCR7-FLAG confirms receptor expression and indicates optimal sample preparation conditions.

(a) Cells transfected with empty vector or CCR7-FLAG were harvested in either TritonX, SDS Urea or RIPA lysis buffer, and reduced with 100 or 400 mM DTT before being separated by SDS-PAGE and transferred to PVDF membrane, then incubated with antibodies sensitive to FLAG-tag and human GAPDH. (b) Lysate from CCR7-FLAG transfected HEK293T cells was subjected to varying denaturing temperatures and incubation times at a constant DTT concentration of 100 mM.

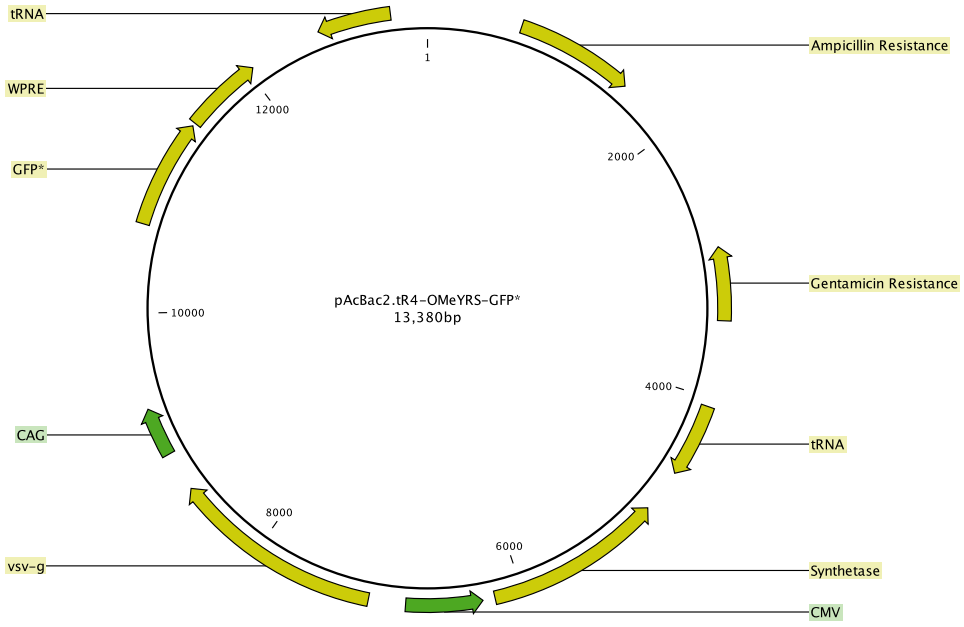

Figure 3.2.6 Plasmid map of pAcBac2.tR4-OMeYRS-GFP*

The above plasmid map was generated using CLC Genomics software and the complete plasmid sequence, provided by Addgene. Feature sequences are highlighted where possible from information provided in the original reference (see text).

CMV: Cytomegalovirus immediate early promoter

CAG: synthetic promoter consisting of the CMV early enhancer element, the promoter, first exon and first intron of the chicken β-actin gene and the splice acceptor of the rabbit β-globin gene.

VSV-G: viral envelope glycoprotein

GFP*: amber stop codon bearing mutant of GFP

WPRE: Woodchuck Hepatitis Virus (WHP) Posttranscriptional Regulatory Element

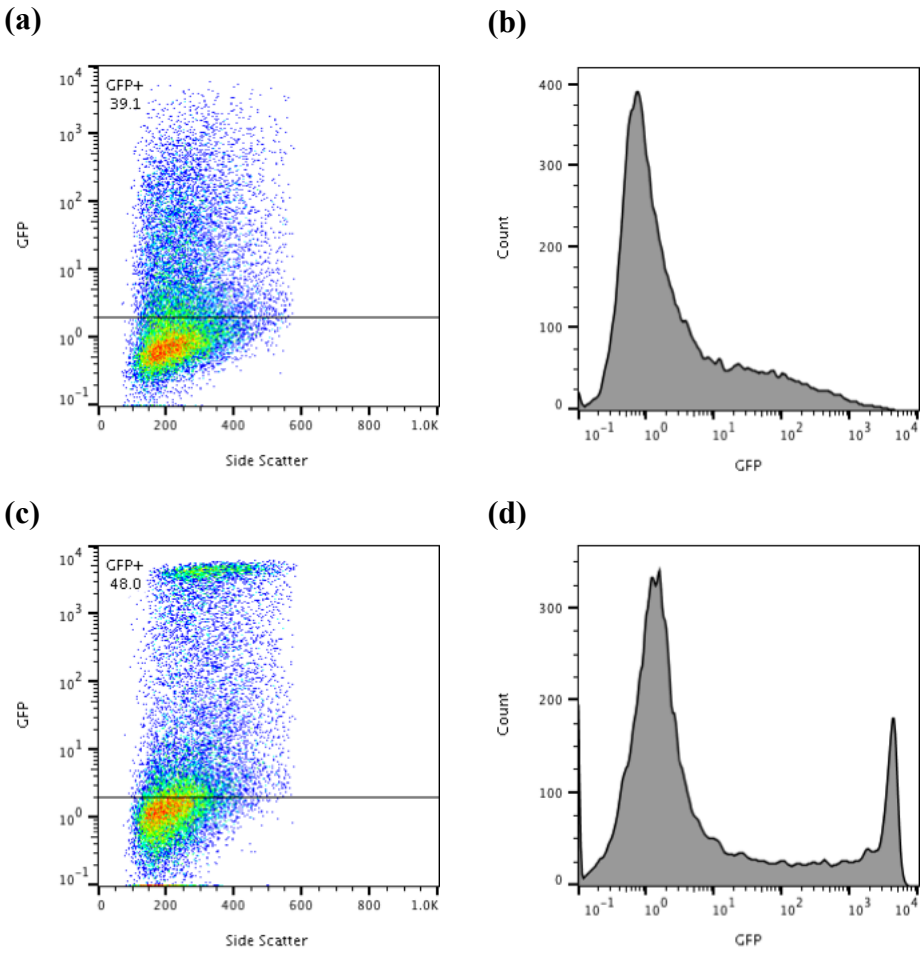

Figure 3.2.7 Expression of UAA bearing GFP in HEK293T cells.

HEK293T cells were transiently transfected with pAcBac2.tR4-OMeYRS-GFP* and maintained in media either free from (a&b) or supplemented with (c&d) 1 mM p-azidophenylalanine, and expression of GFP assessed by flow cytometry. GFP+ gate was applied based on cells transfected with empty vector only.

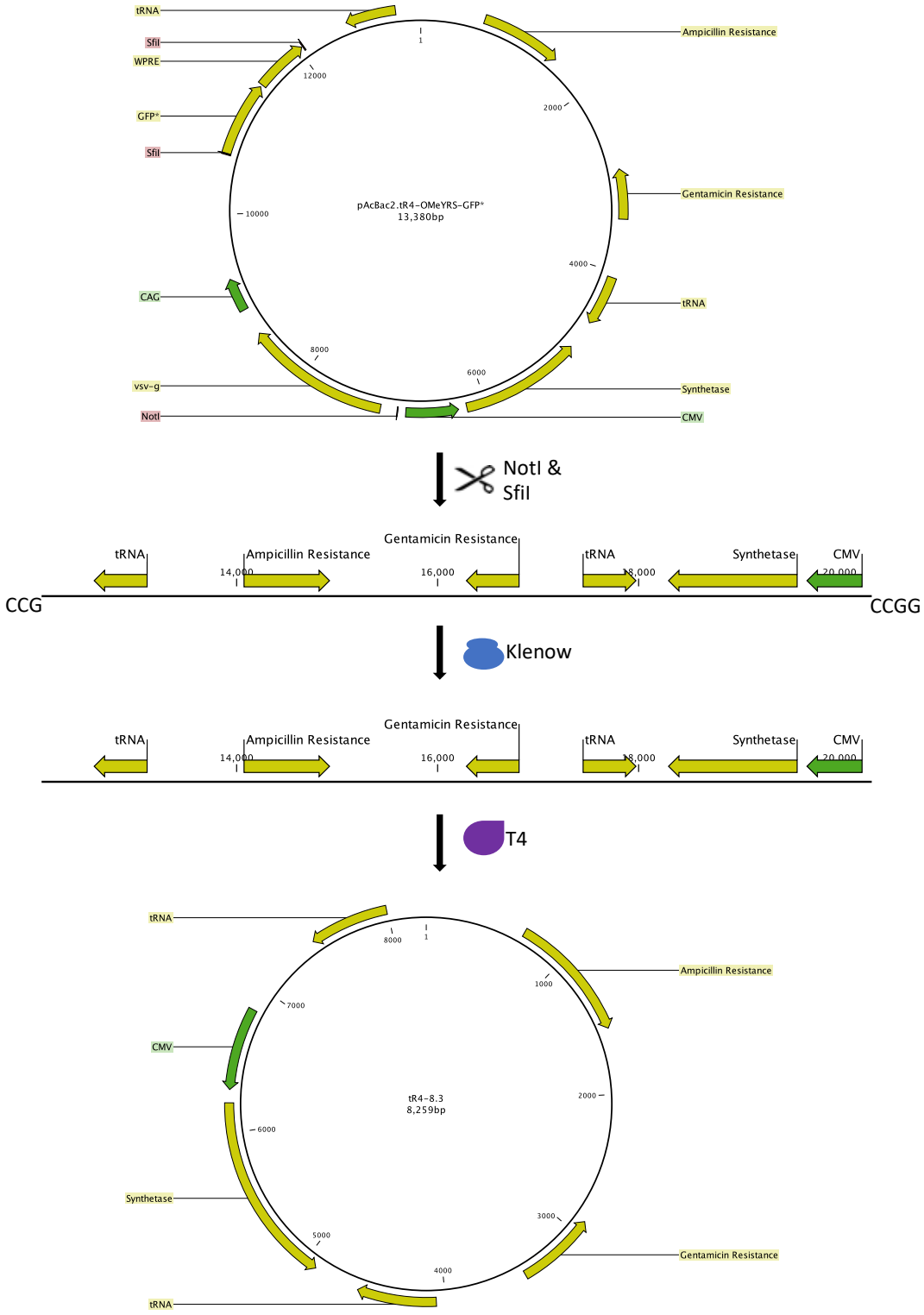

Figure 3.2.8 Graphical summary of tR4-8.3 restriction strategy.

The original pAcBac2.tR4-OMeYRS-GFP* plasmid was subjected to a 2-step digestion first with NotI then SfiI. The 8.3 kb linear product that resulted was then purified and treated with Klenow polymerase fragment, removing the 3' overhangs left from the restriction reaction. This was then blunt end ligated with T4 DNA ligase, to close this into a new plasmid dubbed "tR4-8.3", ready for bacterial transformation.

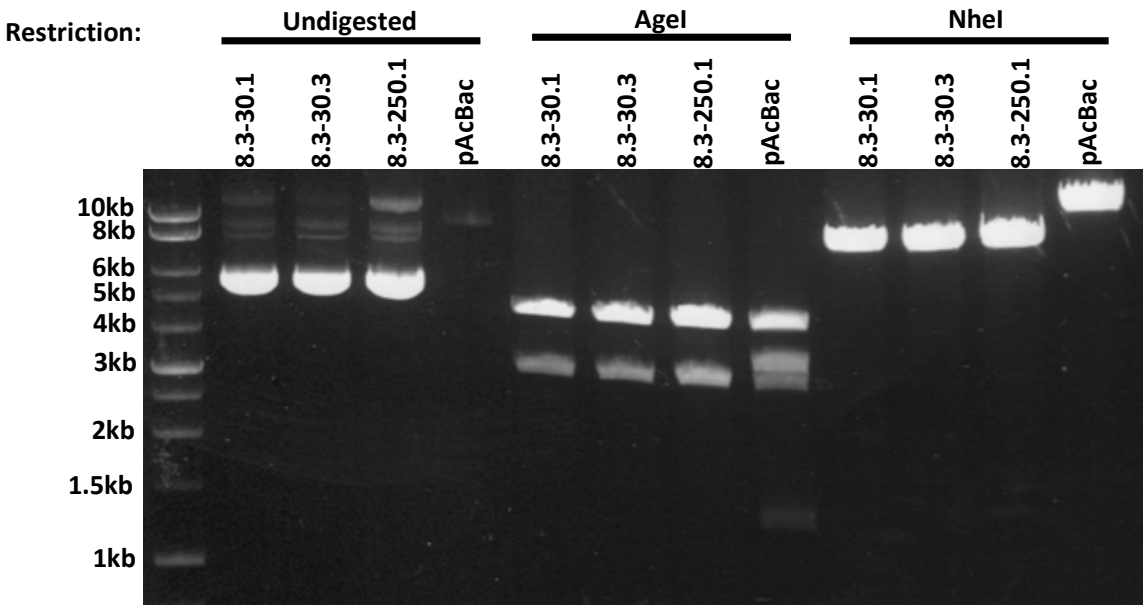

Figure 3.2.9 Restriction digest of tR4-8.3 with AgeI and NheI.

To evaluate the new tR4-8.3 construct 3 clones were picked, plasmid prepared, restriction digest carried out with 2 different enzymes, AgeI and NheI, and comparison made with the unaltered pAcBac2.tR4-OMeYRS-GFP*. This reaction is predicted to result in the following fragment sizes:

AgeI; pAcBac2.tR4-OMeYRS-GFP = 4.9, 3.8, 3.3 & 1.4 kb.

tR4-8.3 = 4.9 & 3.3 kb.

NheI; pAcBac2.tR4-OMeYRS-GFP = 13.4 kb.

tR4-8.3 = 8.3 kb.

A single clone, 8.3.250.1, was used from this point forward.

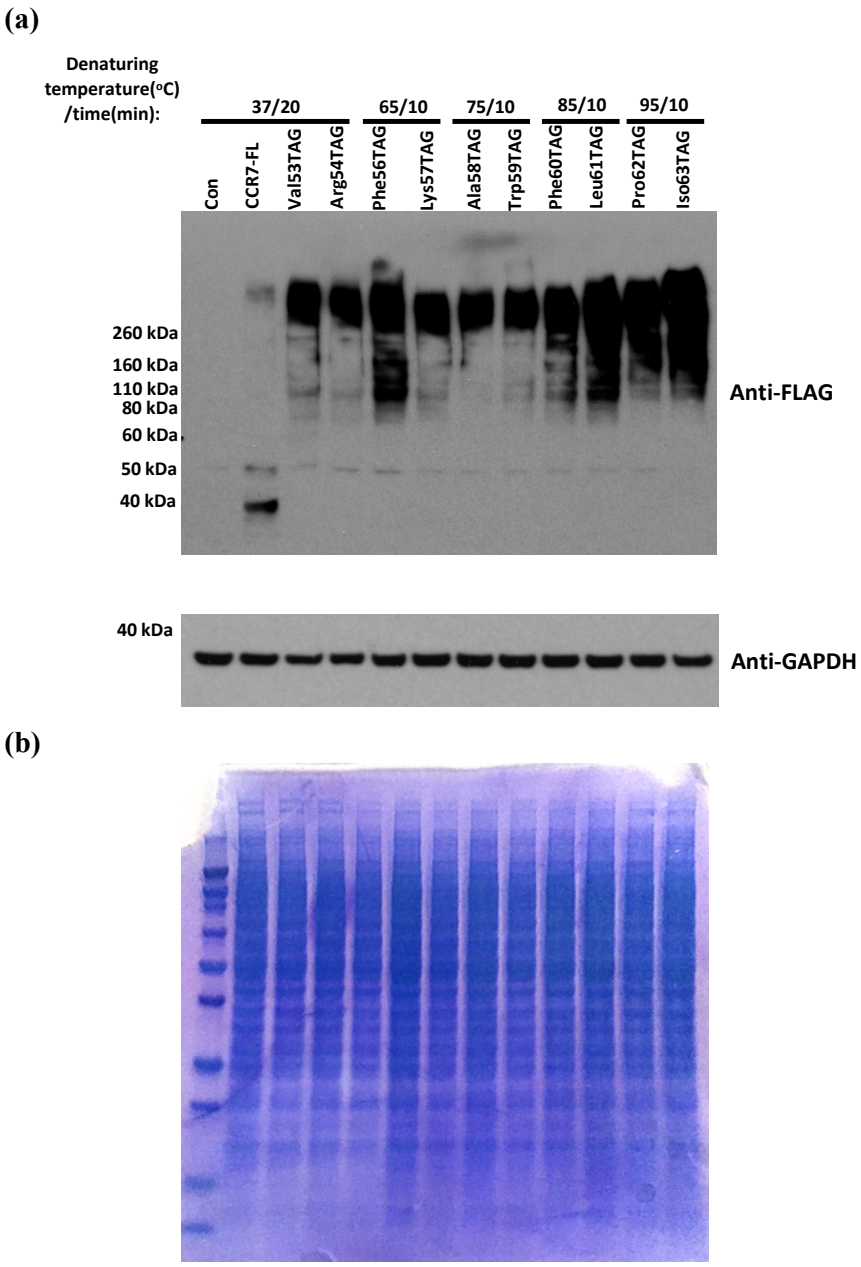

Figure 3.2.10 TAG substitution mutants of CCR7 are expressed in the absence of both UAA or compatible tRNA/synthetase: western blot & Coomassie blue staining.

(a) Whole cell lysate from HEK293T transfected with either empty vector, WT CCR7-FLAG or one of the TAG substitution mutants of CCR7-FLAG were reduced, denatured using a final concentration of 100 mM DTT with varying temperatures and incubation times, then assessed by western blotting for FLAG (CCR7) and human GAPDH (loading control). (b) Coomassie blue staining of an identical gel was also done to reveal total protein distribution.

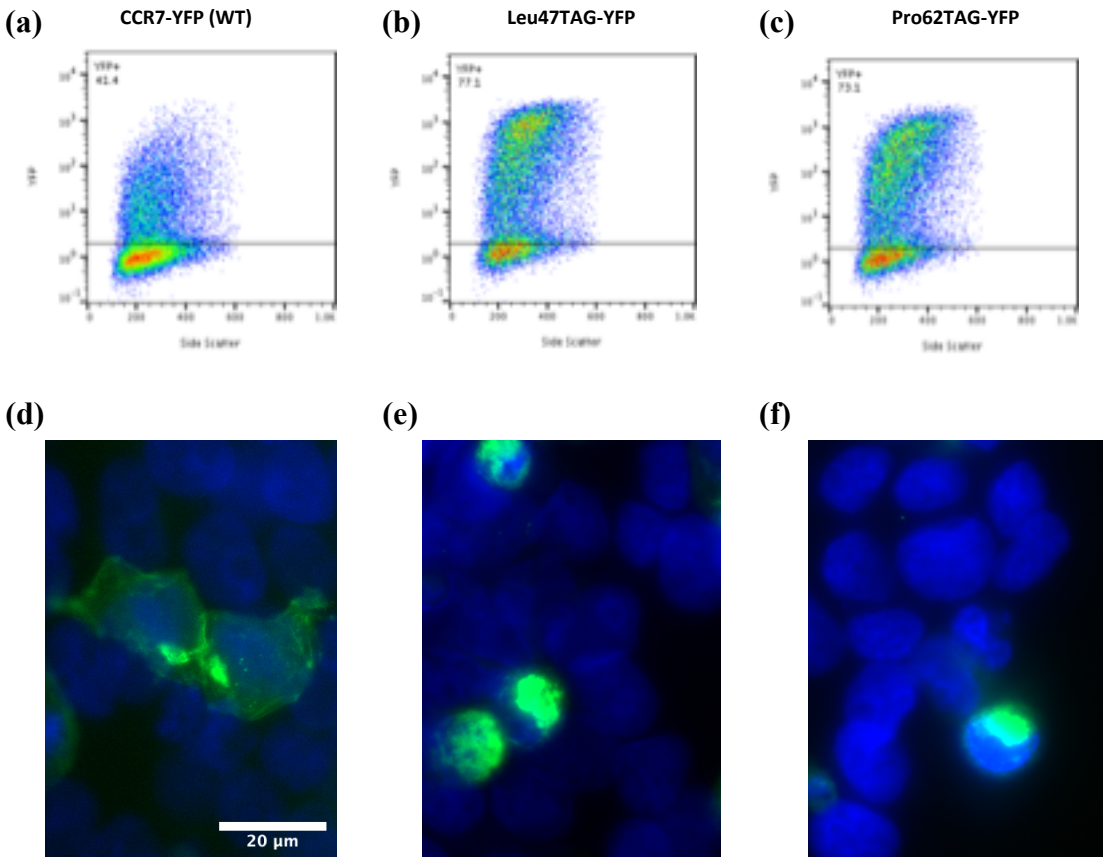

Figure 3.2.11 TAG substitution mutants of CCR7 are expressed in the absence of both UAA or a compatible tRNA/synthetase pair: FACS and epiflourescence microscopy.

Plasmids expressing WT CCR7-YFP (a&d), Leu47TAG CCR7-YFP (b&e) and Pro62TAG CCR7-YFP (c&f), were transfected into HEK293T cells, then evaluated by flow cytometry (a-c) or epiflourescence microscopy (d-f). A YFP+ gate was applied based on the empty vector control from the same experiment. Images are representative of multiple fields of view.

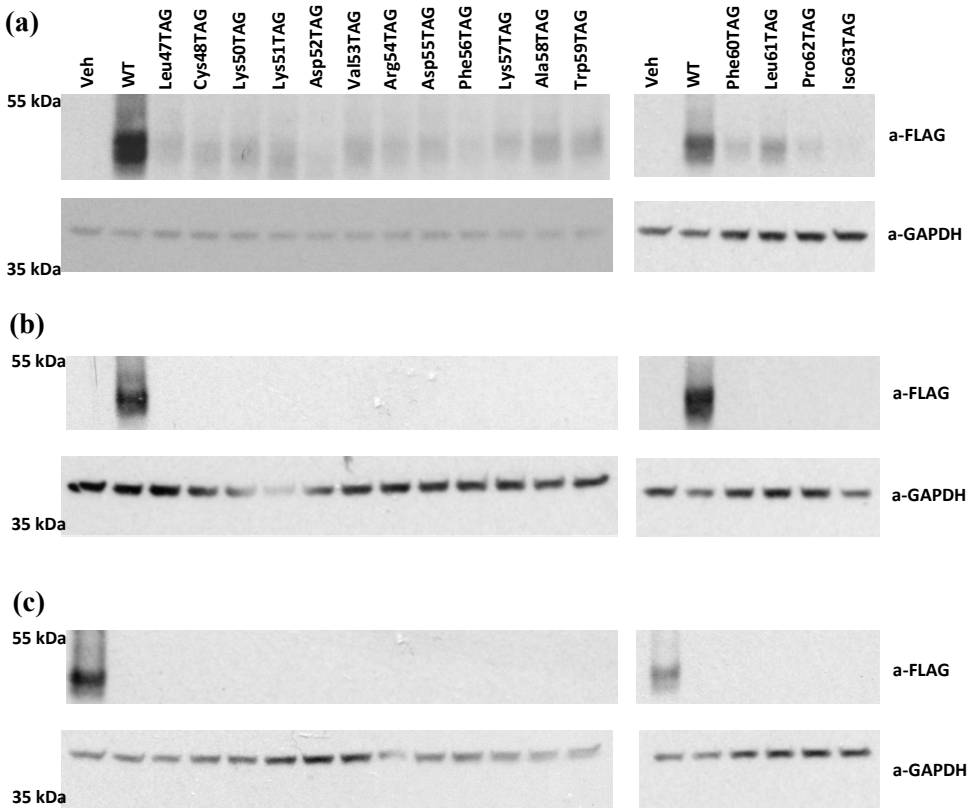

Figure 3.2.12 Integration of p-azidophenylalanine into CCR7; western blotting.

HEK293T cells were transiently transfected with empty vector, CCR7-FLAG or one of the 16 TAG substitution mutants of CCR7-FLAG, whole cell lysate obtained, and the resultant blots probed for full length CCR7 expression (FLAG) and GAPDH. Cells were (a) additionally transfected in a 1:1 ratio with tR4-8.3 and media supplemented with 1 mM p-azidophenylalanine, (b) transfected with tR4-8.3 but not supplemented with the UAA or (c) transfected with empty vector in place of tR4-8.3 and media supplemented with UAA. n.b. Vehicle and wild type controls were swapped in (c), the loading order is otherwise unchanged from (a) and (b).

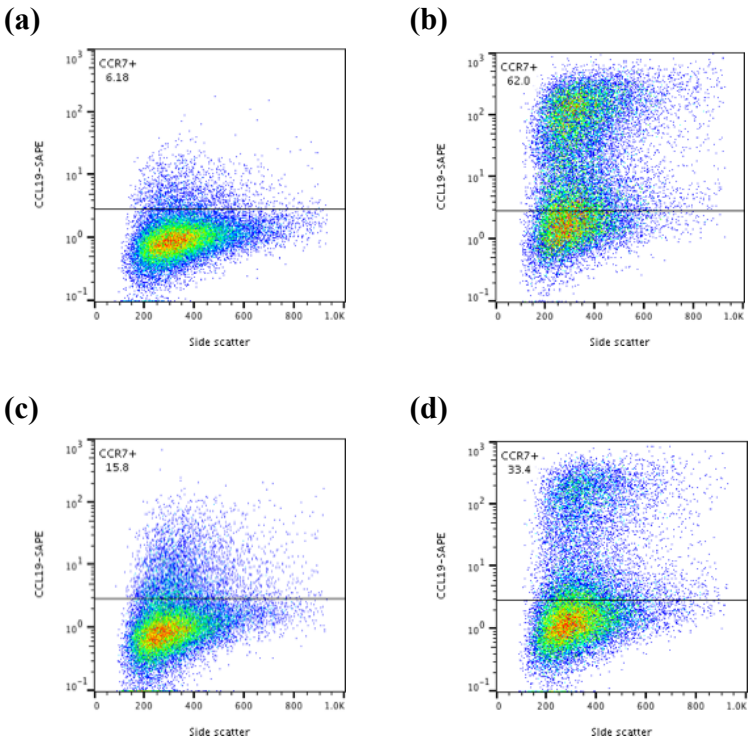

Figure 3.2.13 Integration of p-azidophenylalanine into CCR7; flow cytometry.

Cell surface expression of CCR7 was once again evaluated utilising labelled CCL19. Here exemplar FACS plots from HEK293T cells transiently transfected with tR4-8.3 and either empty vector (a), wild type CCR7 (b) or a selection of 2 TAG substitution CCR7 mutants (c&d) are shown.

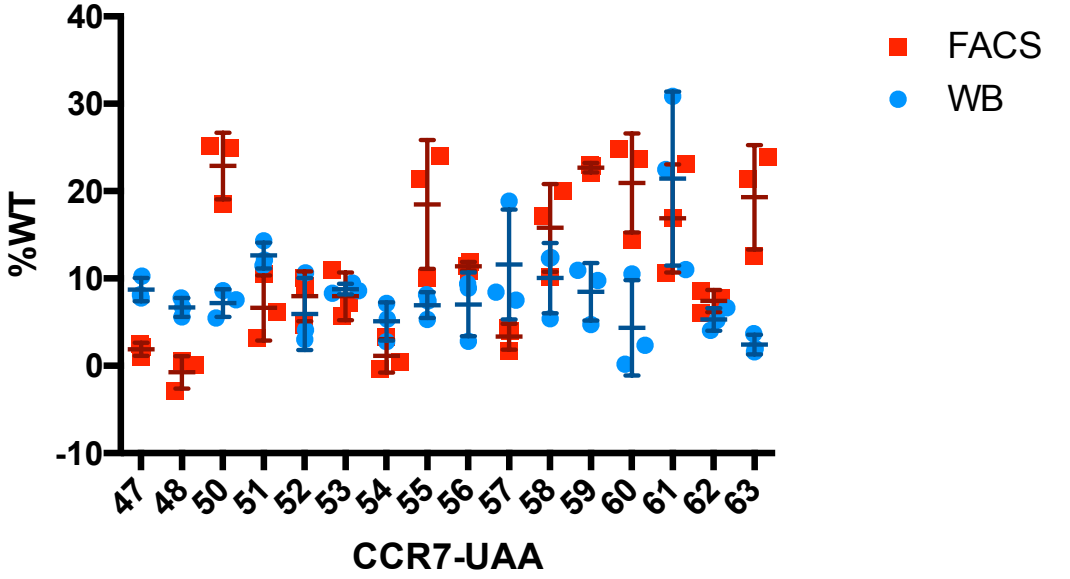

Figure 3.2.14 Integration of p-azidophenylalanine into CCR7; western blotting compared with flow cytometry.

Expression as evaluated by both western blotting of whole cell lysate (blue), and assessment of binding to fluorescently labelled CCL19 by flow cytometry (red), were compared. Band densitometry was determined using the ImageJ gel analyser tool for both FLAG (CCR7) and GAPDH (loading control), with relative expression calculated as FLAG/GAPDH, which was then expressed as a percentage of wild type CCR7 in the same experiment. CCL19 staining was enumerated as a percentage of wild type CCR7 for all 16 TAG substitution mutants by obtaining mean fluorescence intensity (MFI) values of all cells in the live singlet population in the PE channel, and subtracting the MFI from empty vector transfected controls from all samples as non-specific chemokine binding/background prior to calculating percentage. (n=3 biological replicates ± SD)

Substitution:	WB mean:	FACS mean:	Difference:	P value:
47	8.7	1.9	6.8	0.00150
48	6.7	-0.7	7.4	0.00390
50	7.2	22.9	-15.7	0.00276
51	12.6	6.6	6.0	0.06059
52	5.9	8.0	-2.0	0.52253
53	8.8	8.0	0.8	0.63698
54	5.1	1.1	3.9	0.07851
55	7.0	18.5	-11.5	0.05651
56	7.0	11.4	-4.4	0.11028
57	11.6	3.3	8.3	0.09178
58	10.0	15.8	-5.7	0.19697
59	8.5	22.7	-14.2	0.00180
60	4.4	20.9	-16.6	0.02163
61	21.4	16.9	4.6	0.53680
62	5.3	7.4	-2.1	0.11270
63	2.4	19.3	-16.9	0.00864

Table 3.2.1 Integration of p-azidophenylalanine into CCR7; summary of differences in receptor expression as determined by Western blotting and flow cytometry.

Evaluation of expression of UAA bearing mutants of CCR7, as determined by either Western blotting or flow cytometry, revealed significant differences between the two modalities. Here the data presented in figure 3.2.14 is listed and compared. The mean value (% of wild type CCR7) of 3 biological replicates obtained from each is listed here, along with the "difference" between measures (WB mean - FACS mean = difference), and the statistical significance of this difference expressed with the P value (one-way ANOVA with post hoc Holm-Sidak correction).

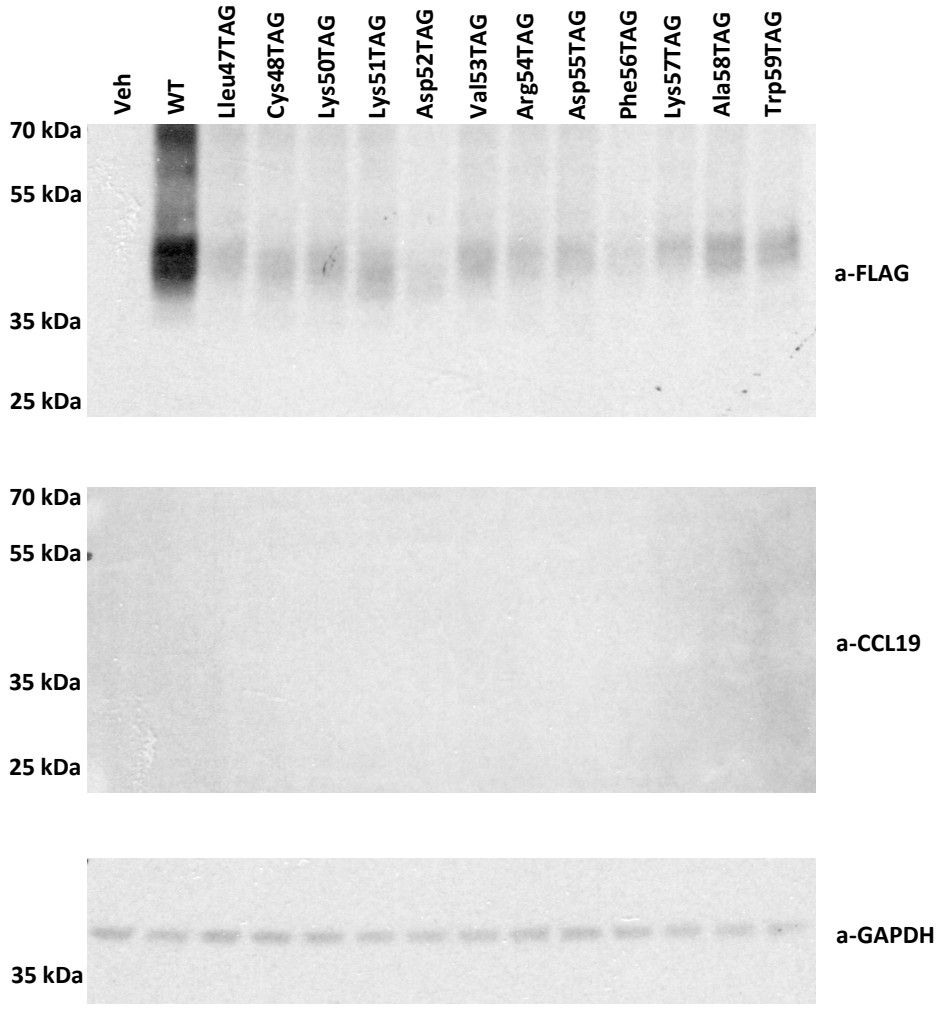

Figure 3.2.15 Photoactivation of p-azidophenylalanine fails to capture chemokine at any substitution site; CCL19 (cuvette)

Cells expressing either WT CCR7-FLAG or one of the 16 UAA bearing mutants (selection of 12 shown here) were lifted by mechanical disruption of the cell layer in ice-cold PBS, incubated with 100 nM CCL19 and transferred to cuvettes before being exposed to UV radiation. Whole cell lysate was obtained and evaluated for CCL19, FLAG (CCR7) and GAPDH by western blotting. Representative of 3 independent experiments.

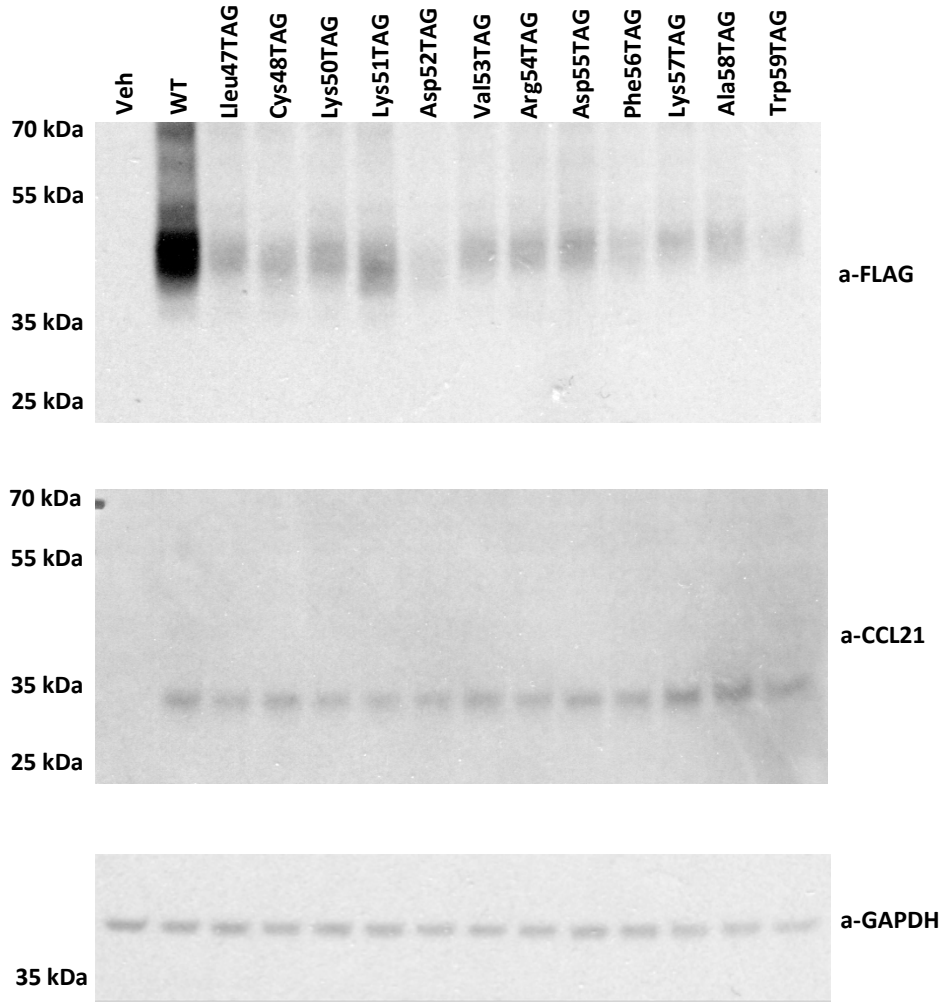

Figure 3.2.16 Photoactivation of p-azidophenylalanine fails to capture chemokine at any substitution site; CCL21 (cuvette)

Cells expressing either WT CCR7-FLAG or one of the 16 UAA bearing mutants (selection of 12 shown here) were lifted, incubated with 100 nM CCL21 and transferred to cuvettes before being exposed to UV radiation. Whole cell lysate was obtained and evaluated for CCL21, FLAG (CCR7) and GAPDH by western blotting. Representative of 3 independent experiments.

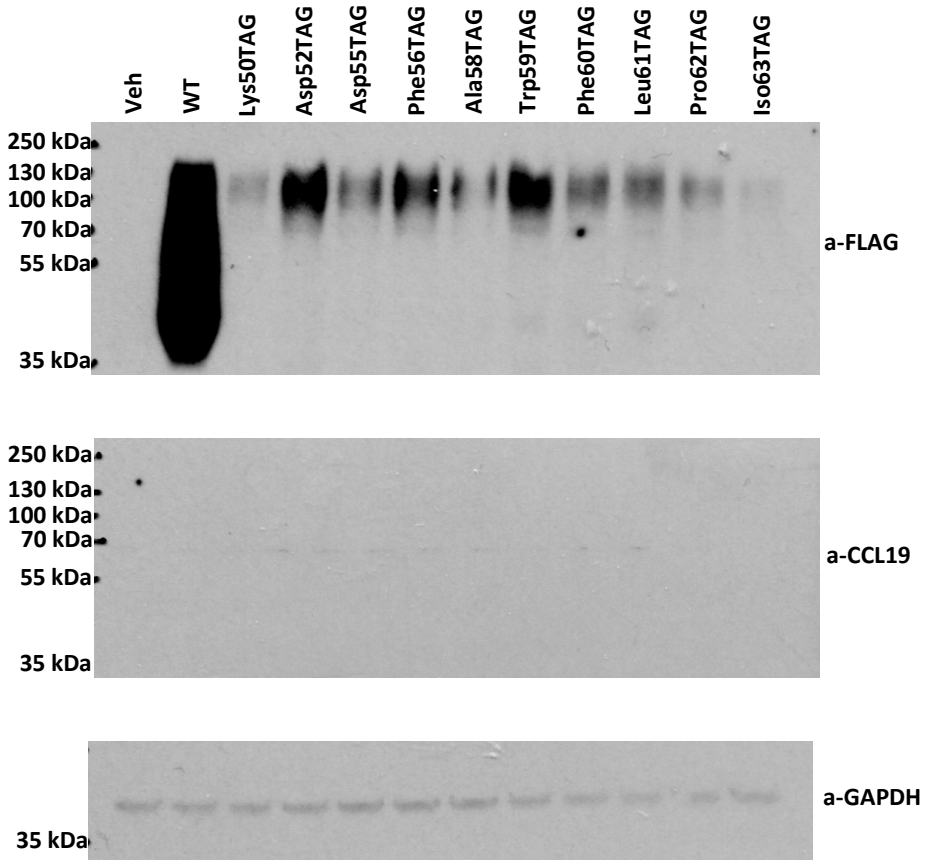

Figure 3.2.17 Photoactivation of p-azidophenylalanine fails to capture chemokine at any substitution site; CCL19 (plate)

Cells expressing either WT CCR7-FLAG or one of a selection of 10 of the original 16 UAA bearing mutants were incubated with 100 nM CCL19 before being exposed to UV radiation on the tissue culture plate. Whole cell lysate was obtained and evaluated for CCL19, FLAG (CCR7) and GAPDH by western blotting.

Site:	aa:	"Difference":	MW (Da):	inc/dec (Da):	Polar (Y/N):	changed (Y/N):	Hydrophobic (Y/N):	changed (Y/N):2	Charged (+/-):	changed (Y/N):3
47	leucine	6.8	131.08	75.125			Y	N		
48	cysteine	7.4	103.01	103.195	Y	Y				
50	lysine	-15.7	128.09	78.115					+	Y
59	tryptophan	-14.2	186	20.205	Y	Y				
60	phenylalanine	-16.6	147.07	59.135			Y	N		
63	isoleucine	-16.9	113.08	93.125			Y	N		
	p-azido-phenylalanine		206.205		N		Y		neu	

Table 3.2.2 Changes in amino acid characteristics between WT and UAA mutants demonstrating significant differences between ligand binding and expression

4 Evaluation of the ligand bias of CCR4, CCR7 and CCR10

4.1 Introduction

Chemokine biology is marked by both a high number of gene duplication events, low sequence homology and functional redundancy of ligands (often seen in inflammatory chemokine signalling), as well as highly conserved single ligand/receptor couplings that have endured more or less unchanged since first emerging. This disparity can be quite jarring. For example, CCR2 can bind CCL2, 7, 8, 11, 13, 16 and 26 (Charo and Ransohoff, 2006), whereas CXCR4, frequently regarded as the primordial chemokine receptor, has only ever demonstrated binding to one chemokine, CXCL12 (Gangadhar, Nandi and Salgia, 2010). Evolutionary forces have driven extensive gene duplication for the ligands of CCR2, presumably pushed by the needs of an increasingly complex immune system, while conserving the status quo in the CXCL12/CXCR4 signalling axis (Zlotnik, Yoshie and Nomiyama, 2006). Indeed, genetic ablation of either CXCR4 or CXCL12 is perinatally lethal, with significant defects in haematopoiesis and bone marrow engraftment, angiogenesis and cardiac formation, neurogenesis and renal development, suggesting the requirement for conservation over divergence in this coupling (Ara *et al.*, 2005; Takabatake *et al.*, 2009; Zhu and Murakami, 2012). Conversely CCR2 knockout animals have few overt physiological differences to wild type, with defects in myeloid recruitment and a resultant altered phenotype only readily apparent during models of inflammation, injury and cancer (Boring *et al.*, 1997; Willenborg *et al.*, 2012; Li *et al.*, 2013).

However, there are multiple chemokine receptors that have evolved to interact with only a pair of ligands. As mentioned previously these include CCR4, CCR7 and CCR10. Perhaps more interesting though is that within each signalling axis a very similar pattern of biased agonism has developed, with one arrestin (CCL22, CCL19, CCL27) and one G-protein (CCL17, CCL21, CCL28) biased chemokine interacting with each receptor (Mariani *et al.*, 2004; Rajagopal *et al.*, 2013; Corbisier *et al.*, 2015). Additionally, high sequence conservation has resulted in chemokines capable of cross-species receptor interaction in the case of CCL19 with CCR7 (previous unpublished observations from our group). This implies some evolutionary advantage in initially duplicating a single chemokine for each receptor and permitting divergence in signalling properties and/or tissue expression pattern within this pair. However subsequent to this these chemokine pairs are maintained with minor, or no, further duplication events, which has occurred on at least 3 separate occasions.

We know from knockout studies in mice that loss of CCL19 and CCL21 carry distinct phenotypes. Loss of both CCL19 and CCL21(ser) in plt/plt mice results in significantly altered secondary lymphoid organ (SLO) architecture, with the distinction between T-cell and B-cell zones lost, and an attenuation of recruitment of T-cells and DCs to SLOs resulting in impaired/delayed antigen specific immune responses (Gunn *et al.*, 1999). CCL19 knockout alone however demonstrates normal SLO structure and cellular recruitment to SLOs in these animals, but poorer naive T-cell survival, as demonstrated by adoptive transfer experiments (Britschgi, Favre and Luther, 2010). Additionally, CCL19 and CCL21 have distinct tissue distributions. Due to its avid glycan binding capacity, CCL21 gradients have been demonstrated within the lymphatic vessels of the skin (Weber *et al.*, 2013) and the roof of the subcapsular sinus of LNs, maintained by the atypical chemokine receptor ACKR4 (Ulvmar *et al.*, 2014), in one of the only demonstrations of chemokine gradients in vivo. CCL21 is expressed by HEVs and fibroblastic reticular cells of the T-cell zones (Carlsen *et al.*, 2005). Basal expression of CCL19 however is restricted to just fibroblastic reticular cells of the T-cell zone (Link *et al.*, 2007). This, in conjunction with their unique signalling profiles, would indicate that duplication of an ancestral chemokine in this case was not to introduce redundancy into the system and has instead resulted in functionally distinct ligands for CCR7.

The ligands of CCR10 have an even more disparate tissue distribution at rest; CCL27 is expressed almost exclusively by keratinocytes in the skin (Morales *et al.*, 1999) and drives the recruitment of a selection of skin-tropic T-cell subsets to this organ. CCL28 on the other hand is expressed by the mucosal epithelium of various tissues (Pan *et al.*, 2000), where it is thought to act to retain IgA producing plasmablasts in these tissues and may additionally act directly as an anti-microbial agent due to its elongated and charged C-terminus. These distinct tissue distributions also fit well with the presumed biased agonism of CCR7 and CCR10; with a G-protein biased agonist retaining/guiding cells into tissues, and a β-arrestin biased agonist guiding cells within tissues, eventually leading to desensitisation of their cognate receptors and loss of localisation cues from these chemokines.

Given the intriguing and complex evolutionary history of this 2-chemokine model, as well as the potential implications in both healthy and disease states, there is a need to further evaluate receptors that demonstrate this curious property. This is particularly true of CCR4, which lacks the more detailed signalling data available for CCR7 and CCR10 (Rajagopal *et al.*, 2013; Corbisier *et al.*, 2015). Like CCR7, distribution of the cognate ligands of CCR4 is presumed to follow a similar pattern of a G-protein biased agonist (CCL17)

providing initial guidance cues, in this case resulting in extravasation of CCR4 expressing T-cells from the blood into skin, and an arrestin biased agonist (CCL22) providing guidance within the tissue before desensitising these cells to CCR4 signalling (Yoshie and Matsushima, 2015).

Expression of CCL17 and CCL22 was evaluated in inflamed tissues compared to untreated, in order to determine if the normally controlled expression of these homeostatic chemokines is altered in response to inflammatory insult and determine what (if any) bearing this might have on CCR4 activity. The recruitment of specific signalling apparatus to CCR4, CCR7 and CCR10 as a result of interaction with their cognate ligands was assessed, with the intention to create a more complete signalling profile than that currently available, in particular for CCR4. Bioluminescence resonance energy transfer (BRET) based assays were used to evaluate the association of signalling machinery and chemokine receptors in response to chemokine. BRET is described as the non-radiative transfer of energy from a 'donor', typically a luciferase, to an 'acceptor' fluorescent protein whose excitation spectrum overlaps with the emission spectrum of the 'donor', like YFP (Brown, Blumer and Hepler, 2015). This is in fact a natural process of some marine species (Ward and Cormier, 1979). If the distance between the two closes to less than 10 nm then the luciferase, instead of emitting light, directly transfers the energy required for light emission by a non-radiative process to YFP. This results in a reduction in luciferase output and emission from YFP.

It is possible in HEK293T cells to express both a 'donor' and 'acceptor' fused to proteins of interest in order to analyse the interaction between the two. In the case of β-arrestin recruitment, a fusion of renilla luciferase with either β-arrestin 1 or 2 is co-transfected with C-terminally yellow fluorescent protein (YFP) tagged CCR4 or CCR7. Luciferase and YFP signal can be detected separately, and at rest the gain for each channel is adjusted such that the ratio of YFP/Luciferase signal is as near to 1 as possible. Association of chemokine with the receptors triggers for β-arrestin recruitment, closing the distance between 'donor' and 'acceptor' to below 10 nm, resulting in BRET and consequently an increase in YFP emission. This increases the ratio above 1 giving a "BRET signal", with this increase being proportional to amount of chemokine applied, allowing for the determination of pEC_{50} values of recruitment for each ligand (summarised in figure 4.1.1).

The recruitment of G_{α} subunits to GPCRs by their ligands can also be assessed utilising BRET based methods, however this requires some additional considerations. In this instance, a single molecule construct (known as a systematic protein affinity strength

modulation, or SPASM, biosensor) is used in place of two separate fusion proteins (Malik *et al.*, 2017). Here the chemokine receptor is linked to a fluorescent 'acceptor', nano-luciferase 'donor' and a peptide fragment of a G_{α} subunit sufficient for recruitment to the receptor, with each separated by linker regions that maintain flexibility. Due to the plasmid background in which these constructs sit (pcDNA5/FRT/TO) it is possible to generate stable cell lines using the Flp-In T-Rex system (Ward, Alvarez-Curto and Milligan, 2011). In brief, compatible cell lines (in this case HEK293) have a defined genetic locus into which the plasmid is placed when it is co-transfected with a second plasmid expressing Flp recombinase. The Flp-in T-Rex 293 cell line stably express Tet repressive protein (TetR), which binds compatible elements in the SPASM biosensors promoter, effectively silencing expression. Treatment with doxycycline binds TetR, releasing expression. While it is possible to perform BRET experiments utilising a similar separate luciferase fused G-protein donor (Corbisier *et al.*, 2015), this SPASM system holds a number of advantages. Once established expression is induced by the treatment of doxycycline, saving on the cost and variability of utilising transient transfections, insures a consistent level of expression between cells in a population, with expression level controllable by the administration of varying concentrations of doxycycline where required. As well, the SPASM biosensor guarantees a 1:1 stoichiometry of donor to acceptor, reducing the chances of excessive background donor signal that could result from using a multi-plasmid transfection strategy.

Expression of the biosensor is induced 24 hours prior to analysis, and from here the methodology is much the same as that used to assess β-arrestin recruitment. In essence the gain for 'donor' and 'acceptor' are again adjusted to a ratio of 1. Association of chemokine with receptor initiates recruitment of the G_{α} peptide causing a change in structural conformation that closes the distance between 'donor' and 'acceptor' below 10 nm, resulting in BRET. Again, the change in ratio relative to concentration of chemokine applied can be measured (summarised in figure 4.1.2). Sensors were already available capable of measuring recruitment of Gi1/2 and Gi3 to other receptors (due to sequence conservation Gi1 and Gi2 specific reporters are not available). As such constructs expressing sensors for Gi1/2 and Gi3 recruitment to either CCR4 or CCR7 were created, and stable cell lines generated. Using these, recruitment of signalling apparatus resulting from binding of CCL17 and CCL22 to CCR4, CCL19 and CCL21 to CCR7 and CCL27 and CCL28 to CCR10 was evaluated.

4.2 Assessment of CCR4 ligand expression and biased signalling

4.2.1 Imiquimod treatment of skin decreases expression of the CCR4 ligand CCL22

Daily imiquimod treatment of mouse skin is a well-established model, giving rise to the formation of a psoriasis like skin lesion characterised by hyperkeratosis and an extensive immune cell infiltrate (van der Fits *et al.*, 2009). The latter aspect of imiquimod treatment was of interest as the ligands of CCR4 are frequently associated with trafficking of a number of T-cell subtypes to the skin and expression may be disrupted by the heavy inflammatory insult inflicted by imiquimod treatment. RNA was extracted from lesional skin tissue at various time points as well as from vehicle treated control skin, normalised by RNA concentration and converted to cDNA. Primers were designed for the amplification of CCL17 and CCL22, and expression relative to a housekeeping gene (TBP) determined by qPCR utilising the $2^{-\Delta\Delta CT}$ method of comparative analysis (figure 4.2.1 a&b). Interestingly there was a significant drop ($p=0.0265$) in expression of CCL22 with imiquimod treatment at the 4 and 24-hour timepoints (4h Veh=1.03±0.18, 4h Imq=0.39±0.03, 24h Veh=1.07±0.29, 24 Imq=0.27±0.01. Units are fold change in all uses of $2^{-\Delta\Delta CT}$ comparative analysis. n=3±SEM for 4h and 1d timepoints, n=4±SEM for all others) (figure 4.2.1 b). Although significant differences were not noted at any other timepoint evaluated, there is a trend to lower expression of CCL22 in treated animals compared with vehicle controls. CCL17 expression however appeared unchanged by the treatment conditions across all timepoints (figure 4.2.1 a). These data indicate that CCL22 expression can be modulated by inflammatory conditions despite being characterised as a homeostatic chemokine.

4.2.2 CCL17 and CCL22 demonstrate signalling bias at the level of β-arrestin and G-protein recruitment

The capacity of CCL17 and CCL22 to enlist either β-arrestin 1 or 2 to CCR4 was compared by treatment with a ligand concentration range from 0.01 nM to 1 μM (figure 4.2.2). These data indicated that while both CCL17 and CCL22 could recruit either β-arrestin 1 or 2, with recruitment following a clear dose-response relationship, CCL22 generated a considerably higher Emax of 0.223±0.007 with β-arrestin 1 and 0.280±0.028 with β-arrestin 2 (n=3±SEM. This is consistent for all BRET experiments unless otherwise stated). CCL17 generated Emax values of 0.025±0.002 and 0.033±0.002 in the same

assays. Indeed, values for CCL17 recruitment need to be plotted separately in order to more readily reveal this response (figure 4.2.2 c&d). pEC_{50} of β–arrestin recruitment differed between the two, with a significant drop (p=0.012) between CCL17 and CCL22 potency from 7.63±0.09 to 8.02 ± 0.01 for recruitment of β–arrestin 1, and from 7.72±0.11 to 7.99±0.10 for β–arrestin 2 recruitment (figure 4.2.3 a). When comparing pEC_{50} of β-arrestin 1 or 2 recruitment for each chemokine no significant differences are apparent. Emax achieved by either chemokine within each assay was compared (referred to as Emax here, figure 4.2.3 b) and revealed significant differences in Emax obtained by each chemokine (β-arrestin 1; p=<0.0001. β-arrestin 2; p=0.001). Again, no significant difference is noted between β-arrestin 1 or 2 Emax with either CCL17 or CCL22.

By treating cells with a single concentration of chemokine, in this instance 100 nM, and taking repeated measures over a 30-minute period it is possible to determine the kinetics of β-arrestin 2's association with CCR4 in response to its ligands (figure 4.2.4 a). Kinetics of β-arrestin 1 recruitment were not analysed as the data reported above indicated little appreciable difference between β-arrestin 1 or 2 recruitment. These data indicated that while CCL22 instigated a rapid and lasting association of β-arrestin with CCR4, CCL17 appears to initiate only a short-lived association before becoming indistinguishable from the no-chemokine (NC) control treated cells. BRET ratio values obtained were constrained to the first 3 minutes of measurement (as this was consistently the timepoint at which CCL22 response peaked) and the time to half-maximal signal (half-time) compared between CCL17 and CCL22, assuming a one-phase association (figure 4.2.4 b). This revealed that CCL17 has a significantly lower halftime of 0.60±0.08 minutes compared to CCL22's halftime of 1.00±0.12 minutes (n=3±SEM. This is consistent for all kinetic experiments). Collectively these findings indicate that, while both CCL17 and CCL22 can recruit either β-arrestin, CCL22 is clearly the more potent ligand in this regard. Indeed, CCL17 incubation appeared to result in only minor and momentary recruitment of β-arrestin to CCR4.

Recruitment of Gi1/2 or Gi3 by CCL17 and CCL22 was also evaluated, in this instance using a ligand concentration range from 0.1 nM to 300 nM. Interestingly this revealed that while CCL22 readily recruited both Gi1/2 and Gi3, with an pEC_{50} of 8.05±0.03 , and 8.08±0.06 respectively, CCL17 appeared completely incapable of doing so at any concentration tested (figure 4.2.5 a). Comparison of pEC_{50} for recruitment of Gi1/2 and Gi3 by CCL22 revealed no significant differences (figure 4.2.5 b). This indicated that, in addition to being a poor ligand in terms of β-arrestin recruitment, CCL17 is also attenuated

in its ability to recruit Gi-proteins to CCR4 when compared to CCL22. Relative efficacy (RA) was calculated as described previously (Gundry *et al.*, 2017), with values listed in table 4.2.1.

4.3 Assessment of the ligand bias of CCR7

4.3.1 CCL19 appears dominant in both β-arrestin and Gi recruitment

β-arrestin recruitment to CCR7, induced by either CCL19 or CCL21, was evaluated in the same manner as CCR4. CCL19 and CCL21 were both readily capable of initiating β-arrestin 1&2 recruitment to CCR7 (figure 4.2.6 a&b), with broadly similar Emax values obtained by both chemokines (β-arrestin 1; CCL19=0.868±0.213, CCL21=0.804±0.251. β-arrestin 2; CCL19=0.718±0.040, CCL21=0.652±0.061). pEC_{50} values were significantly different between CCL19 and CCL21 with both β-arrestin 1 (7.77±0.10 and 7.17±0.08 respectively, p=0.0106) and β-arrestin 2 (7.85±0.08 and 7.18±0.01 respectively, p=0.0012) (figure 4.2.6 c). Similar to assessment of CCR4, no significant difference in pEC_{50} between β-arrestin 1 or 2 recruitment is noted with either CCL19 or CCL21. Analysis of the kinetics of β-arrestin 2 recruitment following treatment with 100 nM of either CCL19 or CCL21 revealed that, unlike CCL17 with CCR4, association of β-arrestin 2 and CCR7 in response to CCL21 is sustained and is clearly distinct from vehicle controls (NC) (figure 4.2.7 a). Half-time measurements were again taken and indicated that CCL19 has a significantly lower half-time (p=0.0013) than CCL21 in terms of β−arrestin 2 recruitment to CCR7 (CCL19 = 3.22±0.12 minutes, CCL21 = 6.45±0.39 minutes n=3±SEM, figure 4.2.7 b). It does appear though that, in terms of BRET ratio, there are some differences in these assays compared with what was previously demonstrated in figure 4.2.6 b. CCL19 appears to generate a higher BRET ratio at 100 nM than observed previously (over 2.0 compared with ~1.75), whereas CCL21 conversely generates a lower signal than previously at this concentration (~1.2 compared with ~1.5). This variability is somewhat concerning, however may be attributable to batch variability between different experiments as batch number was not matched between these different sets of experiments. Regardless, it would appear that, while both CCL19 and CCL21 readily cause association of β-arrestin 1 or 2 with CCR7, CCL19 is both faster acting and more potent than CCL21 in these assays.

Recruitment of either Gi1/2 or Gi3 to CCR7 in response to either CCL19 or CCL21 was evaluated in the same manner as previously shown for CCR4 (figure 4.2.8 a&b). These

data indicated a striking difference in the G-protein recruitment profiles of CCL19 and CCL21. Although there is increasing response with rising concentrations of CCL21 for both Gi1/2 and Gi3, the Emax generated is significantly lower than that seen with CCL19 with both G-protein reporters (Gi1/2; CCL19 = 0.113±0.007, CCL21 = 0.017±0.005, p=0.0003. Gi3; CCL19 = 0.175±0.010, CCL21 = 0.043±0.004, p=0.0002. figure 4.2.8 c). Consistent pEC_{50} values were obtained with CCL19 between experiments (Gi1/2 = 7.67±0.03 , Gi3 = 7.67±0.06), with no significant differences noted between Gi1/2 and Gi3 recruitment (figure 4.2.9 d). pEC_{50} of CCL21 mediated Gi-protein recruitment was more variable between repeat experiments (Gi1/2 = 7.24±0.30 , Gi3 = 7.00±0.15 . figure 4.2.9 d), and once again no significant differences were noted in pEC_{50} of recruitment of either Gi1/2 or Gi3 instigated by CCL21. CCL19 did however appear to be a significantly more potent ligand than CCL21 in terms of Gi3 recruitment (p=0.0132, figure 4.2.9d). RA was calculated as before and used to assign a bias factor to CCL21, using CCL19 as the reference ligand, and assigning β-arrestin 2 and Gi3 recruitment as pathway a and b respectively (Gundry *et al.*, 2017). This generated a bias factor of 0.59±0.12. Previous work assessing the ligand bias of CCR7 in a similar manner determined a biased ligand as having a factor greater than 1 (Corbisier *et al.*, 2015). Based on these criteria these data would appear to indicate that CCL21 is a poorer ligand for CCR7 in both signalling pathways, rather than a G-protein biased agonist as reported previously.

4.4 Assessment of the ligand bias of CCR10

Once again, BRET based methods were used to interrogate the signalling profile of the cognate ligands of CCR10, CCL27 and CCL28. Initially, recruitment of β-arrestin 2 was assessed in the same manner as previously conducted, transfecting 'acceptor' (CCR10-YFP) and 'donor' (β-arrestin 2-rLuc) into HEK293T cells at a ratio of 4:1 (as used in CCR4 and CCR7 β-arrestin analysis) in response to a concentration range of CCL27 and CCL28 of 0.1-300 nM (figure 4.2.9 a). This resulted in a similar signalling profile to that seen with CCR4/CCL17&22. CCL27 appeared capable of readily instigating recruitment of β-arrestin 2 to CCR10 with an pEC_{50} of 7.12±0.25 (n=2±SEM), whereas CCL28 appeared incapable of this. However, assessing β-arrestin recruitment in this manner proved difficult to reliably repeat, with significant variation in pEC_{50} of CCL27 mediated recruitment between two repeat measures, and considerable difficulty in obtaining a third. In BRET experiments the best "BRET signal", and consequently best data quality, is obtained when there is no excess of 'donor' proteins (i.e. the luciferase fused with β-arrestin 2) to 'acceptor' (the C-terminal YFP moiety fused to receptors of interest) at the

cell membrane. In an effort to improve data quality and reproducibility an increased 'acceptor' to 'donor' ratio of 9:1 was used when transfecting cells, utilising the same chemokine range (figure 4.2.9 b). These data again indicated that, while CCL27 triggered β-arrestin 2 recruitment by CCR10 with an pEC_{50} of 6.99±0.01 (n=2±SEM), CCL28 remained incapable of doing so. However, while this ratio resulted in more consistent pEC_{50} values for CCL27 between experiments, again obtaining a suitable number of repeat experiments proved difficult. It is unclear as to why this might be, however could be attributable to poor expression and/or cell surface localisation of CCR10 compared with CCR4 and CCR7.

Finally, a β-arrestin 2-nanoluciferase (nLuc) expression vector was used in place of the β-arrestin 2-rLuc construct used previously. A fusion of β-arrestin 2 with nanoluciferase results in a 'donor' capable of producing considerably greater luciferase signal, allowing for higher 'acceptor': 'donor' ratios to be attempted than are possible when using renilla luciferase-based 'donor's. CCR10-YFP and β-arrestin 2-nluc were transfected into HEK293T cells in a ratio of 4.9 μg to 100 ng, and recruitment of β-arrestin 2 in response to a range of CCL27 and CCL28 concentrations from 0.3 nM- 1 μM was assessed (figure 4.2.9 c). Treatment with CCL27 mediated β-arrestin 2 recruitment by CCR10 with an pEC_{50} of 6.99±0.06 , with improved signal (increased BRET ratio) and reproducibility, however CCL28 treatment still had no effect. pEC_{50} values of β-arrestin 2 recruitment achieved by CCL27 were compared between the different experimental conditions tested (figure 4.2.9 d) and indicated no significant differences between pEC_{50} values obtained utilising different 'acceptor': 'donor' ratios. Collectively these data support previous work asserting that CCL27 is an arrestin biased ligand of CCR10 and indicate that CCL28 appears incapable of triggering β-arrestin recruitment by CCR10 at any concentration tested. An RA value for CCL27 was generated based on experiments utilising nLuc fused β-arrestin 2 only and are listed in table 4.2.1.

Recruitment of Gi1/2 (figure 4.2.10 a&c) and Gi3 (figure 4.2.10 b&d) to CCR10 in response to either CCL27 or CCL28 treatment was assessed using SPASM biosensors in the same manner as employed with CCR4 and CCR7. Unfortunately, repeated measures using these biosensors either failed to generate a detectable BRET signal, or in the experiments listed above generated conflicting data. In one experiment (figure 4.2.10 a&c) CCL27 appears to initiate G-protein coupling to CCR10, with a pEC_{50} of 6.98 for Gi1/2 recruitment and 6.81 for Gi3. CCL28 conversely triggered no apparent recruitment of Gi1/2 by CCR10 (figure 4.2.10 a), similar to CCL17 with CCR4 (figure 4.2.5 a), and

relatively poor recruitment of Gi3 with a pEC_{50} of 6.70, similar to CCL21 with CCR7. However, in subsequent experiments CCL28 generated a higher Emax of Gi1/2 recruitment by CCR10 than is obtained by CCL27 (1.073 and 1.038 respectively, figure 4.2.10 c), though also a higher pEC_{50} (5.72 compared with 6.64 for CCL27). Recruitment of Gi3 by CCR10 in response to either CCL27 or CCL28 generated similar Emax values (1.115 and 1.095 respectively, figure 4.2.10 d), but again demonstrated considerable differences in the corresponding pEC_{50} values (6.01 for CCL27 and 2.95 for CCL28). These data would appear to indicate that CCL27 can trigger Gi-protein recruitment by CCR10. However, with the substantial differences between experiments, and the considerably higher than expected pEC_{50} values of CCL28 mediated recruitment that have been obtained, it is unclear if CCL28 can in fact trigger G-protein recruitment to CCR10.

pEC_{50} Emax and RA values are listed in table 4.2.1. Half-time values are summarised in table 4.2.2.

4.5 Development and evaluation of biotinylated chemokines

Given the unexpected signalling profiles of CCL17 and CCL28, there was interest in identifying if these chemokines interact with their cognate receptors in our hands. Cells expressing chemokine receptors of interest can be analysed by flow cytometry using fluorescently labelled chemokines (figure 3.2.3). As well as allowing for the evaluation of chemokine receptor expression, it is also possible to gain additional information about receptor characteristics using labelled chemokines that is not available from traditional antibody staining. For example, by staining with a constant concentration (25 nM) of labelled chemokine in the presence of a range of concentrations of unlabelled competitor chemokine it is possible to gain information on the affinity of the unlabelled chemokines for their cognate receptor in much the same manner as with radiolabel-based assays, but without the requirement for special equipment, training or precautionary measures. However directly fluorescently labelled chemokines, or those with site-specific biotin moieties, are expensive, and in the case of both cognate ligands of CCR10 were simply not available at the time of this analysis. It would be advantageous to be able to develop biotinylated chemokines in-house if possible.

To assess this unlabelled CCL19 was biotinylated using a commercial kit according to the manufacturer's instructions (Miltenyi, One-step antibody biotinylation kit). Staining with this in-house labelled CCL19 was assessed by flow cytometry on cells transfected with

empty vector or CCR7-FLAG and compared with the commercially available site-specific biotinylated CCL19 (Almac) when using a constant staining chemokine concentration of 25 nM (figure 4.2.11). These data indicated that the best staining of CCR7 compared to vector control cells was obtained using the site-specific biotinylated chemokine (CCR7 (almac) MFI= 3868±21.3, Vec (almac) MFI= 343.3±11.3) (figure 4.2.12 a). However, in-house chemokine labelled cells also demonstrated significantly higher MFI values when staining CCR7 expressing cells compared with empty vector controls both when the chemokine was pre-conjugated with SAPE (CCR7 (in-house pre) MFI= 273±3.0, Vec (in-house pre) MFI= 203±2.3), and when cells were initially incubated with the chemokine then subsequently stained with SAPE (CCR7 (in-house post) MFI= 738±11.5, Vec (in-house post) MFI= 222.7±1.3). These data indicated that in-house biotinylation of chemokines is viable in some instances as a means of detecting chemokine receptor expressing cells by flow cytometry. Additionally, a 2-step staining protocol generated a greater distinction in MFI values between CCR7 and empty vector transfected cells. Consequently a 2-step staining protocol was adopted in all subsequent studies of in-house biotinylated chemokines.

CCL22 was biotinylated in the same manner as CCL19 and staining between CCR4-FLAG and empty vector transfected HEK293T assessed for a range of CCL22 label concentrations of 25-100 nM (figure 4.2.12 b). These data revealed that MFI was significantly higher with CCR4 transfected cells than equivalent empty vector controls at all concentrations tested (CCR4 (25 nM)=541.3±14.9, Vec (25 nM)=143±2.6, CCR4 (50 nM)=633±13.1, Vec (50 nM)=162±2, CCR4 (100 nM)=796.3±4.6, Vec (100 nM)=237.3±3.7), indicating that in-house biotinylated CCL22 can be used for labelling of cells expressing CCR4. A staining concentration of 50 nM was selected for subsequent analysis as it demonstrated a greater distinction in MFI between CCR4 and empty vector transfected cells, with little increase in MFI for empty vector controls from that obtained with a staining concentration of 25 nM.

Unfortunately, when attempting the same with biotinylated CCL27 and CCR10-FLAG expressing cells (figure 4.2.12 c), no staining concentration tested resulted in an increase in MFI for CCR10 transfected cells compared with empty vector controls (CCR10 (25 nM)=132±1.0, Vec (25 nM)=142.7±2.8, CCR10 (50 nM)=138.7±0.3, Vec (50 nM)=157.3±1.8, CCR10 (100 nM)=166.7±5.8, Vec (100 nM)=186.3±5.9). Indeed, at 25 and 50 nM staining concentrations the MFI values of CCR10 transfected cells were significantly lower than their relevant empty vector controls. In an effort to address if this represents an issue with binding of the biotinylated chemokine or insufficient CCR10

expression for detection, HEK293T cells were seeded onto 6-well plates and transfected with increasing quantities of CCR10-YFP plasmid per well (1.5-2.5 μg) and stained with a single concentration of biotinylated CCL27 as before (25 nM, figure 4.2.12 a&b). In this case SABV421 was used in place of SAPE to avoid spectral overlap with the YFP moiety on CCR10. Staining of CCR10 expressing cells was once again compared with empty vector controls, as well as empty vector and CCR7-FLAG transfected cells stained with commercially available biotinylated CCL19 pre-conjugated with SABV421. Receptor expression, as determined by MFI for YFP fluorescence, increased with rising plasmid quantities and peaked with the highest used (CCR10 1.5=474.3±7.7, CCR10 2.0=527.3±15.6, CCR10 2.5=2245±50.9, figure 4.2.13 a), and were all significantly higher than MFI obtained for empty vector transfected cells (Vec 1.5=13.5±1.9). However, when evaluating staining with in-house labelled CCL27 little difference is apparent between any CCR10 transfected group and the empty vector control (CCR10 1.5=1078±9.4, CCR10 2.0=1018.0±83.2, CCR10 2.5=1076±20.0, Vec 1.5=1273±28.31, figure 4.2.13 b). Similar to previous experiments (figure 4.2.12 c) MFI values for empty vector controls were in fact significantly higher than that obtained for any CCR10-YFP transfected group. These data indicate that while CCR10 expression can be observed (as indicated by YFP fluorescence), in-house biotinylated CCL27 does not specifically label CCR10 expressing cells under any conditions tested thus far.

These observations, as well as a noted drop in MFI when using in-house biotinylated CCL19 to label CCR7 expressing cells compared to a commercially available counterpart, raised the concern that the process of non-specific biotinylation may alter the binding properties of a chemokine such that it cannot be considered comparable to the unlabelled chemokine. In order to determine if this might be the case biotinylated CCL19 (figure 4.2.14 a) and CCL22 (figure 4.2.14 b) were compared to their un-biotinylated equivalents (labelled “Control” on the relevant figures), in their capacity to recruit β-arrestin 2 to CCR7 or CCR4. These data revealed biotinylated chemokines were near equivalent to their unlabelled counterparts, with comparable pEC50 (CCR7; control=7.59, biotinylated=7.49. CCR4; control=7.98, biotinylated=7.85) and Emax values (CCR7; control=1.20, biotinylated=1.16. CCR4; control=0.32, biotinylated=0.32). In this instance it would appear that the process of biotinylation has not overtly affected the functional activity of these chemokines, and they may be considered comparable to the unlabelled chemokine.

4.6 Assessment of ligand affinities of CCR4 and CCR7

4.6.1 CCL17 and CCL22 demonstrate differing affinities for CCR4 in a FACS based competition assay

Using either CCL22 directly conjugated to AF647 (figure 4.2.15 a), or the in-house biotinylated version of CCL22 conjugated to SAPE (figure 4.2.15 b), and a range of unlabelled competitor chemokine concentrations of 0.03 nM – 1 μM. A labelled chemokine concentration of 25 nM for direct conjugated and 50 nM for the in-house biotinylated CCL22 was employed. The labelled and unlabelled chemokines were introduced to cells simultaneously and incubated on ice for 20 minutes to prevent receptor internalisation and ligand degredation. pK_i generated using the direct conjugated CCL22 were 7.13 for CCL17 and 7.65 for CCL22, and 7.32 and 7.70 when using the in-house labelled chemokine. These data indicated that both CCL17 and CCL22 can compete for receptor occupancy with labelled CCL22, however CCL22 does so more effectively.

4.6.2 CCL21 appears incapable of displacing labelled CCL19 from CCR7 expressing HEK293T cells

Utilising site-specific biotinylated CCL19 conjugated to SAPE, and HEK293T cells transiently transfected with CCR7, the capacity of CCL19 or CCL21 to displace fluorescently labelled CCL19 was assessed (figure 4.2.16 a&b). These data indicated that, while CCL19 could readily out-compete the labelled CCL19, CCL21 was incapable of doing so at either a 20x (figure 4.2.16 a) or 40x (figure 4.2.16 b) molar excess. The indicated pK_i of CCL19 between both sets of experiments was 8.46±0.17 (n=4±SEM). Interestingly the highest concentration of CCL21 competitor appeared to actually increase staining with CCL19-SAPE. Given previous observations that CCL21 can interact with CCR7, resulting in the receptor recruiting β-arrestin 1 and 2 (figure 4.2.6 a&b), CCL21 can interact with CCR7 expressed in HEK293T cells. However, it appears to do so with poorer affinity than CCL19 and is incapable of competing with labelled CCL19 for receptor occupancy at any concentration tested.

4.7 Discussion

4.7.1 CCR4

Further analysis of the perceived ligand bias of CCR4 and CCR7 was conducted, at both the transcriptional and signalling machinery recruitment levels. For the former, the imiquimod model of skin inflammation was used. This is a well-established model in

which daily application of imiquimod cream induces a psoriasiform lesion on mouse dorsal skin, characterised by thickening of the skin, induced expression of a number of inflammatory cytokines including interferon alpha (INFα) and a resultant influx of immune cells such as plasmacytoid DCs, T-cells such as Th17 cells, as well as innate lymphocytes (van der Fits *et al.*, 2009). This results in the formation of plaques much akin to human psoriatic lesions, however unlike the human disease this is not a chronic inflammatory condition. Imiquimod is a potent agonist of Toll-like receptor 7 (TLR7) (Forward *et al.*, 2010), an intracellular sensor of single stranded RNA rich in guanosine and uridine, which is activated by DCs and macrophages in response to phagocytosis of a number of viruses. As such, imiquimod treatment can be considered a molecular mimic of viral infection. With this in mind the observation that, somewhat paradoxically, inflammation dampens expression of CCL22 does fit with the expected pathophysiology. As the predominant chemokine receptor of Th2 and Treg cells (Yoshie and Matsushima, 2015), CCR4 driven chemotaxis of these cells into tissue inflamed during viral infection would be at best unhelpful (in the case of Th2 recruitment), and at worst potentially damaging to the resolution of infection in the case of Treg recruitment.

Subsequent to the analysis described in this chapter it was demonstrated by others that topical imiquimod treatment reduces expression of CCL22 by TAMs 48 hours after administration in a solid subcutaneous B16F10 tumour model, attenuating Treg recruitment and reducing tumour volume (Furudate *et al.*, 2017). Injection of CCL22 neutralising antibody into tumours similarly reduced tumour burden. It is conceivable that we are observing a similar phenotype here. Such studies might also provide mechanistic insight into a synergistic effect noted with concurrent imiquimod treatment when treating various cancers (Mauldin *et al.*, 2016), in its use as an adjuvant to tumour antigen immunisation (O'Hagan and Valiante, 2003), and it's use in direct treatment of superficial basal cell carcinoma (Geisse *et al.*, 2004). Disruption of the CCR4 signalling axis and subsequent interference with Treg recruitment by imiquimod may be a key aspect of its activity in these contexts.

Interestingly, while a significant drop in CCL22 expression is noted over the course of the imiquimod model, no similar change in CCL17 expression is apparent. This is in contrast to a reported reduction in mRNA levels of both CCR4 ligands by TAMs with imiquimod treatment (Furudate *et al.*, 2017). This was with topical imiquimod treatment in solid melanoma tumours, so would differ biologically from the psoriasiform lesions induced here. As such it is unclear what this steady expression could mean. Additional work may be necessary to confirm if this steady expression of CCL17 is consistent and if, in

accordance with the presumed activities of CCL17 and CCL22, Tregs and Th2 cells are still able to extravasate from the blood but are subsequently unable to navigate toward the inflammatory lesion. It may also be of interest to see how expression of CCL22 and CCL17 change in response to different inflammatory mediators, such as those requiring humoral immune responses, or in wound healing models.

Although odd, the lack of any significant changes in CCL17 expression could simply be attributable to the difference in models used but does somewhat conform with the signalling profile generated here. These data indicate that, while CCL22 readily recruits both β-arrestins and Gi proteins to CCR4, CCL17 appears nearly incapable of doing so, with only brief association of β-arrestin 2 with the receptor following incubation with the chemokine, and no apparent association of Gi1/2 or 3 peptides. This was expected with β-arrestin recruitment; CCL22 has been shown to be dominant both in functional CCR4 internalisation assays of Th2 cells and L1.2 cells transfected with CCR4 (Mariani *et al.*, 2004), and in direct assessment of β-arrestin 2 recruitment by enzyme complementation assays (Ajram *et al.*, 2014). Interestingly the latter demonstrated no β-arrestin recruitment in response to CCL17 compared with what is observed here, potentially indicating increased sensitivity with BRET based methods.

However, the complete lack of Gi coupling is in contrast to the reported agonism of CCL17. Previous studies indicate that CCL17 induces chemotaxis in endogenously CCR4 expressing and transfected cells and is PTX sensitive (indicating CCL17/CCR4 coupling signals through Gi/o pathways) (Imai *et al.*, 1997; Mangmool and Kurose, 2011). Previous evaluation of G-protein recruitment to CCR4 with [^{35}S] GTPγS membrane binding also indicated that both CCL17 and CCL22 recruited G-proteins, but that CCL17 produces a lower maximal response than CCL22 in these assays (Ajram *et al.*, 2014). This assay does not differentiate between recruitment of different G_α subunits however.

FACS based competition assays appear to indicate that CCL17 does indeed bind CCR4, displacing labelled CCL22. However, it does so less well than CCL22 and cannot completely abolish labelled CCL22 binding. This is in agreement with previously published observations (Viney *et al.*, 2014b). Here, the authors postulate that CCR4 exists in at least two distinct conformations, one of which can only bind CCL22. It's concerning that IC50 values obtained here are considerably higher than those determined by other means, such as competing with alkaline-phosphatase linked CCL22 (CCL17 = 2.1 nM, CCL22 = 0.65 nM), or radiolabelled CCL22 (CCL17 = 4.1 nM, CCL22 = 1.5 nM) (Imai *et al.*, 1998; Viney *et al.*, 2014a). This could potentially be due to the difference in labelled

chemokine concentration; we have employed a staining concentration of 25 nM CCL22, whereas the above studies utilised 0.5 nM and 0.1 nM respectively. It could also be due to the different cell lines used; all of our assays are performed in HEK293T cells whereas L1.2 cells were used in the above examples, which could be considered more analogous to an endogenous CCR4 expressing cell. However, given that pEC_{50} values generated here for β-arrestin (9.7 & 10.7 nM) and Gi (8.9 & 8.5 nM) recruitment induced by CCL22 are in broad agreement with those obtained by receptor internalisation (~5 nM) and chemotaxis (9.79 nM) assays performed on Th2 and HUT78 cells (Viney *et al.*, 2014a), it may be that issues exist in the methodology applied here that require optimisation. It may be that the label concentration is simply too high in this assay, and could be titrated down. Alternatively, altering incubation time or temperature, introducing the labelled chemokine before cold competitor may bring the data generated by this method more in line with that seen elsewhere.

It is possible that CCL17 signals through CCR4 in a Gi independent manner. Given previous observations of PTX sensitive chemotaxis to CCL17 (Imai *et al.*, 1997), Go-proteins could be utilised by the receptor following CCL17 binding. Additionally, CCL17 has demonstrated a non-chemotactic function in which it is dominant over CCL22, namely the potent induction of calcitonin gene–related peptide (CGRP) expression in airway epithelial cells (Bonner *et al.*, 2013). CGRP acts as a vasodilator in conjunction with other inflammatory mediators and as such it was posited that this activity of CCL17 contributed to CCR4 driven pathogenesis in airway hypersensitisation and asthma models. Such a skew in G-protein recruitment between different chemokines on the same receptor has not been described previously. However, this could be readily assessed in future experiments using SPASM biosensors for other G_{α} subunits.

4.7.2 CCR7

CCL19 and CCL21 readily recruit β-arrestin 1 and 2 to CCR7, and CCL19 is both more potent and faster acting than CCL21. Interestingly, no difference is noted in recruitment of either β-arrestin 1 or 2 in response to either chemokine. This contradicts earlier work which indicated CCL21 did not recruit β-arrestin, and that CCL19 mediated internalisation of CCR7 was β-arrestin 2 specific. siRNA knockdown of either β-arrestin 1, 2 or both in HUT78 cells indicated that CCR7 internalisation in response to CCL19 was β-arrestin 2 dependent (Byers *et al.*, 2008). A rescue experiment conducted in murine embryonic fibroblasts indicated that only co-expression of the receptor and β-arrestin 2 restored internalisation of CCR7 in response to CCL19. This disparity could be due to the radically

different methodologies used; here BRET based methods were employed, measuring specific protein: protein interactions in HEK293T cells. It is conceivable that, in an exogenous-expression system such as this, interactions occur that would not naturally. However, it is unlikely that such interactions would be indistinguishable from the "natural" pairing of CCR7 and β-arrestin 2. Also, in (Byers *et al.*, 2008) internalisation was measured rather than arrestin recruitment directly, and demonstrate their findings initially with siRNA knockdown, which can carry the risk of off-target effects.

CCL21 has previously been reported as equal in G-protein recruitment capacity to CCL19 (Sullivan *et al.*, 1999), and CCL21 induced chemotaxis has been demonstrated as being PTX sensitive (Suzuki *et al.*, 1999). However, when measuring recruitment of G-proteins by CCR7 using SPASM biosensors, CCL19 is clearly superior to CCL21 in both efficacy and potency. Only a moderate rise in BRET ratio is noted with CCL21 treatment at the highest concentrations tested. This is in broad agreement with a recent study characterising G-protein recruitment to CCR7 by means of BRET, using co-transfection of whole G-proteins conjugated to renilla luciferase, and YFP-tagged CCR7 (Corbisier *et al.*, 2015). From these data it would appear that in HEK293T cells CCR7 signalling does not demonstrate true bias, and CCL21 is simply a poorer ligand for both β-arrestin and Gi-protein recruitment in these assays.

This is in contrast to both the reported bias of CCR7 and the pathophysiology in mice resulting from knockout of CCR7 ligands. Initial characterisation of CCL21 in L1.2 cells expressing CCR7 demonstrated essentially equivalent potency in calcium mobilisation and chemotaxis (Yoshida *et al.*, 1998). Both CCL19 and CCL21 were shown to recruit G-proteins to the membrane via [^{35}S] GTPγS binding and mobilise intracellular calcium near-equally in a human T-cell lymphoma cells (Kohout *et al.*, 2004). However, CCL19 appeared more potent in downstream activation of the MAPK pathway and phosphorylation of CCR7 when assessed in HEK293 cells (Sullivan *et al.*, 1999). A more recent study indicated that CCL21 signals through entirely unique pathways. Here it was demonstrated that oligomerisation of CCR7 allowed for the phosphorylation of CCR7 by SRC kinases, resulting in signalling through SHP2 by CCL21, but not CCL19 (Hauser *et al.*, 2016). This would certainly fit with the differences between CCL19 knockout alone and CCL19 and CCL21 abrogation in the plt/plt mouse line. The former demonstrates little overt phenotypic changes from wild-type, however the latter demonstrates rapidly altered LN structure and attenuated/delayed antigen specific immune responses (Gunn *et al.*, 1999; Britschgi, Favre and Luther, 2010). Collectively this would certainly implicate CCL21 as the dominant ligand in CCR7 activity, not CCL19.

It is interesting that β-arrestin recruitment by CCL21 is robust despite the clearly skewed G-protein recruitment profile between CCL19 and CCL21. In general, β-arrestin recruitment is considered a later event in receptor activation, following G-protein binding and receptor phosphorylation by GPCR kinases (GRKs) (Hanlon and Andrew, 2015). Previous work indicated that, in HEK293 cells, CCL19 and CCL21 demonstrated comparable G-protein activity (as demonstrated by inhibition of forskolin mediated cAMP build up), but CCL19 was a more potent agonist in terms of receptor phosphorylation and recruited a wider repertoire of GRKs (GRK3 and GRK6) to CCR7 than CCL21 (GRK6) (Zidar *et al.*, 2009). It is certainly possible that, while evaluation of specific G-protein recruitment indicated little Gi-coupling resulting from CCL21 interaction, endogenous G-proteins could bind the receptor, leading to phosphorylation and subsequent β-arrestin recruitment. However, previously a β-arrestin biased mutant of the dopamine D2 receptor (D2R) could be seen to directly activate GRK2 without G protein coupling (Pack *et al.*, 2018), with an additive effect observed when using an artificial agonist known to preferentially recruit β-arrestins to D2R. It would be interesting to evaluate if direct GRK recruitment to CCR7 by CCL21 can be observed in G-protein knockout cell lines, possibly via BRET based means.

Another interesting observation is that CCL21 is incapable of competing for receptor occupancy with labelled CCL19, even at a 40x molar excess. This is despite clear evidence of receptor activation in the form of β-arrestin recruitment. These findings contrast with previous characterisation of CCR7, again using both alkaline-phosphatase bound and radiolabelled ligands, which demonstrated similar affinity of CCL19 and CCL21, and the ability of each chemokine to compete with labelled versions of the other (Yoshida *et al.*, 1998; Sullivan *et al.*, 1999). Again, there are considerable differences in terms of label concentration, however in this instance the IC50 values obtained here for CCL19 are comparable to those determined before. As such the key difference may be in the different cell lines used. L1.2 and other lymphoid derived cells have been utilised previously (giving an IC50 of 6.1 nM for CCL19 and 8.2 nM for CCL21 when competing with labelled CCL19 in L1.2 cells (Yoshida *et al.*, 1998), as have CHO-K1 cells (8.5 nM and 8.1 nM respectively) (Corbisier *et al.*, 2015). There may be subtle differences in the characteristics of CCR7 expressed in different cell lineages that results in this intriguing ligand binding profile that we do not consider when utilising HEK293T cells. It is interesting that the highest concentrations of CCL21 competitor actually appear to improve staining of CCR7 expressing cells by labelled CCL19. Given the avid binding profile of CCL21, it is possible

that CCL21 out-competes the labelled CCL19 for non-specific glycan binding, improving specific staining with the chemokine.

Unfortunately, while a bias factor could be applied to CCL21, this was not possible with either CCL17 or CCL28 due to the lack of response in both the β-arrestin and Gi-protein pathways.

4.7.3 CCR10

Previous assessment of CCR4 and CCR7 recruitment of β-arrestin indicated little difference between β-arrestin 1 or 2, so only β-arrestin 2 was assessed with CCR10. Initial attempts to characterise β-arrestin recruitment by CCR10 proved difficult. Issues with data quality and reproducibility were resolved by increasing the ratio of 'acceptor' to ''donor'' (i.e. β-arrestin to receptor). BRET presents the highest "signal" when there is no excess of ''donor'' to ''acceptor'', this could indicate lower expression (or cell surface localisation) of CCR10-YFP compared to CCR4 or CCR7. However, in all assessments of β-arrestin 2 recruitment the same pattern emerged. While interaction with CCL27 recruited β-arrestin 2 to CCR10, CCL28 interaction resulted in no observable recruitment. This is in-keeping with the reported bias of this receptor (Xiong *et al.*, 2012).

Difficulties were also encountered when assessing recruitment of Gi-proteins by CCR10. Previous assessments of CCR10 have indicated that both CCL27 and CCL28 can induce calcium mobilisation when CCR10 is expressed in BAF/3 cells (a pro B cell line) (Wang *et al.*, 2000). Additionally, a more recent evaluation of the signalling bias of CCR10 utilised enzyme fragment complementation-based assays to assess inhibition of cAMP formation following forskolin treatment (a readout of Gi activation) and β-arrestin recruitment (Rajagopal *et al.*, 2013). In this study it was demonstrated that β-arrestin recruitment to CCR10 occurred after CCL27 treatment only, but both CCL27 and CCL28 inhibited cAMP accumulation (EC50; CCL27=7.9 nM, CCL28=127 nM). Using SPASM biosensors two distinct signalling profiles have been generated; one in which CCL28 generated a limited BRET signal compared to CCL27 with Gi3 only (similar to CCL21/CCR7), and another where CCL27 and CCL28 generated a comparable BRET signal with both Gi1/2 and Gi3 recruitment but a considerably higher pEC_{50} for CCL28 (Gi1/2; CCL27=-6.63 , CCL28=-5.72 . Gi3; CCL27=-6.01 , CCL28=-2.96). Despite numerous attempts it has not been possible to reproduce either result. Consequently, it isn't possible to definitively determine which represents the most accurate picture of CCR10 signalling behaviour. However, given that the pEC_{50} values generated in the latter experiments are rather high,

and that the signalling profiles generated by the former closely resemble what has been observed in similar assessments of CCR4 and CCR7, it is likely that in these assays CCL28 also appears to not signal through Gi coupling to CCR10.

4.7.4 Biotinylation of chemokines

Using a kit intended for the biotinylation of antibodies it was possible to create biotinylated versions of CCL19 and CCL22 that could be used for receptor characterisation by flow cytometry and were near-indistinguishable from their unlabelled counterparts in a functional assay. These chemokines stained receptor-expressing cells best when a 2-step process was employed as opposed to pre-conjugation of the biotinylated chemokine with SAPE or SBV421, as done previously. Biotinylation kits non-specifically label any lysine residues in a protein, whereas commercially available labelled chemokines have a single biotin moiety, or are directly conjugated to a fluorophore, at their C-terminus. As such, pre-conjugation of in-house labelled chemokines may result in increased disruption to chemokine structure, reducing receptor binding. Unfortunately, similar attempts to biotinylate CCL27 and label cells expressing CCR10 proved unsuccessful. CCL19 and CCL22 contain 4 lysine residues each, whereas CCL27 contains 7. It is possible that biotinylation of CCL27 therefore introduces too much structural disruption for receptor binding.

4.7.5 Conclusion

In closing it appears that, while CCR4, CCR7 and CCR10 are all reported as following a very similar model of biased agonism, there are definite differences in signalling behaviour between these receptors. All of the “balanced” ligands (CCL22, CCL19 and CCL27) do indeed fit with their presumed signalling properties, readily initiating recruitment of both β-arrestin and Gi-proteins by their relevant receptors. However, when assessing chemokines previously demonstrated as being G-protein biased differences emerge. CCL21 readily recruits β-arrestin to CCR7 with near identical maximal responses to CCL19 but poorer potency. CCL17 on the other hand causes little recruitment of β-arrestin by CCR4, and CCL28 appears completely incapable of initiating β-arrestin recruitment by CCR10. Additionally, CCL17, CCL21 and CCL28 all appear almost incapable of Gi-protein recruitment with either little (CCL21 and CCL28) or no (CCL17) recruitment initiated by their receptors following chemokine treatment. This would indicate that while there are certainly differences both within and between each of these ligand pairs, the label of biased agonism may have been misapplied. However, given the differences between the

data generated here and previous work analysing these receptors and ligands, significant further work would be required before definitively drawing such a conclusion.

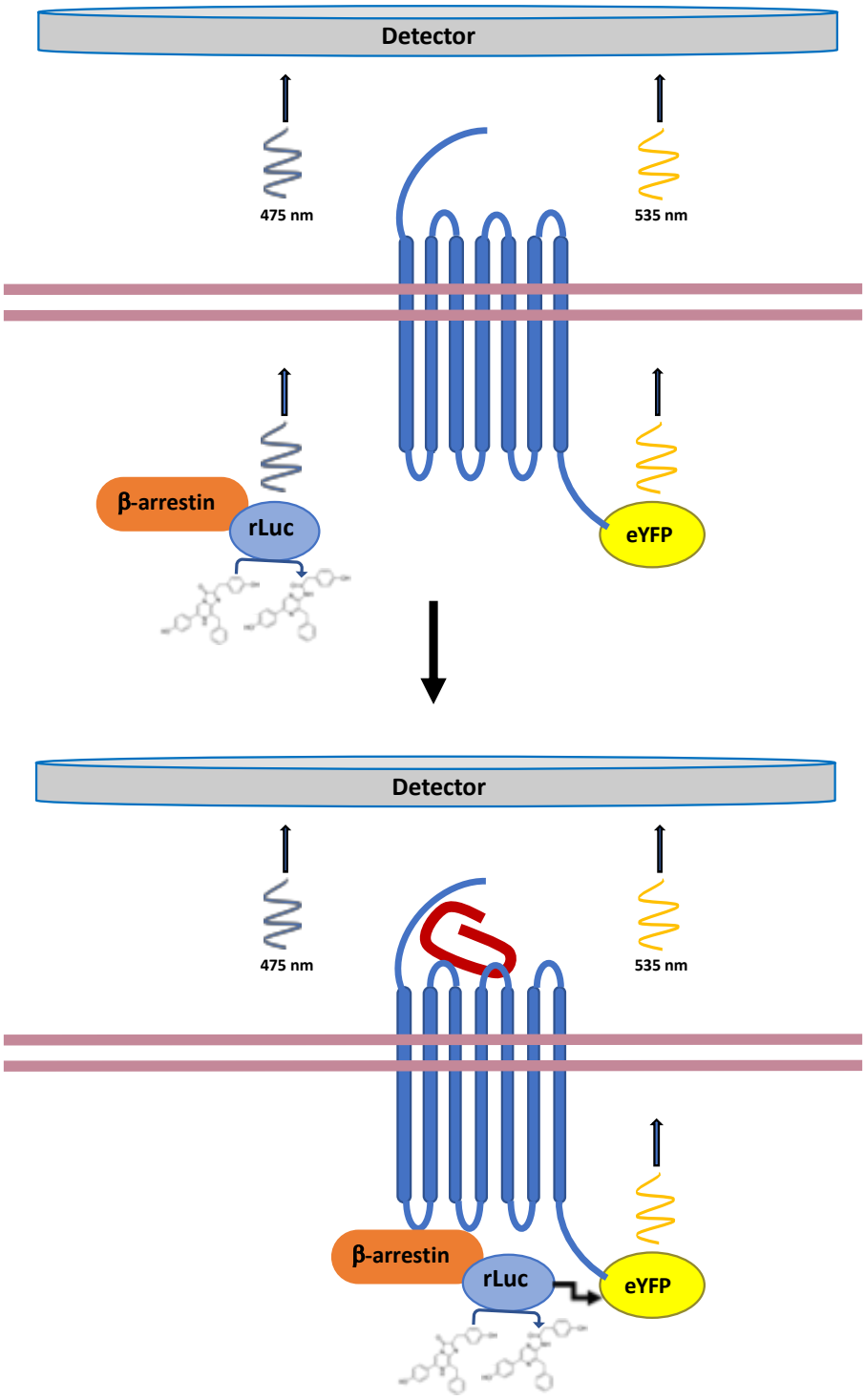

Figure 4.1.1 Schematic representation of BRET based β-arrestin recruitment assay

(a) C-terminal YFP tagged GPCR is co-transfected into HEK293T cells with renilla luciferase tagged β-arrestin 1 or 2. After 24 hours these cells were seeded onto a 96-well plate and analysed after a further 24 hours using a plate reader capable of measuring luciferase and YFP emissions separately. Cells are incubated with Coelentrazine H at 37 ºC for 5 minutes, which is catalysed by rLuc, producing a detectable signal. Gain for the donor and acceptor channels is adjusted so that at

rest the ratio of YFP/luciferase signal intensity is around 1. (b) Chemokine is then introduced to the wells and left to incubate for 5 minutes at room temperature. Incubation with compatible ligands recruits β-arrestin to the receptor, closing the gap between luciferase and YFP to under 10 nm. This allows energy transfer to occur, resulting in reduction in luciferase signal and a concomitant increase in YFP signal, increasing the ratio of YFP/luciferase above 1. This increase in BRET ratio is proportional to the degree of receptor recruitment and increases or decreases depending on the concentration of ligand applied.

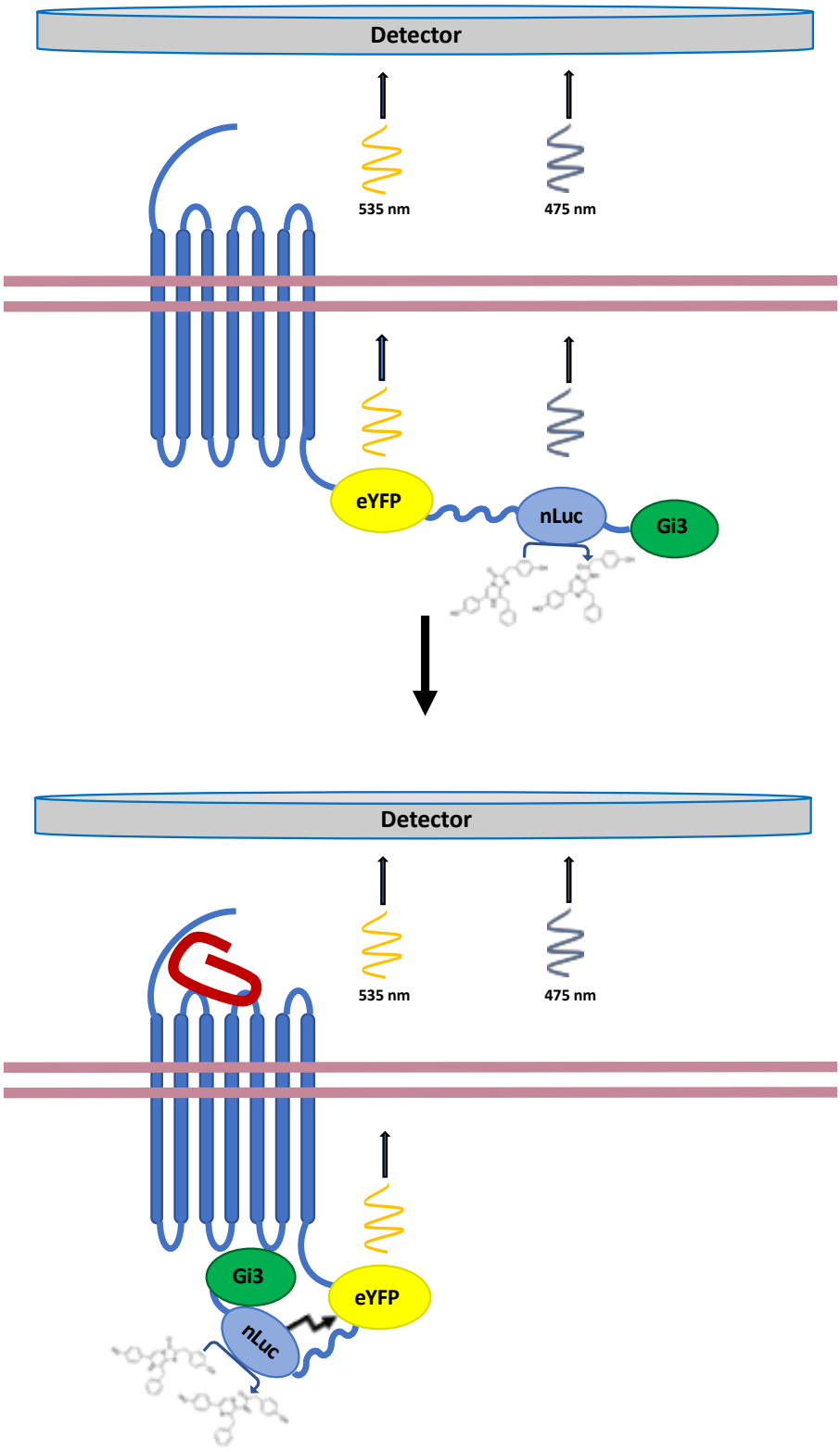

Figure 4.1.2 Schematic representation of the use of SPASM Gi reporting biosensors

(a) The SPASM biosensor consists of a single macromolecular reporter encoding the GPCR of interest, a YFP 'acceptor' and nano-luciferase 'donor' separated by flexible ER/K linker. The C-terminus of a G_a subunit, which is sufficient for receptor recruitment, separated by flexible ER/K linker is separated from the nano-luciferase moiety by a

repeating glycine/serine sequence which insures rotational freedom. This is encoded in a backbone compatible with the Flp-In T-Rex stable cell line system, allowing for genomic insertion in a defined locus and doxycycline inducible expression in HEK293 cells. Generated stable cell lines are induced with doxycycline and seeded onto 96-well plates 24 hours before analysis. From here the same basic methodology used in β-arrestin recruitment assays is employed, with the exception of a longer incubation time with the chemokine of 10 minutes. (b) Incubation with compatible ligands recruits the G-protein peptide to the receptor, resulting in a conformational change that closes the distance between ‘donor’ and ‘‘acceptor’’ to under 10 nm, increasing the calculated BRET ratio in a ligand concentration dependent manner.

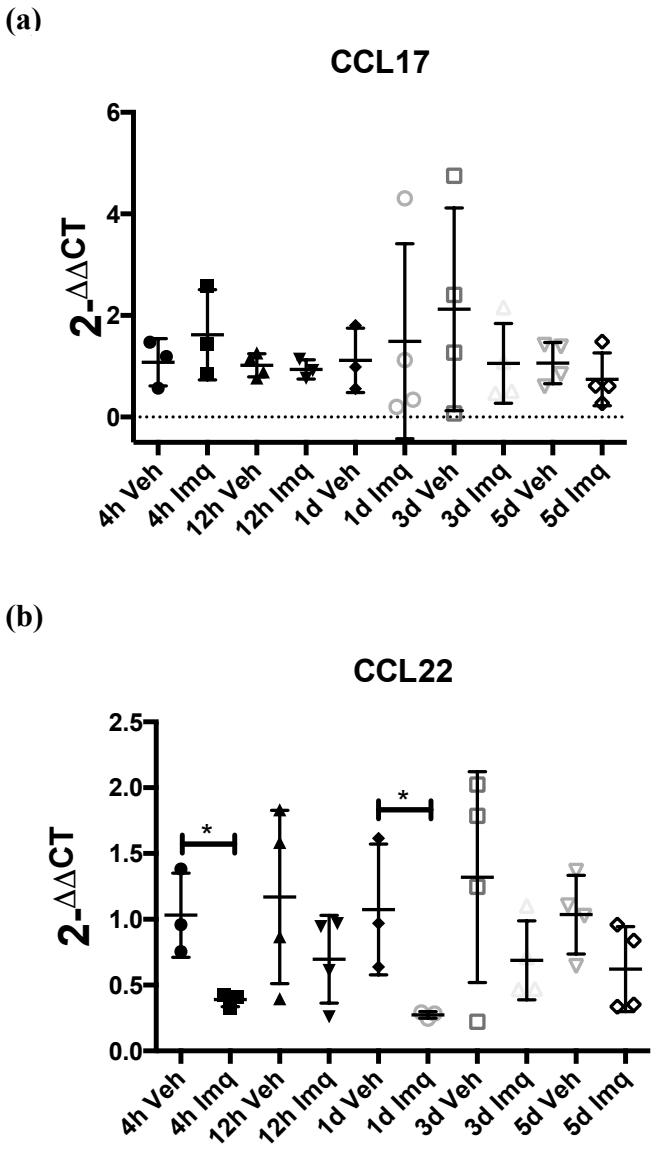

Figure 4.2.1 Expression of ligands of CCR4 in the skin during imiquimod treatment as assessed by qPCR.

Expression of CCL17 (a) and CCL22 (b) were evaluated at the mRNA level by RT-qPCR in skin treated with the TLR7 agonist imiquimod. Treatment was applied every 24 hours, samples harvested at 4, 12 hours and 1 day after the first treatment and 1 day after the 3- and 5-day treatments, and RNA extracted. Each data point represents an individual animal, error bars represent SD. Statistically significant differences between vehicle and imiquimod treated groups were determined by unpaired T-test, $p \leq 0.05$=*.

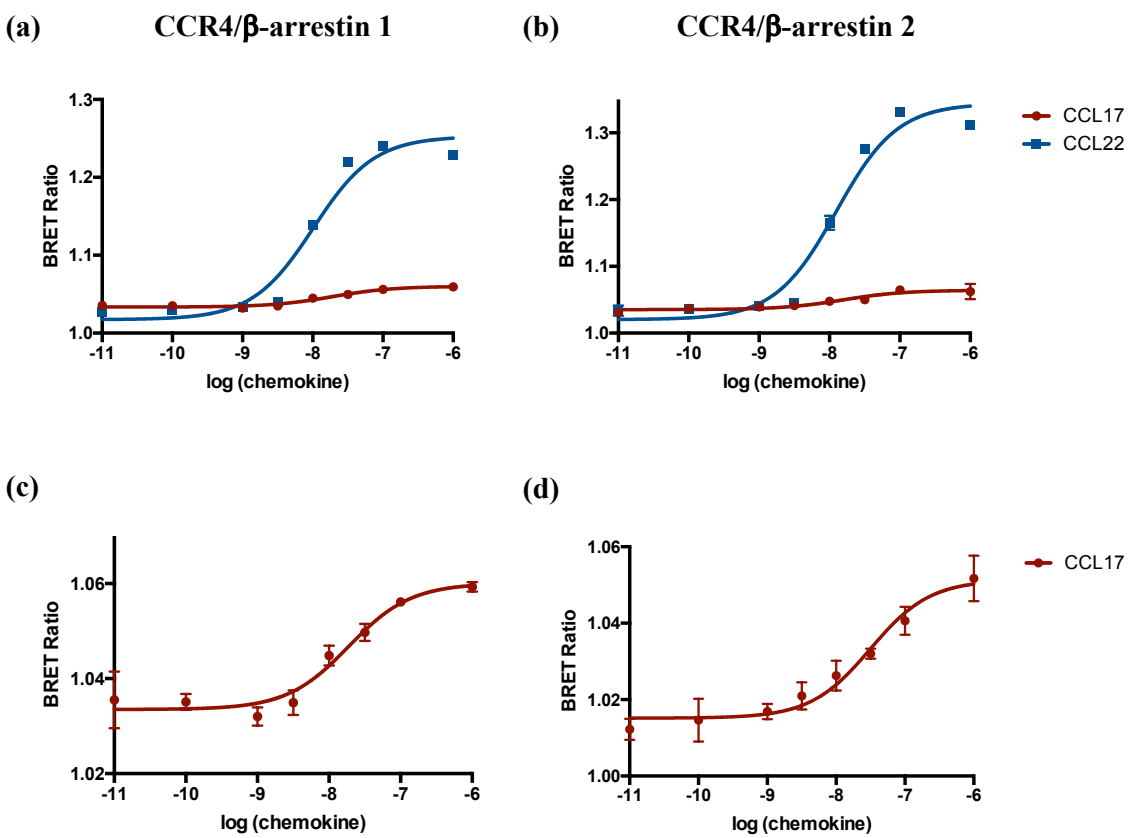

Figure 4.2.2 Recruitment of β-arrestin 1&2 to CCR4 by CCL17 or CCL22, as assessed by BRET.

Recruitment of either β-arrestin 1 (a) or 2 (b) to CCR4 in response to increasing concentrations of either CCL17 or CCL22 was assessed by BRET. Due to comparatively low signal, values obtained for CCL17 were re-plotted excluding those obtained for CCL22 (c&d). (n=3 +/- SD, representative plot selected from 3 independent experiments each).

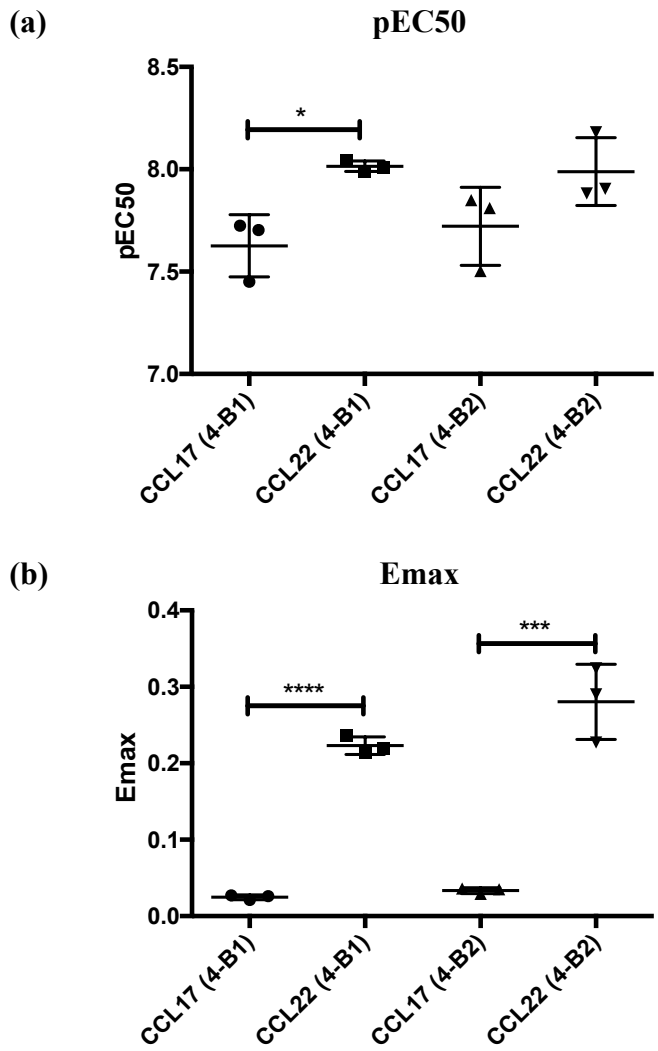

Figure 4.2.3 Comparison of pEC50 values and Emax obtained for CCL17 or CCL22.

(a) Values obtained for the pEC_{50} of β-arrestin recruitment were compared between CCL17 and CCL22, and between β-arrestin 1 and 2 for each ligand. (b) Emax was also compared between CCL17 and CCL22 with either β-arrestin 1 or 2. (n=3 biological replicates. Statistically significant differences between each parameter were determined by unpaired T-test, $p \leq 0.05$=*, $p \leq 0.01$=**, $p \leq 0.001$=***). 4-B1=CCR4/β-arrestin 1 transfection, 4-B2=CCR4/β-arrestin 2 transfection.

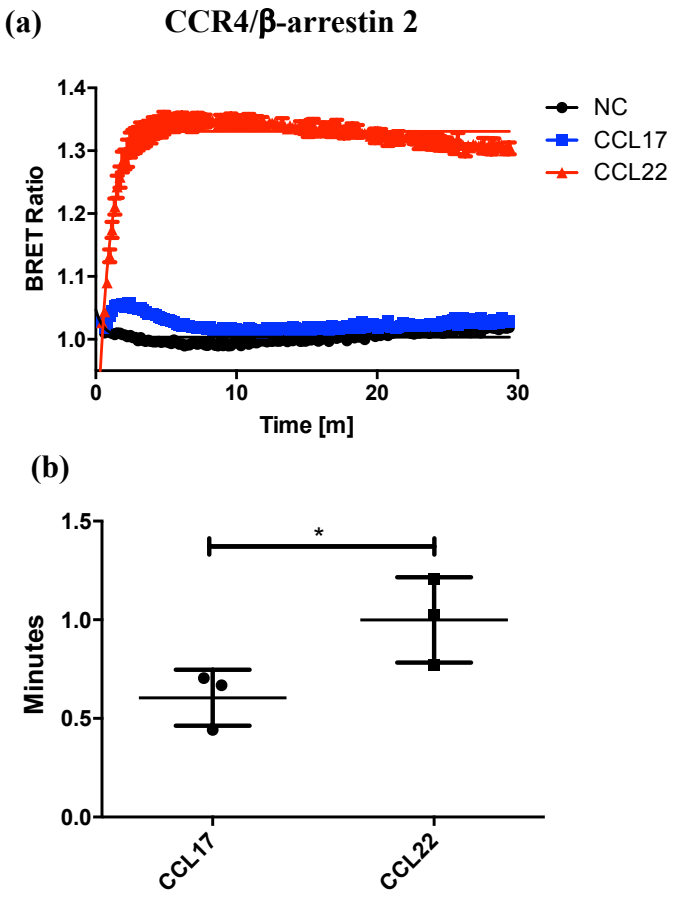

Figure 4.2.4 Kinetics of β-arrestin 2 recruitment to CCR4 induced by CCL17 or CCL22 interaction.

(a) Recruitment of β-arrestin 2 to CCR4 in response to a single concentration (100 nM) of either CCL17 or CCL22 was continuously assessed over a 30-minute period (n=3 +/- SD, representative plot selected from 3 independent experiments). (b) The halftime to maximal signal obtained in response to either CCL17 or CCL22 in these assays were compared (n=3 biological replicates +/- SD, statistically significant differences between each parameter were determined by paired T-test, $p \leq 0.05$=*).

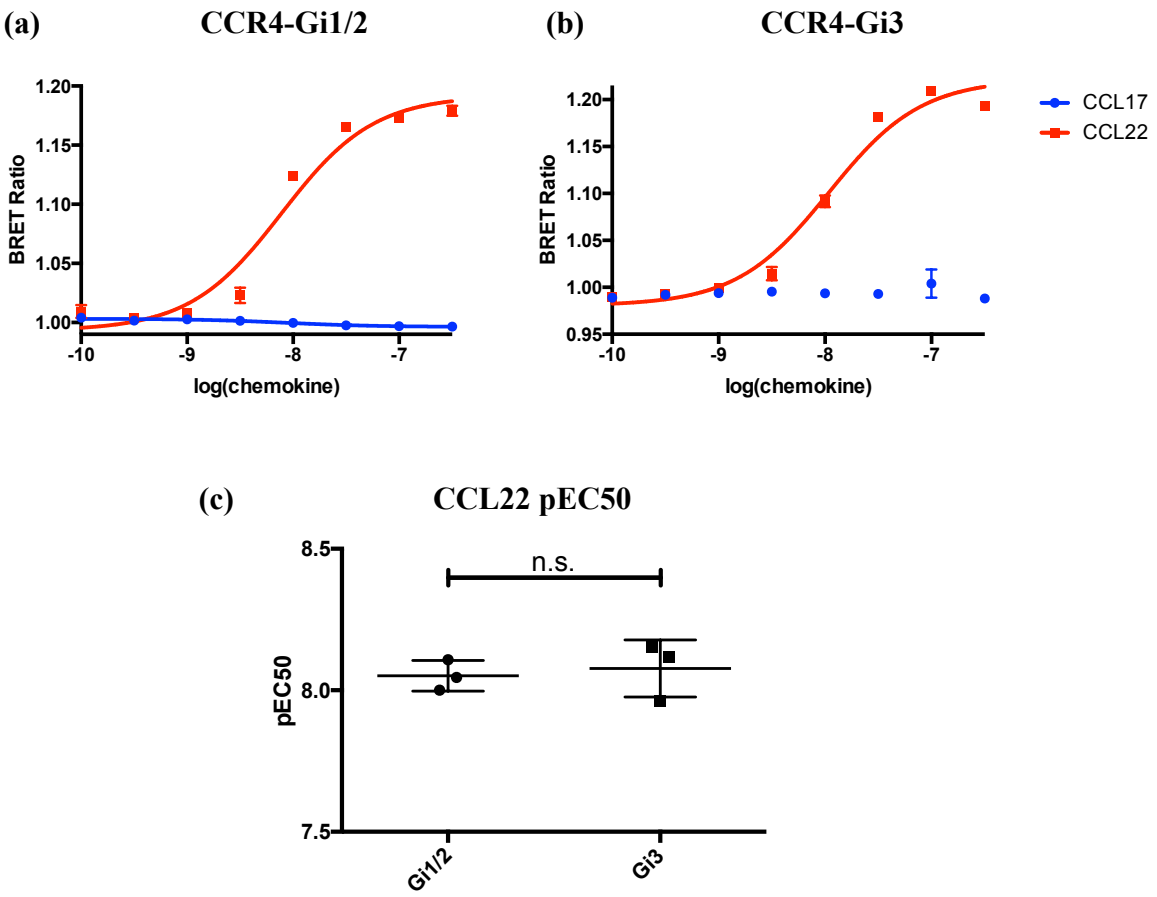

Figure 4.2.5 Recruitment of Gi subunits to CCR4 by CCL17 or CCL22 was assessed utilising SPASM biosensors.

Stable cell lines were generated for the expression of SPASM constructs measuring recruitment of Gi1/2 (a) or Gi3 (b) to CCR4. Expression was induced with doxycycline for 24 hours and cell exposed to increasing concentrations of either CCL17 or CCL22 (n=3 +/- SD, representative plot selected from 3 independent experiments each). All subsequent experiments utilising SPASM biosensors followed the same methodology unless otherwise stated. (c) pEC_{50} values for CCL22 were compared between Gi1/2 and Gi3 recruitment assays (n=3 biological replicates. Statistical significance was evaluated by unpaired T-test).

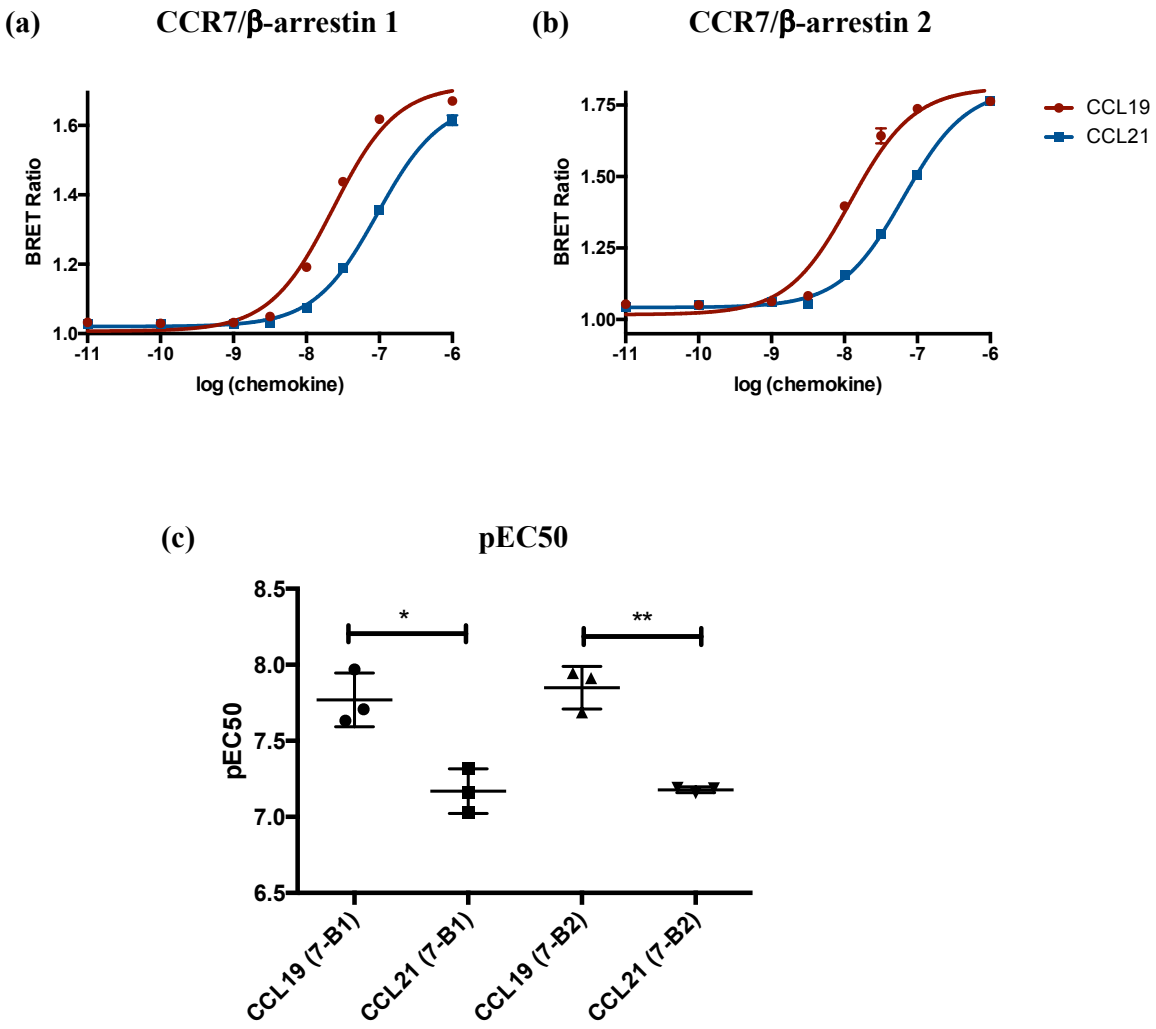

Figure 4.2.6 Recruitment of β-arrestin 1&2 to CCR7 by CCL19 or CCL21, as assessed by BRET.

Recruitment of either β-arrestin 1 (a) or 2 (b) to CCR7 in response to increasing concentrations of either CCL19 or CCL21 was assessed by BRET (n=3 +/- SD, representative plot selected from 3 independent experiments each). (c) Resultant pEC_{50} values were compared between CCL19 and CCL21, and between β-arrestin 1 and 2 for each ligand. (n=3 biological replicates. Statistically significant differences between each parameter were determined by unpaired T-test, $p \leq 0.05$=*, $p \leq 0.01$=**, $p \leq 0.001$=***). 7-B1=CCR7/β-arrestin 1 transfection, 7-B2=CCR7/β-arrestin 2 transfection.

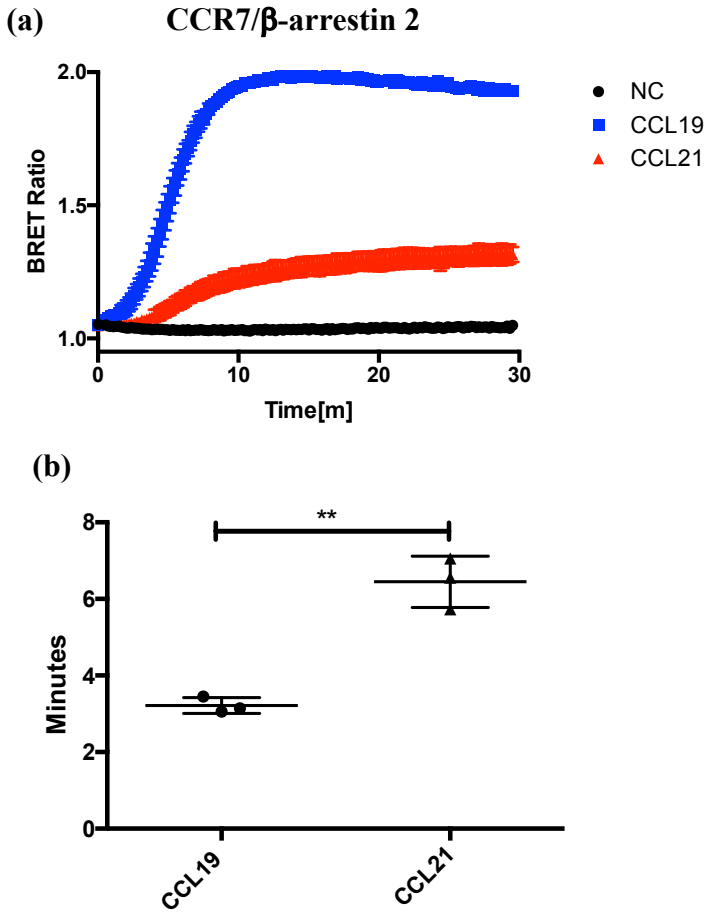

Figure 4.2.7 Kinetics of β-arrestin 2 recruitment to CCR7 induced by CCL19 or CCL21 interaction.

(a) Recruitment of β-arrestin 2 to CCR7 in response to a single concentration (100 nM) of either CCL19 or CCL21 was continuously assessed over a 30-minute period (n=3 +/- SD, representative plot selected from 3 independent experiments). (b) The halftime to maximal signal obtained in response to either CCL19 or CCL21 were compared (n=3 biological replicates +/- SD, statistically significant differences between each parameter were determined by paired T-test, $p \leq 0.01$=**).

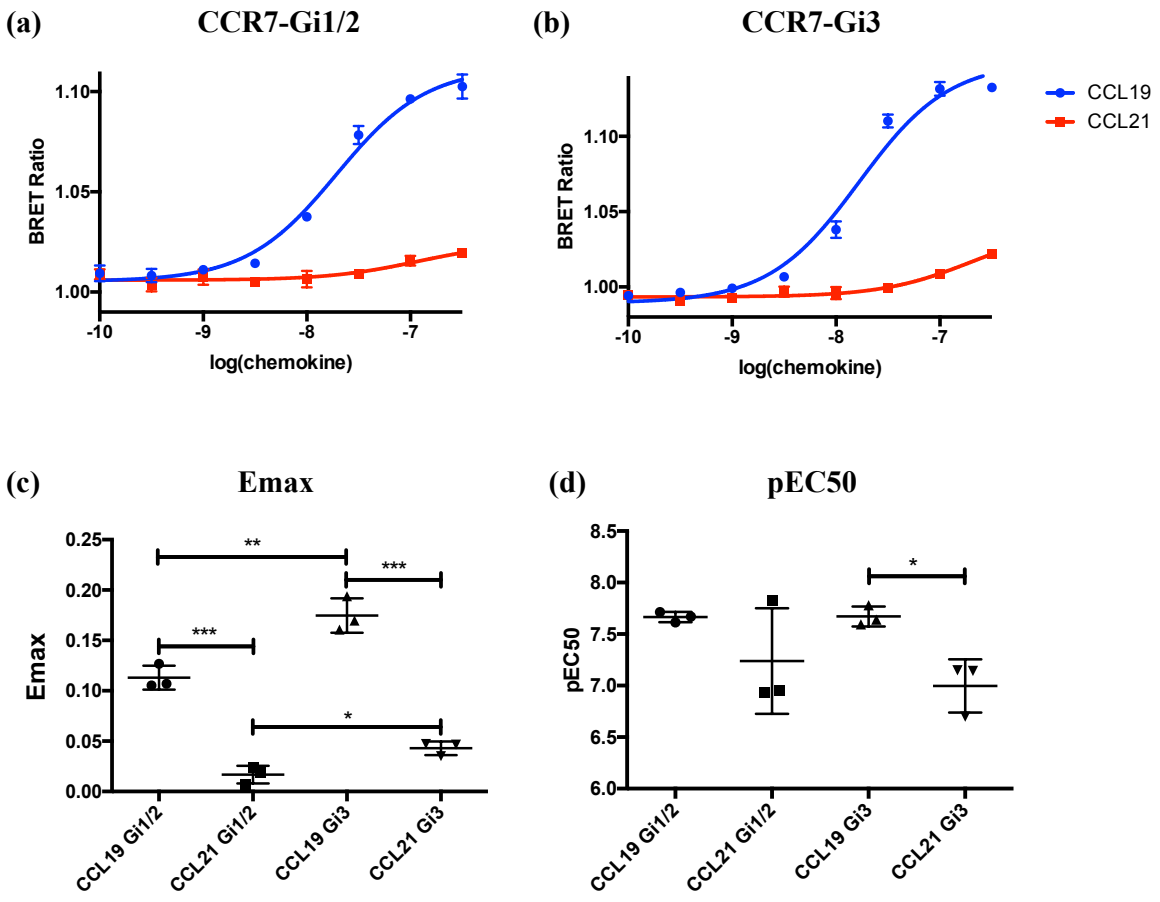

Figure 4.2.8 Recruitment of Gi subunits to CCR7 by CCL19 or CCL21 was assessed utilising SPASM biosensors.

Stable cell lines were generated for the expression of SPASM constructs measuring recruitment of Gi1/2 (a) or Gi3 (b) to CCR7. Expression was induced with doxycycline for 24 hours, with cells exposed to increasing concentrations of either CCL19 or CCL21 then analysed by BRET (n=3 +/- SD, representative plot selected from 3 independent experiments each). (c) Emax values were compared between Gi1/2 and Gi3 recruitment assays for both CCL19 and CCL21. (d) pEC_{50} values from these experiments were also compared. (n=3 biological replicates in both instances. Statistical significance was evaluated by unpaired T-test, $p \leq 0.05$=*, $p \leq 0.01$=**, $p \leq 0.001$=***).

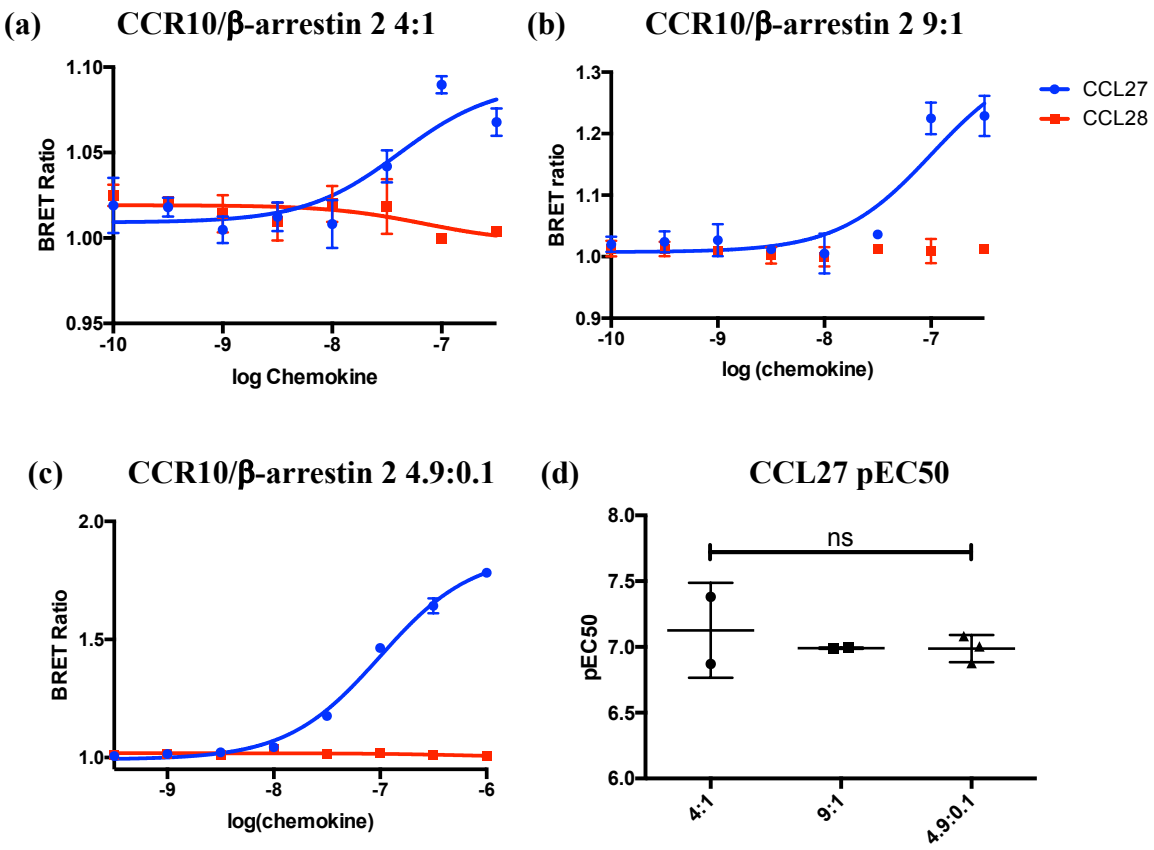

Figure 4.2.9 Recruitment of β-arrestin 2 to CCR10 in response to CCL27 or CCL28, as assessed by BRET.

Recruitment of β-arrestin 2 to CCR10 in response to increasing concentrations of either CCL27 or CCL28 was assessed by BRET when 'acceptor' (CCR10) and 'donor' (β-arrestin 2) were transfected into HEK293T cells in a ratio of either (a) 4:1, (b) 9:1 or (c) 4.9:0.1. In (a) and (b) the same construct was used as before (β-arrestin 2-rLuc). In (c) β-arrestin 2 is expressed in a different construct, fused to nano-luciferase. (a&b; n=3 ± SD, representative plot of 2 independent experiments. c; n=3 ± SD, representative plot of 3 independent experiments). (d) pEC_{50} values for CCL27 mediated β-arrestin 2 recruitment were compared between experiments utilising different 'acceptor':'donor' ratios (a&b n=2 ± SD, c n=3 ±SD. Statistical differences were assessed by unpaired T-test.)

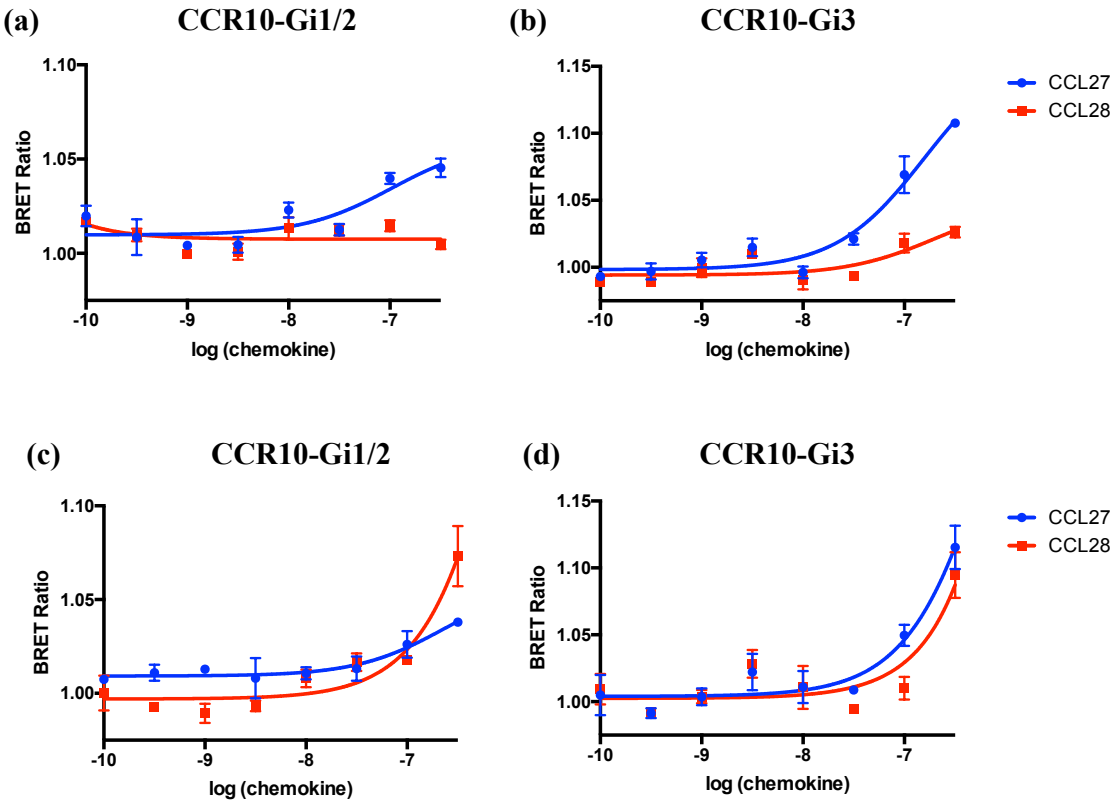

Figure 4.2.10 Recruitment of Gi subunits to CCR10 in response to CCL27 or CCL28 was assessed utilising SPASM biosensors.

Stable cell lines were generated for the expression of SPASM constructs measuring recruitment of Gi1/2 (a) or Gi3 (b) to CCR10. Expression was induced with doxycycline for 24 hours, with cells exposed to increasing concentrations of either CCL27 or CCL28 then analysed by BRET (n=3 +/- SD). (a) and (c) represent repeated experiments assessing recruitment of Gi1/2 to CCR10, and (b) and (d) represent the same for Gi3 recruitment.

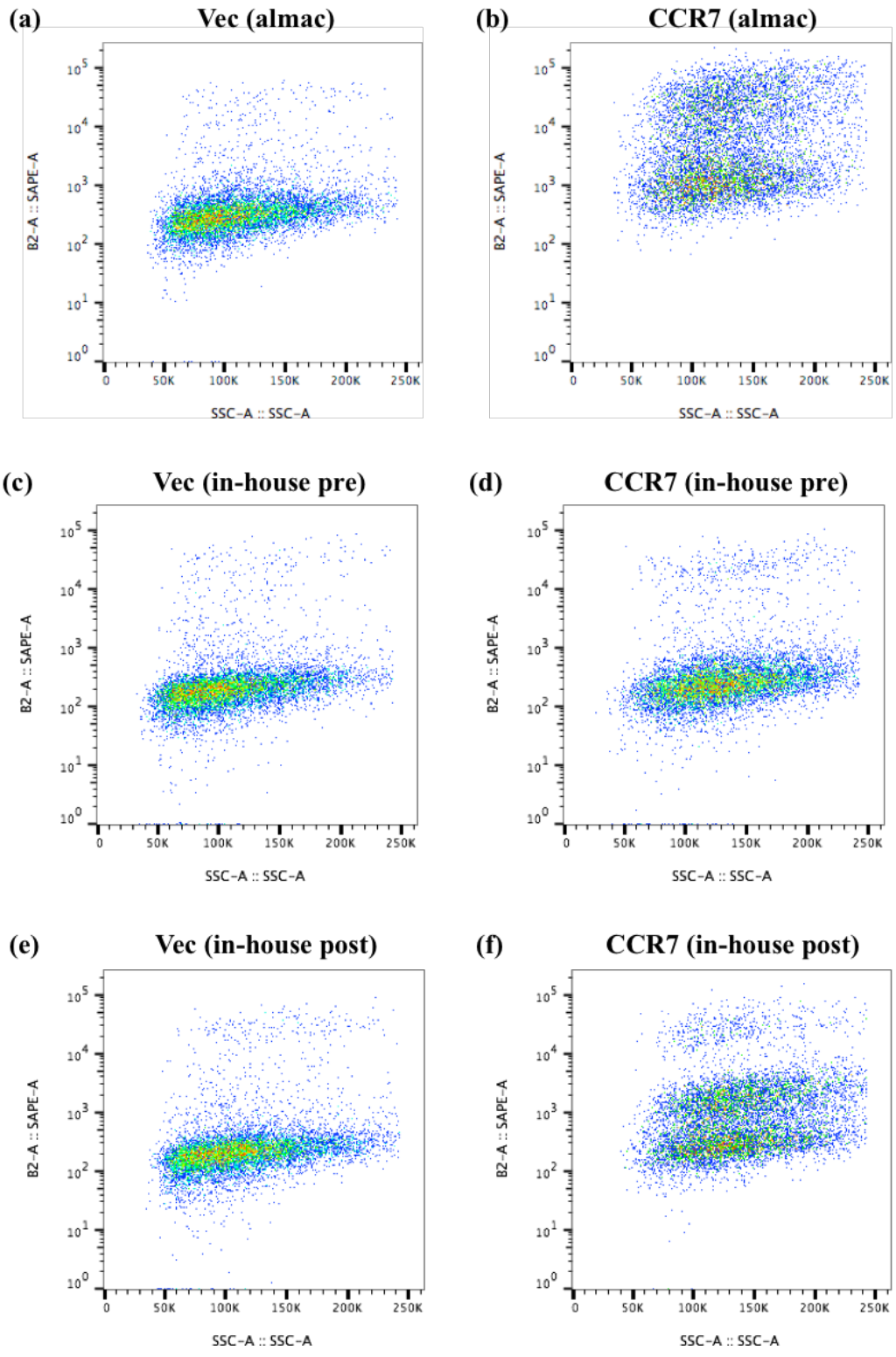

Figure 4.2.11 Assessment of receptor staining by flow cytometry with in-house biotinylated chemokines.

HEK293T cells were transfected with empty vector (Vec, a,c&d) or CCR7-FLAG (CCR7, b,d&f). Transfected cells were prepared for flow cytometry and stained with either biotinylated CCL19 from almac pre-conjugated with SAPE (a&b), in-house biotinylated CCL19 pre-conjugated to SAPE (c&d), or in-house biotinylated CCL19 used initially unconjugated, with cells stained after chemokine incubation with SAPE (e&f). Representative plots from 3 repeat measures are shown.

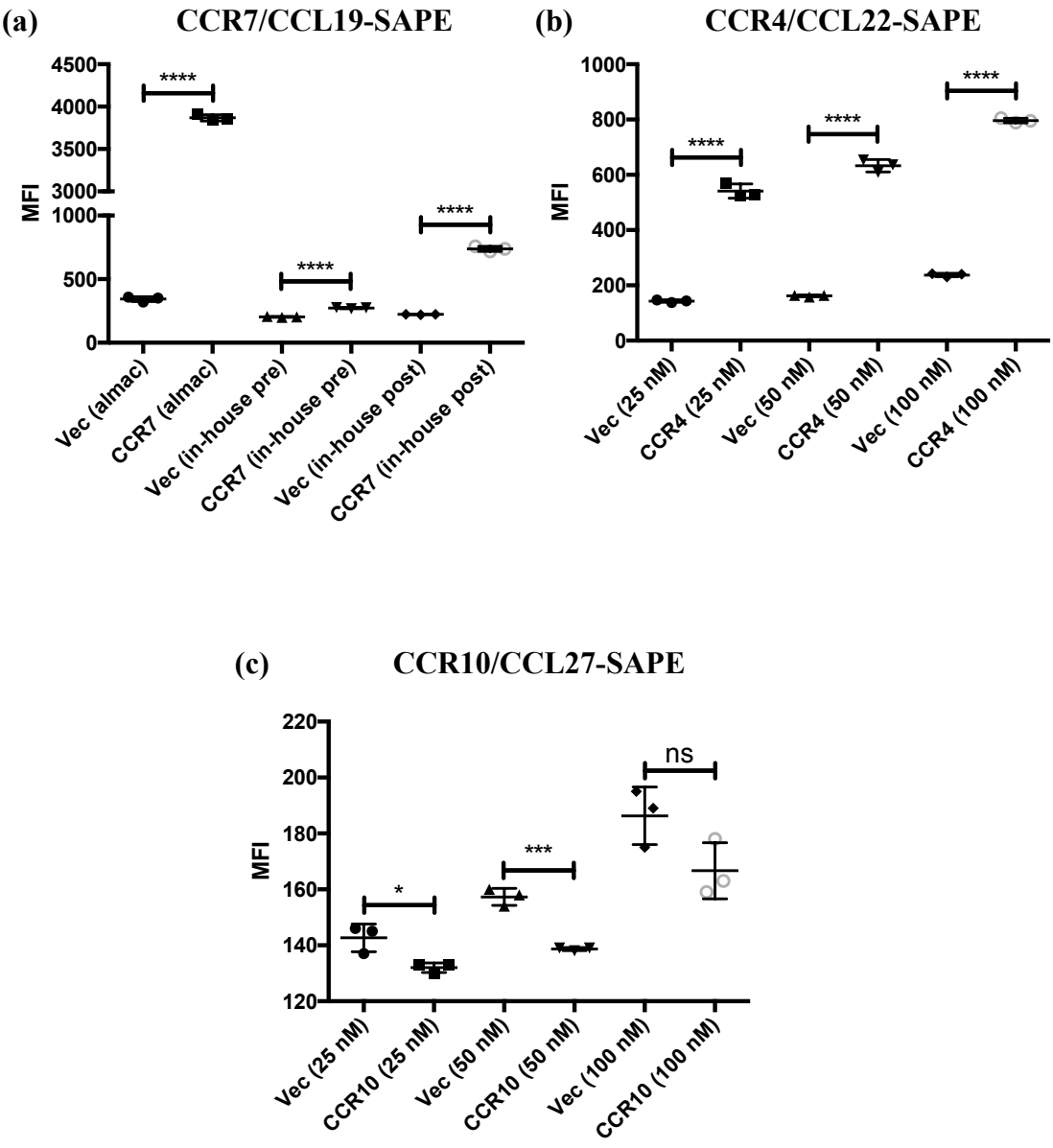

Figure 4.2.12 Assessment of receptor staining by flow cytometry with in-house biotinylated chemokines.

HEK293T cells were transfected with empty vector (Vec), (a) CCR7-FLAG, (b) CCR4-FLAG or (c) CCR10-FLAG. MFI was determined in the PE channel for all cells in the live singlet gate in all instances. (a) Staining with commercially available biotinylated CCL19 (Vec (almac) & CCR7 (almac)) was compared to in-house biotinylated CCL19 either pre-conjugated to SAPE (Vec (in-house pre) & CCR7 (in-house pre)) or cells stained by first chemokine then SAPE separately (Vec (in-house post) & CCR7 (in-house post)). Increasing concentrations (25-100 nM) of biotinylated CCL22 (b) or CCL27 (c) were used to stain either empty vector (Vec), CCR4 or CCR10 transfected cells, with SAPE staining carried out separately as before. (n=3 ±SD in all instances. Statistical significance was evaluated by unpaired T-test, $p \leq 0.05$=*, $p \leq 0.001$=***, $p \leq 0.0001$=****).

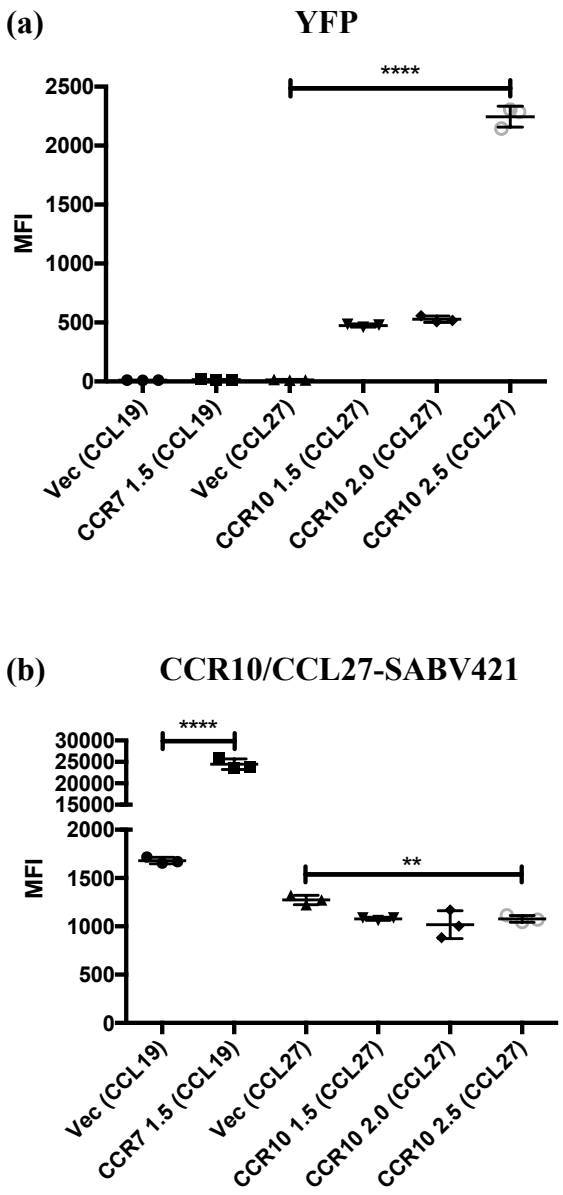

Figure 4.2.13 CCL27 staining was assessed with increasing quantities of CCR10-YFP.

HEK293T cells seeded on a 6-well plate were transfected when near-confluent with either 1.5 µg empty vector, 1.5 µg CCR7-FLAG, and either 1.5, 2.0 or 2.5 µg CCR10-YFP. (a) Expression of CCR10-YFP was determined by flow cytometry. (b) Staining with a constant concentration of biotinylated CCL27 (25 nM) of empty vector/CCR10 transfected cells was assessed as described previously (with SABV421 in place of SAPE) and compared with staining of empty vector and CCR7 transfected cells stained with commercially biotinylated CCL19 pre-conjugated to SABV421. (n=3 ±SD in all instances. Statistical significance was evaluated by unpaired T-test, $p \leq 0.01$=**, $p \leq 0.0001$=****).

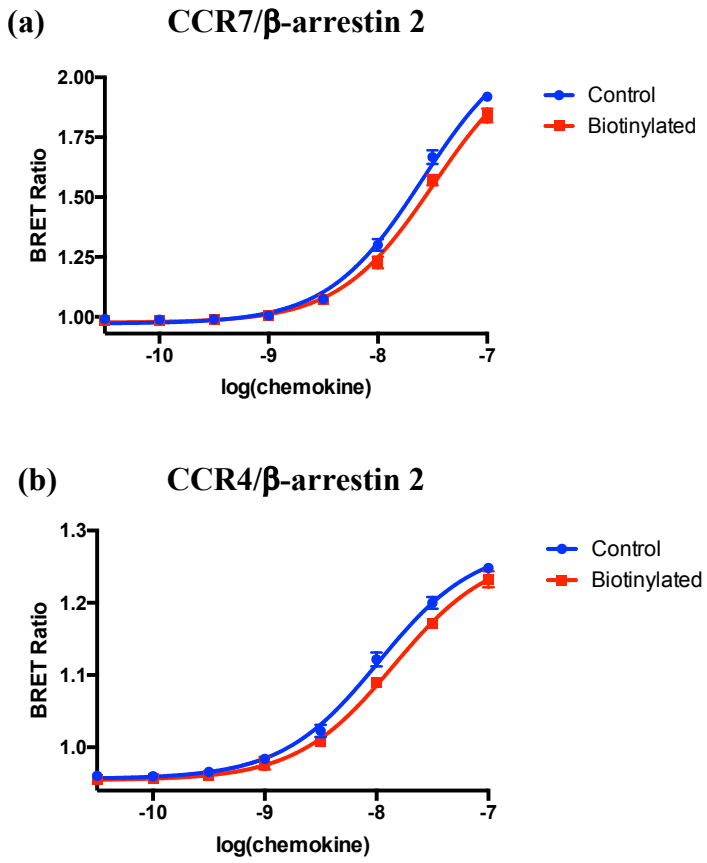

Figure 4.2.14 Recruitment of β-arrestin in response to biotinylated CCL19 and CCL22 was compared with unlabelled chemokine

Recruitment of β-arrestin 2 to either CCR7 (a) or CCR4 (b) in response to increasing concentrations of either unlabelled (Control) or biotinylated CCL19 (a) or CCL22 (b) was assessed by BRET. (n=3 ± SD in both experiments)

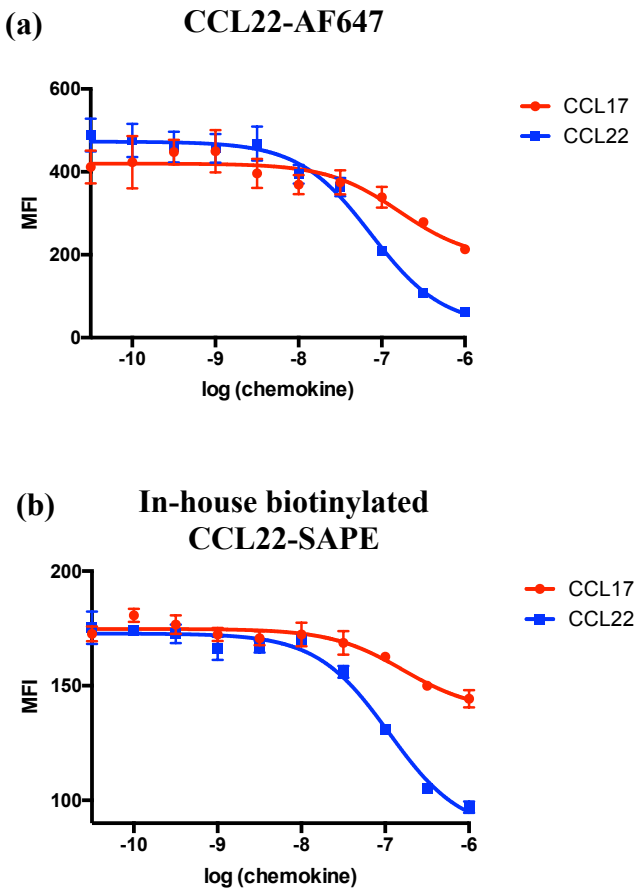

Figure 4.2.15 Affinity of CCL17 or CCL22 for CCR4 expressed on HEK293T cells was assessed via a FACS based competition assay.

HEK293T cells were transiently transfected with CCR4 and subsequently stained with either directly labelled (a) or in-house biotinylated (b) CCL22 in the presence of increasing concentrations of unlabelled CCL17 or CCL22, and evaluated by flow cytometry. IC50 was determined from the MFI obtained from the live singlet population in each respective channel at each inhibitor concentration. (a; n=4±SD, b; n=3±SD)

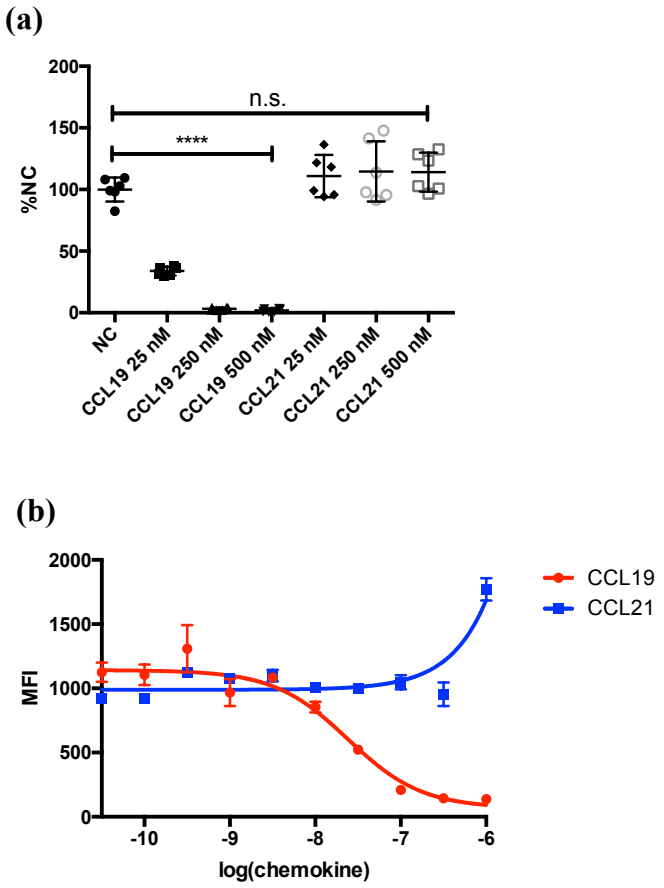

Figure 4.2.16 Determination of CCL19 or CCL21 binding to CCR7 expressed on HEK293T cells as assessed by competition assays.

HEK293T cells were transiently transfected with CCR7 and stained with 25 nM CCL19-SAPE in the presence of increasing concentrations of unlabelled CCL19 or CCL21 as described previously. (a) Displacement of labelled CCL19 by 25, 250 or 500 nM of either unlabelled CCL19 or CCL21 was determined by obtaining MFI values for live single cells in the PE channel, subtracting MFI values obtained with those from the empty vector control group as background, and expressing this as a percentage of cells stained without unlabelled competitor (NC). (n=6±SD, 3 technical replicates each from 2 independent experiments. Statistically significant differences between parameters were determined by unpaired T-test, $p \leq 0.0001$=****). (b) Affinity of CCL19 and CCL21 was evaluated by displacement of CCL19-SAPE by unlabelled competitor with a concentration range from 0.03 nM to 1 mM. IC50 was determined from the MFI obtained from the live singlet population in the PE channel at each inhibitor concentration. (n=3±SD. Representative plot of 2 independent experiments).

Chemokine/ receptor:	arrestin 1			arrestin 2			Gi1/2			Gi3		
	pEC50 (logM±SEM)	Emax (±SEM)	RA (x10^6±SEM)	pEC50 (logM±SEM)	Emax (±SEM)	RA (x10^6±SEM)	pEC50 (logM±SEM)	Emax (±SEM)	RA (x10^6±SEM)	pEC50 (logM±SEM)	Emax (±SEM)	RA (x10^6±SEM)
CCL17/CCR4	7.63±0.09	0.025±0.002	1.067±0.177	7.72±0.11	0.033±0.002	1.835±0.385	nd	nd	nd	nd	nd	nd
CCL22/CCR4	8.01±0.01	0.223±0.007	23.070±0.300	8.00±0.10	0.280±0.028	29.070±7.843	8.05±0.03	0.207±0.010	26.430±1.928	8.08±0.06	0.2126±0.015	27.380±3.020
CCL19/CCR7	7.77±0.10	0.869±0.213	60.550±29.880	7.85±0.08	0.718±0.040	52.500±9.406	7.66±0.03	0.113±0.007	5.259±0.480	7.67±0.06	0.175±0.010	8.230 ±0.725
CCL21/CCR7	7.17±0.08	0.804±0.251	11.820±3.579	7.18±0.01	0.652±0.061	9.874±1.131	7.24±0.30	0.0168±0.005	0.289±0.101	7.00±0.15	0.0168±0.005	0.461±0.1124
CCL27/CCR10	nd	nd	nd	6.99±0.06	0.845±0.023	8.430±1.307	6.98	0.049	0.472	6.8	0.1657	1.059
CCL28/CCR10	nd	nd	nd	nd	nd	nd	nd	nd	nd	nd	nd	nd

Table 4.2.1: Summary of pEC50, Emax and RA values generated in this chapter

Chemokine:	Receptor:	Recruiting:	Halftime (min):	±:
CCL17	CCR4	β-arrestin 2	0.6	0.08
CCL22	CCR4	β-arrestin 2	1.0	0.12
CCL19	CCR7	β-arrestin 2	3.2	0.12
CCL21	CCR7	β-arrestin 2	6.4	0.39

Table 4.2.2: Summary of halftime values obtained for β-arrestin recruitment induced by 100 nM chemokine

5 Polysialylation of chemokine receptors and its impact on the perception of biased agonism

5.1 Introduction

In chapter 4 a curiosity in the relationship between CCL21 and its cognate receptor CCR7 presented itself. It appeared that, rather than demonstrating the widely reported G-protein bias, CCL21 signalling in fact seemed skewed in favour of β-arrestin. Additionally, it appeared that CCL21 had such poor affinity for CCR7 that it was incapable of competing for receptor occupancy with CCL19, up to a 40x molar excess of labelled chemokine. These findings contrast with previous evaluations of the CCL19/CCL21:CCR7 signalling axis, and it is perhaps hasty to attribute this contrast solely to differences in methodology. Recent work utilising similar BRET based methods and the HEK293 cell line demonstrated broadly similar results in terms of β-arrestin and G_{α}-protein recruitment to the studies presented in this thesis, and also concluded that CCR7 does not demonstrate true biased agonism (Corbisier *et al.*, 2015). However, CCL21 is considered the dominant ligand of CCR7 in vivo; singularly sufficient for migration of DCs to LNs and able to engage unique signalling pathways (Gunn *et al.*, 1999; Hauser *et al.*, 2016). In addition, combined CCL21 and CCL19 knockout results in a more profound phenotype than CCL19 KO alone (Britschgi, Favre and Luther, 2010), and more closely mirrors that seen with loss of CCR7 itself (Kobayashi *et al.*, 2017). This would imply some difference between the characteristics of CCR7 expressed in primary cells, in vivo and in cell lines of the lymphoid and myeloid lineages, and in the HEK293T cell line frequently used in more detailed assessment of the receptors signalling properties.

This raised an interesting question; what differences in the translational/post-translational machinery of lymphoid/myeloid cells and HEK293T cells might explain this apparent discrepancy? Recent work on the sialyltransferase ST8sia4 may provide some insight. ST8sia4 catalyses the formation of large α2,8-linked homopolymers of sialic acid ranging from a minimum of 8 subunits to over 100, giving rise to a large, highly restricted additional PTM of a handful of glycosylated proteins known as polysialic acid (pSia) (Mori *et al.*, 2017). pSia is attached to both O- and N-linked glycans and is perhaps best characterised on the neural cell adhesion molecule (NCAM). Polysialylation of NCAM occurs only on the 140 and 180 kDa forms of NCAM, but not the 120 kDa form of the protein found throughout most of the adult central nervous system (CNS). In this context it

is considered vital to neurogenesis during foetal development and neuronal plasticity in the adult CNS (such as in the olfactory bulb) and mediates its activity through inhibition of cell-cell/substrate interactions by attenuating NCAM binding and as a result increasing cellular motility (Windfuhr *et al.*, 2000; Röckle and Hildebrandt, 2016; Zerwas *et al.*, 2016). Polysialylation is catalysed by 2 sialyltransferases, ST8sia2 and ST8sia4, with the former considered more vital in neurogenesis during development and the latter vital to plasticity in the adult CNS (Zerwas *et al.*, 2016). Knockout of ST8sia4 results in generally normal neuronal development however it is associated with a number of learning and behavioural defects attributable to loss of neuronal plasticity (Calandreau *et al.*, 2010; Zerwas *et al.*, 2016). Alteration of cell-surface glycosylation is also a common feature of cancer (Pearce and Läubli, 2015). Indeed, increased polysialylation can be associated with late stage non-small cell lung cancer, metastatic neuroblastoma and increased metastatic potential of breast cancer, and is believed to aid cancer development via a similar contact-inhibition dependent increase in cellular motility, as seen in neuronal plasticity (Tanaka *et al.*, 2000; Cheung, Vickers and Cheung, 2006; Wang *et al.*, 2016). Targeting of ST8sia4 expression with microRNAs has been shown to reduce the aggressive phenotype of breast cancer cell lines and increase susceptibility of multi-drug resistant leukaemia to chemotherapeutic agents, and the use of pharmacological inhibitors of pSia is being evaluated as a novel cancer therapy (Al-Saraireh *et al.*, 2013; Ma *et al.*, 2016; Zhao *et al.*, 2016).

Of more interest however is the observation that pSia is detectable on the surface of DCs, with an increase in surface pSia associated with DC maturation (Curreli *et al.*, 2007). This was believed to be mainly attributable to polysialylation of neuropilin 2 (NRP2), more typically known as a receptor for vascular endothelial growth factors and semaphorins. Additionally, pSia was demonstrated to bind CCL21 both directly and on the surface of DCs, and this binding could be abrogated by the pre-treatment of DCs with endoneuraminidase-N (endo-N), which cleaves pSia from proteins (Bax *et al.*, 2009). Treatment of DCs with endo-N also reduced their migratory capacity to CCL21. It was also demonstrated that, while reduction in chemotactic response to full length CCL21 could be observed following endo-N treatment, no similar reduction was noted in migration of DCs to CCL21 lacking its characteristic extended C-terminus, signifying that this region of CCL21 is critical in pSia mediated regulation (Rey-Gallardo *et al.*, 2010). In the same study it was demonstrated that siRNA knockdown of ST8sia4 also attenuated DC migration toward CCL21.

More recently though it was revealed in a series of elegant experiments that CCR7 is a target of ST8sia4 mediated polysialylation, and that CCL21 signalling is dependent on this PTM (Kiermaier *et al.*, 2016). St8sia4 KO demonstrated a similar immunophenotype to CCR7 KO, with diminished LN size at rest and poor increase in cellularity under inflammatory insult. Bone marrow derived DCs (BMDCs) from ST8sia4 KO animals were profoundly attenuated in their ability to migrate to full-length CCL21 but unaffected in CCL19 migratory capacity in vitro, and ST8sia4 KO DCs demonstrated almost no recruitment to LNs in vivo, or into the afferent lymphatics of skin explants. ST8sia4 KO BMDCs also demonstrated attenuated downstream signalling responses from CCL21 treatment. Migration of NRP2 KO DCs presented no defect in CCL21 migration, indicating that while pSia appears critical to CCL21 mediated chemotaxis it is not dependent on NRP2 polysialylation. Subsequently CCR7 was shown to be directly polysialylated IP experiments, and CCR7 deficient DCs demonstrated reduced pSia levels compared to WT cells. Finally, it was revealed by nuclear magnetic resonance spectroscopy that, in the absence of pSia CCL21, adopts an auto-inhibitory conformation. Interaction with pSia releases CCL21 from this, allowing it to fully interact with CCR7 (select findings summarised in figure 5.1.1).

The idea that, in the absence of pSia, CCL21 maintains an auto-inhibitory conformation that attenuates its ability to interact with CCR7 might help to address some of the more curious findings presented in Chapter 4. Consequently, validation of the FACS based competition assay was sought using BMDCs from wild type mice and CCR7 and ST8sia4 assessed during BMDC differentiation. This would help establish a baseline for affinity of CCL19 and CCL21 in a cell model endogenously expressing CCR7, as well as revealing the expression dynamics of CCR7 and ST8sia4 during development. Expression of ST8sia4 was assessed in HEK293T cells, comparing this to other commonly used adherent and readily transfectable cell lines and a selection of myeloid/lymphoid cell lines. Recruitment assays for CCR4 and CCR7 were repeated with the inclusion ST8sia4, and the resultant data compared with that obtained previously. Lastly, CCR10 was demonstrated as a novel target of ST8sia4 mediated polysialylation, with effects on signalling potential of both of its cognate ligands.

5.2 Evaluation of CCR7 ligand affinity and CCR7 and ST8sai4 mRNA expression in BMDCs

BMDCs were generated as described in materials and methods. In brief; bone marrow from WT mice was resuspended in complete RPMI+ supplemented with 20 ng/ml GM-CSF.

Every two days non-adherent cells were transferred to fresh plates and media refreshed. Adherent cells were discarded. On day 7 cells were stimulated with ovalbumin for 4 hours before being resuspended in media supplemented with 100 ng/ml LPS and 50 ng/ml TNF for overnight stimulation. For FACS analysis day 8 stimulated cells were used. For qPCR, aliquots of cells from unstimulated bone marrow (D0), day 4 of the differentiation protocol (D4) and day 7 of the protocol (D7) were harvested for mRNA which was converted to cDNA, and analysis performed.

BMDCs were stained with biotinylated CCL19 from almac pre-conjugated with SAPE at a concentration of 25 nM, in the presence of increasing concentrations of unlabelled CCL19 or CCL21, with a range of competitor chemokine from 0.03 nM to 1 μM, performed in the same manner as described previously. pK_i was calculated from the MFI of live single cells in the PE channel by flow cytometry at each competitor concentration (figure 5.2.1 a). Both CCL19 and CCL21 could compete for receptor occupancy, with indicated pK_i values of -.80±0.19 for CCL19 and 7.93±0.10 for CCL21 (n=3±SEM). While previous studies determined that affinities between CCL19 and CCL21 were comparable, here CCL19 demonstrates a significantly lower pK_i than CCL21 (p=0.0162, figure 5.2.1 b). These data indicated that CCR7 expressed in BMDCs has different ligand binding properties from CCR7 expressed in HEK293T cells (figure 4.2.16 a&b).

Primers were designed for the amplification of murine CCR7 and ST8sia4, qPCR performed, and expression normalised to a housekeeping gene (TBP), and induction of expression relative to unstimulated bone marrow determined by the $2^{-\Delta\Delta CT}$ method of comparative analysis as before. These data indicated that CCR7 expression was effectively absent in bone marrow, however its expression is strongly induced during the differentiation protocol, peaking on day 7 (D0=1.0±0.1 n=3±SEM, D4=2.8±0.7 n=3±SEM, D7=45.8±7.1 n=10±SEM, figure 5.2.2 a. Units are fold change, n and unit is the same for below). ST8sia4 expression meanwhile remained steady during the maturation of BMDCs, demonstrating a trend of increased expression between stages of differentiation but no significant differences (D0=1.1±0.4, D4=1.1±0.1, D7=1.7±0.2, figure 5.2.2 b). As such it would appear that while CCR7 expression is upregulated in response to the maturation protocol, ST8sia4 expression is steady and may precede it. This would allow for appropriate polysialylation of the receptor once its expression was up-regulated.

5.3 The role of ST8sia4 in the perceived ligand bias of CCR7

5.3.1 ST8sia4 is robustly expressed in myeloid/lymphoid cell lines, but near absent in HEK293T cells

Due to the observation that CCL21 appears attenuated in activity when performing assays in HEK293T cells, and recent publications indicating that polysialylation by ST8sia4 is critical to CCL21:CCR7 interaction, expression of ST8sia4 in HEK293T was evaluated and compared with other commonly used cell lines. To address this, mRNA was harvested from a selection of other frequently used human/simian (HUT78, U937, THP1, COS-7 & HEK293T, figure 5.2.3 a) and murine (L1.2, 3T3 & RAW, figure 5.2.3 b) cell lines and converted to cDNA. In this case analysis by $2^{-\Delta\Delta CT}$ was not appropriate as each cell line would need to act as its own control group and analysis of baseline ST8sia4 expression was sought, not induction. Consequently, a copy number of ST8sia4 and TBP mRNA was determined via qPCR by comparison to known standard curves for each gene. Expression of ST8sia4 is displayed relative to 1000 copies of the housekeeping gene(mTBP). These data indicated that in both human and murine myeloid/lymphoid derived cell lines, ST8sia4 was robustly expressed (HUT78=711.7±139.5, U937=286.9±14.1, THP1=289.3±18.9, L1.2=5101±1269 & RAW=7028±11.8. n=4 in all cases except RAW cells, where n=2. Units are copy number per 1000 copies of TBP). However, in all adherent, fibroblastic/epithelial derived cell lines tested ST8sia4 expression was minimal/absent (HEK293T=45.1±5.4, COS-7=18.0±0.5 and 3T3=1.1±0.3). Consequently, it would appear that adherent, readily transfectable cell lines are deficient in ST8sia4 expression when compared to cells of the lymphoid/myeloid lineage.

5.3.2 CCR7/ST8sia4 co-expression allows CCL21 to out-compete labelled CCL19

Having determined that ST8sia4 expression in HEK293T cells is effectively absent, an ST8sia4-HA expression vector was generated, and previous assessments of CCR7 (chapter 4) repeated, now including ST8sia4 in the transfection strategy. Polysialylation of CCR7 restores CCL21/CCR7 interaction in HEK293T cells in repeats of the competition assay (figure 5.2.4 a&b, compared with figure 4.2.15 b). CCL21 is now capable of competing with the labelled CCL19 for receptor occupancy. CCL21/CCR7 interaction is improved when an increased quantity of ST8sia4 plasmid was used in the transfection. When increased from 1 μg (figure 5.2.4 a) to 4 μg (figure 5.2.4 b), there is a reciprocal drop in pK_i for CCL21 from 7.25 to 8.01 (pK_i for CCL19 was 8.08 and 8.52 respectively). Given

that expression vectors for ST8sia4 and CCR7 are of near equal size (6.2 kb and 6.3 kb respectively), these data appeared to indicate that a near-equimolar transfection strategy is preferable. As such this was used in all subsequent experiments. When directly comparing CCL19:CCL19 competition between cells transfected with and without ST8sia4 (figure 5.2.4 c), no overt differences in CCL19 affinity were noted, with IC50 values of 8.3 and 9 nM respectively. These data agree with previous assessments of CCR7 polysialylation that indicated that pSia had no effect on CCL19 activity, and confirm that the absence of polysialylation of CCR7 in HEK293T cells could account for previous discrepancies when assessing CCL21/CCR7 interactions.

5.3.3 Polysialylation of CCR7 considerably alters CCL21 signalling profile

Assessment of β–arrestin 2 recruitment to CCR7 was repeated, now including ST8sia4-HA in the transfection of cells. A range of concentrations of either CCL19 or CCL21 from 0.1 nM to 300 nM was applied, and recruitment assessed as described previously. When CCR7 was polysialylated CCL21 performs better as a ligand of CCR7 (figure 5.2.5 a, in comparison with 4.2.6 b) with a significant drop in pEC_{50} of β–arrestin 2 recruitment from previous experiments without ST8sia4 co-transfection (CCL21-=7.18±0.01, CCL21+=7.99±0.03, figure 5.2.5 b. p=<0.0001). pEC_{50} for β–arrestin 2 recruitment by polysialylated CCR7 was significantly lower for CCL21 than CCL19 (CCL19+=7.66±0.04, CCL21+=7.99±0.03, p=0.0018). No significant difference was noted between CCL19 pEC_{50} with or without ST8sia4 co-transfection (CCL19-=7.83±0.08, CCL19+=7.66±0.04). In a repeat of previous evaluations of the kinetics of β–arrestin 2 recruitment, with ST8sia4 now included, CCL21 generated a higher maximal BRET signal than CCL19 (CCL19=1.58±0.01 minutes, CCL21=1.63±0.02 minutes, n=3±SEM. Figure 5.2.6 a, compared with 4.2.7 a). CCL21 also appeared to be a faster acting ligand when CCR7 is polysialylated (figure 5.2.6 b), with a reduction in half-time to maximal signal from 6.4±0.4 minutes to 4.1±0.3 minutes. Once again, no significant differences in CCL19 half-times are noted. Collectively, these data indicate that rather than being G-protein biased, CCL21 is a more potent ligand than CCL19 in terms of β–arrestin 2 recruitment. This is in contrast with previous assessments of β–arrestin recruitment by CCR7 in HEK293T cells and may indicate that CCR7 polysialylation had not been accounted for.

Recruitment of Gi3 proteins to CCR7 was re-assessed with receptor polysialylation now included. Initially this was attempted using the previously established stable cell line expressing CCR7-Gi3 reporter used in chapter 4 (figure 4.2.8 a&b). Subsequent transient

transfection of this cell line with ST8sia4-HA was attempted (figure 5.2.7 a), assessing the recruitment of Gi3 to CCR7 with the same concentration range as used previously. While this did result in a lower and more consistent pEC_{50} for CCL21, this was not significantly lower than that achieved previously (CCL21-=7.00±0.15, n=3±SEM. CCL21+(stable)=7.16±0.07, n=2±SEM. Figure 5.2.7 c). This moderate effect was somewhat surprising given the fundamental effect CCR7 polysialylation had when assessing β–arrestin recruitment in response to CCL21. Unpublished observations indicated that stable cell lines generated using this system are refractory to subsequent transient transfection. Consequently, a purely transient transfection of this cell line with ST8sia4-HA was attempted in an effort to address this, co-transfecting the CCR7-Gi3 biosensor construct and ST8sia4-HA into HEK293T cells (figure 5.2.7 b). These data demonstrated a recruitment profile much more in-line with that observed when assessing β-arrestin recruitment to the receptor, resulting in an indicated pEC_{50} of 7.84±0.27 (n=2±SEM) for CCL21. However, despite the considerable increase in indicate potency this did not prove significantly lower than previous measures of pEC_{50} (figure 5.2.7 c). Similar to what was seen when assessing β-arrestin recruitment by CCR7, polysialylation of the receptor had no effect on pEC_{50} of CCL19 mediated Gi3 recruitment (CCL19-=7.67±0.06, n=3±SEM. CCL19+(stable) = 7.70±0.08, n=3±SEM. CCL19+(trans) =7.70±0.08, n=2±SEM). This would indicate that, rather than being G-protein biased, CCL21 is a balanced ligand of CCR7 and can initiate recruitment of both β–arrestin and Gi-proteins by CCR7. It is also apparent that polysialylation of CCR7 has had no effect on CCL19 signalling potential.

5.4 CCL17 signalling potential through CCR4 is unaffected by ST8sia4 co-transfection

Given the somewhat similar dearth of CCL17 signalling (particularly at the level of Gi signalling), and the profound effects polysialylation had on CCL21/CCR7 interaction, CCL17/CCR4 interaction was re-evaluated with ST8sia4 included. This was done in an effort to determine if CCR4 could potentially also be a target of ST8sia4 mediated polysialylation. However, when assessed at the β-arrestin 2 level (figure 5.2.8 a, compared with 4.2.2 b), or at the level of Gi3 protein recruitment (figure 5.2.8 b, compared with 4.2.5 b), CCL17 signalling potential appeared unaffected by the inclusion of ST8sia4 transfection. pEC_{50} values obtained for CCL22 were near comparable to those obtained previously (β–arrestin 2; -ST8sia4=7.99±0.10, n=3±SEM. +ST8sia4=7.99. Gi3; -ST8sia4=8.10±0.06, n=3±SEM. +ST8sia4=7.99). These data indicated that ST8sia4 co-

transfection had no measurable effect on CCL17/CCR4 interaction, and CCR4 is therefore unlikely to be a target of ST8sia4 mediated polysialylation.

5.5 CCR10 is a novel target of ST8sia4 driven polysialylation

5.5.1 Immunoprecipitation of CCR7 and CCR10 confirm polysialylation of these receptors

The posited mode of action for pSia interaction with CCL21 is that the positively charged extended C-terminus of the chemokine interacts with the highly negatively charged pSia, releasing CCL21 from an otherwise auto-inhibitory conformation and allowing it to interact more completely with the receptor. CCL28, like CCL21, has an extended and charged C-terminus, and also has a hexa-cysteine motif instead of the typical tetracysteine motif of chemokines. Additionally, CCL28 is also considered the G-protein biased ligand in a signalling axis with CCL27 and the receptor CCR10, much the same as CCL21/CCL19/CCR7. Given these similarities CCL28 might also require polysialylation of its receptor in order to fully interact, and therefore CCR10 might represent a novel target of ST8sia4 mediated polysialylation.

CCR7-FLAG and CCR10-FLAG were co-transfected into HEK293T cells with either empty vector or ST8sia4-HA. IP was performed against the resulting lysates using an anti-FLAG antibody to enrich for receptor, and western blotting performed to determine if pSia can be detected in the purified lysate of cells transfected with both chemokine receptor and ST8sia4. This would indicate that the receptor is potentially polysialylated (figure 5.2.9). These data indicated that IP of CCR7-FLAG and CCR10-FLAG display a positive signal for pSia only with ST8sia4 co-transfection. As well as confirming the findings of Kiermaier et al regarding CCR7 polysialylation, these data indicate that CCR10 may also be polysialylated.

An IP against pSia itself (probing for receptor to confirm polysialylation of CCR7 and CCR10) proved technically challenging and required considerable optimisation. In brief; the receptor construct used was changed from C-terminally FLAG tagged versions of CCR7 and CCR10 to the Gi3 biosensor construct of these receptors. This was done as the resultant protein product appeared more immunogenic when detected by western blotting using an in-house generated anti-GFP antibody. Immunoprecipitated protein was directly denatured in 2x LDS loading buffer with 100 mM DTT, as opposed to elution in glycine buffer as performed before, in the hopes of maximising protein yield. Additionally, IP time

was shortened from overnight to 4 hours, as pSia is prone to degradation and may have been adversely affected by an extended incubation. Finally, a different anti-pSia antibody was used for detection by western blotting from that used to perform the IP, as the anti-pSia used to perform the IP gave a very strong background signal. The result of this is that a specific band can be seen for GFP only when CCR10-Gi3 and ST8sia4 are co-transfected (figure 5.2.10), further suggesting that CCR10 is polysialylated by ST8sia4. No signal is seen for CCR7, indicating it has not been successfully immunoprecipitated with pSia under these conditions. Given the relative difference in pSia signal seen previously (figure 5.2.9), and the difficulties encountered here, it is possible there simply is not sufficient protein obtained for detection of CCR7.

5.5.2 ST8sia4/CCR10 co-transfection alters signalling properties of both CCL27 and CCL28

In order to determine if polysialylation is likely to contribute to CCR10 signalling, β-arrestin recruitment by the receptor in response to CCL27 and CCL28 was assessed. These experiments were performed in the same manner as previously described (figure 4.2.9 c), now with the inclusion of ST8sia4 when transfecting cells (figure 5.2.11 a). These data indicated that while β-arrestin 2 recruitment was induced by CCL27 with or without ST8sai4 co-transfection, recruitment by CCL28 could only be observed when ST8sia4 was included. It should be noted however that CCL28 generated a detectable BRET signal only at the highest concentrations tested (>100 nM). Interestingly, indicated pEC_{50} for CCL27 dropped significantly from 6.99±0.06 (n=3±SEM) without ST8sia4, to 7.27±0.06 (n=3±SEM) when the receptor is polysialylated (figure 5.2.11 b). These data further suggest that CCR10 is polysialylated, and that polysialylation aids receptor interaction of both its cognate ligands.

5.5.3 Expression of CCR10 and ST8sia4 can be simultaneously detected in primary murine cells

Publicly available RNA-seq data was used to determine if CCR10 and ST8sia4 expression are likely to occur in the same cells. The Immunological Genome Project's Skyline (RNA-seq) data set was used, with 6 cell types known to express CCR10 (consisting of 3 each of B-cell and γδ T-cell subsets) evaluated. A selection of DC populations was included as means of comparison for ST8sia4 expression. These were then assessed for CCR10 (figure 5.2.12 a) and ST8sia4 (figure 5.2.12 b) expression. These data indicated that in each cell subset expressing CCR10, ST8sia4 expression was also present. This would suggest that CCR10 polysialylation is likely in vivo. ST8sia4 expression was comparable between 2

DC subsets and the cells expressing CCR10, but considerably lower than 1. This could potentially indicate different requirements of pSia between cell types.

5.5.4 Development of polycistronic vectors compatible with stable cell line generation

While it was possible to assess CCR7 recruitment of Gi3 with receptor polysialylation by using the SPASM biosensor in a transient transfection model (figure 5.2.7 b), repeat measures proved difficult. This is possibly because these biosensors have been optimised for use in an inducible stable cell line, rather than via transient transfection, and perform better in this set-up (unpublished observations from the lab). Generally speaking, transient transfections result in a highly heterogenous population, with some cells expressing no or very little of the desired protein, and others expressing a high copy number of it. In the case of the SPASM biosensor, it's large size increases the probability of it being retained intracellularly, particularly when highly expressed. This would result in reporter proteins still producing light following Coelentrazine H administration but unable to interact with ligand, increasing background luciferase signal and consequently effecting BRET signal. However, as observed when attempting a subsequent transfection of ST8sia4 into stable cell lines generated with the CCR7-Gi3 biosensor, little effect is noted on CCL21/CCR7 interaction. This would indicate that ST8sia4 expression was poor or absent, and that these stable cell lines are refractory to further transfection. As well, the observation that both ligands of CCR10 benefit from receptor polysialylation might provide an indication of why previous assessment of CCR10 G-protein recruitment has been problematic. If CCL27 is attenuated in its capacity to trigger Gi3 recruitment by CCR10 when the receptor is not polysialylated, then it could be that without this G-protein recruitment is not detectable. In an effort to address these issues, polycistronic vectors for the expression of both ST8sia4-HA and the Gi1/2 or GI3 biosensors for CCR4, CCR7 and CCR10 were developed, and placed in a plasmid background compatible with the generation of stable cell lines as before. Plasmids were also generated for expression of ST8sia4 and the YFP tagged versions of CCR4, CCR7 and CCR10 in an effort to simplify transfection strategies going forward. These were based on the TaV2A motif; a 20 amino acid virus-derived sequence that allows for the expression of multiple protein products from a single ORF by initiating what is assumed to be a "skip" in translation by the ribosome upon encountering the sequence (Donnelly *et al.*, 2001). A 2-step process was devised for generating these plasmids, wherein primers were designed to introduce TaV2A and a compatible restriction site downstream of ST8sia4. A new plasmid was generated with this product. Primers were then designed to amplify the Gi biosensor constructs with compatible restrictions sites, and

this product was ligated into the new ST8sia4/TaV2A plasmid (summarised in figure 5.2.13).

Prior to establishing stable cell lines, these constructs were evaluated for expression of both proteins by transient transfection into HEK293T and subsequent western blotting. These data indicated that ST8sia4-HA expression could be detected at equivalent levels to the ST8sia4-HA only transfected controls, and that pSia was generated as a result (a-HA & a-pSia respectively, figure 5.2.14). Unfortunately, protein levels of the chemokine receptors were low for every construct tested (a-GFP (low)), and only readily detectable with longer exposure times (a-GFP (high)). As such it would appear that, while both proteins can be expressed from the single vector, there are significant issues with expression of the second product and these constructs are unlikely to express both required proteins at suitable levels in a stable cell line.

5.6 Discussion

A number of novel findings are described in this chapter, related to the role played by ST8sia4 driven polysialylation in the function of multiple chemokine receptors.

5.6.1 CCR7

Following from observations in the previous chapter regarding CCL21/CCR7 interaction, CCL21/CCR7 affinity was evaluated in a cell type endogenously expressing CCR7. BMDCs were used in a FACS based competition assay, and both CCL19 and CCL21 were shown to compete for receptor occupancy with the CCL19-SAPE, in stark contrast to the same assay performed with CCR7 expressing HEK293T cells (figure 4.2.10 b). While these data are more in-line with previous characterisation of CCR7 and its ligands, CCL21 competes with CCL19-SAPE less effectively than CCL19, generating a significantly higher IC50 value. As stated before, CCL19 and CCL21 are considered to be essentially of equal affinity for CCR7. Again, this could be attributable to differences in methodology, such as the increased staining concentration, or that in this instance non-species matched ligands were used. However, this clear contrast in CCL21 activity in the same assay between BMDCs and HEK293T cells added credence to the hypothesis that specific differences in the molecular characteristics of CCR7 exist between different expression systems. No overt difference is noted in IC50 of CCL19 between assays performed in BMDCs or HEK293T cells.

CCR7 and ST8sia4 expression was assessed during various stages of BMDC differentiation. As expected, CCR7 expression significantly increased during maturation of BMDCs, however somewhat surprisingly ST8sia4 expression remained comparatively steady. This is in contrast with previous studies which demonstrated increasing ST8sia4 expression between monocytes, immature and mature DCs (Curreli *et al.*, 2007). In these studies, human monocytes were sorted and differentiated into DCs. Here however a mixed population (bone marrow) was used to generate DCs. It is possible that, in comparing the induction of expression from a mixed population such as bone marrow instead of purified monocytes it is not possible to determine differences in expression. However, there is also little increase in ST8sia4 expression between cells harvested midway through the differentiation protocol (D4) and those harvested near the end (D7), making this less likely to be the case.

Instead these differences could be attributable to how the DCs were generated from human monocytes. In these studies, Il-4 was used in addition to GM-CSF to induce differentiation into DCs. Beyond the obvious difference in species, it is possible that this change in cytokine treatment results in a DC population with subtly different properties. This might provide something of an explanation for CCL21 demonstrating poorer affinity than CCL19 for CCR7 on BMDCs. It is possible that, if ST8sia4 expression is not induced as potently as it can be, CCR7 expressed in these cells might not be fully polysialylated and therefore attenuated in its capacity to interact with CCL21. DCs can be generated in vitro in two main ways; treatment with GM-CSF and IL-4 or treatment with Flt3 ligand. The latter has been described previously as superior in migratory capacity to LNs, and more akin to steady-state resident DCs (Xu *et al.*, 2007). The observation that the GM-CSF derived DCs used here appear less capable of interacting with CCL21 and have little/no increase in ST8sia4 expression during differentiation could provide a mechanistic explanation for these observations. It would be interesting to see if generating DCs via Flt3 ligand treatment altered ST8sia4 expression profiles and therefore CCL21 binding properties.

The fact that CCL21 was able to compete for receptor occupancy on BMDCs at all however raised an obvious question; do HEK293T cells express ST8sia4? Lack of receptor polysialylation would account for the poor affinity and diminished signalling potential of CCL21. ST8sia4 expression was evaluated in a panel of human and murine cell lines. Interestingly, all cells of the lymphoid/myeloid lineage robustly expressed ST8sia4, whereas expression was either entirely, or near, absent in 3T3, COS-7 and HEK293T cells. An expression vector for ST8sia4 was developed and previous assessments of CCR7 signalling properties were repeated now including polysialylation of the receptor.

Polysialylation of CCR7 in HEK293T cells allowed CCL21 to compete with CCL19-SAPE, with comparable IC50 values to those obtained with BMDCs when CCR7 and ST8sia4 were transfected in near equimolar proportions. No difference was seen in CCL19 affinity, in agreement with previous assessments of CCR7. Interestingly, CCL21 is not able to completely out-compete CCL19-SAPE at a 40x molar excess in this assay, as was seen with BMDCs. This is possibly due to the simultaneous introduction of CCR7 and ST8sia4 into the cells. qPCR data on BMDC indicated that expression of ST8sia4 preceded that of CCR7. By introducing both simultaneously there could be a lag period in which CCR7 is produced but not polysialylated, resulting in a proportion of CCR7 still attenuated in CCL21 binding. There might also be additional PTMs of CCR7 not considered here. For example, CCR7 sulfation has been shown to enhance CCL21 binding (Phillips *et al.*, 2017), and sulfation of CCR7 (or lack thereof) has not been addressed here. It is also possible that, inclusion of a C-terminal epitope tag for ease of detection may have altered ST8sia4 function. Comparison could be made quite easily with new constructs expressing an untagged version of ST8sia4.

Polysialylation profoundly alters the signalling properties of CCL21. When CCR7 is polysialylated, CCL21 appeared dominant to CCL19 in initiating β-arrestin recruitment. pEC_{50} of CCL21 in these assays drops dramatically and is significantly lower than CCL21 when CCR7 is not polysialylated, but also lower than CCL19 when it is. However, while CCL21 is faster acting in the presence of pSia, it is still slower than CCL19. This increase in β–arrestin recruitment potency above that of CCL19 is interesting when considering previous observations that receptor internalisation is instigated either entirely or predominantly by CCL19 (Bardi *et al.*, 2001; Otero, Groettrup and Legler, 2006). These studies were performed using T-cells and peripheral blood lymphocytes, and it has been suggested that T-cell and B-cells exhibit lower surface pSia compared to DCs (Kiermaier *et al.*, 2016), which could account for this difference. However, given that CCL21 avidly binds glycan there may be issues with steric hinderance that could complicate internalisation of non-soluble chemokine in vivo. It would be of interest to determine if CCL21 is internalised efficiently by HEK293T cells expressing CCR7 and ST8sia4. As mentioned previously, CCL19 and CCL21 have been shown to recruit different GRKs to CCR7 (Zidar *et al.*, 2009). Given that this study was conducted in HEK293 cells it would be prudent to repeat this analysis including ST8sia4 transfection and evaluate if this apparent bias still exists when CCR7 is polysialylated.

There were technical issues when attempting to assess recruitment of Gi3 by polysialylated CCR7. The CCR7-Gi3 stable cell line appears to be refractory to subsequent transient

transfection, with little effect noted when attempting to introduce ST8sia4 expression. Although difficult to repeat, transient transfection with CCR7-Gi3/ST8sia4 resulted in a considerable drop in pEC_{50} of CCL21 compared to that obtained when ST8sia4 was either entirely absent or introduced by subsequent transfection. Collectively these data indicate that polysialylation of CCR7 improves receptor affinity and signalling capacity of CCL21, however has no effect on CCL19/CCR7 interaction.

5.6.2 CCR4

Inclusion of ST8sia4 while assessing signalling properties of CCR4 did not alter the signalling profile of either CCL17 or CCL22. CCL22 generated recruitment responses much in line with our previous assessments, while CCL17 still appeared near silent. This is perhaps not surprising when considering the proposed mode of action of pSia; that it interacts with the extended C-terminus of CCL21. CCL17 presents a more classic chemokine structure and does not have an extended C-terminus. As mentioned previously, it is possible that CCL17 acts through other signalling pathways not assessed here. Previous evaluations of CCL17/CCL22 affinity indicate that CCL17 binds CCR4 (Godiska *et al.*, 1997), so assessing receptor activation in a blunter fashion (pERK induction for example), would confirm that CCL17 is active on the receptor. It would then be a matter of determining with other G-protein biosensors if CCL17 is selectively signalling through other G-protein couplings to CCR4 to induce chemotaxis or CGRP expression.

5.6.3 CCR10

Based on the proposed activity of CCL21/pSia interaction, CCR10 presented itself as a likely candidate for ST8sia4 mediated polysialylation. Like CCR7, CCR10 has previously been reported to demonstrate biased agonism between a ligand pair, one of which has an extended and positively charged C-terminus (CCL28) (Rajagopal *et al.*, 2013). Indeed, when performing an IP against receptor there is a clear signal for pSia when CCR10 and ST8sia4 are co-transfected into HEK293T cells, which is considerably stronger than that observed for CCR7. While pSia and receptor cannot be readily co-localised on the blot, this appears to be quite common when blotting for ST8sia4 and has previously been attributed to the antibody against pSia detecting multiple epitopes along a single molecule and the fact that pSia self-cleaves, rendering it unstable in solution (Manzi *et al.*, 1994). Additionally, although it is not possible to determine with CCR7, a higher molecular weight band is seen with CCR10-only transfection that is not visible with ST8sia4 co-transfection. If this represents the mature glycosylated form of CCR10 it is conceivable that, when polysialylated, this shifts from this position. As mentioned previously, pSia can

degrade resulting in a highly mixed MW, it may therefore not be possible to visualise a single discreet band for polysialylated receptor. Performing IP against pSia itself did prove technically challenging when using antibody capture. Kiermaier et al had performed this using catalytically inactivate endo-N coupled to magnetic beads, however this was not a feasible option here. After considerable optimisation it was possible to visualise a specific band for the receptor with CCR10/ST8sia4 co-transfection, confirming that CCR10 represents an entirely novel target of ST8sia4 mediated polysialylation.

To determine if CCR10 polysialylation affected ligand activity, β-arrestin recruitment in response to CCL27 or CCL28 was assessed when CCR10 was polysialylated. Polysialylation resulted in CCL28 consistently recruiting β-arrestin to the receptor, albeit with poor efficiency and only at the highest concentrations tested. Perhaps more interesting is that the pEC_{50} of CCL27 is significantly lower when CCR10 is polysialylated. Analysis of CCR7 in this chapter, and by others, demonstrated that the previously reported β-arrestin biased ligand (CCL19) was completely unaffected by receptor polysialylation in multiple different assays. This is clearly not the case with CCL27 however. At 12.6 kDa CCL27 is larger than typical for a chemokine (8-10 kDa), though is not quite as sizable as CCL21 and CCL28 (14.6 and 14.3 kDa respectively). CCL27 has been described as having a large and unstructured C-terminus (Jansma *et al.*, 2010), which is dissimilar to the majority of chemokines but quite like CCL21 and CCL28. The C-terminal region of the chemokine also harbours a number of positively charged residues, another similarity it shares with CCL21 and CCL28. It is possible that, like CCL21, both CCL27 and CCL28 exist in auto-inhibitory conformations maintained by their extended C-terminus, until released by interaction with the negatively charged pSia decorating their receptor. This may also be representative of a common mode of action of pSia in chemokine biology.

By mining publicly available RNA-seq databases it is clear that, if a cell expresses CCR10, it expresses ST8sia4 as well. This would suggest that the observation that CCR10 is polysialylated, and that this PTM alters signalling properties of both CCL27 and CCL28, is unlikely to be an artefact of utilising in-vitro systems and is likely critical to its biological functions. It is also clear that, unlike with CCR7, the previously reported arrestin bias cannot be attributed simply to an absence of pSia. While CCL28 is capable of recruiting β–arrestin it can only do so poorly and at the highest concentrations tested. Given that other studies have previously shown signalling events downstream of CCR10 consistent with Gi activation by CCL28, this would appear to confirm that, unlike with CCR7, the reported bias of this receptor is not attributable to a lack of pSia modifications in these studies.

5.6.4 Polycistronic vector development

Obtaining reproducible measures of Gi protein recruitment using purely transient transfection proved challenging. Consequently, it was decided to develop a double expression system for these biosensors and ST8sia4-HA compatible with the development of stable cell lines. Unfortunately, although expression of ST8sia4-HA was comparable to single transfected controls, little expression of the chemokine receptor could be observed with these new plasmids. Although slightly larger than ST8sia4-HA from a single expression vector (presumably due to remaining residues from the TaV2A sequence), the sialyltransferase appeared to still be functional in the generation of pSia. This would indicate that TaV2A self-processing has occurred successfully and separated the 2 protein products from the same ORF, and that either translation of the downstream chemokine receptor has been attenuated, or the resulting protein product was rapidly degraded. Poor expression of the secondary product downstream of TaV2A has been reported previously (Momose and Morikawa, 2016), suggested to be the result of proteasomal degradation of the downstream product. However, it has also been shown that re-introducing the initiating methionine (removed from the second ORF) can improve stability of downstream products, as can changing the order in which proteins are encoded. As such it may be possible to generate a new construct with these conditions in mind that can successfully express both cassettes. However, it might ultimately be necessary to repeat the assays described here in an adherent cell line of an immune lineage, such as RAW cells, to insure robust expression of ST8sia4, CCR7/CCR10 and any BRET donor proteins required.

5.6.5 Conclusion

Described here are a number of novel findings related to the polysialylation of chemokine receptors. For example, CCL21/CCR7 signalling behaviour is rapidly altered in HEK293T cells when the receptor is polysialylated. This could go some way to explain the noted discrepancy in assessments of CCR7 signalling between studies using different cell types, as CCL21 now appears to be dominant in CCR7 activation over CCL19 in HEK293T cells which is more in keeping with the observable biology of this receptor. In addition, CCR4 appears to not be polysialylated, or at the least polysialylation has no impact on signalling activity of either CCL22 or CCL17. Previous work does indicate that CCL17 can interact with CCR4 in HEK293T cells (figure 4.2.2 & 4.2.14), so questions remain as to what this interaction initiates downstream of the receptor. Finally, CCR10 presented itself as a previously undescribed candidate for ST8sia4 polysialylation. The presence of pSia on CCR10 improved signalling in response to both CCL27 and CCL28, which distinguishes it from CCR7 which demonstrates effects of receptor polysialylation with CCL21 only.

When considering the ligand characteristics this does make some sense, as unlike CCL19, CCL27 can also be described as having an extended and positively charged C-terminus. This also suggests to a common mode of action of pSia on chemokine receptors, namely the release of chemokines from auto-inhibitory conformations via interaction with their C-terminus.

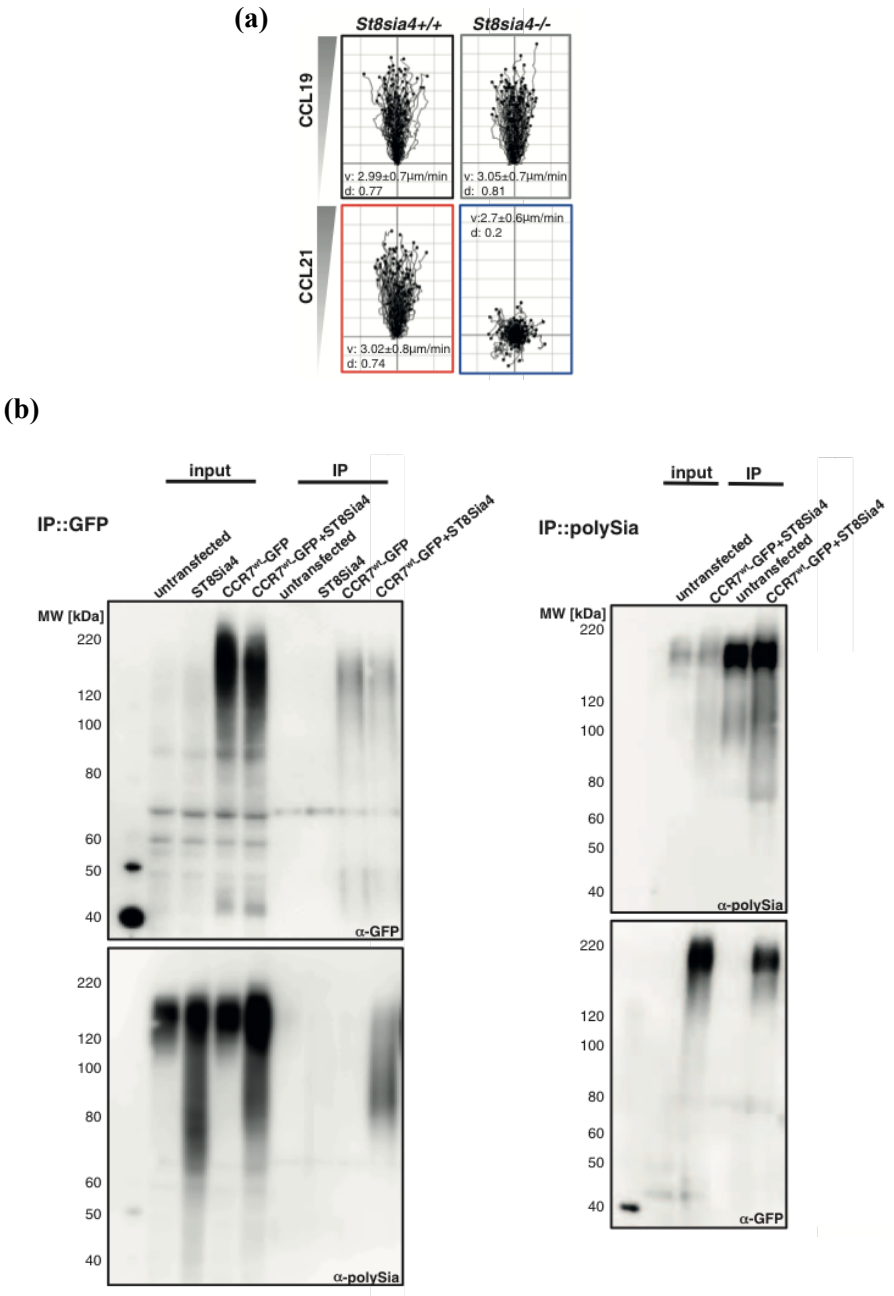

Figure 5.1.1 Polysialylation of CCR7 is critical to CCL21 migratory activity

(a) BMDCs generated from ST8sia4 KO mice demonstrate unchanged migratory capacity to CCL19 but are nearly incapable of migration to CCL21 when compared to BMDCs from WT animals. (b) IP against CCR7 and pSia results in positive signal for both the receptor and the pSia in both cases, indicating that CCR7 is a polysialylated protein. Adapted from Kiermaier et al, 2016.

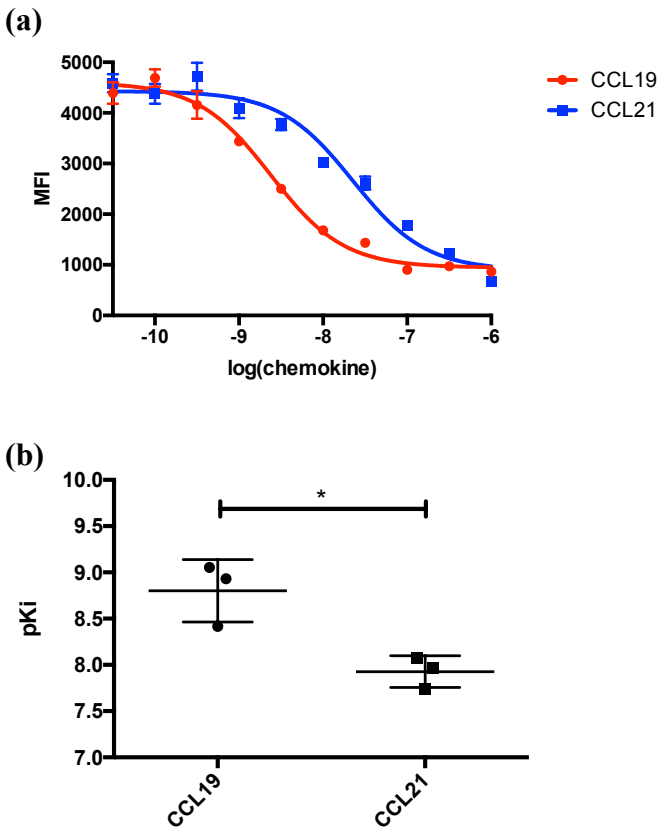

Figure 5.2.1 Determination of CCL19 and CCL21 affinity on endogenous CCR7 expressing BMDCs.

(a) In vitro differentiated BMDCs were labelled with 25 nM fluorescently labelled CCL19 in the presence of increasing concentrations of unlabelled CCL19 or CCL21. MFI was determined for all live single cells in the PE channel (n=3 +/- SD, representative plot selected from 3 independent experiments). (b) pK_i values obtained were compared between CCL19 and CCL21 (n=3 biological replicates +/- SD, statistically significant differences between each parameter were determined by unpaired T-test, $p \leq 0.05$=*).

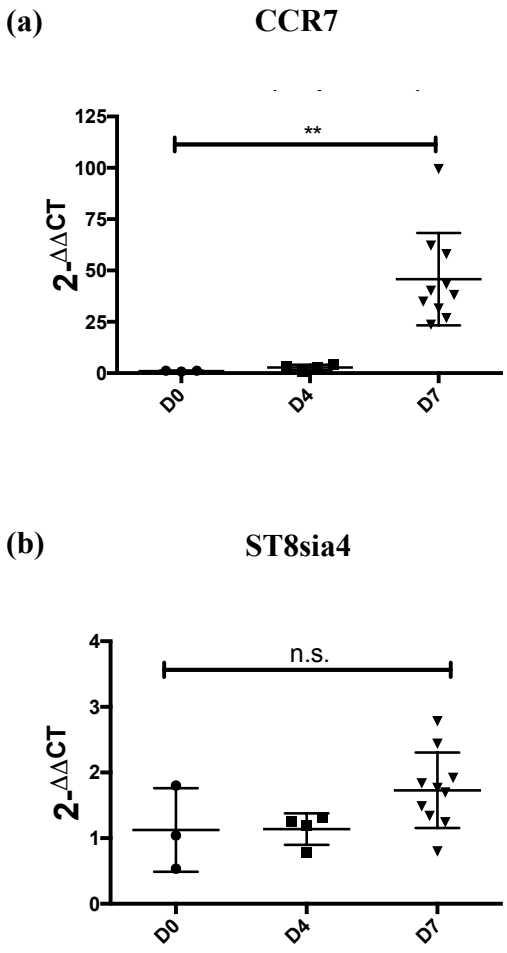

Figure 5.2.2 Expression of CCR7 and ST8sia4 during BMDC differentiation were compared by qPCR

BMDCs were derived from murine bone marrow by repeated treatment with GM-CSF at day 0, 2 and 4. Levels of either (a) CCR7 or (b) ST8sia4 mRNA were assessed by RT-qPCR relative to day 0 bone marrow (D0) at day 4 of BMDC differentiation (D4) and on day 7 (D7) (each data point represents a biological replicate, error bars = +/- SD, statistically significant differences between each parameter were determined by unpaired T-test, $p \leq 0.01$=**).

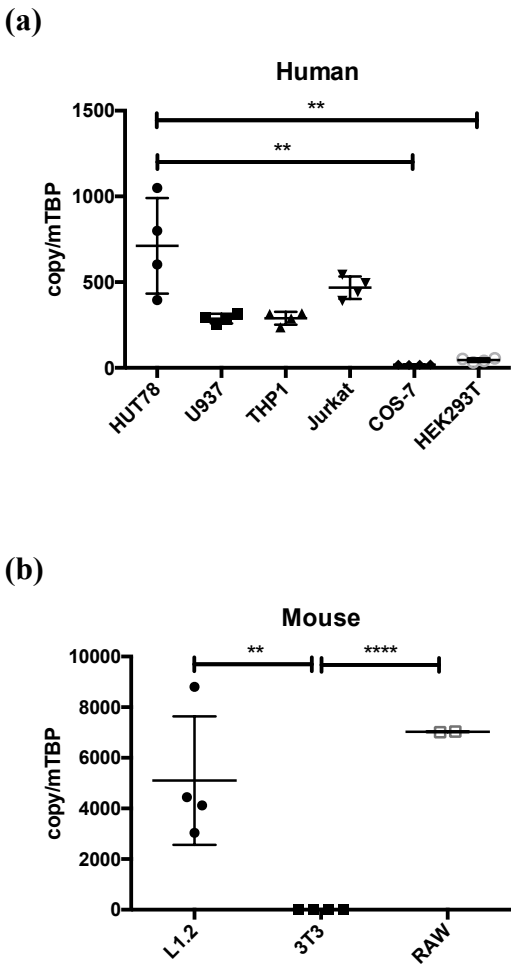

Figure 5.2.3 ST8sia4 expression in a panel of lymphoid/myeloid and adherent cell lines was compared by qPCR

Quantities of ST8sia4 mRNA in a panel of commonly used (a) human and (b) mouse cell lines were assessed by RT-qPCR, compared to a known standard curve and expressed relative to the quantity of a housekeeping gene (TBP) (each data point represents a biological replicate, error bars = +/- SD, statistically significant differences between parameters were determined by unpaired T-test, $p \leq 0.01$=**, $p \leq 0.0001$=****).

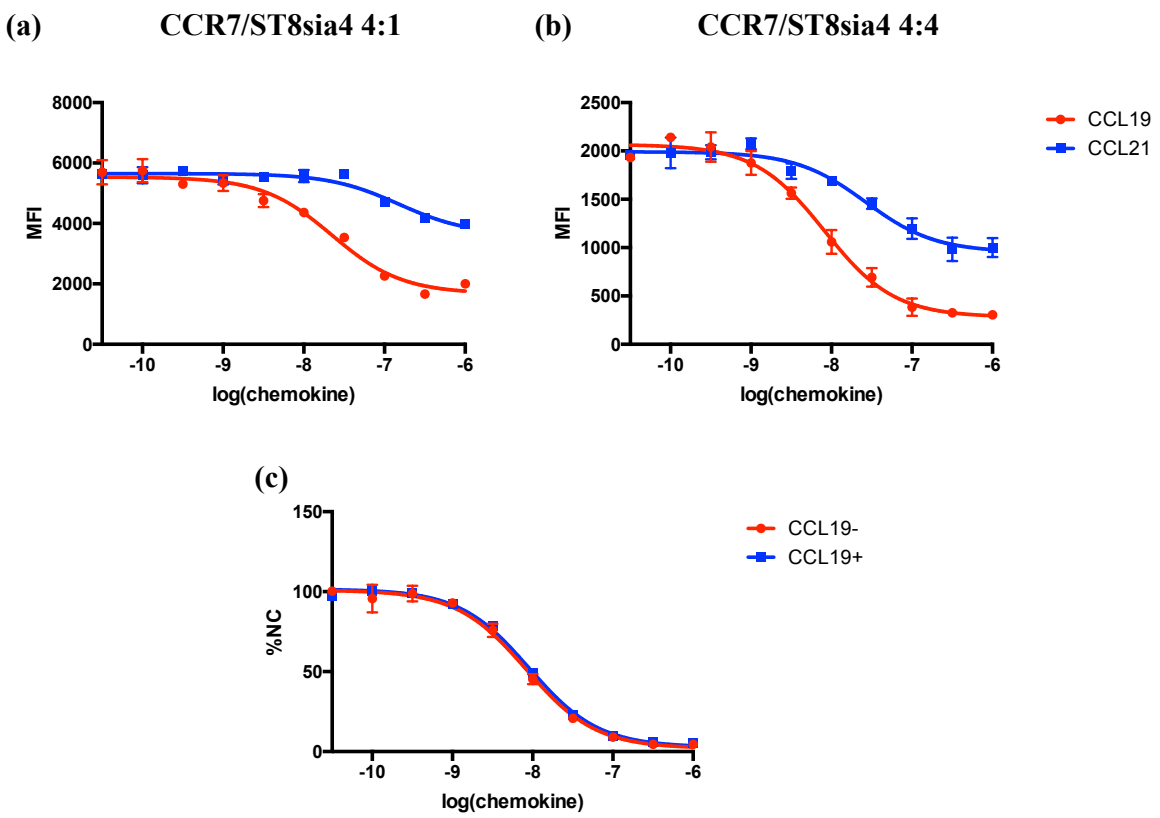

Figure 5.2.4 ST8sia4 expression restores CCL21's ability to compete for receptor occupancy

HEK293T cells were seeded on a 10 cm^2 tissue culture dish and transfected when near-confluent with CCR7 and ST8sia4 in a ratio of either (a) 4 µg: 1 µg or (b) 4 µg; 4 µg. Transfected cells were analysed 48 hours later and affinity of either CCL19 or CCL21 determined using a FACS-based competition assays as described previously, staining with 25 nM labelled CCL19. (c) Affinity of CCL19 was compared between HEK293T expressing CCR7 alone (CCL19-) and those expressing CCR7 and ST8sia4 (CCL19+). Percentage of non-competitor controls (%NC) was calculated by obtaining MFI values for live single cells in the PE channel, subtracting MFI values obtained with those from the empty vector control group as background, and expressing this as a percentage of cells stained with labelled CCL19 only. (n = 3 +/- SD, in all instances).

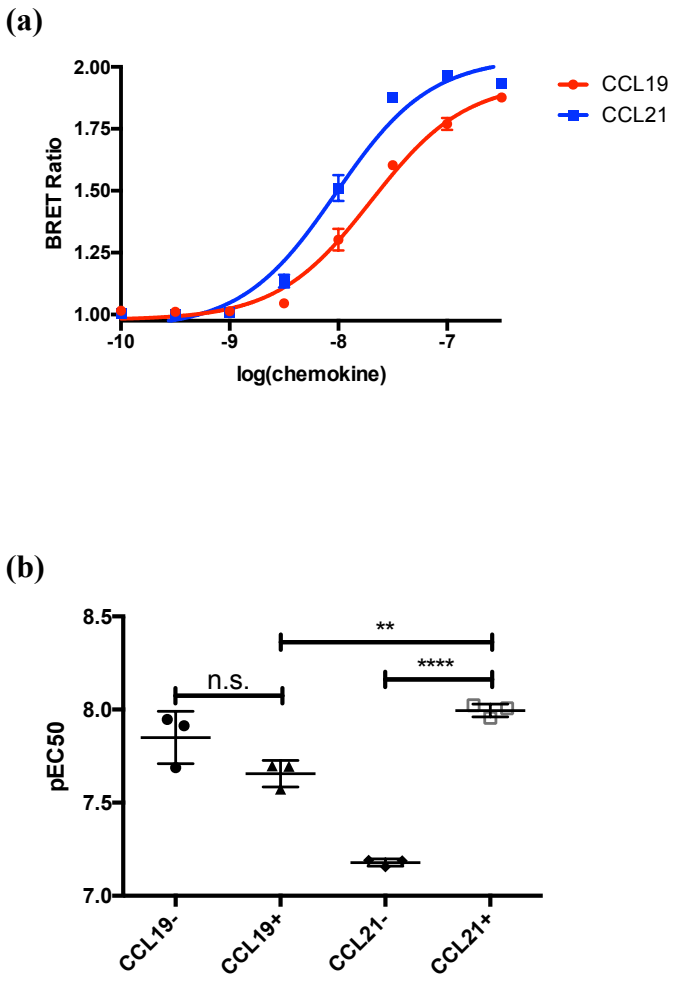

Figure 5.2.5 CCL21 is more effective for β–arrestin recruitment in the presence of polysialic acid

(a) Potency of either CCL19 or CCL21 for recruitment of β-arrestin 2 was assessed in HEK293T cells expressing both the receptor and β-arrestin 2 as well as ST8sia4 (n = 3 +/- SD, representative plot selected from 3 independent experiments). (b) pEC_{50} values obtained for each chemokine (CCL19+ & CCL21+) were compared to those obtained previously in the same assay without ST8sia4 co-transfection (CCL19- & CCL21-) (n=3 biological replicates +/- SD, statistically significant differences between parameters were determined by unpaired T-test, p≤0.01=**, p ≤0.0001=****).

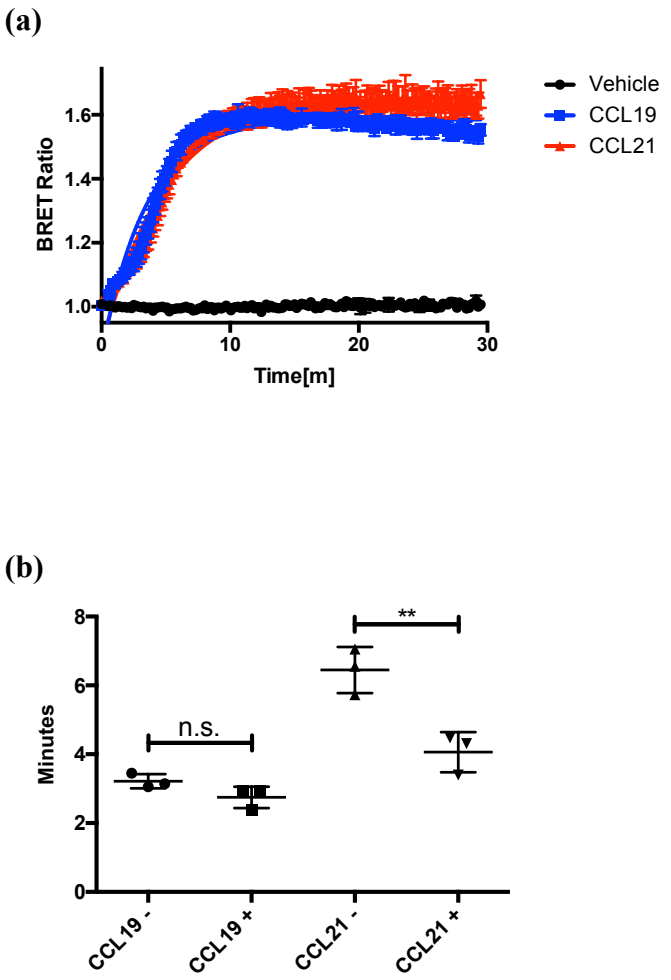

Figure 5.2.6 CCL21 is also faster acting when CCR7 is polysialylated

(a) Once again recruitment of β-arrestin 2 to 100 nM of either CCL19 or CCL21 was continuously assessed over a 30-minute period using HEK293T cells transfected with β-arrestin 2, CCR7-YFP and ST8sia4-HA (n = 3 +/- SD, representative plot selected from 3 independent experiments). (b) Halftime to maximal BRET ratio obtained by each chemokine was compared without (CCL19- & CCL21-) and with (CCL19+ & CCL21+) ST8sia4 co-transfection (n=3 biological replicates +/- SD, statistically significant differences between parameters were determined by unpaired T-test, $p \leq 0.01$=**).

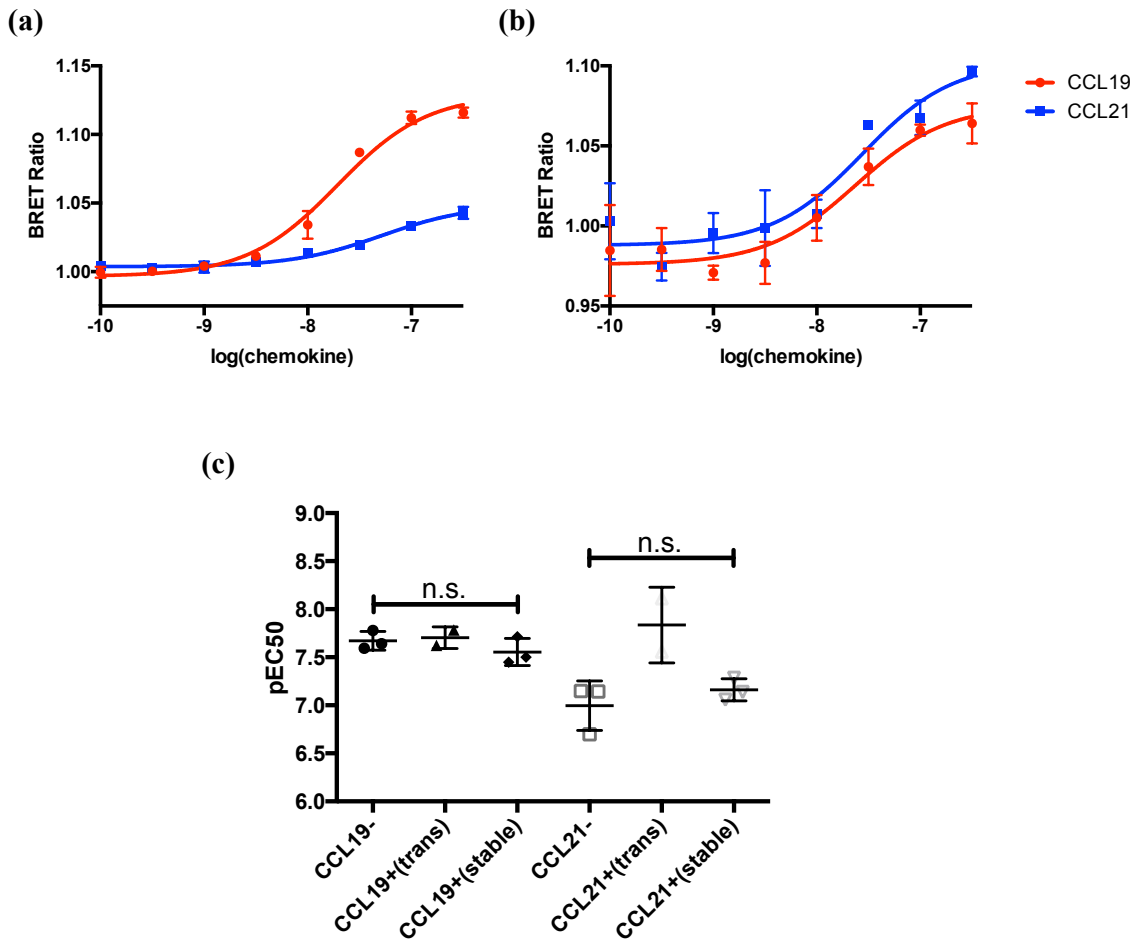

Figure 5.2.7 Polysialylation of CCR7 alters Gi3 recruitment profile of CCL21

(a) Stable cell lines expressing the CCR7-Gi3 biosensor were transiently transfected with ST8sia4-HA 48 hours prior to analysis. 24-hours later expression of the biosensor was induced with doxycycline, cells seeded on a 96-well plate and analysis performed a further 24 hours later (n = 3 +/- SD, representative plot selected from 3 independent experiments). (b) HEK293T cells seeded on a 10 cm^2 dish were transiently transfected when near confluent with the CCR7-Gi3 biosensor and ST8sia4 in a ratio of 1 µg sensor: 1 µg ST8sia4. 24 hours later cells were transferred to a 96-well plate and Gi3 recruitment assessed a further 24 hours after this (n = 3 +/- SD, representative plot selected from 2 independent experiments). (c) The pEC_{50} values obtained for each chemokine were compared between those generated previously (CCL19- & CCL21-), those achieved with stable cell lines subsequently transfected with ST8sia4 (CCL19+(stable) & CCL21+(stable)), and those obtained with fully transiently transfected cells (CCL19+(trans) & CCL21+(trans)) (each point represents a biological replicate, error bars represent SD. Statistically significant differences between parameters were evaluated by unpaired T-test, $p \leq 0.05$=*).

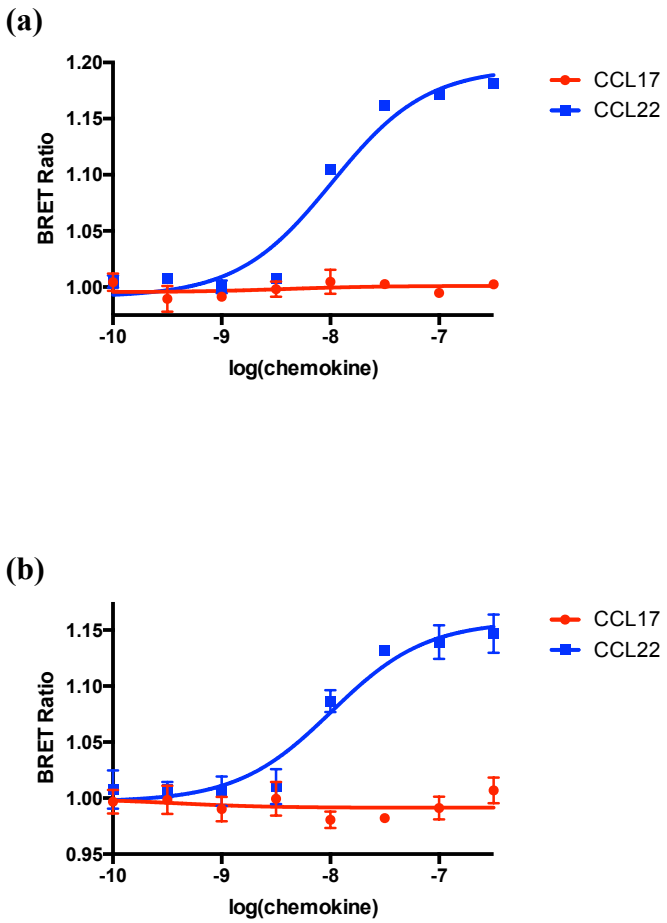

Figure 5.2.8 Co-transfection of CCR4 with ST8sia4 does not appear to affect CCL17 signalling potential

(a) Assessment of β–arrestin recruitment was performed with cells expressing CCR4-YFP, β–arrestin 2-rluc and ST8sia4-HA (n = 3 +/- SD). (b) Recruitment of Gi3 was assessed by transient transfection of the appropriate biosensor with ST8sia4 in a 1:1 ratio into HEK293T cells as described previously (n=3 +/- SD).

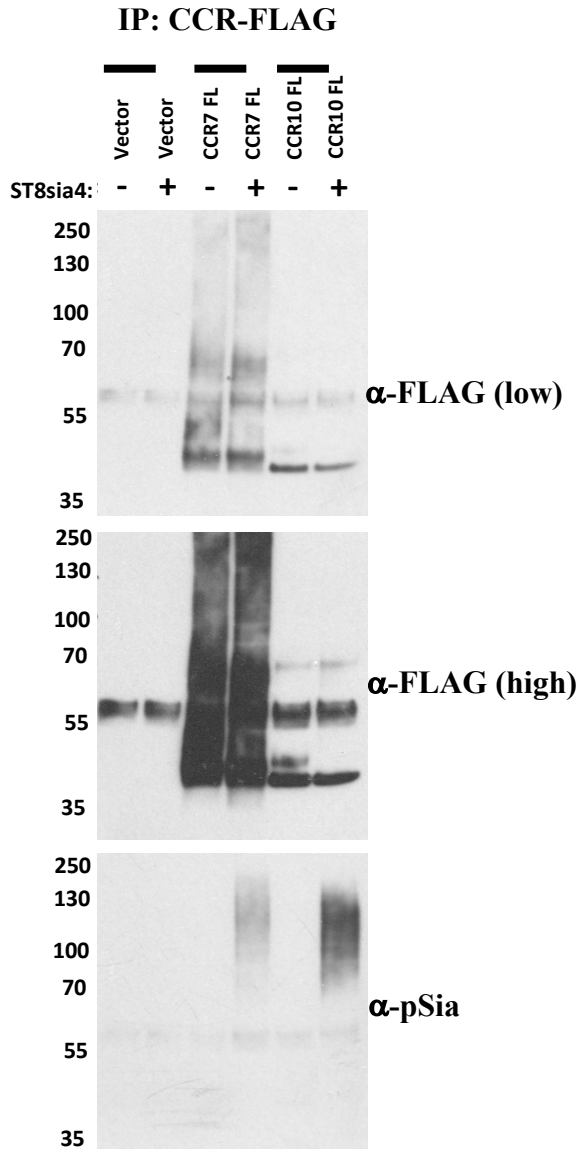

Figure 5.2.9 IP experiments indicated polysialylation of both CCR7 and CCR10

HEK293T cells were seeded onto 10 cm^2 dishes and co-transfected when near-confluent with either 4 μg empty vector, CCR7-FLAG or CCR10-FLAG and either a further 4 μg empty vector or ST8sia4-HA. Whole cell lysate was obtained 48 hours later, pre-cleared with isotype antibody and Protein L PLUS-Agarose beads, and receptor then pulled down with anti-FLAG (M2) antibody and agarose beads, with protein eluted in glycine-elution buffer (pH2.5). Eluted protein was denatured and run as previously described for western blotting, and the resultant blots interrogated with antibodies against FLAG and polysialic acid. α-FLAG (low) and α-FLAG (high) represent different exposure times of the same membrane. (representative example of 4 independent experiments)

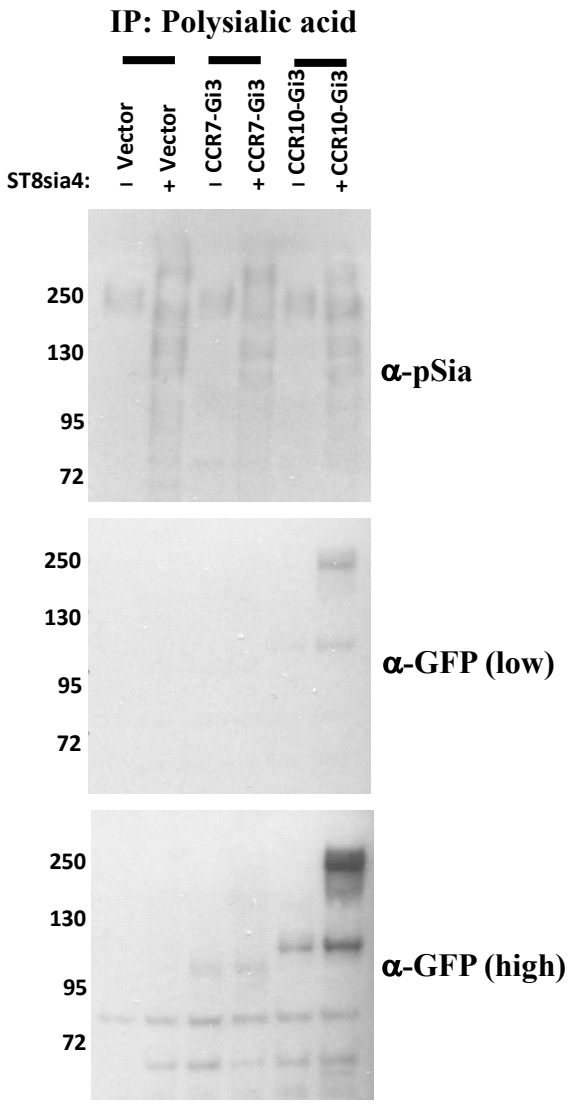

Figure 5.2.10 IP against pSia confirms polysialylation of CCR10

HEK293T cells were seeded and transfected as described previously except that the Gi3 biosensor for either CCR7 or CCR10 was used in place of the FLAG tagged versions of these receptors. IP was performed as before using anti-pSia(735) antibody and protein eluted by direct pellet disruption and denatured/reduced in 2x loading buffer + 100 mM DTT. This was then run as previously described for western blotting, and blots probed with antibodies against GFP (receptor) and polysialic acid. α-GFP (low) and α-GFP (high) represent different exposure times of the same membrane. (representative example of 2 independent experiments)

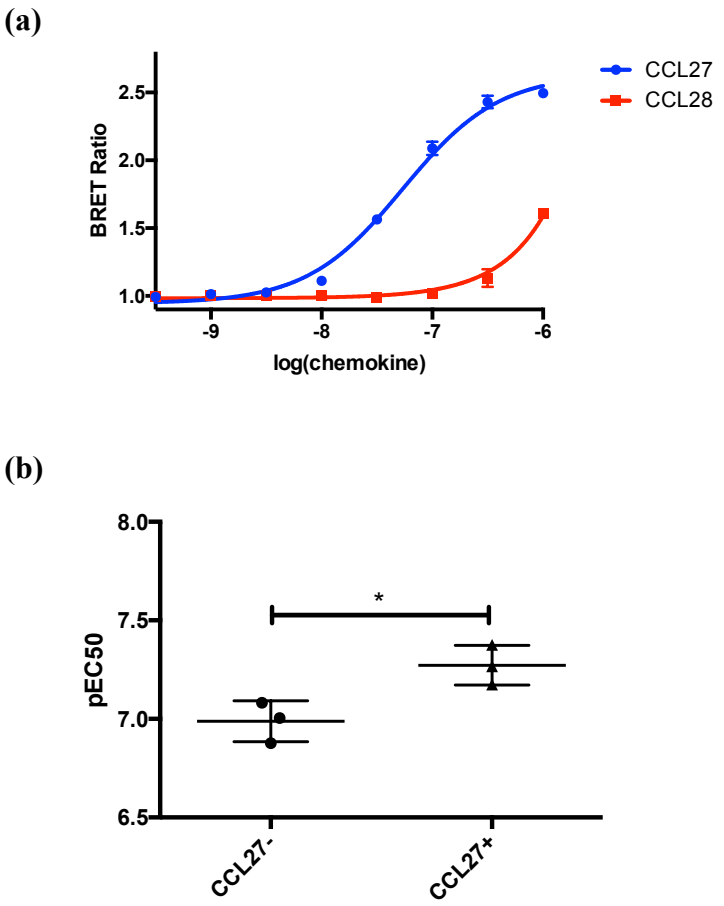

Figure 5.2.11 Polysialylation of CCR10 alters the recruitment profile of CCL27 and CCL28

(a) CCR10-YFP and β–arrestin 2-nluc were transfected into HEK293T cells in a ratio of 4.9 µg:100 ng (+ 4 µg ST8sia4), and recruitment of β–arrestin 2 by CCL27 and CCL28 assessed as before (n = 3 +/- SD, representative plot selected from 3 independent experiments). (b) pEC_{50} values obtained for CCL27 with (CCL27+) and without (CCL27-) polysialylation were compared (n=3 biological replicates +/-SD. Statistically significant differences were determined by unpaired T-test, $p \leq 0.05$=*).

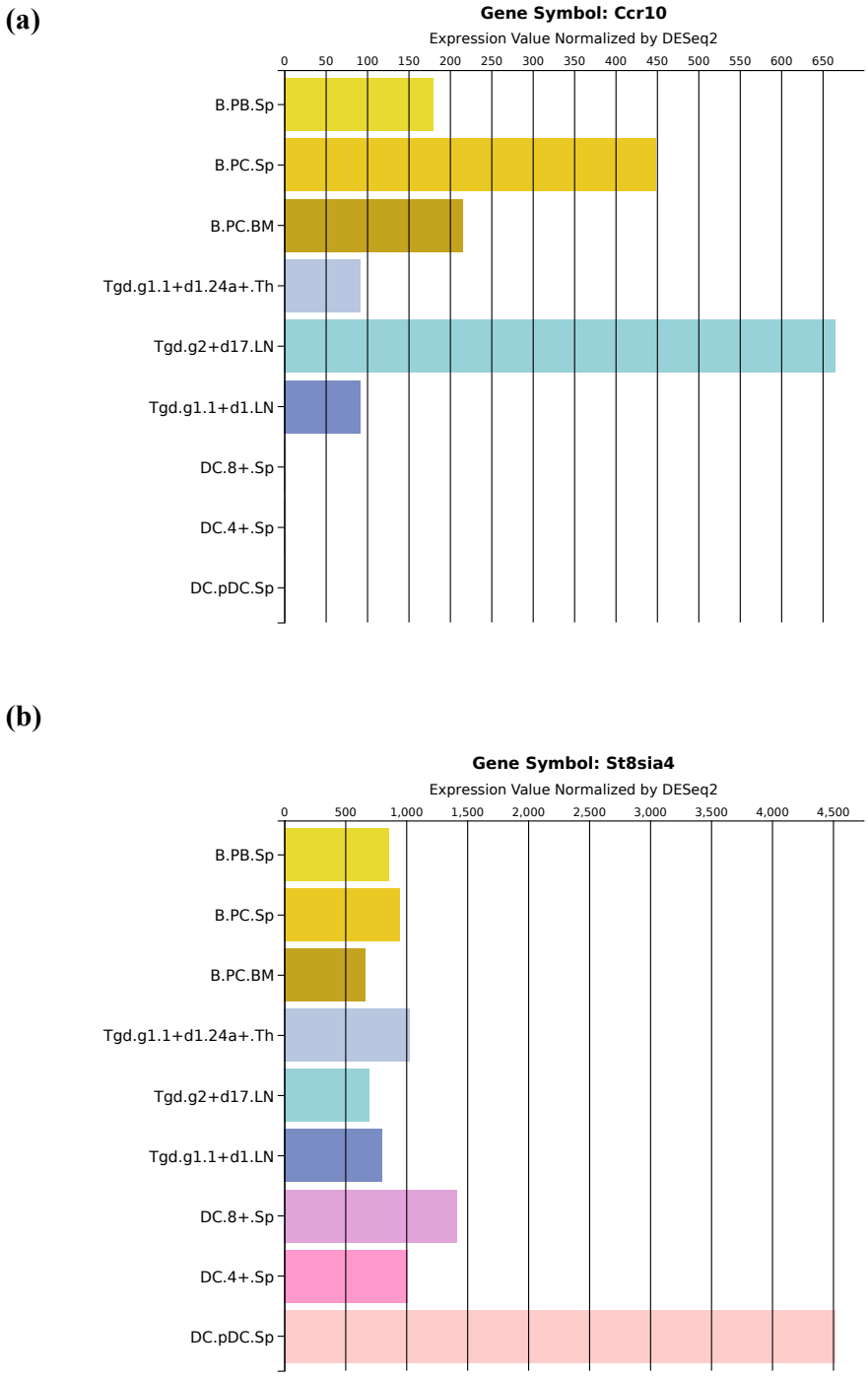

Figure 5.2.12 Expression of CCR10 correlates with expression of ST8sia4 in primary murine cells

The publicly available Gene Skyline (RNA-seq) dataset of murine primary immune cells was accessed via the Immunological Genome Project's web portal (http://rstats.immgen.org/Skyline/skyline.html). The 6 highest CCR10 expressing cell subsets available were selected and graphs generated to display (a) CCR10 and (b) ST8sia4 expression. In addition, 3 DC sub-populations are included for comparison purposes.

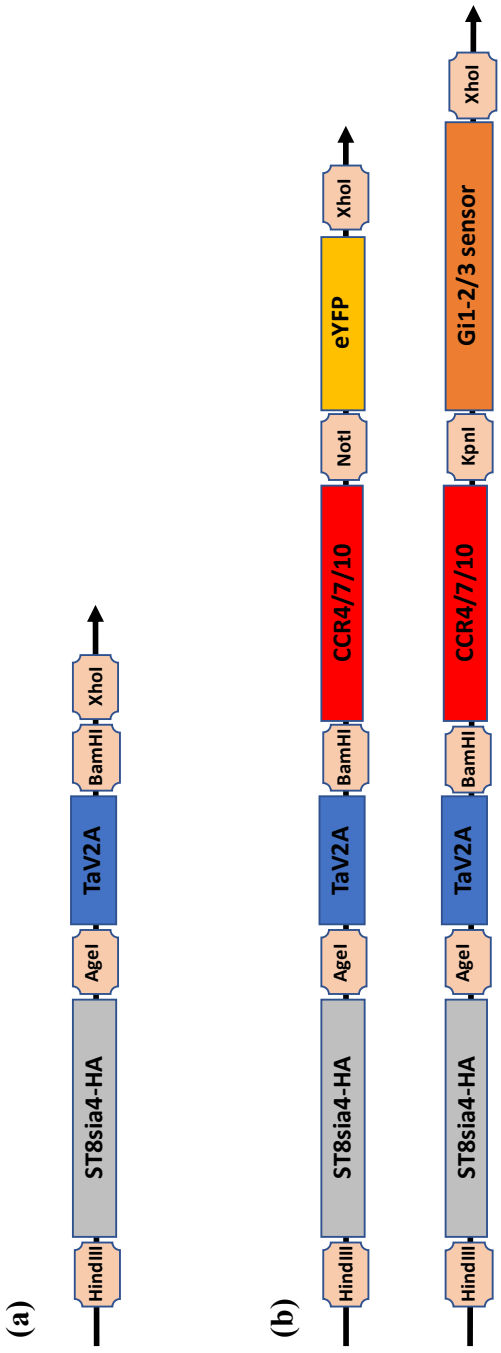

Figure 5.2.13 Schematic representation of TaV2A double-expression plasmid development

(a) A first generation plasmid was developed that encoded for ST8sia4-HA and the TaV2A sequence, flanked by restriction sites allowing for insertion of chemokine receptors/reporter constructs downstream. (b) Subsequently, the chemokine receptors were inserted downstream of TaV2A, generating a new series of polycistronic expression vectors.

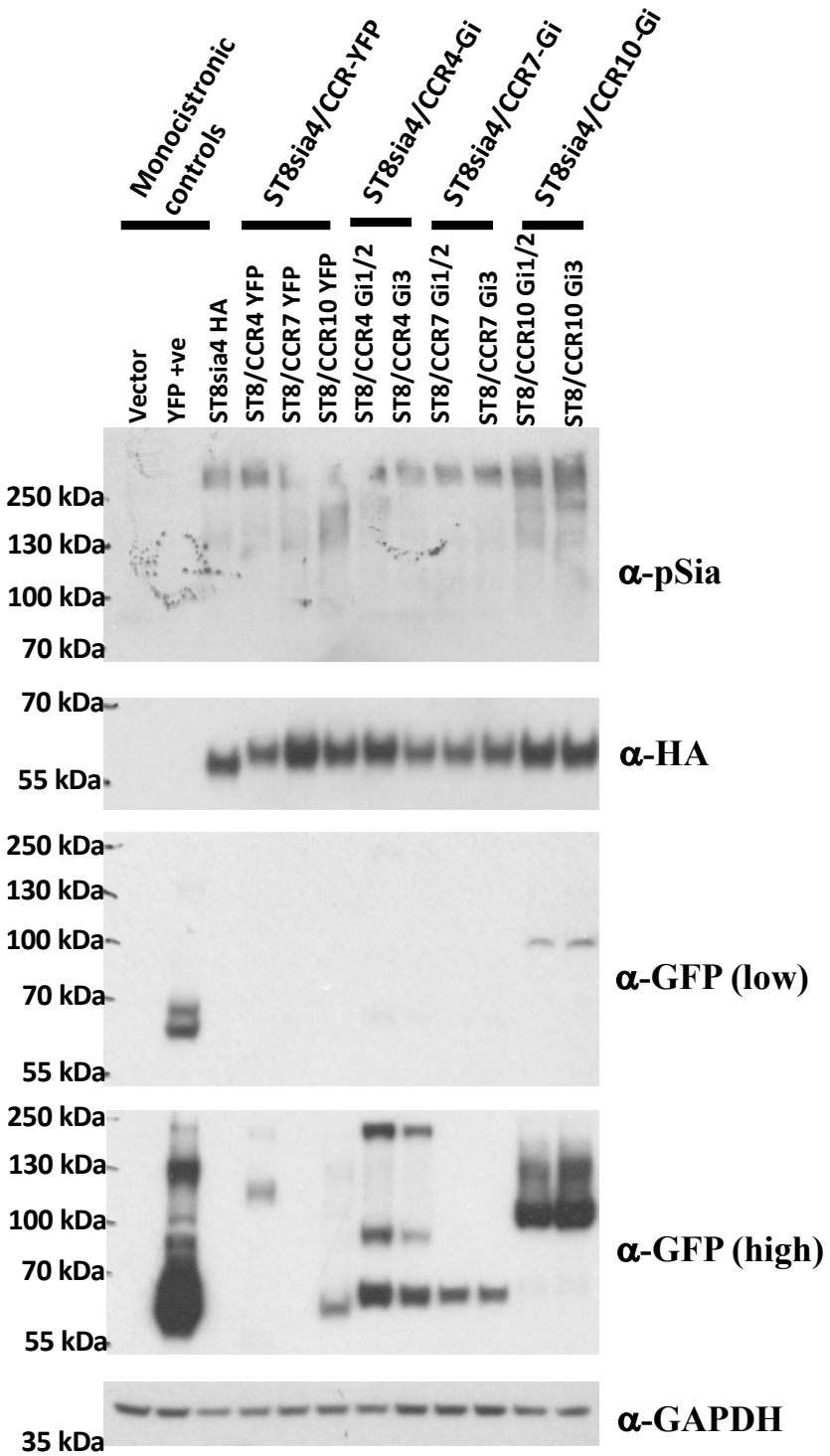

Figure 5.2.14 Assessment of expression by TaV2A plasmids

HEK293T cells were transiently transfected with all of the TaV2A plasmids generated. Whole cell lysate was then tested by western blotting for expression of ST8sia4 (a-HA), chemokine receptor/SPASM biosensor (a-GFP (low) & a-GFP (high)), a housekeeping protein (a-GAPDH) as well as pSia (a-pSia). α-GFP (low) and α-GFP (high) represent different exposure times of the same membrane.

6 Discussion

The data described in this thesis present a number of novel findings that may have wide reaching implications. Firstly, CCR10 is novel target of ST8sia4 mediated polysialylation. This in and of itself is interesting, however potentially also alludes to a common feature of pSia in chemokine biology. This being that chemokines featuring an extended C-terminus with multiple positively charged amino acids may require polysialylation of their receptors in order to fully signal through them. This would mean that CCR3 (which also binds CCL28), CCR6 (CCL20) and CCR9 (CCL25) could for example be polysialylated proteins (Svensson *et al.*, 2002; Schutyser, Struyf and Van Damme, 2003; Danilova *et al.*, 2015). This does make a certain measure of sense. Analysis of publicly available expression data from the likes of Immgen or the Human Protein Atlas indicates that ST8sia4 is widely expressed in the immune system. However, pSia is considered a highly restricted PTM, described on only a handful of proteins, namely NCAM, NRP2, CD36, synaptic cell adhesion molecule 1, the α subunit of voltage dependent sodium channel, the poly-sialyltransferase themselves, and most recently CCR7 (Colley, Kitajima and Sato, 2014; Kiermaier *et al.*, 2016). This would certainly imply that there are more targets of ST8sia4 mediated polysialylation expressed by cells of the immune system than have been identified thus far.

The profound effects that polysialylation (or lack thereof) can have on signalling behaviour and biological activity also raises another intriguing possibility. As described by Kiermaier et al, DCs exhibit higher surface pSia than T-cell and B-cells, presumably as a consequence of varying expression of ST8sia4 between these cell types. As has been mentioned previously, CCL21 recruits fewer GRKs than CCL19 when CCR7 is presumably not polysialylated in HEK293 cells. Additionally, the data presented here indicate that CCL21 is also deficient in recruitment of certain G-proteins, demonstrating a skewed signalling profile when CCR7 is not polysialylated. It is conceivable that, by altering the level of polysialylation, the same receptor expressed in different cell types could demonstrate divergent ligand preferences, which would represent a subtle means of fine-tuning the chemotactic response to certain chemokines. The observation that Flt3 ligand derived BMDCs are more chemotactic than those derived from GM-CSF treatment could represent an example of this, however this has not been specifically addressed yet.

It would be of interest to determine if, as with CCR7, primary cells expressing CCR10 demonstrate varying levels of pSia, and see if this consideration fits with the observable biology of these cells. This also raises another interesting prospect; that it might be

possible to selectively target one ligand over another on the same receptor by disrupting pSia formation. As has been seen, removal of pSia can fundamentally impair the signalling functions of a chemokine, so conceptually this could be replicated in vivo via pharmacological intervention. As mentioned previously targeting of pSia pharmacologically is already being considered as a novel cancer therapy, and small molecule antagonists that effectively abrogate cell surface sialylation have been evaluated in models of cancer where they demonstrate no cytotoxicity but inhibit the metastatic phenotype of cancer cell lines (Chiang *et al.*, 2010). Targeting of the chemokine system in this manner could hold a number of benefits. Antagonists targeting chemokine receptors rarely reach their intended clinical outcomes in trials, frequently attributed to the inability of these drugs to reach a threshold of receptor coverage sufficient to block chemotactic activity entirely. By targeting pSia one could conceptually bypass this issue, as cells expressing these receptors would be highly refractory to any chemokine like CCL21 CCL28 that require pSia to be released from an auto-inhibitory conformation. As well, the lack of cytotoxicity would mean that cells expressing polysialylated receptors would still be able to migrate in response to other chemokines that don't require this release, and as such could selectively silence one ligand on a receptor while otherwise leaving the signalling axis unperturbed. However, polysialyltransferases do target a number of proteins. While it is regarded as a highly-restricted PTM, consideration would need to be made of side-effects associated with potentially abrogating polysialylation on other targeted proteins.

The findings presented here also allude to an important but often overlooked consideration when using cell lines and in vitro means of evaluating receptors; that different cells exhibit differences in PTMs. ST8sia4 expression was readily detectable in every immune derived cell evaluated, however it is either completely absent (3T3, COS-7) or only found at the limits of detection (HEK293T) in the epithelial/fibroblast like cells tested. This makes some sense biologically as these are immortalised somatic cells from non-neuronal lineages that form a cohesive monolayer in culture. As such they are unlikely to have expressed ST8sia4 before being cultured and would have little use for pSia in culture given its contact inhibitory properties. These are all cell lines frequently used in detailed receptor analysis and molecular biology generally. This is because they are adherent, easily grown and maintained and can be readily transfected in transient and stable expression systems. This is especially true when compared with lymphoid/myeloid derived cells, which are often difficult to transfect.

However, as demonstrated here, the lack of this very specific PTM in these cells can fundamentally alter the data obtained from these studies. In the case of CCR7, consideration of polysialylation alters the perception of signalling bias of this receptor substantially. As mentioned, the previously reported bias of CCR7 is that CCL19 readily recruits G-proteins and β-arrestin to the receptor, but that CCL21 preferentially signals through G-protein coupling (Förster, Davalos-Misslitz and Rot, 2008). However, unlike in previous direct evaluations of recruitment of signalling machinery to CCR7, evaluation here indicates that CCL21 is, if anything, more potent in triggering recruitment of β-arrestin by CCR7 than CCL19. It is likely that previous reports to the contrary are due to the lack of polysialylation of the receptor in the cell lines used, and that while bias has been observed in terms of signalling (SHP2) it is not the classical bias described previously.

Interestingly, in a similar BRET based study evaluating CCR7 bias, HEK293 cells were used in all assays directly assessing recruitment but CHO-K1 cells were used to evaluate receptor affinity (Corbisier *et al.*, 2015). In this study a signalling profile of CCL19 and CCL21 was presented that closely mirrored the findings presented in Chapter 4 of this thesis. However, when ligand affinity was assessed in this study, using CCR7 expressed in CHO-K1 cells, CCL19 and CCL21 were effectively equivalent in displacing radiolabelled CCL19. Wild-type CHO-K1 cells do express ST8sia4 and NCAM, so have pSia on their surface (Windfuhr *et al.*, 2000). Consequently, CCR7 expressed in these cells is likely polysialylated and the observation of equivalent receptor affinity of CCL19 and CCL21 for CCR7 expressed in these cells is perhaps unsurprising.

However, this does raise an interesting point; that while evaluating polysialylated proteins careful consideration of the specific properties of the cell line used need to be made. It simply is not feasible to easily perform the kinds of BRET based assays presented here in lymphoid/myeloid cell lines, and while CHO-K1 and RAW cells (an adherent macrophage line) represent an attractive test-bed for working with polysialylated proteins, these carry caveats also. In our hands they are less readily transfectable than HEK293T (unpublished observations), and in the BRET based assays we have been using, the ratio of donor to acceptor proteins needs to be well controlled. A more difficult transfection could complicate this. However, as was seen when assessing Gi3 recruitment to CCR7, subsequent transient transfections of ST8sia4 into the stable cell lines used for this analysis is difficult. Also, relying on purely transient transfection is either sub-optimal or simply not possible when using SPASM biosensors. As such considerations must be made when designing future experiments working with polysialylated proteins to ensure a workable

balance of sufficient expression of the sialyltransferase, its target and any reporter/donor proteins, in a cell type amenable to the intended analysis to be performed.

6.1 Future directions

The data presented here appeared to indicate that CCL21 is a balanced ligand, rather than a G-protein biased one. This is in contrast with previous reports on CCL21 which indicate that it is poorly internalised. However, as mentioned before, differences in the kind of cells used, and in particular the lack of polysialylation of CCR7, are likely to have contributed to this disparity. It would be of interest to measure internalisation directly in HEK293T cells, potentially utilising a pH dependent dye such as pHrodo avidin conjugated to a biotin labelled CCL21, should one become available. This would determine if the recruitment of β-arrestin by CCL21 observed here results in the expected functional consequence of CCR7 internalisation, or if this finding is incidental or serves other signalling functions for the receptor.

It would also be a priority to establish a means of consistently evaluating G-protein recruitment in cells expressing ST8sia4. This would be of particular interest for CCR10 as it would help to affirm that pSia is important in its biological activity and could help to confirm the perceived bias of this receptor. Polycistronic vectors were established to express both ST8sia4 and chemokine receptors of interested, with the intention being to establish stable cell lines that would express both near-equally. However, while expression of the first protein (ST8sia4) could be readily demonstrated, little to no expression was noted for the second (chemokine receptors/SPASM biosensors). Seemingly this is a known issue when using the TaV2A domain to express multiple proteins from a single ORF and has been attributed to both poor translation of the second protein and rapid proteasomal degredation of the resulting product (Momose and Morikawa, 2016). Conceptually a vector expressing multiple copies of the second protein each separated by a distinct 2A peptide, or reintroducing the initiating methionine of the second protein, might be able to overcome this issue. It might be simpler to transfect the stable cell lines already generated with an expression vector for ST8sia4 that can be selected for with an additional antibiotic. However, there may be some issues with such an approach. As demonstrated when trying to introduce ST8sia4 via transient transfection, these stable cell lines are refractory to subsequent transfection. As well, a step-wise establishment of double-stable cell lines in this manner is likely to require selection, expansion and evaluation of individual clones. This would result in a high passage number before cells are even useable. It might

therefore be easier to establish stable expression of SPASM biosensors in a cell lineage known to express ST8sia4 at rest, such as CHO-K1 or RAW cells.

Establishing if low/no ST8sia4 expression is a common feature of HEK293 cells and their derivatives would also be of considerable interest. It has been demonstrated that, in the HEK293T cells used here, ST8sia4 expression is effectively absent. Additionally, inclusion of ST8sia4 in transfections of HEK293T with CCR7 restored CCL21 interaction. Similarly, evaluation of Gi-protein recruitment by CCR7 in response to CCL21 indicated that signalling potential of the chemokine is blunted. This would imply that the HEK293 derived Flp-In TRex cell line used to generate the stable lines used in these assays is similarly deficient in ST8sia4 expression. However, at least one study evaluated CCL19/CCL21 affinity for CCR7 in a HEK293 derived cell line (HEK293E) and demonstrated the same comparable affinity of these chemokines as has been seen elsewhere (Sullivan *et al.*, 1999). The HEK293E were generated by inducing stable expression of the *Epstein barr* virus protein EBNA1, and are most frequently used in the large-scale production of recombinant proteins (Tom, Bisson and Durocher, 2008). When used in this manner they are grown in suspension rather than as an adherent cell layer. Consequently, it is possible that they may bear pSia on their cell surface as it's contact inhibitory properties might aid this phenotype. Differences in methodology are again quite apparent, namely that affinity was assessed on cell membranes rather than whole live cells, using picomolar concentrations of radiolabelled CCL19 or CCL21. However, given the total absence of CCL21 competition observed in Chapter 4 of this thesis, it is difficult to ignore the disparity. Variable receptor polysialylation could account for the differences noted when evaluating CCR7 signalling in different cell lineages. Additionally, HEK293 derived cells are used almost universally in receptor characterisation and compound screenings. It would be important to evaluate ST8sia4 expression in HEK293 cells from multiple sources. This would help to establish if the lack of ST8sia4 expression observed here is indicative of all/most HEK293 derived cell lines, or simply a peculiarity of the cells used in this thesis

Finally, it would be beneficial to determine if primary cells expressing CCR10 do indeed bear pSia on their surface, and if this PTM modifies CCR10 activity in vivo. The former would be a relatively simple matter of harvesting CCR10 expressing cells, such as γδ T-cells or plasmablasts, from mouse tissues and evaluating surface pSia and CCR10 by flow cytometry. The latter however requires additional consideration. Purifying CCR10 expressing cell types, treating them with endo-N or PNGase F and evaluating chemotaxis by transwell or 3D migration could determine if stripping CCR10 of polysialylation affects

the chemotactic potential of CCL27 and CCL28 for primary cells in a similar manner to simply deglycosylating them. Alternatively, purifying these cells from ST8sia4 KO mice could achieve a similar effect without the need for additional enzymatic treatment of cells. It would also be possible to assess if there is altered cellularity in tissues where CCR10 expressing cells could be expected, such as in the skin and mucosal epithelium. In either case, this would indicate if pSia on CCR10 results in functional consequences for endogenously CCR10 expressing cells, and hopefully validate the in vitro findings presented here.

References

Airoldi, I. and Ribatti, D. (2011) 'Regulation of angiostatic chemokines driven by IL-12 and IL-27 in human tumors', *Journal of Leukocyte Biology*. doi: 10.1189/jlb.0511237.

Ajram, L. *et al.* (2014) 'Internalization of the chemokine receptor CCR4 can be evoked by orthosteric and allosteric receptor antagonists', *European Journal of Pharmacology*. doi: 10.1016/j.ejphar.2014.02.007.

Al-Saraireh, Y. M. J. *et al.* (2013) 'Pharmacological Inhibition of polysialyltransferase ST8SiaII Modulates Tumour Cell Migration', *PLoS ONE*. doi: 10.1371/journal.pone.0073366.

Alexeev, V. *et al.* (2013) 'Analysis of chemotactic molecules in bone marrow-derived mesenchymal stem cells and the skin: Ccl27-Ccr10 axis as a basis for targeting to cutaneous tissues', *Cytotherapy*. doi: 10.1016/j.jcyt.2012.11.006.

Allavena, P. *et al.* (2008) 'The inflammatory micro-environment in tumor progression: The role of tumor-associated macrophages', *Critical Reviews in Oncology/Hematology*. doi: 10.1016/j.critrevonc.2007.07.004.

Allen, S. J., Crown, S. E. and Handel, T. M. (2007) 'Chemokine:Receptor Structure, Interactions, and Antagonism', *Annual Review of Immunology*, 25(1), pp. 787–820. doi: 10.1146/annurev.immunol.24.021605.090529.

Anders, H. J., Romagnani, P. and Mantovani, A. (2014) 'Pathomechanisms: Homeostatic chemokines in health, tissue regeneration, and progressive diseases', *Trends in Molecular Medicine*. doi: 10.1016/j.molmed.2013.12.002.

Anderson, C. A., Solari, R. and Pease, J. E. (2016) 'Biased agonism at chemokine receptors: obstacles or opportunities for drug discovery?', *Journal of Leukocyte Biology*. doi: 10.1189/jlb.2MR0815-392R.

Ansel, K. M. *et al.* (2000) 'A chemokine-driven positive feedback loop organizes lymphoid follicles', *Nature*. doi: 10.1038/35018581.

Ara, T. *et al.* (2005) 'The role of CXCL12 in the organ-specific process of artery

formation', *Blood*. doi: 10.1182/blood-2004-07-2563.

Banfield, G. *et al.* (2010) 'CC Chemokine Receptor 4 (CCR4) in human allergen-induced late nasal responses', *Allergy: European Journal of Allergy and Clinical Immunology*. doi: 10.1111/j.1398-9995.2010.02327.x.

Bannert, N. *et al.* (2001) 'Sialylated O-Glycans and Sulfated Tyrosines in the NH $_2$ -Terminal Domain of CC Chemokine Receptor 5 Contribute to High Affinity Binding of Chemokines', *The Journal of Experimental Medicine*. doi: 10.1084/jem.194.11.1661.

Bardi, G. *et al.* (2001) 'The T cell chemokine receptor CCR7 is internalized on stimulation with ELC, but not with SLC', *European Journal of Immunology*. doi: 10.1002/1521-4141(200111)31:11<3291::AID-IMMU3291>3.0.CO;2-Z.

Bax, M. *et al.* (2009) 'Interaction of polysialic acid with CCL21 regulates the migratory capacity of human dendritic cells', *PLoS ONE*. doi: 10.1371/journal.pone.0006987.

Behm, B. *et al.* (2012) 'Cytokines, chemokines and growth factors in wound healing', *Journal of the European Academy of Dermatology and Venereology*. doi: 10.1111/j.1468-3083.2011.04415.x.

Belperio, J. A. *et al.* (2000) 'CXC chemokines in angiogenesis.', *Journal of leukocyte biology*. doi: 10.1160/TH07.

Berchiche, Y. A. *et al.* (2011) 'Different Effects of the Different Natural CC Chemokine Receptor 2b Ligands on -Arrestin Recruitment, G i Signaling, and Receptor Internalization', *Molecular Pharmacology*. doi: 10.1124/mol.110.068486.

Berger, E. A., Murphy, P. M. and Farber, J. M. (1999) 'CHEMOKINE RECEPTORS AS HIV-1 CORECEPTORS: Roles in Viral Entry, Tropism, and Disease', *Annual Review of Immunology*. doi: 10.1146/annurev.immunol.17.1.657.

Bermudez, D. M. *et al.* (2011) 'Inhibition of stromal cell-derived factor-1α further impairs diabetic wound healing', *Journal of Vascular Surgery*. doi: 10.1016/j.jvs.2010.10.056.

Bizzarri, C. *et al.* (2006) 'ELR+ CXC chemokines and their receptors (CXC chemokine receptor 1 and CXC chemokine receptor 2) as new therapeutic targets', *Pharmacology and Therapeutics*. doi: 10.1016/j.pharmthera.2006.04.002.

Bonecchi, R. *et al.* (1998) 'Differential Expression of Chemokine Receptors and Chemotactic Responsiveness of Type 1 T Helper Cells (Th1s) and Th2s', *The Journal of Experimental Medicine*. doi: 10.1084/jem.187.1.129.

Bonner, K. *et al.* (2013) 'CCL17/thymus and activation-regulated chemokine induces calcitonin gene-related peptide in human airway epithelial cells through CCR4', *Journal of Allergy and Clinical Immunology*. Elsevier Ltd, 132(4), p. 942–950.e3. doi: 10.1016/j.jaci.2013.04.015.

Boring, L. *et al.* (1997) 'Impaired monocyte migration and reduced type 1 (Th1) cytokine responses in C-C chemokine receptor 2 knockout mice', *Journal of Clinical Investigation*. doi: 10.1172/JCI119798.

Borsig, L. *et al.* (2014) 'Inflammatory chemokines and metastasis-tracing the accessory', *British Dental Journal*. doi: 10.1038/onc.2013.272.

Britschgi, M. R., Favre, S. and Luther, S. A. (2010) 'CCL21 is sufficient to mediate DC migration, maturation and function in the absence of CCL19', *European Journal of Immunology*. doi: 10.1002/eji.200939921.

Le Brocq, M. L. *et al.* (2014) 'Chemokines as Novel and Versatile Reagents for Flow Cytometry and Cell Sorting', *The Journal of Immunology*. doi: 10.4049/jimmunol.1303371.

Brown, N. E., Blumer, J. B. and Hepler, J. R. (2015) 'Bioluminescence resonance energy transfer to detect protein-protein interactions in live cells', in *Protein-Protein Interactions: Methods and Applications: Second Edition*. doi: 10.1007/978-1-4939-2425-7_30.

Burg, J. S. *et al.* (2015) 'Structural basis for chemokine recognition and activation of a viral G protein-coupled receptor', *Science*. doi: 10.1080/11038128.2016.1198419.

Byers, M. A. *et al.* (2008) 'Arrestin 3 Mediates Endocytosis of CCR7 following Ligation of CCL19 but Not CCL21', *The Journal of Immunology*. doi: 10.4049/jimmunol.181.7.4723.

Calandreau, L. *et al.* (2010) 'Differential impact of polysialyltransferase ST8SiaII and ST8SiaIV knockout on social interaction and aggression', *Genes, Brain and Behavior*. doi: 10.1111/j.1601-183X.2010.00635.x.

Carlsen, H. S. *et al.* (2005) 'Disparate lymphoid chemokine expression in mice and men: No evidence of CCL21 synthesis by human high endothelial venules', *Blood*. doi: 10.1182/blood-2004-11-4353.

Cha, H.-R. *et al.* (2011) 'Mucosa-Associated Epithelial Chemokine/CCL28 Expression in the Uterus Attracts CCR10+ IgA Plasma Cells following Mucosal Vaccination via Estrogen Control', *The Journal of Immunology*. doi: 10.4049/jimmunol.1100402.

Charo, I. F. and Ransohoff, R. M. (2006) 'The Many Roles of Chemokines and Chemokine Receptors in Inflammation', *New England Journal of Medicine*. doi: 10.1056/NEJMra052723.

Chatterjee, A. *et al.* (2012) 'Chemokines and Chemokine Receptors in susceptibility to HIV-1 infection and progression to AIDS', *Disease Markers*. doi: 10.3233/DMA-2011-0874.

Chatterjee, A. *et al.* (2013) 'Efficient viral delivery system for unnatural amino acid mutagenesis in mammalian cells', *Proceedings of the National Academy of Sciences*. doi: 10.1073/pnas.1309584110.

Chen, L. *et al.* (2014) 'Upregulation of chemokine receptor CCR10 is essential for glioma proliferation, invasion and patient survival', *Oncotarget*. doi: 10.18632/oncotarget.2134.

Cheung, I. Y., Vickers, A. and Cheung, N. K. V (2006) 'Sialyltransferase STX (ST8SiaII): A novel molecular marker of metastatic neuroblastoma', *International Journal of Cancer*, 119(1), pp. 152–156. doi: 10.1002/ijc.21789.

Chi, B. J. *et al.* (2015) 'Silencing of CCR7 inhibits the growth, invasion and migration of prostate cancer cells induced by VEGFC', *International Journal of Clinical and Experimental Pathology*.

Chiang, C. H. *et al.* (2010) 'A novel sialyltransferase inhibitor AL10 suppresses invasion and metastasis of lung cancer cells by inhibiting integrin-mediated signaling', *Journal of Cellular Physiology*. doi: 10.1002/jcp.22068.

Clark-Lewis, I. *et al.* (1994) 'Structural requirements for interleukin-8 function identified by design of analogs and CXC chemokine hybrids', *Journal of Biological Chemistry*.

Coin, I. *et al.* (2013) 'XGenetically encoded chemical probes in cells reveal the binding path of urocortin-i to CRF class B GPCR', *Cell*. doi: 10.1016/j.cell.2013.11.008.

Colley, K. J., Kitajima, K. and Sato, C. (2014) 'Polysialic acid: Biosynthesis, novel functions and applications', *Critical Reviews in Biochemistry and Molecular Biology*. doi: 10.3109/10409238.2014.976606.

Comerford, I. *et al.* (2013) 'A myriad of functions and complex regulation of the CCR7/CCL19/CCL21 chemokine axis in the adaptive immune system', *Cytokine and Growth Factor Reviews*. doi: 10.1016/j.cytogfr.2013.03.001.

Corbisier, J. *et al.* (2015) 'Biased signaling at chemokine receptors', *Journal of Biological Chemistry*. doi: 10.1074/jbc.M114.596098.

Corsiero, E. *et al.* (2012) 'Role of lymphoid chemokines in the development of functional ectopic lymphoid structures in rheumatic autoimmune diseases', *Immunology Letters*. doi: 10.1016/j.imlet.2012.04.013.

Cotton, M. and Claing, A. (2009) 'G protein-coupled receptors stimulation and the control of cell migration', *Cellular Signalling*. doi: 10.1016/j.cellsig.2009.02.008.

Cowan, J. E. *et al.* (2014) 'Differential Requirement for CCR4 and CCR7 during the Development of Innate and Adaptive T Cells in the Adult Thymus', *The Journal of Immunology*. doi: 10.4049/jimmunol.1400993.

Culley, F. J. *et al.* (2006) 'Role of CCL5 (RANTES) in Viral Lung Disease', *Journal of Virology*. doi: 10.1128/JVI.00496-06.

Curiel, T. J. *et al.* (2004) 'Specific recruitment of regulatory T cells in ovarian carcinoma fosters immune privilege and predicts reduced survival', *Nature Medicine*. doi: 10.1038/nm1093.

Curreli, S. *et al.* (2007) 'Polysialylated neuropilin-2 is expressed on the surface of human dendritic cells and modulates dendritic cell-T lymphocyte interactions', *Journal of Biological Chemistry*. doi: 10.1074/jbc.M702965200.

Dai, Y. *et al.* (2017) 'Association of CXCR4, CCR7, VEGF-C and VEGF-D expression with lymph node metastasis in patients with cervical cancer', *European Journal of*

Obstetrics Gynecology and Reproductive Biology. doi: 10.1016/j.ejogrb.2017.04.043.

Dairaghi, D. J. *et al.* (2011) 'Pharmacokinetic and pharmacodynamic evaluation of the novel CCR1 antagonist CCX354 in healthy human subjects: Implications for selection of clinical dose', *Clinical Pharmacology and Therapeutics*. doi: 10.1038/clpt.2011.33.

Danilova, E. *et al.* (2015) 'A role for CCL28-CCR3 in T-cell homing to the human upper airway mucosa', *Mucosal Immunology*. doi: 10.1038/mi.2014.46.

Davalos-Misslitz, A. C. M. *et al.* (2007) 'Generalized multi-organ autoimmunity in CCR7-deficient mice', *European Journal of Immunology*. doi: 10.1002/eji.200636656.

Devine, S. M. *et al.* (2008) 'Rapid mobilization of functional donor hematopoietic cells without G-CSF using AMD3100, an antagonist of the CXCR4/SDF-1 interaction', *Blood*. doi: 10.1182/blood-2007-12-130179.

Donnelly, M. L. L. *et al.* (2001) 'Analysis of the aphthovirus 2A/2B polyprotein "cleavage" mechanism indicates not a proteolytic reaction, but a novel translational effect: A putative ribosomal "skip"', *Journal of General Virology*, 82(5), pp. 1013–1025. doi: 10.1099/0022-1317-82-5-1013.

Ehrlich, L. I. R. *et al.* (2009) 'Differential Contribution of Chemotaxis and Substrate Restriction to Segregation of Immature and Mature Thymocytes', *Immunity*. doi: 10.1016/j.immuni.2009.09.020.

Eyerich, S. *et al.* (2009) 'Th22 cells represent a distinct human T cell subset involved in epidermal immunity and remodeling', *Journal of Clinical Investigation*. doi: 10.1172/JCI40202.

Farajzadeh Valilou, S. *et al.* (2018) 'The role of inflammatory cytokines and tumor associated macrophages (TAMs) in microenvironment of pancreatic cancer', *Cytokine and Growth Factor Reviews*. doi: 10.1016/j.cytogfr.2018.01.007.

Farzan, M. *et al.* (1999) 'Tyrosine sulfation of the amino terminus of CCR5 facilitates HIV-1 entry', *Cell*. doi: 10.1016/S0092-8674(00)80577-2.

van der Fits, L. *et al.* (2009) 'Imiquimod-Induced Psoriasis-Like Skin Inflammation in Mice Is Mediated via the IL-23/IL-17 Axis', *The Journal of Immunology*. doi:

10.4049/jimmunol.0802999.

Förster, R. *et al.* (1999) ‘CCR7 coordinates the primary immune response by establishing functional microenvironments in secondary lymphoid organs’, *Cell*. doi: 10.1016/S0092-8674(00)80059-8.

Förster, R., Davalos-Misslitz, A. C. and Rot, A. (2008) ‘CCR7 and its ligands: Balancing immunity and tolerance’, *Nature Reviews Immunology*. doi: 10.1038/nri2297.

Forward, N. a *et al.* (2010) ‘Signaling through TLR7 enhances the immunosuppressive activity of murine CD4+CD25+ T regulatory cells’, *J.Leukoc.Biol.* doi: 10.1189/jlb.0908559.

Fujita, Y. *et al.* (2006) ‘Presence of circulating CCR10+ T cells and elevated serum CTACK/CCL27 in the early stage of mycosis fungoides’, *Clinical Cancer Research*. doi: 10.1158/1078-0432.CCR-05-1513.

Furudate, S. *et al.* (2017) ‘Immunomodulatory Effect of Imiquimod Through CCL22 Produced by Tumor-associated Macrophages in B16F10 Melanomas’, *Anticancer Research*, 37(7), pp. 3461–3471. doi: 10.21873/anticanres.11714.

Gangadhar, T., Nandi, S. and Salgia, R. (2010) ‘The role of chemokine receptor CXCR4 in lung cancer’, *Cancer Biology and Therapy*. doi: 10.4161/cbt.9.6.11233.

Geisse, J. *et al.* (2004) ‘Imiquimod 5% cream for the treatment of superficial basal cell carcinoma: Results from two phase III, randomized, vehicle-controlled studies’, *Journal of the American Academy of Dermatology*. doi: 10.1016/j.jaad.2003.11.066.

Ghosh, E. *et al.* (2015) ‘Methodological advances: The unsung heroes of the GPCR structural revolution’, *Nature Reviews Molecular Cell Biology*. doi: 10.1038/nrm3933.

Gobert, M. *et al.* (2009) ‘Regulatory T cells recruited through CCL22/CCR4 are selectively activated in lymphoid infiltrates surrounding primary breast tumors and lead to an adverse clinical utcome’, *Cancer Research*. doi: 10.1158/0008-5472.CAN-08-2360.

Godiska, R. *et al.* (1997) ‘Human macrophage-derived chemokine (MDC), a novel chemoattractant for monocytes, monocyte-derived dendritic cells, and natural killer cells.’, *The Journal of experimental medicine*. doi: 10.1084/jem.185.9.1595.

Grant, A. J. *et al.* (2002) 'Hepatic expression of secondary lymphoid chemokine (CCL21) promotes the development of portal-associated lymphoid tissue in chronic inflammatory liver disease', *American Journal of Pathology*. doi: 10.1016/S0002-9440(10)62570-9.

Groer, C. E. *et al.* (2011) 'Agonist-directed interactions with specific β-arrestins determine μ-opioid receptor trafficking, ubiquitination, and dephosphorylation', *Journal of Biological Chemistry*. doi: 10.1074/jbc.M111.248310.

Gundry, J. *et al.* (2017) 'A practical guide to approaching biased agonism at G protein coupled receptors', *Frontiers in Neuroscience*, 11(JAN), pp. 1–6. doi: 10.3389/fnins.2017.00017.

Gunn, M. D. *et al.* (1999) 'Mice Lacking Expression of Secondary Lymphoid Organ Chemokine Have Defects in Lymphocyte Homing and Dendritic Cell Localization', *The Journal of Experimental Medicine*. doi: 10.1084/jem.189.3.451.

Hanahan, D. and Weinberg, R. A. (2011) 'Hallmarks of cancer: The next generation', *Cell*. doi: 10.1016/j.cell.2011.02.013.

Hanlon, C. D. and Andrew, D. J. (2015) 'Outside-in signaling - a brief review of GPCR signaling with a focus on the Drosophila GPCR family', *Journal of Cell Science*. doi: 10.1242/jcs.175158.

Hauser, A. S. *et al.* (2017) 'Trends in GPCR drug discovery: New agents, targets and indications', *Nature Reviews Drug Discovery*. doi: 10.1038/nrd.2017.178.

Hauser, M. A. *et al.* (2016) 'Inflammation-Induced CCR7 Oligomers Form Scaffolds to Integrate Distinct Signaling Pathways for Efficient Cell Migration', *Immunity*. doi: 10.1016/j.immuni.2015.12.010.

Hendrix, C. W. *et al.* (2004) 'Safety, pharmacokinetics, and antiviral activity of AMD3100, a selective CXCR4 receptor inhibitor, in HIV-1 infection', *Journal of Acquired Immune Deficiency Syndromes*. doi: 10.1097/01.qai.0000137371.80695.ef.

Hieshima, K. *et al.* (2003) 'CCL28 Has Dual Roles in Mucosal Immunity as a Chemokine with Broad-Spectrum Antimicrobial Activity', *The Journal of Immunology*. doi: 10.4049/jimmunol.170.3.1452.

Hirahara, K. *et al.* (2006) 'The Majority of Human Peripheral Blood CD4+CD25highFoxp3+ Regulatory T Cells Bear Functional Skin-Homing Receptors', *The Journal of Immunology*. doi: 10.4049/jimmunol.177.7.4488.

Homey, B. *et al.* (2000) 'Cutting Edge: The Orphan Chemokine Receptor G Protein-Coupled Receptor-2 (GPR-2, CCR10) Binds the Skin-Associated Chemokine CCL27 (CTACK/ALP/ILC)', *The Journal of Immunology*. doi: 10.4049/jimmunol.164.7.3465.

Homey, B. *et al.* (2002) 'CCL27-CCR10 interactions regulate T cell-mediated skin inflammation', *Nature Medicine*. doi: 10.1038/nm0202-157.

Horuk, R. (2009) 'Chemokine receptor antagonists: Overcoming developmental hurdles', *Nature Reviews Drug Discovery*. doi: 10.1038/nrd2734.

Hu, C. *et al.* (2013) 'CXCL12/CXCR4 axis promotes mesenchymal stem cell mobilization to burn wounds and contributes to wound repair', *Journal of Surgical Research*. doi: 10.1016/j.jss.2013.01.019.

Hu, Z. *et al.* (2015) 'CCR4 promotes medullary entry and thymocyte–dendritic cell interactions required for central tolerance', *The Journal of Experimental Medicine*. doi: 10.1084/jem.20150178.

Hughes, C. E. and Nibbs, R. J. B. (2018) 'A guide to chemokines and their receptors', *FEBS Journal*. doi: 10.1111/febs.14466.

Huskens, D. *et al.* (2007) 'The role of N-glycosylation sites on the CXCR4 receptor for CXCL-12 binding and signaling and X4 HIV-1 viral infectivity', *Virology*. doi: 10.1016/j.virol.2007.01.031.

Imai, T. *et al.* (1996) 'Molecular cloning of a novel T cell-directed CC chemokine expressed in thymus by signal sequence trap using Epstein-Barr virus vector', *Journal of Biological Chemistry*. doi: 10.1074/jbc.271.35.21514.

Imai, T. *et al.* (1997) 'The T cell-directed CC chemokine TARC is a highly specific biological ligand for CC chemokine receptor 4', *Journal of Biological Chemistry*. doi: 10.1074/jbc.272.23.15036.

Imai, T. *et al.* (1998) 'Macrophage-derived chemokine is a functional ligand for the CC

chemokine receptor 4.', *The Journal of biological chemistry*, 273(3), pp. 1764–8. doi: 10.1074/jbc.273.3.1764.

Imai, T. *et al.* (1999) 'Selective recruitment of CCR4-bearing T(h)2 cells toward antigen-presenting cells by the CC chemokines thymus and activation-regulated chemokine and macrophage-derived chemokine', *International Immunology*. doi: 10.1093/intimm/11.1.81.

Ishida, T. *et al.* (2013) 'Stevens-Johnson Syndrome associated with mogamulizumab treatment of adult T-cell leukemia/lymphoma', *Cancer Science*. doi: 10.1111/cas.12116.

Janetopoulos, C., Jin, T. and Devreotes, P. (2016) 'Receptor-Mediated Activation of Heterotrimeric G-Proteins in Living Cells Author(s)':, 60(3), pp. 348–360.

Jansma, A. L. *et al.* (2010) 'NMR analysis of the structure, dynamics, and unique oligomerization properties of the chemokine CCL27', *Journal of Biological Chemistry*. doi: 10.1074/jbc.M109.091108.

Jin, Y. *et al.* (2010) 'CCR10 Is Important for the Development of Skin-Specific T Cells by Regulating Their Migration and Location', *The Journal of Immunology*. doi: 10.4049/jimmunol.1001612.

Jørgensen, A. S., Rosenkilde, M. M. and Hjortø, G. M. (2018) 'Biased signaling of G protein-coupled receptors – From a chemokine receptor CCR7 perspective', *General and Comparative Endocrinology*. doi: 10.1016/j.ygcen.2017.07.004.

Karube, K. *et al.* (2004) 'Expression of FoxP3, a key molecule in CD4+CD25+ regulatory T cells, in adult T-cell leukaemia/lymphoma cells', *British Journal of Haematology*. doi: 10.1111/j.1365-2141.2004.04999.x.

Katada, T. (2012) 'The inhibitory G protein G(i) identified as pertussis toxin-catalyzed ADP-ribosylation.', *Biological {&} pharmaceutical bulletin*. doi: 10.1248/bpb.b212024.

Katou, F. *et al.* (2003) 'Differential expression of CCL19 by DC-lamp+mature dendritic cells in human lymph node versus chronically inflammed skin', *Journal of Pathology*. doi: 10.1002/path.1255.

Kenakin, T. and Christopoulos, A. (2013) 'Signalling bias in new drug discovery: Detection, quantification and therapeutic impact', *Nature Reviews Drug Discovery*. doi:

10.1038/nrd3954.

Kiermaier, E. *et al.* (2016) 'Polysialylation controls dendritic cell trafficking by regulating chemokine recognition', *Science*. doi: 10.1126/science.aad0512.

Kobayashi, D. *et al.* (2017) 'Regulation of CCR7-dependent cell migration through CCR7 homodimer formation', *Scientific Reports*. doi: 10.1038/s41598-017-09113-4.

Kohout, T. A. *et al.* (2004) 'Differential desensitization, receptor phosphorylation, ??-arrestin recruitment, and ERK1/2 activation by the two endogenous ligands for the CC chemokine receptor 7', *Journal of Biological Chemistry*, 279(22), pp. 23214–23222. doi: 10.1074/jbc.M402125200.

Koressaar, T. and Remm, M. (2007) 'Enhancements and modifications of primer design program Primer3', *Bioinformatics*. doi: 10.1093/bioinformatics/btm091.

Kraynyak, K. A. *et al.* (2010) 'Systemic immunization with CCL27/CTACK modulates immune responses at mucosal sites in mice and macaques', *Vaccine*. doi: 10.1016/j.vaccine.2009.10.095.

Kühnelt-Leddihn, L. *et al.* (2012) 'Overexpression of the chemokine receptors CXCR4, CCR7, CCR9, and CCR10 in human primary cutaneous melanoma: A potential prognostic value for CCR7 and CCR10?', *Archives of Dermatological Research*. doi: 10.1007/s00403-012-1222-8.

Lazareno, S. and Birdsall, N. J. M. (1993) 'Estimation of competitive antagonist affinity from functional inhibition curves using the Gaddum, Schild and Cheng-Prusoíf equations', *British Journal of Pharmacology*. doi: 10.1111/j.1476-5381.1993.tb13737.x.

Leach, K., Charlton, S. J. and Strange, P. G. (2007) 'Analysis of second messenger pathways stimulated by different chemokines acting at the chemokine receptor CCR5', *Biochemical Pharmacology*. doi: 10.1016/j.bcp.2007.06.019.

Lebre, M. C. *et al.* (2011) 'Why CCR2 and CCR5 blockade failed and why ccr1 blockade might still be effective in the treatment of rheumatoid arthritis', *PLoS ONE*. doi: 10.1371/journal.pone.0021772.

Lee, I. *et al.* (2005) 'Recruitment of Foxp3 $^{+}$ T regulatory cells mediating allograft

tolerance depends on the CCR4 chemokine receptor', *The Journal of Experimental Medicine*. doi: 10.1084/jem.20041709.

Li, K. *et al.* (2016) 'CCR7 regulates Twist to induce the epithelial-mesenchymal transition in pancreatic ductal adenocarcinoma', *Tumor Biology*. doi: 10.1007/s13277-015-3819-y.

Li, M. *et al.* (2013) 'A role for CCL2 in both tumor progression and immunosurveillance', *OncoImmunology*. doi: 10.4161/onci.25474.

Lin, H. yu *et al.* (2017) 'CCR10 activation stimulates the invasion and migration of breast cancer cells through the ERK1/2/MMP-7 signaling pathway', *International Immunopharmacology*. doi: 10.1016/j.intimp.2017.07.018.

Link, A. *et al.* (2007) 'Fibroblastic reticular cells in lymph nodes regulate the homeostasis of naive T cells', *Nature Immunology*. doi: 10.1038/ni1513.

Loughran, G. *et al.* (2018) 'Stop codon readthrough generates a C-terminally extended variant of the human vitamin D receptor with reduced calcitriol response', *Journal of Biological Chemistry*. doi: 10.1017/S096702629700139X.

Lovell, K. M. *et al.* (2015) 'Structure-Activity Relationship Studies of Functionally Selective Kappa Opioid Receptor Agonists that Modulate ERK 1/2 Phosphorylation while Preserving G Protein over βarrestin2 Signaling Bias', *ACS Chemical Neuroscience*. doi: 10.1021/acschemneuro.5b00092.

Luttrell, L. M. *et al.* (1999) 'β-arrestin-dependent formation of β2 adrenergic receptor-src protein kinase complexes', *Science*. doi: 10.1126/science.283.5402.655.

Ma, Q. *et al.* (1998) 'Impaired B-lymphopoiesis, myelopoiesis, and derailed cerebellar neuron migration in CXCR4- and SDF-1-deficient mice', *Proceedings of the National Academy of Sciences*. doi: 10.1073/pnas.95.16.9448.

Ma, X. *et al.* (2016) 'Functional roles of sialylation in breast cancer progression through miR-26a/26b targeting ST8SIA4', *Cell death & disease*. doi: 10.1038/cddis.2016.427.

Makita, S. and Tobinai, K. (2017) 'Mogamulizumab for the treatment of T-cell lymphoma', *Expert Opinion on Biological Therapy*. doi: 10.1080/14712598.2017.1347634.

Malik, R. U. *et al.* (2017) ‘ER/K linked GPCR-G protein fusions systematically modulate second messenger response in cells’, *Scientific Reports*. doi: 10.1038/s41598-017-08029-3.

Malpica, L. *et al.* (2018) ‘Epidemiology, clinical features, and outcome of HTLV-1–related ATLL in an area of prevalence in the United States’, *Blood Advances*. doi: 10.1182/bloodadvances.2017011106.

Mangmool, S. and Kurose, H. (2011) ‘Gi/oprotein-dependent and -independent actions of pertussis toxin (ptx)’, *Toxins*, 3(7), pp. 884–899. doi: 10.3390/toxins3070884.

Mantovani, A. (1999) ‘The chemokine system: Redundancy for robust outputs’, *Immunology Today*. doi: 10.1016/S0167-5699(99)01469-3.

Manzi, A. E. *et al.* (1994) ‘Intramolecular self-cleavage of polysialic acid’, *Journal of Biological Chemistry*.

Maolake, A. *et al.* (2016) ‘Tumor-associated macrophages promote prostate cancer migration through activation of the CCL22–CCR4 axis’, *Oncotarget*. doi: 10.18632/oncotarget.14185.

Marchese, A. and Benovic, J. L. (2001) ‘Agonist-promoted Ubiquitination of the G Protein-coupled Receptor CXCR4 Mediates Lysosomal Sorting’, *Journal of Biological Chemistry*. doi: 10.1074/jbc.C100527200.

Mariani, M. *et al.* (2004) ‘Dominance of CCL22 over CCL17 in induction of chemokine receptor CCR4 desensitization and internalization on human Th2 cells’, *European Journal of Immunology*. doi: 10.1002/eji.200324429.

Matloubian, M. *et al.* (2004) ‘Lymphocyte egress from thymus and peripheral lymphoid organs is dependent on S1P receptor 1’, *Nature*. doi: 10.1038/nature02284.

Mauldin, I. S. *et al.* (2016) ‘Topical treatment of melanoma metastases with imiquimod, plus administration of a cancer vaccine, promotes immune signatures in the metastases’, *Cancer Immunology, Immunotherapy*. doi: 10.1007/s00262-016-1880-z.

Mirshahpanah, P. *et al.* (2008) ‘CCR4 and CCR10 ligands play additive roles in mouse contact hypersensitivity’, *Experimental Dermatology*. doi: 10.1111/j.1600-0625.2007.00630.x.

Miyazato, P. and Matsuoka, M. (2014) 'Human T-cell leukemia virus type 1 and Foxp3 expression: Viral strategy in vivo', *International Immunology*. doi: 10.1093/intimm/dxu048.

Mizukami, Y. et al (2008) 'CCL17 and CCL22 chemokines within tumor microenvironment are related to accumulation of Foxp3+ regula- tory T cells in gastric cancer.', *Int J Cancer*. doi: 10.1002/ijc.23392.

Momose, F. and Morikawa, Y. (2016) 'Polycistronic expression of the influenza A virus RNA-dependent RNA polymerase by using the Thosea asigna virus 2A-like self-processing sequence', *Frontiers in Microbiology*. doi: 10.3389/fmicb.2016.00288.

Morales, J. *et al.* (1999) 'CTACK, a skin-associated chemokine that preferentially attracts skin-homing memory T cells', *Proceedings of the National Academy of Sciences*. doi: 10.1073/pnas.96.25.14470.

Mori, A. *et al.* (2017) 'Different properties of polysialic acids synthesized by the polysialyltransferases ST8SIA2 and ST8SIA4', *Glycobiology*, 27(9), pp. 834–846. doi: 10.1093/glycob/cwx057.

Morimoto, Y. (2005) 'Induction of surface CCR4 and its functionality in mouse Th2 cells is regulated differently during Th2 development', *Journal of Leukocyte Biology*. doi: 10.1189/jlb.0305139.

Morteau, O. *et al.* (2008) 'An Indispensable Role for the Chemokine Receptor CCR10 in IgA Antibody-Secreting Cell Accumulation', *The Journal of Immunology*. doi: 10.4049/jimmunol.181.9.6309.

Na, I. K. *et al.* (2008) 'Identification of truncated chemokine receptor 7 in human colorectal cancer unable to localize to the cell surface and unreactive to external ligands', *International Journal of Cancer*. doi: 10.1002/ijc.23704.

Nibbs, R. J. B. and Graham, G. J. (2013) 'Immune regulation by atypical chemokine receptors', *Nature Reviews Immunology*. doi: 10.1038/nri3544.

Nomiyama, H., Osada, N. and Yoshie, O. (2011) 'A family tree of vertebrate chemokine receptors for a unified nomenclature', *Developmental and Comparative Immunology*. doi: 10.1016/j.dci.2011.01.019.

Notohamiprodjo, M. *et al.* (2005) ‘CCR10 is expressed in cutaneous T-cell lymphoma’, *International Journal of Cancer*. doi: 10.1002/ijc.20922.

O’Hagan, D. T. and Valiante, N. M. (2003) ‘Recent advances in the discovery and delivery of vaccine adjuvants’, *Nature Reviews Drug Discovery*. doi: 10.1038/nrd1176.

Ohl, L. *et al.* (2003) ‘Cooperating Mechanisms of CXCR5 and CCR7 in Development and Organization of Secondary Lymphoid Organs’, *The Journal of Experimental Medicine*. doi: 10.1084/jem.20030169.

Ohl, L. *et al.* (2004) ‘CCR7 governs skin dendritic cell migration under inflammatory and steady-state conditions’, *Immunity*. doi: 10.1016/j.immuni.2004.06.014.

Ondondo, B. *et al.* (2013) ‘Home sweet home: The tumor microenvironment as a haven for regulatory T cells’, *Frontiers in Immunology*. doi: 10.3389/fimmu.2013.00197.

Oppermann, M. *et al.* (1999) ‘Differential effects of CC chemokines on CC chemokine receptor 5 (CCR5) phosphorylation and identification of phosphorylation sites on the CCR5 carboxyl terminus’, *Journal of Biological Chemistry*. doi: 10.1074/jbc.274.13.8875.

Otero, C., Groettrup, M. and Legler, D. F. (2006) ‘Opposite Fate of Endocytosed CCR7 and Its Ligands: Recycling versus Degradation’, *The Journal of Immunology*. doi: 10.4049/jimmunol.177.4.2314.

Ourne, H. E. R. B. (1997) ‘Receptors induce chemotaxis by releasing the ␣ subunit of G i ’, 94(December), pp. 14489–14494.

Pack, T. F. *et al.* (2018) ‘The dopamine D2 receptor can directly recruit and activate GRK2 without G protein activation’, *Journal of Biological Chemistry*. doi: 10.1074/jbc.RA117.001300.

Palczewski, K. *et al.* (1991) ‘Mechanism of rhodopsin kinase activation’, *Journal of Biological Chemistry*.

Pan, J. *et al.* (2000) ‘Cutting Edge: A Novel Chemokine Ligand for CCR10 And CCR3 Expressed by Epithelial Cells in Mucosal Tissues’, *The Journal of Immunology*. doi: 10.4049/jimmunol.165.6.2943.

Park, C. *et al.* (2012) 'Lymph node B lymphocyte trafficking is constrained by anatomy and highly dependent upon chemoattractant desensitization', *Blood*. doi: 10.1182/blood-2011-06-364273.

Pearce, O. M. T. and Läubli, H. (2015) 'Sialic acids in cancer biology and immunity', *Glycobiology*. doi: 10.1093/glycob/cwv097.

Percherancier, Y. *et al.* (2001) 'Palmitoylation-dependent Control of Degradation, Life Span, and Membrane Expression of the CCR5 Receptor', *Journal of Biological Chemistry*. doi: 10.1074/jbc.M104013200.

Pere, H. *et al.* (2011) 'ACCR4 antagonist combined with vaccines induces antigen-specific CD8+T cells and tumor immunity against self antigens', *Blood*. doi: 10.1182/blood-2011-01-329656.

Peterson, Y. K. and Luttrell, L. M. (2017) 'The Diverse Roles of Arrestin Scaffolds in G Protein–Coupled Receptor Signaling', *Pharmacological Reviews*. doi: 10.1124/pr.116.013367.

Phillips, A. J. *et al.* (2017) 'CCR7 sulfotyrosine enhances CCL21 binding', *International Journal of Molecular Sciences*. doi: 10.3390/ijms18091857.

Proudfoot, A. E. I. *et al.* (1996) 'Extension of recombinant human RANTES by the retention of the initiating methionine produces a potent antagonist', *Journal of Biological Chemistry*. doi: 10.1074/jbc.271.5.2599.

Qin, L. *et al.* (2015) 'Crystal structure of the chemokine receptor CXCR4 in complex with a viral chemokine', *Science*. doi: 10.1126/science.1261064.

Rainone, V. *et al.* (2011) 'CCL28 induces mucosal homing of HIV-1-specific IgA-secreting plasma cells in mice immunized with HIV-1 virus-like particles', *PLoS ONE*. doi: 10.1371/journal.pone.0026979.

Rajagopal, S. *et al.* (2013) 'Biased agonism as a mechanism for differential signaling by chemokine receptors', *Journal of Biological Chemistry*. doi: 10.1074/jbc.M113.479113.

Rajagopalan, L. and Rajarathnam, K. (2006) 'Structural basis of chemokine receptor function - A model for binding affinity and ligand selectivity', *Bioscience Reports*. doi:

10.1007/s10540-006-9025-9.

Raman, D., Sobolik-Delmaire, T. and Richmond, A. (2011) ‘Chemokines in health and disease’, *Experimental Cell Research*. doi: 10.1016/j.yexcr.2011.01.005.

Rankin, S. M. (2012) ‘Chemokines and adult bone marrow stem cells’, *Immunology Letters*. doi: 10.1016/j.imlet.2012.04.009.

Rankovic, Z., Brust, T. F. and Bohn, L. M. (2016) ‘Biased agonism: An emerging paradigm in GPCR drug discovery’, *Bioorganic and Medicinal Chemistry Letters*. doi: 10.1016/j.bmcl.2015.12.024.

Reiss, Y. *et al.* (2001) ‘CC Chemokine Receptor (CCR)4 and the CCR10 Ligand Cutaneous T Cell–attracting Chemokine (CTACK) in Lymphocyte Trafficking to Inflamed Skin’, *The Journal of Experimental Medicine*. doi: 10.1084/jem.194.10.1541.

Rey-Gallardo, A. *et al.* (2010) ‘Polysialylated neuropilin-2 enhances human dendritic cell migration through the basic C-terminal region of CCL21’, *Glycobiology*. doi: 10.1093/glycob/cwq078.

Röckle, I. and Hildebrandt, H. (2016) ‘Deficits of olfactory interneurons in polysialyltransferase- and NCAM-deficient mice’, *Developmental Neurobiology*. doi: 10.1002/dneu.22324.

Rollins, B. J. (1997) ‘Chemokines’, *Blood Journal*. doi: 10.1111/j.1365-2036.2011.04980.x.

Rot, A. and von Andrian, U. H. U. H. (2004) ‘Chemokines in innate and adaptive host defense: basic chemokinese grammar for immune cells.’, *Annual review of immunology*. doi: 10.1146/annurev.immunol.22.012703.104543.

Rummel, P. C. *et al.* (2013) ‘Extracellular Disulfide Bridges Serve Different Purposes in Two Homologous Chemokine Receptors, CCR1 and CCR5’, *Molecular Pharmacology*. doi: 10.1124/mol.113.086702.

Sallusto, F. *et al.* (1998) ‘Rapid and coordinated switch in chemokine receptor expression during dendritic cell maturation’, *European Journal of Immunology*. doi: 10.1002/(SICI)1521-4141(199809)28:09<2760::AID-IMMU2760>3.0.CO;2-N.

Sallusto, F. *et al.* (2014) 'Two subsets of memory T lymphocytes with distinct homing potentials and effector functions', *Journal of Immunology*. doi: 10.1126/science.1058867.

Sanz, M. J. and Kubes, P. (2012) 'Neutrophil-active chemokines in in vivo imaging of neutrophil trafficking', *European Journal of Immunology*. doi: 10.1002/eji.201142231.

Sather, B. D. *et al.* (2007) 'Altering the distribution of Foxp3 $^{+}$ regulatory T cells results in tissue-specific inflammatory disease', *The Journal of Experimental Medicine*. doi: 10.1084/jem.20070081.

Schaeuble, K. *et al.* (2011) 'Cross-talk between TCR and CCR7 signaling sets a temporal threshold for enhanced T lymphocyte migration.', *The Journal of Immunology*. doi: 10.4049/jimmunol.1101850.

Schmid, C. L. and Bohn, L. M. (2010) 'Serotonin, But Not N-Methyltryptamines, Activates the Serotonin 2A Receptor Via a -Arrestin2/Src/Akt Signaling Complex In Vivo', *Journal of Neuroscience*. doi: 10.1523/JNEUROSCI.1665-10.2010.

Schmied, W. H. *et al.* (2014) 'Efficient multisite unnatural amino acid incorporation in mammalian cells via optimized pyrrolysyl tRNA synthetase/tRNA expression and engineered eRF1', *Journal of the American Chemical Society*. doi: 10.1021/ja5069728.

Schneider, M. A. *et al.* (2007) 'CCR7 is required for the in vivo function of CD4 $^{+}$ CD25 $^{+}$ regulatory T cells', *The Journal of Experimental Medicine*. doi: 10.1084/jem.20061405.

Schutyser, E., Struyf, S. and Van Damme, J. (2003) 'The CC chemokine CCL20 and its receptor CCR6', *Cytokine and Growth Factor Reviews*. doi: 10.1016/S1359-6101(03)00049-2.

Shannon, L. A. *et al.* (2012) 'CCR7/CCL19 controls expression of EDG-1 in T cells', *Journal of Biological Chemistry*. doi: 10.1074/jbc.M111.310045.

Shao, N. *et al.* (2015) 'Site Specific Genetic Incorporation of Azidophenylalanine in Schizosaccharomyces pombe', *Scientific Reports*. doi: 10.1038/srep17196.

Soler, D. *et al.* (2003) 'CCR4 versus CCR10 in human cutaneous TH lymphocyte trafficking', *Blood*. doi: 10.1182/blood-2002-07-2348.

Stone, M. J. *et al.* (2017) 'Mechanisms of regulation of the chemokine-receptor network', *International Journal of Molecular Sciences*. doi: 10.3390/ijms18020342.

Strieter, R. M. *et al.* (1995) 'The functional role of the ELR motif in CXC chemokine-mediated angiogenesis', *Journal of Biological Chemistry*. doi: 10.1074/jbc.270.45.27348.

Sugiyama, D. *et al.* (2013) 'Anti-CCR4 mAb selectively depletes effector-type FoxP3+CD4+ regulatory T cells, evoking antitumor immune responses in humans', *Proceedings of the National Academy of Sciences*. doi: 10.1073/pnas.1316796110.

Sullivan, S. K. *et al.* (1999) 'Pharmacological and signaling analysis of human chemokine receptor CCR-7 stably expressed in HEK-293 cells: High-affinity binding of recombinant ligands MIP-3β and SLC stimulates multiple signaling cascades', *Biochemical and Biophysical Research Communications*. doi: 10.1006/bbrc.1999.1442.

Sun, L. *et al.* (2015) 'CCL21/CCR7 up-regulate vascular endothelial growth factor-D expression via ERK pathway in human non-small cell lung cancer cells', *International Journal of Clinical and Experimental Pathology*.

Sun, X. *et al.* (2010) 'CXCL12 / CXCR4 / CXCR7 chemokine axis and cancer progression', *Cancer and Metastasis Reviews*. doi: 10.1007/s10555-010-9256-x.

Suzuki, G. *et al.* (1999) 'Pertussis toxin-sensitive signal controls the trafficking of thymocytes across the corticomedullary junction in the thymus', *Journal of immunology (Baltimore, Md : 1950)*. doi: 10.4049/jimmunol.176.1.401.

Svensson, H. *et al.* (2012) 'Accumulation of CCR4+CTLA-4hiFOXP3+CD25hiregulatory T cells in colon adenocarcinomas correlate to reduced activation of conventional T cells', *PLoS ONE*. doi: 10.1371/journal.pone.0030695.

Svensson, M. *et al.* (2002) 'CCL25 mediates the localization of recently activated CD8αβ+lymphocytes to the small-intestinal mucosa', *Journal of Clinical Investigation*. doi: 10.1172/JCI0215988.

Szekanecz, Z. *et al.* (2006) 'Chemokines in rheumatic diseases', *CURRENT DRUG TARGETS*. doi: 10.2174/138945006775270231.

Szpakowska, M. *et al.* (2012) 'Function, diversity and therapeutic potential of the N-

terminal domain of human chemokine receptors', *Biochemical Pharmacology*. doi: 10.1016/j.bcp.2012.08.008.

Takabatake, Y. *et al.* (2009) 'The CXCL12 (SDF-1)/CXCR4 Axis Is Essential for the Development of Renal Vasculature', *Journal of the American Society of Nephrology*. doi: 10.1681/ASN.2008060640.

Takahama, Y. (2006) 'Journey through the thymus: Stromal guides for T-cell development and selection', *Nature Reviews Immunology*. doi: 10.1038/nri1781.

Takimoto, J. K. *et al.* (2009) 'Improving orthogonal tRNA-synthetase recognition for efficient unnatural amino acid incorporation and application in mammalian cells', *Molecular BioSystems*. doi: 10.1039/b904228h.

Tan, Q. *et al.* (2013) 'Structure of the CCR5 chemokine receptor-HIV entry inhibitor maraviroc complex', *Science*. doi: 10.1126/science.1241475.

Tanaka, F. *et al.* (2000) 'Expression of polysialic acid and STX, a human polysialyltransferase, is correlated with tumor progression in non-small cell lung cancer', *Cancer Research*. doi: 10.1016/s0959-4388(97)80083-9.

Tom, R., Bisson, L. and Durocher, Y. (2008) 'Culture of HEK293-EBNA1 cells for production of recombinant proteins', *Cold Spring Harbor Protocols*. doi: 10.1101/pdb.prot4976.

Ulvmar, M. H. *et al.* (2014) 'The atypical chemokine receptor CCRL1 shapes functional CCL21 gradients in lymph nodes', *Nature Immunology*. doi: 10.1038/ni.2889.

Ulvmar, M. H., Hub, E. and Rot, A. (2011) 'Atypical chemokine receptors.', *Experimental cell research*. doi: 10.1016/j.yexcr.2011.01.012.

Vestergaard, C. *et al.* (2003) 'Expression of the T-helper 2-specific chemokine receptor CCR4 on CCR10-positive lymphocytes in atopic dermatitis skin but not in psoriasis skin', *British Journal of Dermatology*. doi: 10.1046/j.1365-2133.2003.05505.x.

Viney, J. M. *et al.* (2014a) 'Distinct Conformations of the Chemokine Receptor CCR4 with Implications for Its Targeting in Allergy', *The Journal of Immunology*. doi: 10.4049/jimmunol.1300232.

Viney, J. M. *et al.* (2014b) 'Distinct Conformations of the Chemokine Receptor CCR4 with Implications for Its Targeting in Allergy', *The Journal of Immunology*, 192(7), pp. 3419–3427. doi: 10.4049/jimmunol.1300232.

Violin, J. D. *et al.* (2010) 'Selectively Engaging -Arrestins at the Angiotensin II Type 1 Receptor Reduces Blood Pressure and Increases Cardiac Performance', *Journal of Pharmacology and Experimental Therapeutics*. doi: 10.1124/jpet.110.173005.

Violin, J. D., Soergel, D. G. and Lark, M. W. (2012) 'Beta-arrestin-biased ligands at the AT1R: A novel approach to the treatment of acute heart failure', *Drug Discovery Today: Therapeutic Strategies*. doi: 10.1016/j.ddstr.2014.01.001.

Wang, L. and Schultz, P. G. (2002) 'Expanding the genetic code', *Chemical Communications*. doi: 10.1039/b108185n.

Wang, W. *et al.* (2000) 'Identification of a novel chemokine (CCL28), which binds CCR10 (GPR2)', *Journal of Biological Chemistry*. doi: 10.1074/jbc.M001461200.

Wang, X. *et al.* (2016) 'Enhanced expression of polysialic acid correlates with malignant phenotype in breast cancer cell lines and clinical tissue samples', *International Journal of Molecular Medicine*. doi: 10.3892/ijmm.2015.2395.

Ward, R. J., Alvarez-Curto, E. and Milligan, G. (2011) 'Using the Flp-In™ T-Rex™ system to regulate GPCR expression', *Methods in Molecular Biology*. doi: 10.1007/978-1-61779-126-0_2.

Ward, W. W. and Cormier, M. J. (1979) 'An energy transfer protein in coelenterate bioluminescence. Characterization of the Renilla green-fluorescent protein.', *Journal of Biological Chemistry*.

Watanabe, Y. *et al.* (2010) 'Tumor-infiltrating lymphocytes, particularly the balance between CD8+T cells and CCR4+regulatory T cells, affect the survival of patients with oral squamous cell carcinoma', *Oral Surgery, Oral Medicine, Oral Pathology, Oral Radiology and Endodontology*. doi: 10.1016/j.tripleo.2009.12.015.

Weber, M. *et al.* (2013) 'Interstitial Dendritic Cell Guidance by Haptotactic Chemokine Gradients', *Science*. doi: 10.1126/science.1228456.

Wengner, A. M. *et al.* (2007) 'CXCR5- and CCR7-dependent lymphoid neogenesis in a murine model of chronic antigen-induced arthritis', *Arthritis and Rheumatism*. doi: 10.1002/art.22939.

Willenborg, S. *et al.* (2012) 'CCR2 recruits an inflammatory macrophage subpopulation critical for angiogenesis in tissue repair', *Blood*. doi: 10.1182/blood-2012-01-403386.

Windfuhr, M. *et al.* (2000) 'Molecular defects that cause loss of polysialic acid in the complementation group 2A10', *Journal of Biological Chemistry*. doi: 10.1074/jbc.M003507200.

Worbs, T. *et al.* (2007) 'CCR7 ligands stimulate the intranodal motility of T lymphocytes in vivo', *The Journal of Experimental Medicine*. doi: 10.1084/jem.20061706.

Xia, M. *et al.* (2014) 'CCR10 regulates balanced maintenance and function of resident regulatory and effector T cells to promote immune homeostasis in the skin', *Journal of Allergy and Clinical Immunology*. doi: 10.1016/j.jaci.2014.03.010.

Xiong, N. *et al.* (2012) 'CCR10 and its ligands in regulation of epithelial immunity and diseases', *Protein and Cell*. doi: 10.1007/s13238-012-2927-3.

Xiong, Y. *et al.* (2017) 'CCL21/CCR7 interaction promotes cellular migration and invasion via modulation of the MEK/ERK1/2 signaling pathway and correlates with lymphatic metastatic spread and poor prognosis in urinary bladder cancer', *International Journal of Oncology*. doi: 10.3892/ijo.2017.4003.

Xu, B. *et al.* (2017) 'CCR7 mediates human breast cancer cell invasion, migration by inducing epithelial–mesenchymal transition and suppressing apoptosis through AKT pathway', *Cancer Medicine*. doi: 10.1002/cam4.1039.

Xu, Y. *et al.* (2007) 'Differential Development of Murine Dendritic Cells by GM-CSF versus Flt3 Ligand Has Implications for Inflammation and Trafficking', *The Journal of Immunology*. doi: 10.4049/jimmunol.179.11.7577.

Ye, J. *et al.* (2012) 'Primer-BLAST: a tool to design target-specific primers for polymerase chain reaction.', *BMC bioinformatics*. doi: 10.1186/1471-2105-13-134.

Yoshida, R. *et al.* (1998) 'Secondary lymphoid-tissue chemokine is a functional ligand for

the CC chemokine receptor CCR7', *Journal of Biological Chemistry*. doi: 10.1074/jbc.273.12.7118.

Yoshie, O. *et al.* (2002) 'Frequent expression of CCR4 in adult T-cell leukemia and human T-cell leukemia virus type 1-transformed T cells', *Blood*. doi: 10.1182/blood.V99.5.1505.

Yoshie, O. and Matsushima, K. (2015) 'CCR4 and its ligands: From bench to bedside', *International Immunology*. doi: 10.1093/intimm/dxu079.

Yu, S. *et al.* (2011) 'The chemokine receptor CXCR7 functions to regulate cardiac valve remodeling', *Developmental Dynamics*. doi: 10.1002/dvdy.22549.

Zerwas, M. *et al.* (2016) 'Environmental enrichment rescues memory in mice deficient for the polysialytransferase ST8SiaIV', *Brain Structure and Function*. doi: 10.1007/s00429-015-0991-1.

Zhang, L. *et al.* (2017) 'Inhibition of CCR7 promotes NF-KB-dependent apoptosis and suppresses epithelial-mesenchymal transition in non-small cell lung cancer', *Oncology Reports*. doi: 10.3892/or.2017.5524.

Zhang, Y. *et al.* (2017) 'A new antagonist for CCR4 attenuates allergic lung inflammation in a mouse model of asthma', *Scientific Reports*. doi: 10.1038/s41598-017-11868-9.

Zhao, L. *et al.* (2016) 'Upregulation of miR-181c inhibits chemoresistance by targeting <i>ST8SIA4</i> in chronic myelocytic leukemia', *Oncotarget*. doi: 10.1007/978-3-319-70742-6_20.

Zhong, G. *et al.* (2017) 'Chemokine (C-C motif) ligand 21/C-C chemokine receptor type 7 triggers migration and invasion of human lung cancer cells by epithelial-mesenchymal transition via the extracellular signal-regulated kinase signaling pathway', *Molecular Medicine Reports*. doi: 10.3892/mmr.2017.6534.

Zhou, L. *et al.* (2013) 'Development of functionally selective, small molecule agonists at kappa opioid receptors', *Journal of Biological Chemistry*. doi: 10.1074/jbc.M113.504381.

Zhu, B. *et al.* (2012) 'CXCL12 enhances human neural progenitor cell survival through a CXCR7- and CXCR4-mediated endocytotic signaling pathway', *Stem Cells*. doi: 10.1002/stem.1239.

Zhu, Y. and Murakami, F. (2012) ‘Chemokine CXCL12 and its receptors in the developing central nervous system: Emerging themes and future perspectives’, *Developmental Neurobiology*. doi: 10.1002/dneu.22041.

Ziarek, J. J. *et al.* (2017) ‘Structural basis for chemokine recognition by a G protein–coupled receptor and implications for receptor activation’, *Science Signaling*. doi: 10.1126/scisignal.aah5756.

Zidar, D. A. *et al.* (2009) ‘Selective engagement of G protein coupled receptor kinases (GRKs) encodes distinct functions of biased ligands’, *Proceedings of the National Academy of Sciences*. doi: 10.1073/pnas.0904361106.

Zlotnik, A. and Yoshie, O. (2000) ‘Chemokines: A new classification system and their role in immunity’, *Immunity*. doi: 10.1016/S1074-7613(00)80165-X.

Zlotnik, A. and Yoshie, O. (2012) ‘The Chemokine Superfamily Revisited’, *Immunity*. doi: 10.1016/j.immuni.2012.05.008.

Zlotnik, A., Yoshie, O. and Nomiyama, H. (2006) ‘The chemokine and chemokine receptor superfamilies and their molecular evolution’, *Genome Biology*. doi: 10.1186/gb-2006-7-12-243.